

**Late Aptian-Albian of the Vocontian Basin (SE-France)
and Albian of NE-Texas:
Biostratigraphic and paleoceanographic implications by
planktic foraminifera faunas.**

Dissertation
zur Erlangung des Grades eines Doktors der Naturwissenschaften

der Geowissenschaftlichen Fakultät
der Eberhard-Karls-Universität Tübingen

vorgelegt von
Kerstin Reichelt
aus Helmstedt

2005

Tag der mündlichen Prüfung: 27.01.2005

Dekan: Prof. Dr. K.-G. Nickel

1. Berichterstatter: Prof. Dr. Ch. Hemleben

2. Berichterstatter: Priv.-Doz. Dr. R. Schiebel

Zusammenfassung

Zur Entwicklung einer hochauflösenden Biostratigraphie des Ober Apt bis Ober Alb des Vokontischen Beckens (SE-Frankreich) und des Mittel bis Ober Alb in NE-Texas wurden planktische Foraminiferen und stabile Isotope des Kohlenstoffs untersucht. Basierend auf Korrelationen der Kohlenstoffisotopenkurve aus SE-Frankreich, des östlichen (DSDP 547, Mazagan Plateau) und westlichen (ODP 1052; Blake Nose Plateau) Atlantik sowie des Golf von Mexicos (NE-Texas) konnte eine hochauflösende Kohlenstoffisotopen Stratigraphie (CIS) des Alb entwickelt werden.

Anhand von Faunendaten planktischer Foraminiferen wurde die Evolution der planktischen Foraminiferen der Mittleren Kreide (Ober Apt bis Ober Alb, 113-98 Ma) nachvollzogen.

Durch die hochauflösende Kohlenstoffisotopen Stratigraphie konnte diachrones Erstauftreten von stratigraphisch gut untersuchten planktischen Foraminiferen zwischen dem Vokontischen Becken (westliche Tethys), dem Mazagan Plateau (östlicher Atlantik), dem Blake Nose Plateau (westlicher Atlantik) und NE-Texas (Golf von Mexiko) aufgezeigt werden. Die Gründe für dieses zeitlich ungleiche Erstauftreten können durch paläoceanographische und paläoklimatische Veränderungen, welche das Strömungssystem sowie die Struktur der Wassersäule und die Nahrungsverteilung möglicherweise beeinflussten, gegeben sein.

Zusätzlich konnte nachgewiesen werden, dass das Erstauftreten sowie die Entwicklung von planktischen Foraminiferen in NE-Texas stark von Transgressions/Regressions Zyklen abhängig sein können.

Abstract

Planktic foraminifera fauna and carbon isotopes of the bulk rock have been investigated to compile a high resolution biostratigraphy for the Late Aptian to Late Albian in the Vocontian Basin (SE-France) and for the Middle and Late Albian in NE-Texas. A high resolution carbon isotope stratigraphy (CIS) has been established for the Albian of the Vocontian Basin, and partially correlated with sections in the eastern (ODP 547, Mazagan Plateau) and western (ODP 1052; Blake Nose Plateau) Atlantic as well as in the Gulf of Mexico (NE-Texas).

The high resolution carbon isotope stratigraphy possibly revealed diachronous first appearances of stratigraphically well constrained planktic foraminifera in the Vocontian Basin (western Tethys), at the Mazagan Plateau (eastern Atlantic), the Blake Nose Plateau (western Atlantic), and NE-Texas (Gulf of Mexico). The causes for the non-simultaneous occurrences may be palaeoceanographic and palaeoclimatic changes, which may have affected the water current system, the water column structure and the nutrient distribution.

In addition, the planktic foraminiferal data of the first appearance in NE-Texas show that the evolution of planktic foraminifera in NE-Texas may depend highly on transgression/regression cycles.

Danksagung

Für die Betreuung der Arbeit, die intensive Unterstützung und Bereitstellung der Arbeitsmittel gebührt Herrn Prof. Dr. Christoph Hemleben mein besonderer Dank.

PD Dr. R. Schiebel übernahm freundlicherweise die Zweitbegutachtung dieser Arbeit.

Dr. J. Herrle (South Hampton) und Dr. J. Lehmann (Bremen) danke ich im besonderen für Arbeitsanregungen, interessante Diskussionen, Probenmaterial, ergänzende Daten und Ratschläge.

Die Geländearbeit in Texas (Fort Worth) wäre ohne die vorab Versorgung mit Literatur und tatkräftige Mithilfe von Dr. Robert W. Scott (Tulsa) nicht möglich gewesen. Vielen Dank!

Ebenso möchte ich Oliver Friedrich danken, der mir bei Geländearbeiten und mit zahl- und ergebnisreichen Diskussionen sehr geholfen hat.

Meinen Kollegen Dr. Ralf Schiebel (ETH Zürich), Dr. Gerhard Schmiedl (Leipzig) und Dr. Petra Heinz (Tübingen) möchte ich für ihre immerwährende Diskussionsbereitschaft danken.

Für die Photoaufnahmen der REM-Bilder danke ich Frau Margaret Bayer.

Mein herzlicher Dank gilt allen Mitarbeitern und Mitarbeiterinnen des Geologischen Institutes, besonders der Abteilung Mikropaläontologie, die stets für ein angenehmes Arbeitsklima sorgten.

Die finanzielle Unterstützung dieser Arbeit war durch ein DFG-Projekt (Klank) gesichert. Danke!

Mein persönlicher Dank gilt meinen Freunden, im besonderen Birgit Fortenbacher, Ansgar Höckh, Christian Förster, Frank H. Müller und meinen Eltern, die immer ein offenes Ohr hatten.

Zusammenfassung/Abstract	I
Danksagung	II
Contents	III
1. Introduction	1
<i>1.1. Purpose of Investigation</i>	2
<i>1.2. State of the Art</i>	3
1.2.1. Study Areas Vocontian Basin, Mazagan Plateau, Blake Nose Plateau and NE-Texas	3
1.2.2. Planktic Foraminifera	4
1.2.3. Stable Isotopes	6
2. Materials and Methods	6
<i>2.2. Planktic Foraminifera</i>	6
<i>2.3. Stable Isotopes</i>	7
3. SE-France	7
<i>3.1. Geology and Palaeogeography of SE-France</i>	7
<i>3.2. Lithology and Description of Investigated Sections in SE-France</i>	8
3.2.1. Tarendol	8
3.2.2. Pré Guittard	10
3.2.3. Les Oustaus	10
3.2.4. L'Arboudeysse	10
3.2.5. Col de Palluel I	10
3.2.6. Serre Amande	12
3.2.7. Col de Palluel II	13
3.2.8. Col de Palluel III	13
3.2.9. Col de Palluel IV	14
3.2.10. Col de Palluel V	14
3.2.11. Col de Palluel VI	14
<i>3.3. Results SE-France</i>	15
3.3.1. Preservation of Planktic Foraminifera	15
3.3.2. Planktic Foraminiferal Record	15
3.3.3. First and Last Appearance Datums of Planktic Foraminifera	23
3.3.4. Stable Isotopes	24
<i>3.4. Discussion SE-France</i>	26
3.4.1. Preservation of Planktic Foraminifera of SE-France	26
3.4.2. Isotopic Signatures and Diagenesis	27
3.4.3. Planktic Foraminiferal Record	28
3.4.4. Biostratigraphy of the Late Aptian to Late Albian	31
3.4.5. High resolution Carbon Isotope Stratigraphy of the Late Aptian to Late Albian	34
3.4.6. Aptian/Albian Stage and Albian Substage Boundaries in SE-France	37
<i>Aptian/Albian Stage Boundary</i>	37
<i>Early/Middle Albian Substage Boundary</i>	39
<i>Middle/Late Albian Substage Boundary</i>	40
4. NE-Texas	40
<i>4.1. Geology and Paleogeography of Texas</i>	40
<i>4.2. Lithology and Description of Investigated Sections NE-Texas</i>	42
4.2.1. Marys Creek I	42
4.2.2. Marys Creek II	43
4.2.3. Vickery Blvd.	43
4.2.4. Meacham Field	44

4.2.5. Lancaster Avenue	45
4.2.6. Seminary Drive	45
4.2.7. Interstate 30 & Ben Avenue	45
4.2.8. Interstate 30 & Menzer Street	46
4.2.9. Sunset Oaks	46
4.3. Results NE-Texas	47
4.3.1. Preservation of Planktic Foraminifera	47
4.3.2. Planktic Foraminiferal Record	47
4.3.3. First and Last Appearance Datums of Planktic Foraminifera	53
4.3.4. Stable Isotopes	54
4.4. Discussion NE-Texas	56
4.4.1. Preservation of Planktic Foraminifera	56
4.4.2. Planktic Foraminiferal Record	56
4.4.3. Biostratigraphy of the Middle/Late Albian	59
4.4.4. Isotopic Signature and Diagenesis	61
4.4.5. Correlation of the Carbon Isotope Record of NE-Texas with SE-France	61
4.4.6. Albian/Cenomanian Stage and Albian Substage Boundaries in NE-Texas	61
Middle/Late Albian Substage Boundary	61
Albian/Cenomanian Stage Boundary	62
5. Integrated Stratigraphy of the Late Aptian to Late Albian: Implications for Planktic Foraminiferal Evolution	63
5.1. Comparison of First and Last Appearance Datums of Planktic Foraminifera with an isochronous $d^{13}C$ signal	63
5.2. Paleooceanographic Implications of diachronous FADs of <i>R. appenninica</i> and <i>P. buxtorfi</i> at the Mazagan Plateau (eastern Atlantic)	66
5.3. Palaeoecological Implications for diachronous FADs of <i>R. appenninica</i> and <i>P. buxtorfi</i> at the Blake Nose Plateau (western Atlantic)	68
5.4. Transgression related First Appearance Datums in NE-Texas and Implications for Biostratigraphy	70
6. Conclusions	72
7. Literature	74
8. Taxonomy	84
Appendix	94
Plates	112

1. Introduction

The mid-Cretaceous period, from 121 to 89 m.y., is believed to have been different from our present world in several major aspects (Gradstein et al., 1995). The mid-Cretaceous world was possibly characterised by an extreme “greenhouse” climate as indicated by high atmospheric $p\text{CO}_2$ -level (Barron & Washington, 1985) and a high sea-level (Haq et al., 1988). The climate of this period is estimated to have been with a reduced latitudinal temperature gradient (e.g., Huber et al., 1995) and elevated average temperatures (e.g., Sellwood et al., 1994; Barron et al., 1995).

northern hemisphere and Africa, South America and Antarctica in the southern hemisphere (Fig.1). The northern and southern continents were separated by the large east-west extended Tethys and the small Central Atlantic. Ongoing from the Jurassic the building of the Atlantic continued and a narrow North and South Atlantic were established by the Late Albian (Kennedy & Cooper, 1975). The Tethyan and Atlantic oceans provided a circumglobal oceanic connection. The ocean surface water currents, resulting from general circulation modelling (GCM), indicate stable, westward-

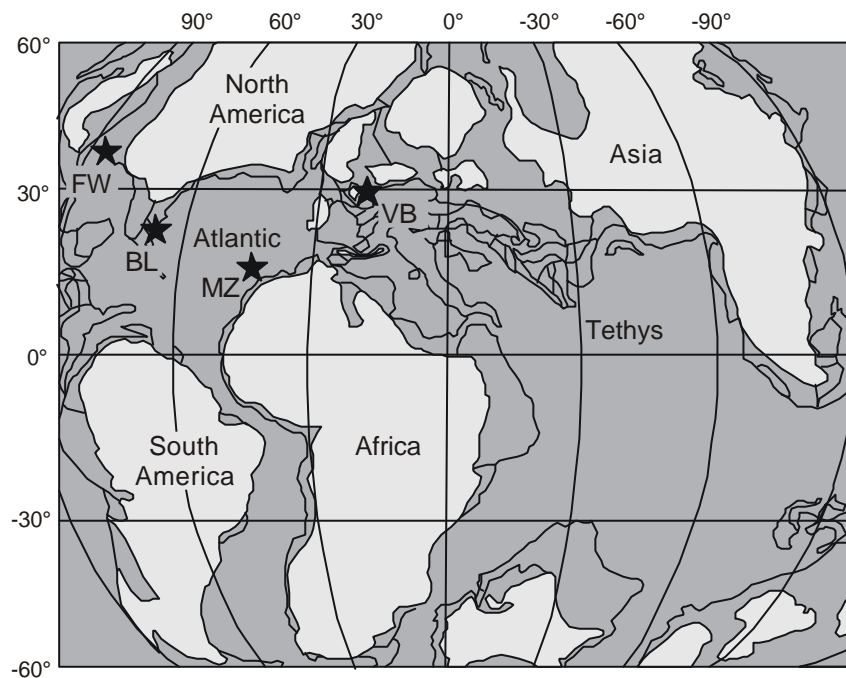


Fig.1: Palaeogeography of the mid-Cretaceous (100 Ma) with high sea-level shorelines (modified after Hay et al., 1999). White areas indicate land. Asterisks mark the study areas in the Vocontian Basin (VB) and in NE-Texas (Fort Worth area = FW) as well as the DSDP Site 545/547 at the Mazagan Plateau (MZ) and ODP Site 1052 at the Blake Nose Plateau (BL).

Based on nannofossil and carbon isotope data, Herrle et al. (2003 b) shows that this “greenhouse” climate was not even as previously thought. The Cretaceous was also a time of major plate movements, which not only changed the palaeogeography, but also influenced the palaeoclimate and the circulation patterns of the oceans. Two major continent complexes dominated the palaeogeographic situation: the North America-Eurasia complex in the

flowing circumglobal currents (Roth, 1986; Barron, 1987). However, Barron & Peterson (1990) and Poulsen et al. (1998) show that the Tethys and the Atlantic were dominated by clockwise gyres (Barron & Peterson, 1990; Poulsen et al., 2001).

The production of new oceanic crust, associated among others with the building of the Atlantic, and the formation of continental flood basalts (Rajmahal, Eastern India; Courtillot et al., 1996)

were enhanced in the Cretaceous and reached a maximum in the Aptian interval (Larson, 1991). The global sea-level was low at the beginning of the Cretaceous but reaches the highest point during the Cenomanian/Turonian (Haq et al., 1988). During the Cretaceous, vast shelf areas were flooded corresponding to globally recognisable transgressions (Hay et al., 1999). The Aptian is one transgressive phase with a mid Aptian break related to a brief sea-level fall. The Albian is characterised by three major flooding events, at or near the substage boundaries.

The extreme oceanic and climatic conditions during the Aptian and Albian advanced the formation of regional and superregional black shales. Superregional black shales appear to be almost synchronous in different marine environments and have therefore been named Oceanic Anoxic Events (OAEs), e.g. OAE 1a (Lower Aptian; Schlanger & Jenkyns, 1976; Arthur et al., 1990; Bralower et al., 1994), OAE 1b (Early Albian; Br  h  ret et al., 1986; Bralower et al., 1993; Erbacher et al., 1999; Herrle et al., 2003 a, b) and OAE 1d (Late Albian; Erbacher et al., 1996; Erbacher & Thurow, 1997; Wilson & Norris, 2001).

The classical method of Cretaceous stratigraphy is biostratigraphy. For example, the twelve Cretaceous stage boundaries are defined by ammonites (Birkelund et al., 1984). The Second International Symposium on Cretaceous Stage Boundaries (1995, Brussels) has encompassed further criteria for stage boundaries, for example microfossil datums, carbon isotope excursions and geomagnetic reversals. But ammonites still dominate the historically founded zonation of the Cretaceous. One major problem of stratigraphy, using Cretaceous ammonites, is that the ammonite fauna of the Aptian and Albian is characterised by a distinct provincialism, which complicates the finding of an international standard marker for the Aptian/Albian stage boundary. This is reflected in problems concerning the correlation of Boreal and Tethyal environments by ammonites (Erba, 1996). For microfossil biostratigraphy mainly planktic foraminifera, calcareous nannofossils, dinoflagellate cysts and calpionellids are used.

Planktic foraminifera become an increasingly important part of marine zooplankton since the beginning of the Cretaceous. Their first and last occurrences are useful datum points for biostratigraphy (e.g. Caron, 1985; Sliter, 1989, 1992; Robaszynski & Caron, 1995). In DSDP and ODP cores, marine microfossils are used for biostratigraphy because of their global distribution and high abundance. Therefore, well dated reference sections, for example DSDP Site 545 (Leckie, 1984) and 547 (Nederbragt et al., 2001) at the Mazagan Plateau and ODP Site 1052 (Bellier & Moullade, 2002) at the Blake Nose Plateau, are available.

Planktic foraminifera exist in sediment cores as well as in land sections, as ammonites are rarely found in cores. Several species of planktic foraminifera can be used as indicators for palaeogeographic and palaeoclimatic changes as well (e.g. Weiss, 1997; Galeotti, 1998; Luciani et al., 2001).

In the past, carbon isotope records have been mainly used for reconstruction of temperature and palaeoproductivity changes in marine environments (e.g. Stoll & Schrag, 2000). The usage of carbon isotope records for stratigraphical purposes exists, but only parts of the Aptian and Albian are discussed or the record is low-resolution (Scholle & Arthur, 1980; Nederbragt et al., 2001). Herrle (2002) established for the first time a high-resolution carbon isotope stratigraphy for the Aptian and lowermost Albian of SE-France.

1.1. Purpose of Investigation

The purpose of this investigation is the revision of the mid-Cretaceous biostratigraphy based on planktic foraminifera and stable isotopes. As time intervals and investigation areas, the Late Aptian to Late Albian in the Western Tethys (Vocontian Basin in SE-France) and the Middle and Late Albian of the Western Atlantic (NE-Texas, area of Fort Worth) are chosen. Main focus is on the following objectives:

- A revised high-resolution biostratigraphy for the Late Aptian to Late Albian of SE-France based on planktic foraminifera.

- A new biostratigraphy for the Middle and Late Albian of NE-Texas.
- Establishment of a carbon isotope stratigraphy for the Late Aptian and Albian of the western Tethys (SE-France)
- Correlation with sections in the eastern (DSDP 545/547, Mazagan Plateau) and western Atlantic (ODP 1052, Blake Nose Plateau; NE-Texas).
- Revision and discussion of the Aptian/Albian stage boundary as well as the Lower/Middle Albian and Middle/Late Albian substage boundaries in SE-France and the Middle/Late Albian and Albian Cenomanian boundary in NE-Texas.
- Assessment of diachronous and synchronous first and last appearances of stratigraphical important planktic foraminifera species.
- Assessment of palaeoecological implications (reconstruction of palaeoceanographic conditions, ocean currents, gateways) of diachronous first occurrences of specialised planktic foraminifera in the mid-Cretaceous.

1.2. State of the Art

1.2.1. Study areas Vocontian Basin, Mazagan Plateau, Blake Nose Plateau and NE-Texas

The Vocontian Basin (“fosse vocontienne”) in SE-France as a sedimentary basin was introduced into the literature by Paquier (1900), who has established this term for the Early Cretaceous pelagic sediments of the South East France Basin in contrast to the marginal facies and the platform carbonates. The basic study of Br  h  ret (1997) gives an overview of the sedimentary, geochemical and palaeontological development of the hemipelagic to pelagic Vocontian Basin in the mid-Cretaceous. Multiproxy studies (foraminifera, calcareous nannofossils; palynomorphs and stable isotopes) about the black shale horizons occurring in the Vocontian Basin are recently used to propose climatic as well as palaeoceanographic models for the mid-Cretaceous period (Herrle et al., 2003 a, b).

The proposed isotope stratigraphy (Herrle, 2002; this thesis) clarifies the connection of special black shale horizons of the Vocontian Basin to superregional Oceanic Anoxic Events (OAEs). The Mazagan Plateau was explored during the Deep Sea Drilling Project (DSDP) 79 in four sites (Winterer & Hinz, 1984). In this thesis, site 545 at the base of the steep Mazagan Escarpment and site 547 in a small subbasin adjacent to the basement block (Leckie, 1984) are used for comparison with the investigated sections in SE-France. Site 545 includes a complete succession of early Late Aptian to Middle Cenomanian and site 547 contains an expanded Late Albian to Late Cenomanian succession. Further sedimentological, geochemical, geophysical information are compiled in the Initial Reports of the Deep Sea Drilling Project, Volume 79 (1984). The Mazagan Plateau is a Jurassic to Early Cretaceous carbonate platform offshore Morocco, overlain by Late Cretaceous to Cenozoic hemipelagic and clastic sediments. To the south, the Mazagan Plateau is an offshore extension of the Moroccan Meseta (Jansa et al., 1984). A detailed description of the geological and palaeogeographical situation is given by Winterer & Hinz (1984).

The Blake Nose Plateau was surveyed in 1998 by the Ocean Drilling Program (ODP) Leg 171B in the western Atlantic. Down the spine of the Blake Nose, a salient on the margin of the Blake Plateau, five sites (1049-1053) were drilled. In this thesis, site 1052 at the top of the spine, recovering the Aptian to Turonian (Bellier & Moullade, 2002), is used for correlation and palaeoceanographic reconstruction. Further sedimentological, geochemical, geophysical information are compiled in the Proceedings of the Ocean Drilling Program, Scientific Results Volume 171B (1999). The Blake Nose represents a Jurassic to Lower Cretaceous carbonate platform with buried reef build-ups at the landward end of the Blake Nose, overlain by Middle Cretaceous and younger sediments (claystone and carbonate ooze; Norris et al., 2001).

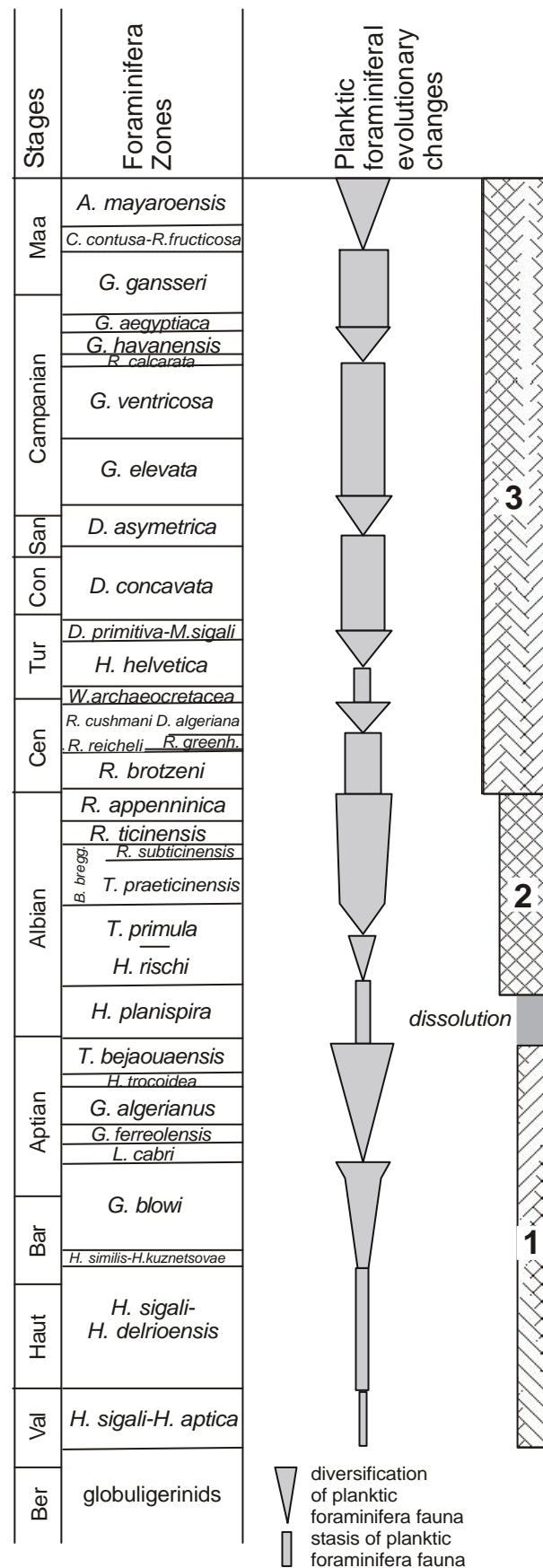
The early history of geological research in Texas has been summarised by Roemer (1849) and Hill (1887) but none of the two has dealt directly

with the Cretaceous of the Fort Worth area. Studies by Lozo (1944), Perkins & Albritton (1955) include the Fort Worth area and focus on stratigraphic purposes. Perkins (1960) was the first giving an overview of the mid-Cretaceous sections in the Fort Worth area and their macrofossil content. The mid-Cretaceous sections in the northern part of the East Texas Embayment are characterised by the shallow marine environment of the Comanche carbonate platform and the long term and short term cyclic sedimentation (transgression and regression of the Gulf of Mexico onto the shelf). The cyclic sediment deposition of NE-Texas has been used in recent papers to correlate and compare sea-level curves and events of the Gulf Coast, NE-Texas, and south eastern Arabia (Immenhauser & Scott, 1999; Scott et al., 2000). For geological and palaeogeographical details about the East Texas Embayment and the Fort Worth area see Chapter 4.1.

1.2.2. Planktic Foraminifera

The first planktic foraminifera have been described from the Middle Jurassic (Bajocian), but play no significant role in marine life until the mid-Cretaceous (Leckie, 1989). Three major adaptive radiations in the evolution of planktic foraminifera can be recognised in the Cretaceous record (Wonders, 1980; Premoli-Silva & Sliter, 1999; Fig. 2). The threefold pattern, from the Lower Valanginian to the Late Aptian, from the Aptian/Albian boundary to the Late Albian and finally to the end of the Cretaceous, is characterised by alternating phases of diversification, stasis, extinction and faunal turnover (Premoli-Silva & Sliter, 1999; Fig. 2).

Fig. 2: Planktic foraminiferal evolutionary changes through the Cretaceous after Premoli-Silva & Sliter (1999) and references therein. The three cross-hatched bars (1, 2 and 3) show the threefold evolutionary pattern of planktic foraminifera in the Cretaceous. The grey shaded bars and arrows a more detailed version of the evolutionary changes. The dark grey shaded area at the Aptian/Albian boundary marks an interval of stasis or enhanced dissolution.



The first continuously increasing diversification extends with a duration of 22 m.y. from the Lower Valanginian to the Late Aptian and is not interrupted by a turnover near the Livello Selli (=OAE 1a; Premoli-Silva & Sliter, 1999) as proposed by Coccioni et al. (1992) and Erba & Premoli-Silva (1994). The Aptian/Albian boundary interval is marked by a phase of stasis or enhanced carbonate dissolution (Fig.2). Leckie et al. (2002) proposed a link between the greatest turnover of planktic foraminifera near the Aptian/Albian boundary and the formation of black shales in this time interval. Both may be triggered among others by submarine volcanism (sea water pH, reduced carbon availability; Leckie et al., 2002). The second radiation interval (Early Albian to Late Albian) is also characterised by increasing diversification but in half of the time (12 m.y.; Premoli-Silva & Sliter, 1999; Fig. 2). The third interval until the end of the Cretaceous differs from the first two. Short periods of rapid diversification and turnover are separated by longer periods of stasis (Premoli-Silva & Sliter, 1999; Fig. 2). Due to the rapid evolution of planktic foraminifera this zooplankton is a reliable tool for biostratigraphy in Cretaceous time. Phases of diversification, like the Late Albian, provide a wide range of possible biostratigraphic horizons. In contrast, phases of stasis like the Aptian/Albian boundary interval with lacking evolution of planktic foraminifera or probably enhanced dissolution complicate the definition of the stage boundary by planktic foraminifera. Throughout the Cretaceous the species richness increased and morphotypes grew more complex (Caron & Homewood, 1983). From the beginning (Jurassic to Albian) the foraminiferal fauna was characterised by small, primitive, globular morphotypes (r-selected; Caron & Homewood, 1983) who have lived in surface waters (Hart & Bailey, 1979; Leckie, 1987; Hart, 1999; Premoli-Silva & Sliter, 1999). In the Late Albian, more advanced morphotypes (k-selected) with a more complicated umbilical system and an additional keel evolved (Wonders, 1980; Caron & Homewood, 1983) and colonised the deeper water (Hart & Bailey, 1979; Leckie, 1987; Hart, 1999).

Isotopic data from Cretaceous planktic foraminifera (e.g. Huber et al., 1995; Price et al., 1998; Wilson & Norris, 2001; Price & Hart, 2002) support this model of depth stratification of Cretaceous planktic foraminifera.

In the Cretaceous, latitudinal differentiation in the faunal composition within the planktic foraminiferal associations can be recognised as well (Haig, 1979; Premoli-Silva & Sliter, 1999). Two provinces, Boreal and Tethys (tropical), separated by a temperate transition zone, can be distinguished. This picture is mirrored to the southern hemisphere (tethyal/tropical-transition-austral). Every province has a characteristic faunal association. The transition zones are marked by a mixture of boreal and tethyal faunal elements. The latitudinally limited distribution of planktic foraminifera complicates the correlation of planktic foraminiferal zones of high and low latitude sections.

For 40-50 years, planktic foraminifera are used as biostratigraphical markers. The steady revision of existing taxa and the description of new species made it possible to modernise continuously the stratigraphical zonation. The first zonation for the mid-Cretaceous (Renz, 1936; Gandolfi, 1942; Bolli, 1945) used planktic foraminifera (*Globotruncanidae*) to date Alpine-Mediterranean sections without proposing zones. First local zonation was established for North African (Sigal, 1952, 1955) and Caribbean (Bolli, 1959) sites. More generalised zonation for the Cretaceous was proposed about 10 years later by van Hinte (1965) and Sigal (1967). The results of Moullade (1966), Caron (1985), Sliter (1989, 1992) and Robaszynski & Caron (1995) among others allowed a refinement of this zonation. This zonation based mainly on first and last appearance datums (FAD and LAD) of planktic foraminifera. Generally, Haynes (1981) pointed out that extinctions related to recent and Pleistocene planktic foraminifera can be locally variable, and according to Blow (1970) LADs show a considerable degree of in-built diachroneity. Therefore, extinctions should be avoided as datum horizon (Blow, 1970; Jenkins, 1971 b). First appearances may also be diachronous (Jenkins, 1971a) as, for example, in the Tertiary

Globoquadrina dehiscens, and treated with caution as biostratigraphic horizon.

1.2.3. Stable Isotopes

The limited use of classical biostratigraphy tools, due to migration, biogeographical endemism (ammonites) and evolutionary crisis (planktic foraminifera) requires an additional, independent stratigraphic control. The possible correlation of carbon isotope records from different facies and environmental conditions makes the stable isotope record (carbon) a reliable tool for stratigraphy.

Different biotic and atmospheric mechanisms affect the distribution of carbon isotopes (^{13}C) in the oceans. The most important biotic mechanism is the preference of surface water organisms and land plants to use ^{12}C for the build-up of organic material. A high bioproductivity in the ocean surface water leads to an enrichment of ^{13}C in this surface water (the lighter ^{12}C is bound to the organic material of organisms and plants). Arthur et al. (1985) assume a relationship between sediment erosion and decreasing $\delta^{13}\text{C}$ values and data from the Late Cenomanian to Early Coniacian support the link between sea-level changes and fluctuation in the $\delta^{13}\text{C}$ record (Voigt & Hilbrecht, 1997). The ^{12}C input into the water, could be forced by erosion of organic matter, stored in sediments before (Voigt & Hilbrecht, 1997). Due to this mechanism, a decrease of $\delta^{13}\text{C}$ values occurs during intervals of sediment erosion (sea-level fall) and an increase of $\delta^{13}\text{C}$ values during sediment accumulation (sea-level rise; Hilbrecht & Hoefs, 1986). The stratification of the water column or palaeocirculation may be another controlling factor of fluctuation in the carbon isotope record (Weissert et al., 1979). When the circulation between surface water and intermediate/bottom water is sluggish, the surface water is enriched in $\delta^{13}\text{C}$, because of the missing dilution with $\delta^{13}\text{C}$ depleted intermediate/bottom water. The intermediate/bottom water depletion is caused by the oxygen consuming and CO_2 releasing decomposition of organic material, setting through the water column. Therefore, enhanced mixing of the

water column would lower the $\delta^{13}\text{C}$ content in the photic zone.

The atmospheric carbon circulation (CO_2 exchange of atmosphere and ocean) depending on sea surface temperature and CO_2 exchange rate influences the variation of $\delta^{13}\text{C}$ in the ocean as well. A very high CO_2 concentration in the atmosphere due to enhanced volcanism, as estimated for the mid-Cretaceous (Larson, 1991) may have influenced the $\delta^{13}\text{C}$ signal (Arthur et al., 1985). Methane gas is also under discussion as having a great effect on $\delta^{13}\text{C}$ values of the atmosphere and the ocean (Jahren & Arens, 1998).

2. Materials and Methods

2.2 Planktic Foraminifera

For biostratigraphic and faunal investigations of the SE-France sections, 526 foraminiferal samples were studied. Additionally, 94 samples were investigated from the section in NE-Texas. The foraminifera samples were prepared using the standard methods (Wick, 1947; Wissig & Herrig, 1999) to receive cleaner foraminifera tests. The raw material was reduced to small pieces, dried and weighed. Subsequently, the material was soaked with 100 ml hydrogenperoxid (3%) for one to 24 hrs, washed over a 63 μm sieve and dried for approximately 24 hrs at 50°C. Thereafter, the sample was soaked in 5-10 ml of ethanol-tenside (REWOQUAD) mixture, left again for 24 to 72 hrs and washed over a 63 μm sieve to remove the remaining sediment. Dry residues were sieved into three fractions of 63-125, 125-250 and 250-500 μm . Planktic foraminifera were determined/classified and counted under a Zeiss Stemi DRC „Binokular” at 12.8x to 128x magnification. A total of 150 to 300 specimens of each fraction were counted. If necessary, samples were splitted with a microsplitter in smaller aliquots and recalculated. The planktic foraminifera data is plotted in order of the first appearance datum (FAD) in a range chart. Faunal assemblages are referred as individuals per gram dried sediment and percentages. The diversity is given by the number of species as additional information.

2.3. Stable Isotopes

A total of 518 bulk rock samples from SE-France and 165 from NE-Texas were taken in a sampling distance between 0.1 and 1 m. The samples have been taken from freshly cut rock pieces and homogenised in an agate mortar. Isotopic measurements were conducted with a Finnigan MAT 251 mass spectrometer at the „Leibniz-Labor für Altersbestimmungen und Isotopenforschung” in Kiel (Germany). The mass spectrometer is coupled on-line to the Carbo-Kiel device I for automated CO₂ preparation from carbonate samples for isotopic analysis. Precision average is 0.02 ‰ for carbon and 0.03 ‰ for oxygen, adjusted to the Pee Dee Belemnite standard (PDB). A part of 56 samples were measured by A. Bornemann with a Finnigan delta S gas mass spectrometer at the “Isotopenlabor” of the Ruhr University Bochum (Bochum). The precision average here for carbon is 0.1 ‰, adjusted to PDB. The carbon and oxygen isotope ratios (R) are expressed on a per mil (‰) basis relative to the Pee Dee Belemnite standard (PDB):

$$\delta_{\text{sample}} = (R_{\text{sample}} - R_{\text{PDB}} / R_{\text{PDB}}) \times 1000$$

$$R = (^{13}\text{C}/^{12}\text{C}) \text{ or } (^{18}\text{O}/^{16}\text{O})$$

δ_{sample} (‰) represents the parts per thousand difference (per mil) between the sample (R_{sample}) ratio and that of the international PDB standard carbonate (R_{PDB}). PDB refers to a selected belemnite from the Cretaceous Pee Dee Formation in South Carolina, U.S.A.

3. SE-France

3.1. Geology and Palaeogeography of SE-France

The geology of SE-France is characterised by the arched mountain chains of the Western Alps. The Western Alps are divided in two major parts, the Internal and the External Zone. The Internal Zone represents the Penninic napes and the Austro-Alpine. The External Zone comprises a

parautochthonous (Ultra-Dauphiné, Ultra-Helvetic) and an autochthonous part (Dauphiné, Helvetic) (Lorenz, 1980; Fig. 3). The whole External Zone was part of the European margin of the Mesozoic Tethys ocean (Arnaud & Lemoine, 1993). Because of the more marginal position of the Dauphiné at the realm of the Alpine geosyncline, this unit is less deformed than the Ultra-Dauphiné (Gwinner, 1971). A second major structure in SE-France is the South-East France Basin (SFB). The SFB represents a Mesozoic sedimentary basin widespread from the Massif Central in the west to the External Zone (Dauphiné) of the Alps in the east and to the Alpine-folded Pyrenean-Provence belt in the south (Arnaud & Lemoine, 1993). The study area in SE-France, the Vocontian Basin, belongs to the Dauphiné part of the SFB.

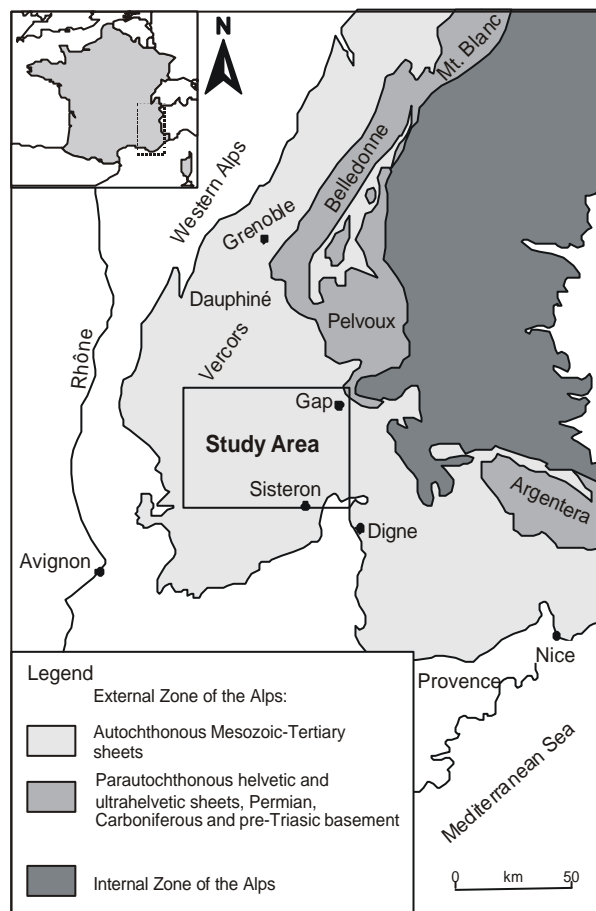


Fig. 3: Geological map of SE-France (modified after Lorenz, 1980) including the study area (Vocontian Basin).

During the Late Jurassic and Early Cretaceous the epicontinental Vocontian basin was a part of the SFB and was located at a palaeolatitude of 25° to 30° N (Savostin et al., 1986; Voigt, 1996; Hay et al., 1999). From the Upper Hauterivian to the Lower Aptian this basin was surrounded by the Urgonian carbonate platforms, the Vercors Platform in the north and the Provence Platform in the south (Arnaud-Vaneau & Arnaud, 1990, 1991). In the Late Aptian to Early Albian these carbonate platforms were drowned (Arnaud & Lemoine, 1993; Weissert et al., 1998). The shallow-water carbonates of the surrounding and later drowned platforms and slopes intercalated with the hemipelagic facies in the centre of the basin (Fig. 4). To the east, the Vocontian basin was open to the Tethyan Ocean (Curnelle & Dubois, 1986; Arnaud & Lemoine, 1993).

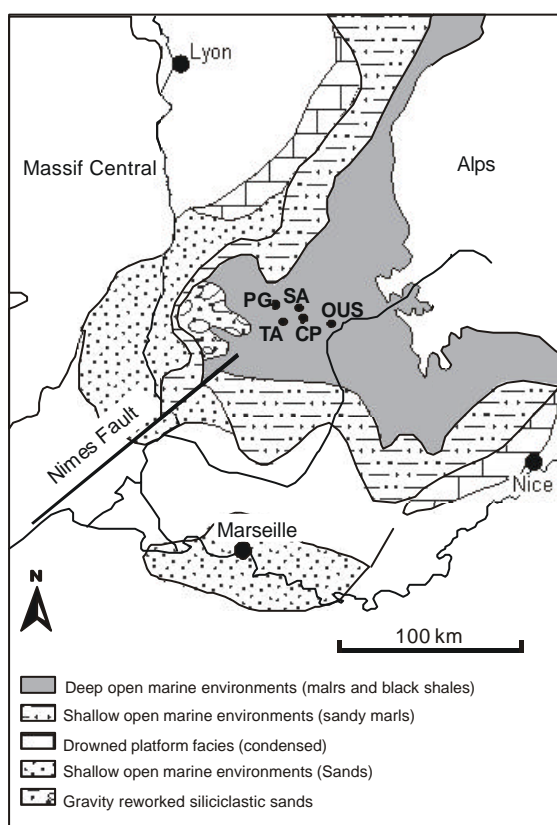


Fig. 4: Palaeogeographic map of the Vocontian Basin during the Late-Aptian and Albian (after Arnaud & Lemoine, 1993) showing the location of studied sections (TA=Tarendol, PG=Pré Guittard, OUS=Les Oustaus, SA=Serre Amande, CP=Col de Palluel with l'Arboudeysse).

The connection is now covered by the thrust fault system of the Penninic Alps (Arnaud & Lemoine, 1993). During the Aptian/Albian the Marnes Bleues (Flandrin, 1963), an up to 750 m thick sediment succession of alternating marl- and limestones with intercalated black shale horizons, were deposited in the Vocontian Basin (Bréhéret, 1988, 1997). The succession was occasionally interrupted by turbidites and slumps (Bréhéret, 1997). Based on faunal and floral data, the palaeo-water depth of the Vocontian Basin is estimated within a range of several hundred metres (Wilpshaar & Leereveld, 1994; Wilpshaar et al., 1997). In contrast, Cotillon & Rio (1984) recommend a palaeo-water-depth of 2000 m for the Vocontian Basin.

3.2 Lithology and Description of Investigated Sections in SE-France

The Late Aptian to Late Albian in SE-France was studied in 11 sections. A total of 909 samples were collected in two field trips in 2000 (Fig. 5). This includes the sections Tarendol, Pré Guittard, Les Oustaus, l'Arboudeysse, Col de Palluel I, Serre Amande and Col de Palluel II-IV. The different sections are correlated with basinwide lithostratigraphic marker horizons described by Bréhéret (1997). The average sample distance is between 0.05 m to 0.60 m. All grid references in the following refer to the Lambert III grid in the Série Bleu maps of the Institute Geographique National (IGN France). A road map of SE-France with the location of these sections is given in Appendix 1.

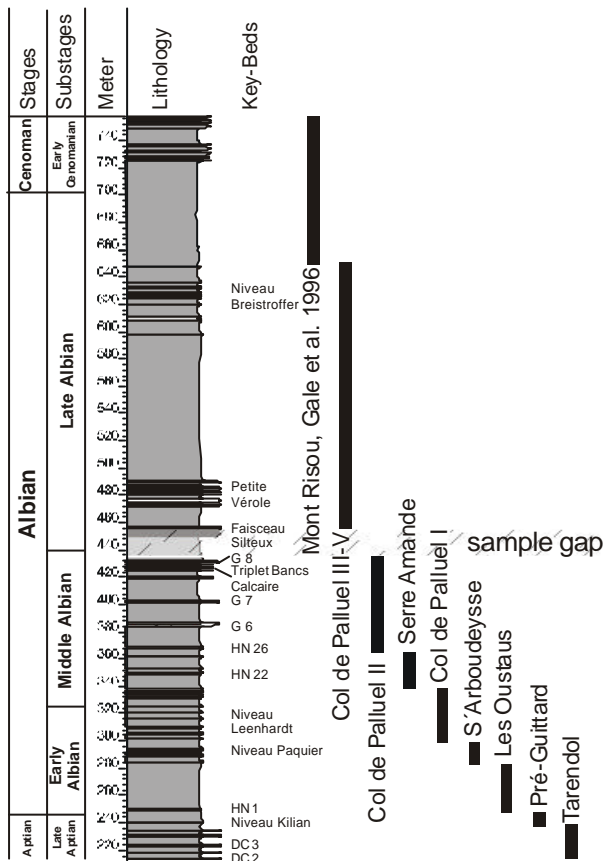
3.2.1. Tarendol

Location and grid reference: The section of Tarendol is situated about 2 km southwest of the village Tarendol, on the eastern side of the St. Etienne hill (Fig. 5). TM 25 Rémuzat, No. 3139 Est, co-ordinates X: 840 200, Y: 3232 300.

Stratigraphic range: Late Aptian.

Lithology: The whole exposure at Tarendol is 47 m thick and comprises an interval from 2 m below the Faisceau Fromaget 3 to the Délits Calcaires 4. In this study the 24 m thick succession from the Délits Calcaires 2 (DC 2) to the Délits Calcaires 4 (DC 4) is investigated.

SE-France



Legend

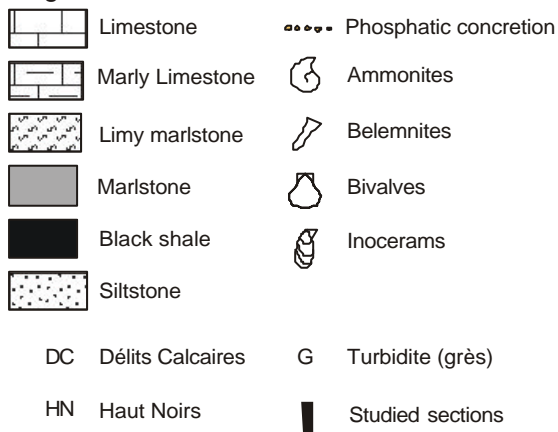
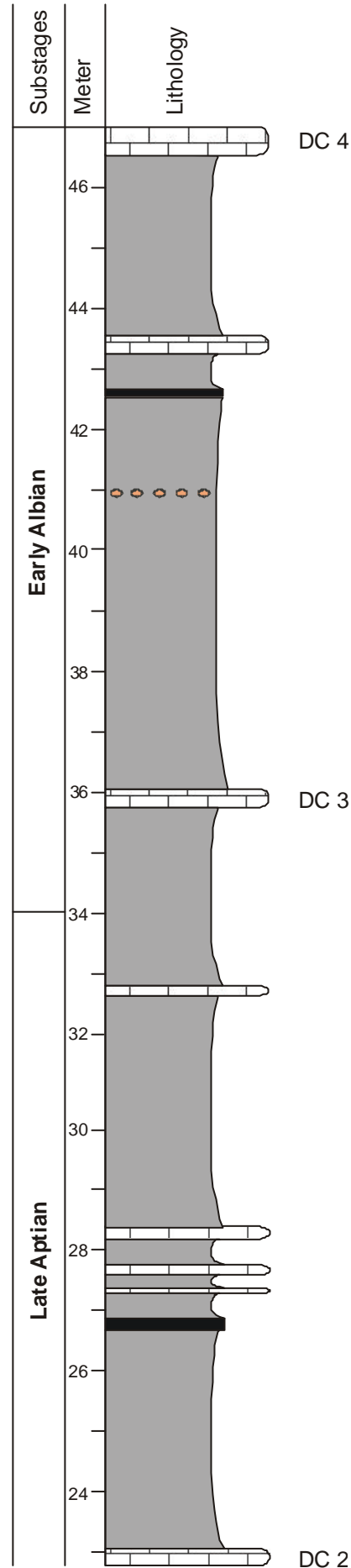


Fig. 5: Overview of the investigated sections and their stratigraphical ranges in SE-France

Fig. 6: Schematic lithological column of the Pré Guittard section. A detailed lithological column with sample distribution is given in Appendix 3. For lithological explanations and abbreviations see Fig. 5.



This interval consists of marlstone intercalated by limestone, marly limestone and black shale. The three most prominent limestone horizons are the Délits Calcaires 2, 3 and 4 (DC 2-4; Bréhéret, 1997; Fig. 6). They are basinwide distributed and partly rich in aucellinids.

3.2.2. Pré Guittard

Location and grid reference: The succession is located about 800 m southeast of Pré Guittard, at the south-eastern-flank of the Serre Sablon (Fig. 5). TM 25 Dieulefit, No. 3138 Ouest, co-ordinates X: 836 800, Y: 3248 825.

Stratigraphic range: Late Aptian.

Lithology: The 8 m thick section of Pré Guittard exposes an interval from the Délits Calcaires 4 (DC 4) to a horizon two metres above the Niveau Kilian. This interval consists of pale and dark marlstone interrupted by the 74 cm thick Niveau Kilian black shale, named by Bréhéret et al. (1986; Fig. 7). The black shale of the Niveau Kilian can be probably correlated with the Monte Nerone black shale horizon in the Umbria Marche Basin, Italy (Erbacher, 1994).

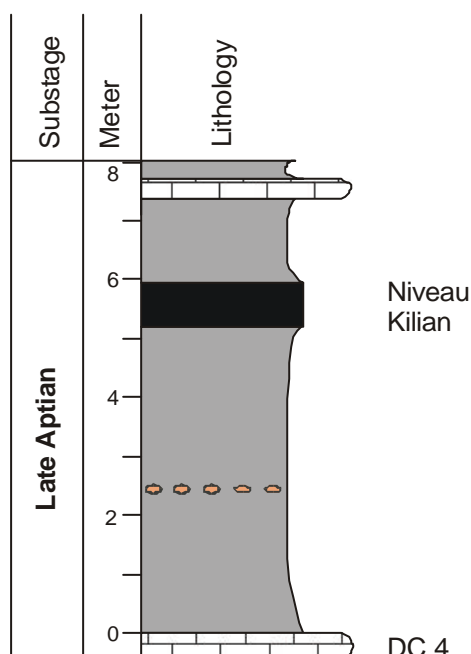


Fig. 7: Schematic lithological column of the Pré Guittard section. A detailed lithological column with sample distribution is given in Appendix 4. For lithological explanations and abbreviations see Fig. 5.

3.2.3. Les Oustaus

Location and grid reference: The succession can be found about 3 km southwest of Esparron and about 500 m northeast of the hill Les Oustaus (Fig. 5). TM 25 Serres/ Veynes, No. 3338 Ouest, co-ordinates X: 887 850, Y: 3242 775.

Stratigraphic range: Late Aptian to Early Albian.

Lithology: The 39 m thick section of Les Oustaus comprises the succession from 2 m above the Niveau Kilian to the Haute Noir 7 (HN 7). This interval consists of dark marlstone with several intercalated black shales known as Haute Noir 1 to 7 (HN 1-7; Bréhéret, 1997; Fig 8). Also several phosphatic concretion horizons are inserted into the marlstone succession.

3.2.4. L'Arboudeysse

Location and grid reference: The outcrop is situated 700 m southwest of l'Arboudeysse, about 900 m east of the Col de Palluel (Fig. 5). TM 25 Rosans, No. 3239 Ouest, co-ordinates X: 854 850 Y: 3238 825.

Stratigraphic range: Early Albian.

Lithology: The 14 m thick section of l'Arboudeysse starts with the Haute Noir 7 (HN 7) and ends 4 m above the Niveau Paquier. This interval consists of marlstone interrupted by the black shale layers Haute Noir 7, Haute Noir 8 (HN 8; Bréhéret, 1997) and the Niveau Paquier (Bréhéret, 1983; Fig. 9). The Niveau Paquier black shale is developed as paper shale and in the upper part interrupted by a 3 cm thick carbonate rich layer, called "à-bed" (Bréhéret, 1983). Lymeriellids are abundant in the Niveau Paquier. The black shale of the Niveau Paquier is supposed to be superregionally distributed (Bréhéret, 1986) and equivalent to the Oceanic Anoxic Event 1b (OAE 1b), recognised in several ODP/DSDP sites in the Atlantic (Bréhéret, 1997; Erbacher et al., 2001; Herrle, 2002).

3.2.5. Col de Palluel I

Location and grid reference: The section is situated 700 m northeast of the Col de Palluel. (Fig. 5). TM 25 Rosans, No. 3239 Ouest, co-ordinates X: 854 225 Y: 3239 300.

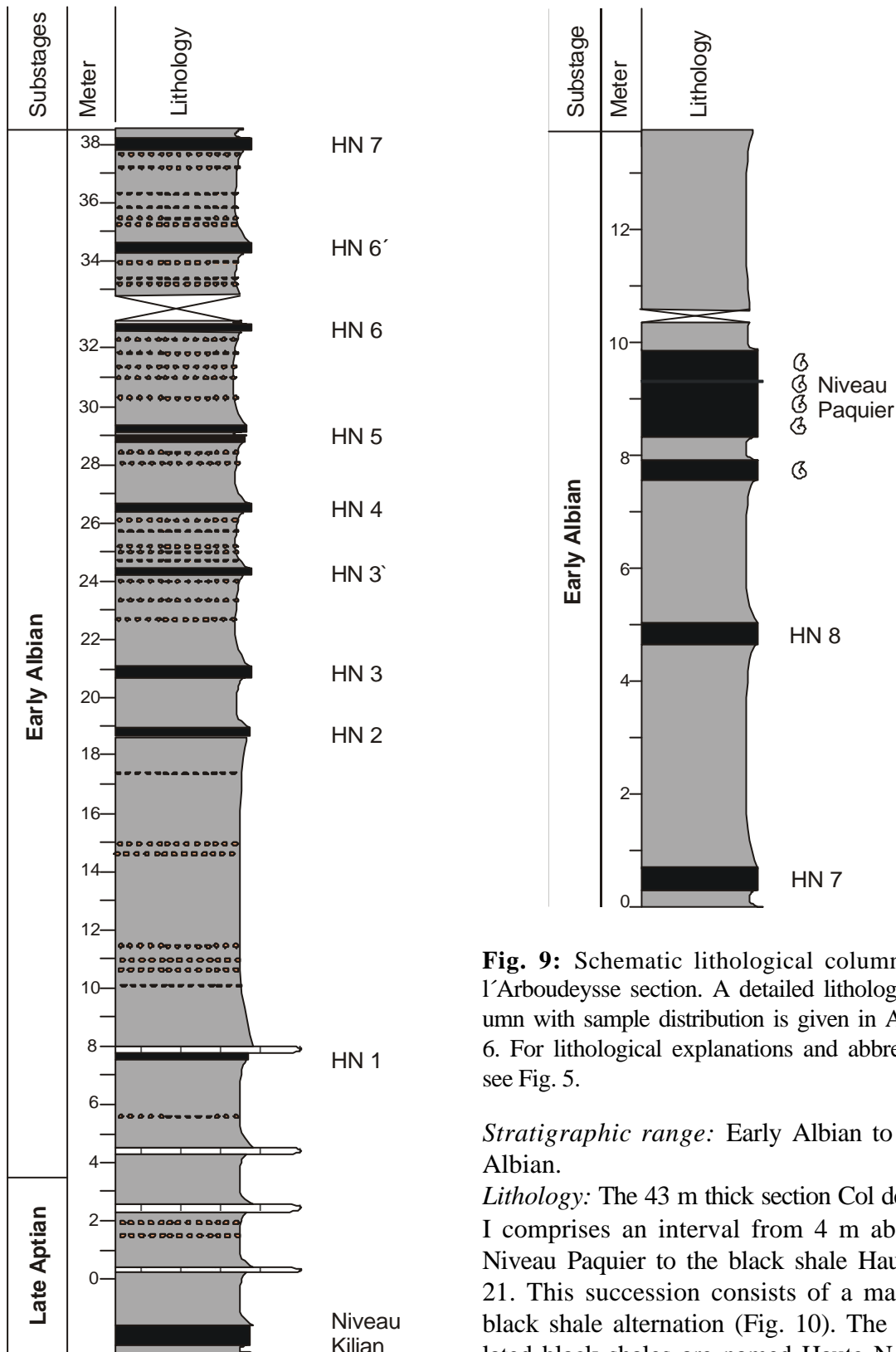


Fig. 8: Schematic lithological column of the Les Oustaus section. A detailed lithological column with sample distribution is given in Appendix 5. For lithological explanations and abbreviations see Fig. 5.

Fig. 9: Schematic lithological column of the l'Arboudeysse section. A detailed lithological column with sample distribution is given in Appendix 6. For lithological explanations and abbreviations see Fig. 5.

Stratigraphic range: Early Albian to Middle Albian.

Lithology: The 43 m thick section Col de Palluel I comprises an interval from 4 m above the Niveau Paquier to the black shale Haute Noir 21. This succession consists of a marlstone-black shale alternation (Fig. 10). The intercalated black shales are named Haute Noire 13-21 (HN 13-21; Bréhéret, 1997), the most prominent black shale is the HN 17, called Niveau Leenhardt, with a basinwide distribution (Bréhéret et al., 1986). Within the black shales of the Niveau Leenhardt inoceramids (*Birostrina concentrica*) are common.

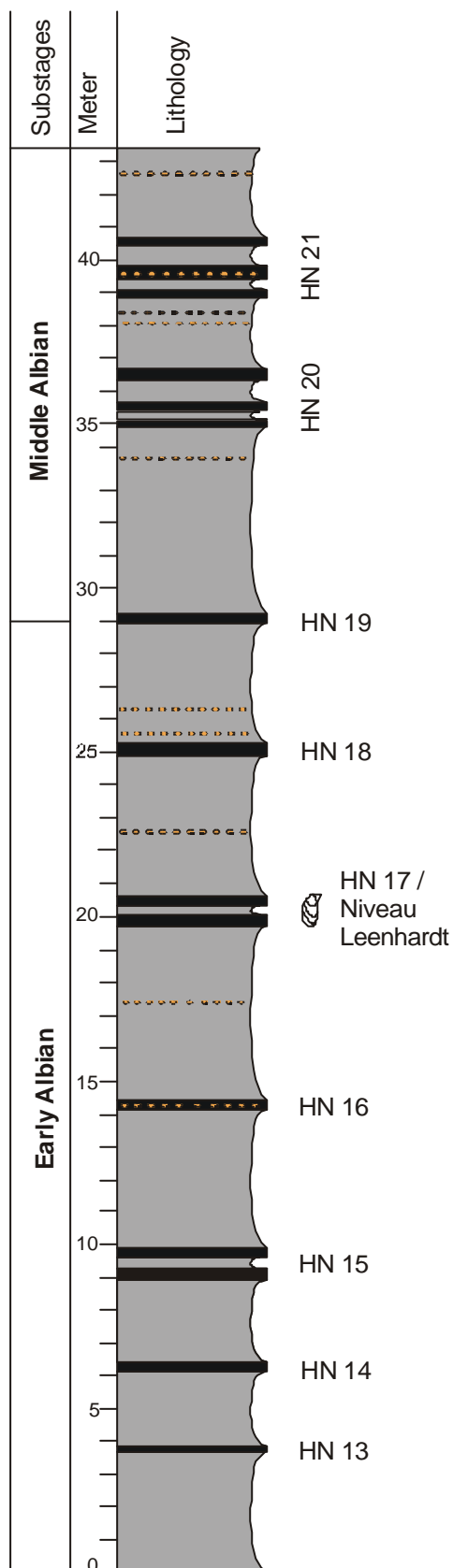


Fig. 10: Schematic lithological column of the Col de Palluel I section. A detailed lithological column with sample distribution is given in Appendix 7. For lithological explanations and abbreviations see Fig. 5.

3.2.6. Serre Amande

Location and grid reference: The section is located about 250 m west of Bruis, at the north-flank of the hill Serre Amande (Fig. 5). TM 25 Luc-en-Diois, No. 3238 Ouest, co-ordinates X: 852 427, Y: 3245 595

Stratigraphic range: Middle Albian.

Lithology: The 28 m thick section of Serre Amande starts with the double black shale of Haute Noir 21 and ends with the black shale triplet of Haute Noir 25. This succession consists of a marlstone-black shale alternation (Fig. 11). The black shales are named Haute Noir 21 to 25 (HN 21-25) after Br  heret (1997). These black shales are characterised by phosphatic or pyritic nodules.

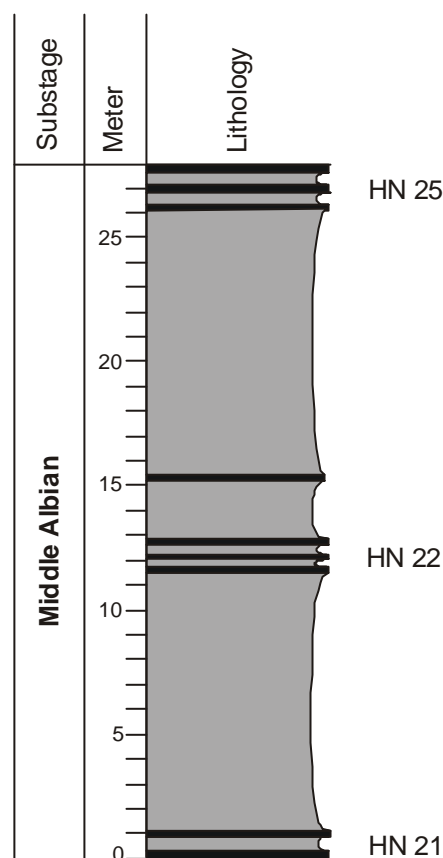


Fig. 11: Schematic lithological column of the Serre Amande section. A detailed lithological column with sample distribution is given in Appendix 8. For lithological explanations and abbreviations see Fig. 5.

3.2.7. Col de Palluel II

Location and grid reference: Roadcut north of the D994 between the Col de Palluel and Moydans, about 150 m west of the Col de Palluel (Fig. 5). TM 25 Rosans, No. 3239 Ouest, co-ordinates X: 853 585, Y: 3238 780.

Stratigraphic range: Middle Albian.

Lithology: The 72 m thick section of Col de Palluel II comprises a succession from Haute Noir 26 (HN 26) to the sandstone layer Grés 8 (G 8). This interval consists of marlstone intercalated by sandy turbidites, numerous silty-sandy dykes and in the top by a triplet of limestone layers. The sandy turbidites are named Grés 6, 7 and 8 (G 6, 7 and 8) and the three limestone layers Triplet Bancs Calcaire (Bréhéret, 1997; Fig. 12). The 2 m thick G 6 in the lower part of the section is characterised by glauconite as well as bivalves and belemnites at its base. Between G 7 and the Triplet Bancs Calcaire ammonites and inoceramids (*Birostrina*; Bréhéret, 1997) are common.

Fig. 12: →

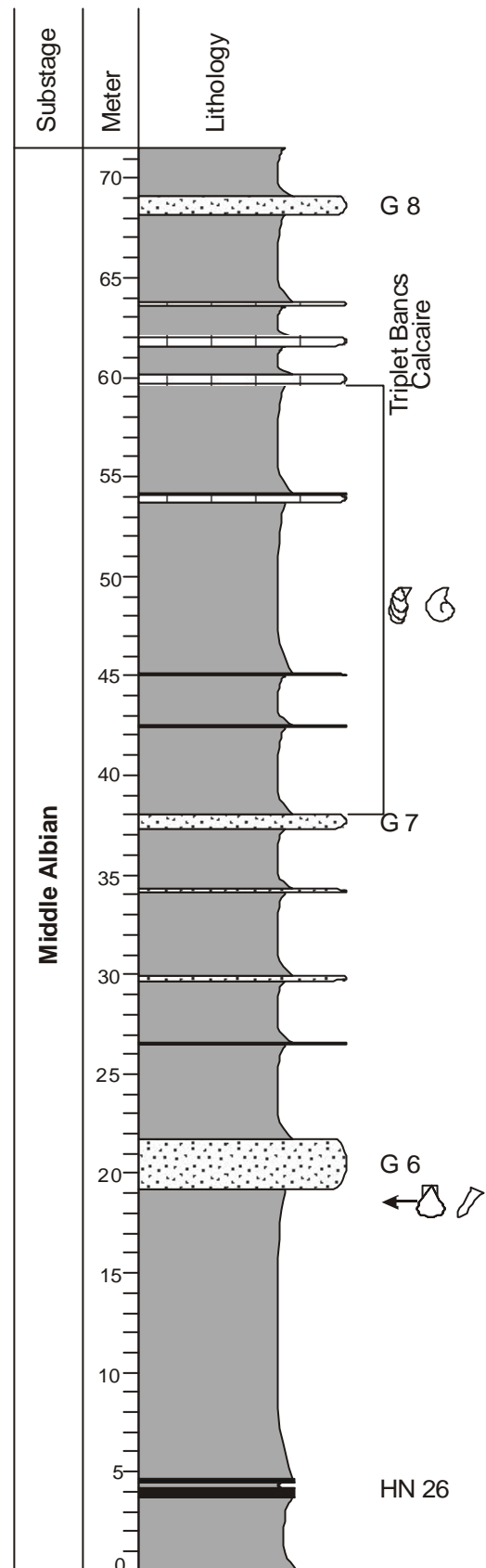
Schematic lithological column of the Col de Palluel II section. A detailed lithological column with sample distribution is given in Appendix 9. For lithological explanations and abbreviations see Fig. 5.

3.2.8. Col de Palluel III

Location and grid reference: This outcrop is located 300 m southwest of the Col de Palluel (south of the road D994) at the northern hillside of the Mont Risou (Fig. 5). TM 25 Rosans, No. 3239 Ouest, co-ordinates X: 853 675, Y: 3228 470.

Stratigraphic range: Late Albian.

Lithology: The section Col de Palluel III that is about 17 m thick, reaches from the topmost layers of the Faisceau Silteux to 6 m below the Petite Vérole. The section starts with a 3.5 m thick succession of marlstone intercalated with 10 to 20 cm thick glauconitic sandstones (Fig. 13). This part represents the top of the Faisceau Silteux (Bréhéret & Delamette, 1987). It is followed by a marlstone succession intercalated by two thin limestone layers.



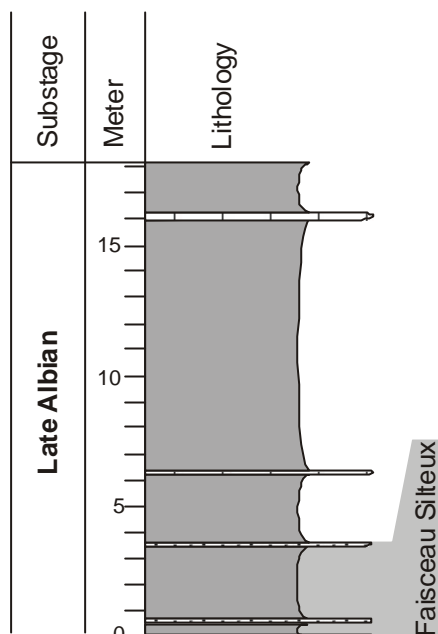


Fig. 13: Schematic lithological column of the Col de Palluel III section. A detailed lithological column with sample distribution is given in Appendix 10. For lithological explanations and abbreviations see Fig. 5.

3.2.9. Col de Palluel IV

Location and grid reference: This outcrop is located 300 m southwest of the Col de Palluel (south of the road D994) at the northern hillside of the Mont Risou a few metres above Col de Palluel III (Fig. 5). TM 25 Rosans, No. 3239 Ouest, co-ordinates X: 853 675, Y: 3228 470.

Stratigraphic range: Late Albian.

Lithology: This 14 m thick section at the Col de Palluel IV comprises the interval from 6 m below to 6 m above the Petite Vérole. The whole succession consists of a marlstone to marly limestone alternation. At about 6.5 m several silty and limy marlstones are intercalated. These glauconitic, bioturbated (*Chondrites*) layers of the Petite Vérole (Bréhéret & Delamette, 1987; Fig. 14) represent an interception in sedimentation (Bréhéret, 1997). The Petite Vérole is characterised by a high abundance of large bivalves (*Pinna*; Bréhéret, 1997), inoceramids (*Birostrina sulcata*) and ammonites (*Puzosia* sp.).

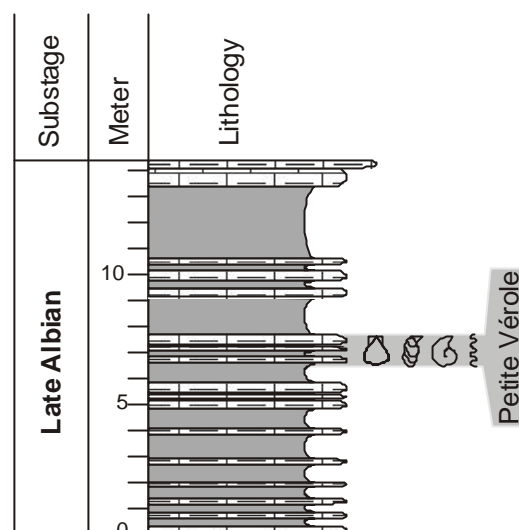


Fig. 14: Schematic lithological column of the Col de Palluel IV section. A detailed lithological column with sample distribution is given in Appendix 11. For lithological explanations and abbreviations see Fig. 5.

3.2.10. Col de Palluel V

Location and grid reference: This outcrop is located 300 m southwest of the Col de Palluel (south of the road D994) at the northern hillside of the Mont Risou a few metres above Col de Palluel IV (Fig. 5). TM 25 Rosans, No. 3239 Ouest, co-ordinates X: 853 675, Y: 3228 470.

Stratigraphic range: Late Albian.

Lithology: The 87 m thick section at the Col de Palluel V starts about 8 m above the Petite Vérole and ends about 48 m below the Niveau Breistroffer. This interval comprises an alternation of marl- and limestone (Fig. 15). The limestone layers have an average thickness of 15 to 40 cm. At the base of this succession bivalves (*Pecten*, Bréhéret, 1997) and various ammonites (*Puzosia mayoriana*) can be found.

3.2.11. Col de Palluel VI

Location and grid reference: This outcrop is located 300 m southwest of the Col de Palluel (south of the road D994) at the northern hillside of the Mont Risou a few metres above Col de Palluel V (Fig. 5). This part of the whole Col de Palluel section is visible from the road D994. TM 25 Rosans, No. 3239 Ouest, co-ordinates X: 853 787, Y: 3228 360

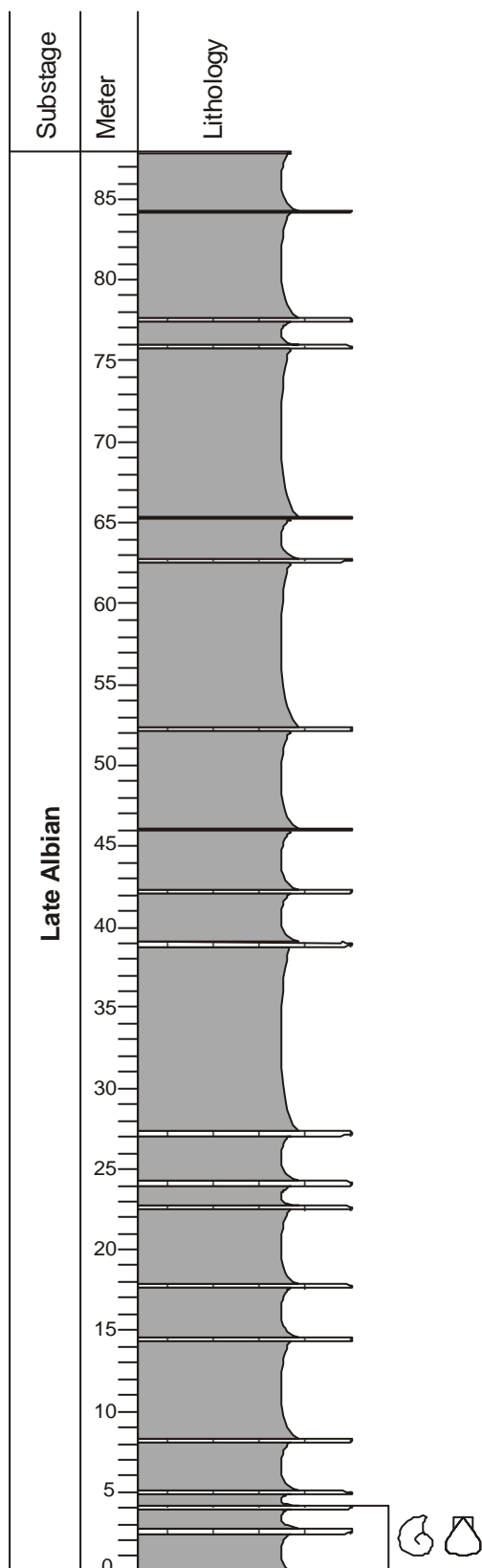


Fig. 15: Schematic lithological column of the Col de Palluel V section. A detailed lithological column with sample distribution is given in Appendix 12. For lithological explanations and abbreviations see Fig. 5.

Stratigraphic range: Late Albian.

Lithology: This 77 m thick section at the Col de Palluel VI starts 48 m below the Niveau Breistroffer and ends 23 m above it. This section consists of marlstone, marly limestone and black shale horizons (Fig. 16). The whole succession can be divided into three parts: the lower part that reaches until 22 m above the base is characterised by an alternation of marlstone and marly limestone. The second part up to 46 m above the base consists of marlstone intercalated by a few marly limestone and the first black shale horizons. The third part up to the end of the section is dominated by a marlstone black shale alternation intercalated by a few limy marlstones. The black shale horizons in the upper part are called Niveau Breistroffer (Bréhéret, 1997). The Niveau Breistroffer event is suggested to be superregional and comparable to the Oceanic Anoxic Event 1d (OAE 1d), found for example in the western Atlantic (Blake Nose; Wilson & Norris, 2001). The Niveau Breistroffer is characterised by pyritised ammonites of various species (among others *Puzosia*, *Stolizskaja*).

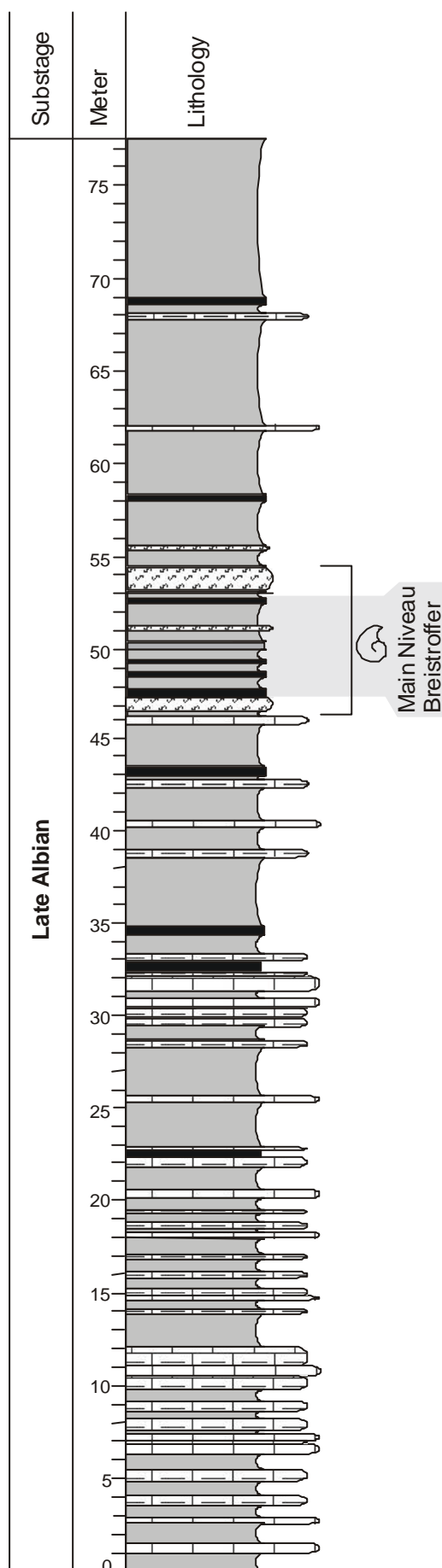
3.3. Results SE-France

3.3.1. Preservation of Planktic Foraminifera

The preservation of the planktic foraminifera in SE-France varies through time and can be described, based on subjective observations during counting, as moderate to good. Generally, the planktic foraminifera in the complete succession are filled with secondary calcite. A comparative count of shell debris and complete shells was not performed, but *Rotalipora* and *Planomalina* could subjectively consider to be better preserved than *Hedbergella*.

3.3.2. Planktic Foraminifera Record

Planktic foraminifera are in general unevenly distributed and vary considerably in their amount throughout the studied section. The planktic foraminiferal assemblage in SE-France is



composed of 27 species belonging to 9 genera. The abundance of all individuals of the fraction 63-500 μm fluctuates between 0 and about 150884 individuals per gram sediment (Ind./g; Fig. 17). The lower part of the combined sections up to 5 m below the Niveau Paquier, is characterised by very low abundances (max. 412 Ind./g; Fig. 17). From 5 m below the Niveau Paquier the abundance increases and shows two maxima (I, II; Fig. 17). The first maximum can be found between the Niveau Leenhardt and the HN 22 (~40000 Ind./g) and the second from the sandlayer G 7 to 20 m above the Petite Vérole (136497 Ind./g). Above Petite Vérole the abundances are decreasing again (Fig. 17). The number of planktic foraminifera of the fraction 250-500 μm decreases between the Délits Calcaires 2 (DC 2) and Délits Calcaires 4 (DC 4) from an average of 0,19 Ind./g to 0 Ind./g (Fig. 17). In the interval between DC 4 and 10 m above the Niveau Leenhardt planktic foraminifera of the fraction 250-500 μm do not exist. About 10 m above the Niveau Leenhardt the abundance of individuals > 250 μm increases again and shows three maxima (I, II, III; Fig. 17) The maxima are characterised by a continuous increase and a drastically decrease of the abundances (Fig. 17). The total abundance of the fraction 63-250 μm shows fluctuation comparable to the total abundance of the fraction 63-500 μm with two maxima (I, II; Fig. 17) near Niveau Leenhardt (~ 40000 Ind./g) and Petite Vérole (136497 Ind./g). The diversity (number of species) shows strong fluctuating values in the lower part of the section (base of the section to Haute Noir 22; Fig. 17). In the upper part (above the HN 22) the diversity is continuously increasing and reaches values up to 22 species.

← **Fig. 16:**

Schematic lithological column of the Col de Palluel VI section. A detailed lithological column with sample distribution is given in Appendix 13. For lithological explanations and abbreviations see Fig. 5.

SE-France

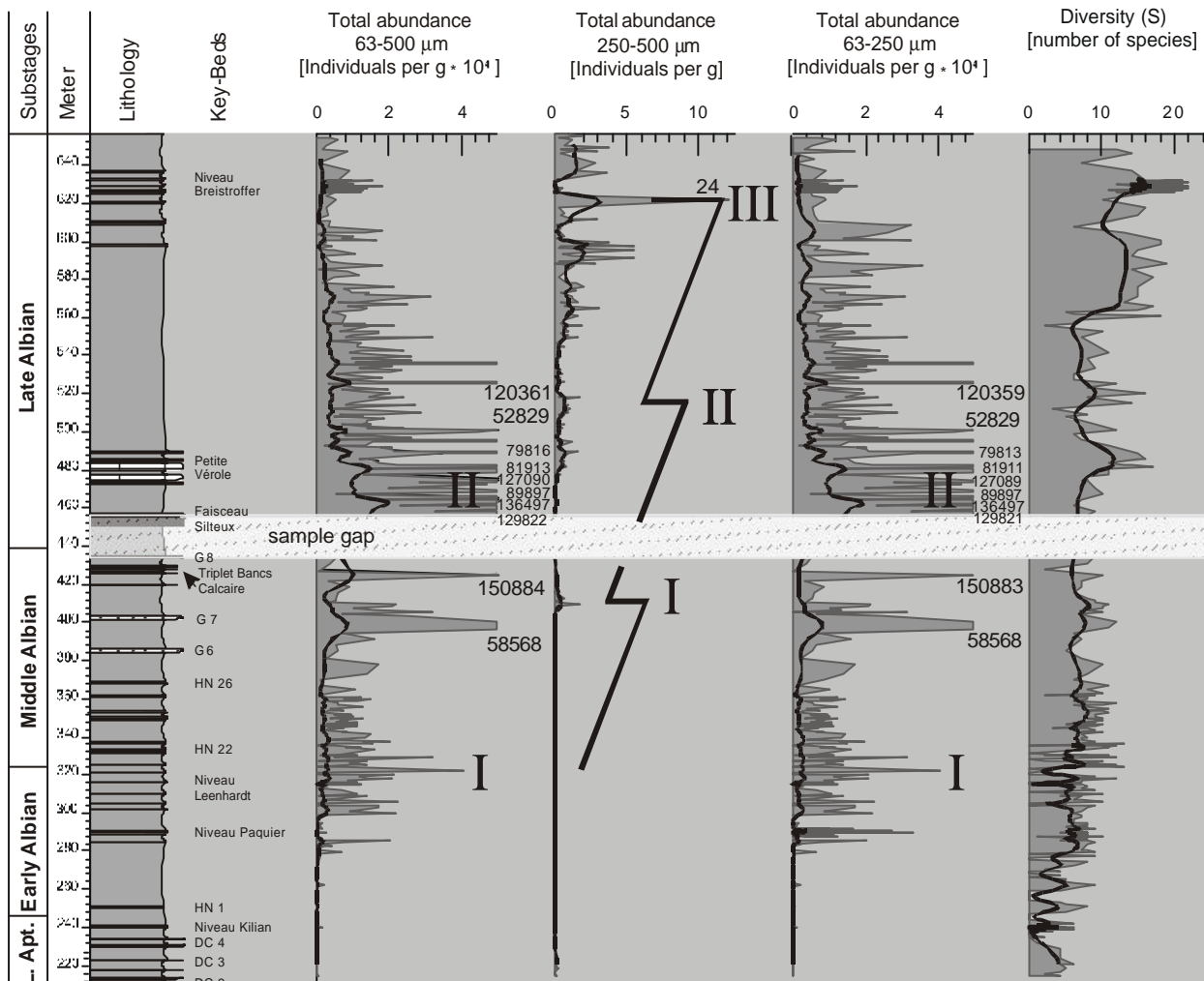


Fig. 17: Total abundance of planktic foraminifera of the fraction 63-500 µm, 250-500 µm and 63-250 µm given in individuals per g sediment, as well as the diversity expressed in number of species in the Late Aptian and Albian succession in SE-France (Vocontian Basin) is shown.

Tab. 1: List of planktic foraminiferal species in SE-France (Vocontian Basin) in alphabetical order

<i>Biticinella breggiensis</i> (Gandolfi, 1942)	<i>Heterohelix moremanni</i> (Cushman, 1938)
<i>Globigerinelloides bentonensis</i> (Morrow, 1934)	<i>Heterohelix reussi</i> (Cushman, 1938)
<i>Globigerinelloides ultramicra</i> (Subbotina, 1949)	<i>Heterohelix striata</i> (Ehrenberg, 1840)
<i>Guembelitra cretacea</i> (Cushman, 1933)	<i>Planomalina buxtorfi</i> (Gandolfi, 1942)
<i>Hedbergella bizoniae</i> (Chevalier, 1961)	<i>Planomalina praebuxtorfi</i> (Wonders, 1975)
<i>Hedbergella delrioensis/infracretacea</i> (Carsey, 1926)	<i>Praeglobotruncana delrioensis</i> (Plummer, 1931)
<i>Hedbergella flandrini</i> (Porthault, 1970)	<i>Rotalipora appenninica</i> (Renz, 1936)
<i>Hedbergella gorbachikae</i> (Longoria, 1974)	<i>Rotalipora subticinensis</i> (Gandolfi, 1942)
<i>Hedbergella maslakovae</i> ()	<i>Rotalipora ticinensis</i> (Gandolfi, 1942)
<i>Hedbergella planispira</i> (Tappan, 1940)	<i>Ticinella bejaouaensis</i> (Sigal, 1966)
<i>Hedbergella sigali</i> (Moullade, 1966)	<i>Ticinella praeticinensis</i> (Sigal, 1966)
<i>Hedbergella simplex</i> (Morrow, 1934)	<i>Ticinella primula</i> (Luterbacher, 1963)
<i>Hedbergella trocoidea</i> (Gandolfi, 1942)	<i>Ticinella raynaudi</i> (Sigal, 1966)
	<i>Ticinella roberti</i> (Gandolfi, 1942)

Biticinella breggiensis occurs only in the Late Albian and shows maximum values of about 560 Ind./g (Fig. 18). *Globigerinelloides* spp., represented by *Globigerinelloides bentonensis*, and *Globigerinelloides ultramicra* occur from the Late Aptian to the Late Albian. *Globigerinelloides bentonensis* shows maximum values of 1934 Individuals per g sediment (Ind./g) in the early Late Albian at the Petite Vérole (Fig. 18). Highest abundances (210 Ind./g) of *G. ultramicra* can be described from the late Late Albian near the Niveau Breistroffer (Fig. 18).

The triserial species *Guembelitra cretacea* occurs in the Late Albian and shows high abundances of 1046 to 2217 Ind./g from the Petite Vérole to 40 m below the Niveau Breistroffer (Fig. 18).

The fauna in SE-France is dominated by nine *Hedbergella* species. *Hedbergella* is the only genus occurring continuously throughout the entire succession (Fig. 19, 20). *Hedbergella bizonae* occurs only in the Early and Middle Albian in low numbers (max. 53 Ind./g). The highest abundance of all planktic foraminifera species can be described from *Hedbergella delrioensis/infracretacea*. This species occurs in all sections and reaches maximum values of about 70562 Ind./g in the early Late Albian between the Faisceau Silteux and the Petite Vérole (Fig. 19). The abundance of *H. delrioensis/infracretacea* shows no distinct fluctuation. *Hedbergella flandrini* occurs only in the Late Albian Niveau Breistroffer and reaches max. values of 0.65 Ind./g (Fig. 19).

SE-France
(Vocontian Basin)

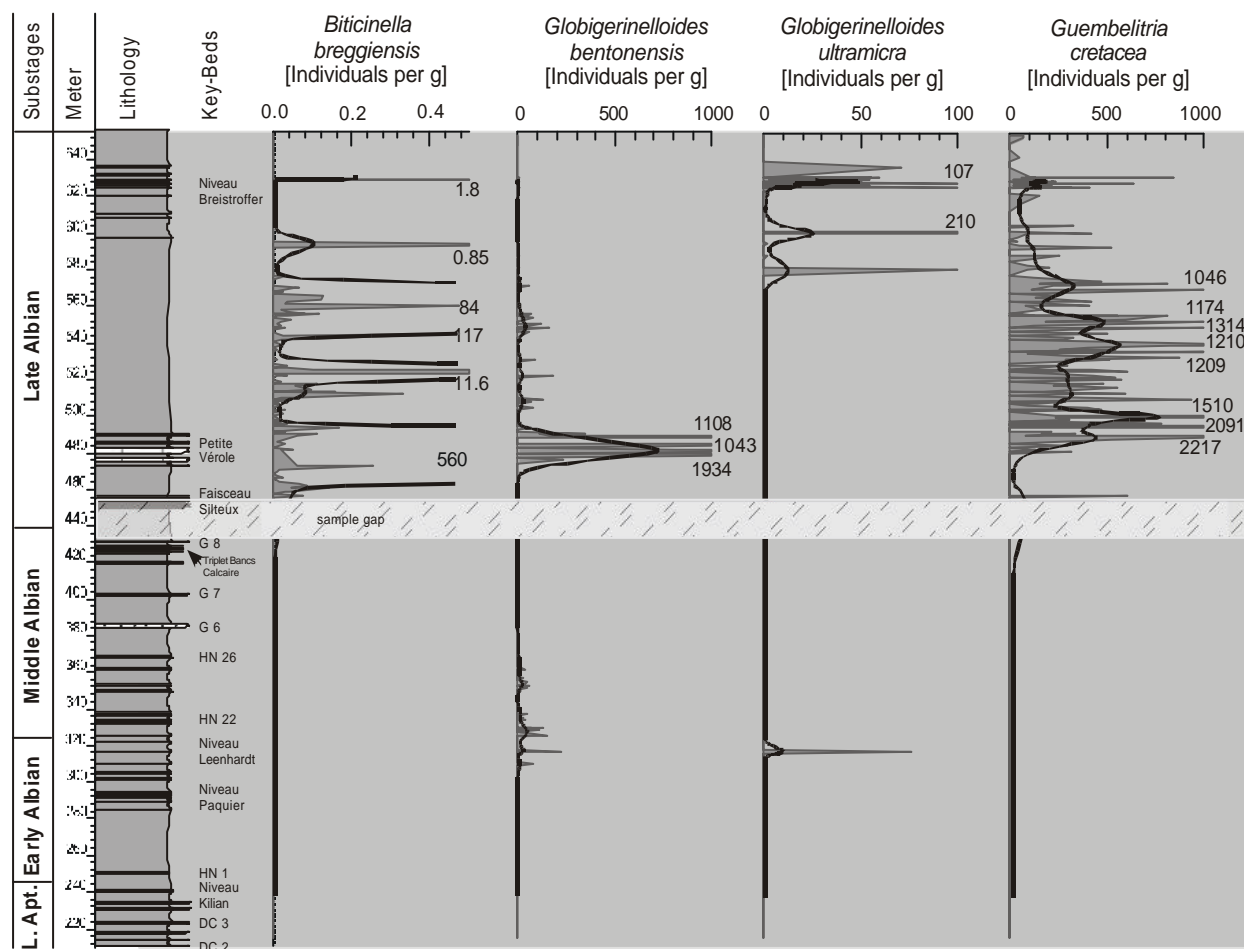


Fig. 18: Abundances of the planktic foraminifera *Biticinella breggiensis*, *Globigerinelloides bentonensis* and *Globigerinelloides ultramicra* as well as *Guembelitra cretacea* given in individuals per g sediment of the Late Aptian to Late Albian in SE-France (Vocontian Basin).

SE-France
(Vocontian Basin)

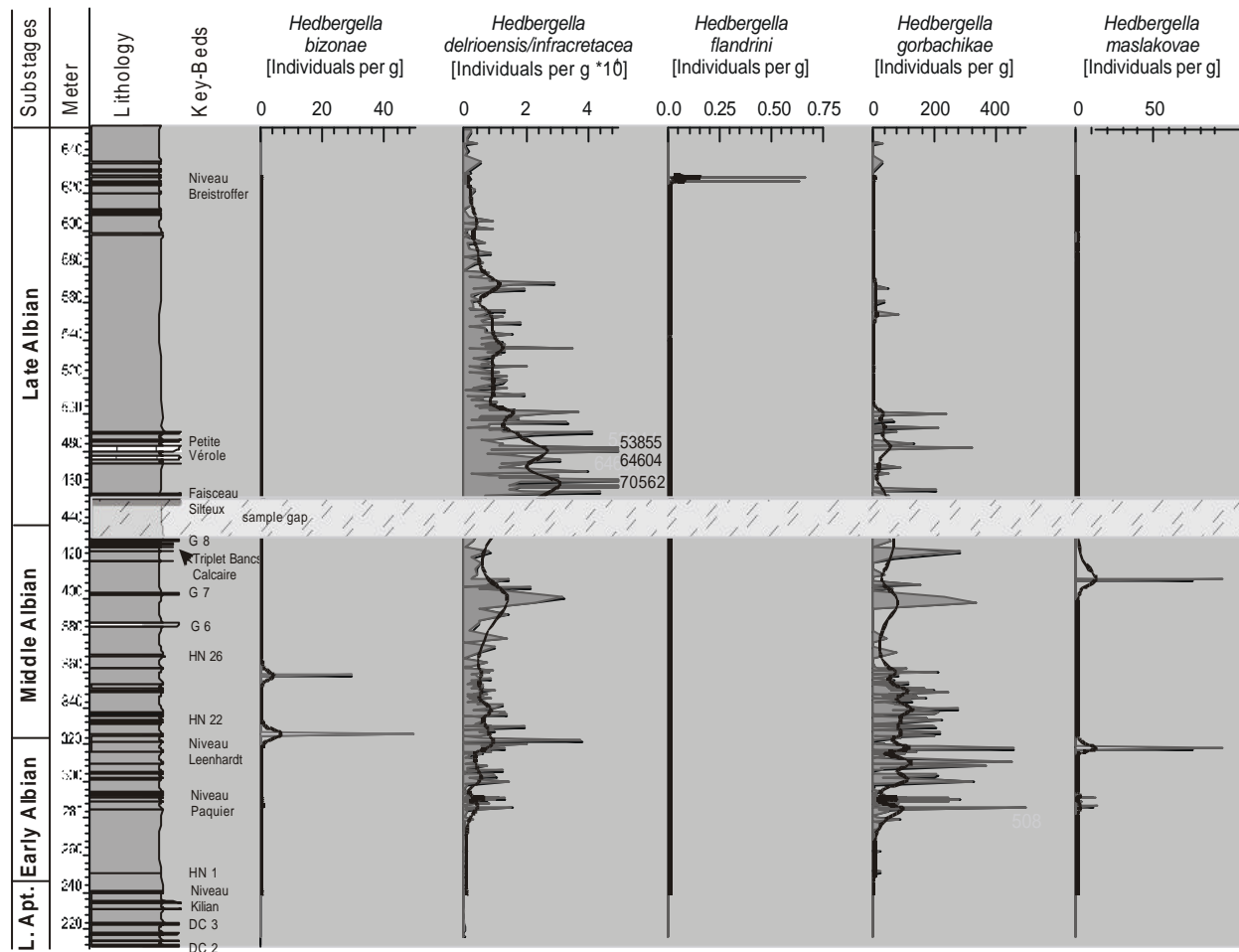


Fig. 19: Abundance of the planktic foraminifera *Hedbergella bizonae*, *Hedbergella delrioensis/infracretacea*, *Hedbergella flandrini*, *Hedbergella gorbachikae* and *Hedbergella maslakovae* given in individuals per g sediment of the Late Aptian to Late Albian in SE-France (Vocontian Basin).

Hedbergella gorbachikae is well distributed in the whole section, but shows higher values in the lower part (Early and Middle Albian). Maximum values (400 – 508 Ind./g) can be described from just below the Niveau Paquier to the Niveau Leenhardt (Fig. 19). *Hedbergella maslakovae* shows only low values with two peaks, at the Niveau Leenhardt and just above the sandlayer G 7 (90 Ind./g; Fig. 19). *Hedbergella planispira* is the planktic foraminiferal species with the second highest abundance in SE-France. This species occurs from the Late Aptian to the Late Albian and reaches maximum values in the early Late Albian between the Faisceau Silteux and the end of the Petite Vérole (12621 Ind./g; Fig. 20). No distinct fluctuation in the abundance of

H. planispira can be described.

From the Late Aptian to the Late Albian, *Hedbergella sigali* shows no distinct fluctuation as well. Maximum values can be observed in the Early Albian (1900 Ind./g) in the Niveau Paquier, in the Middle Albian (1800 Ind./g) just below sandlayer G 7 and in the Late Albian (7413 Ind./g) in the Petite Vérole (Fig. 20). Whereas other species like *H. planispira* and *H. flandrini* show higher values in the Niveau Breistroffer, the abundance of *H. sigali* here is lower than below and above the Niveau Breistroffer.

Hedbergella simplex appears also continuously in the whole section and fluctuates very frequently between 0 Ind./g and maximum values of about 1059 Ind./g (Fig. 20).

SE-France
(Vocontian Basin)

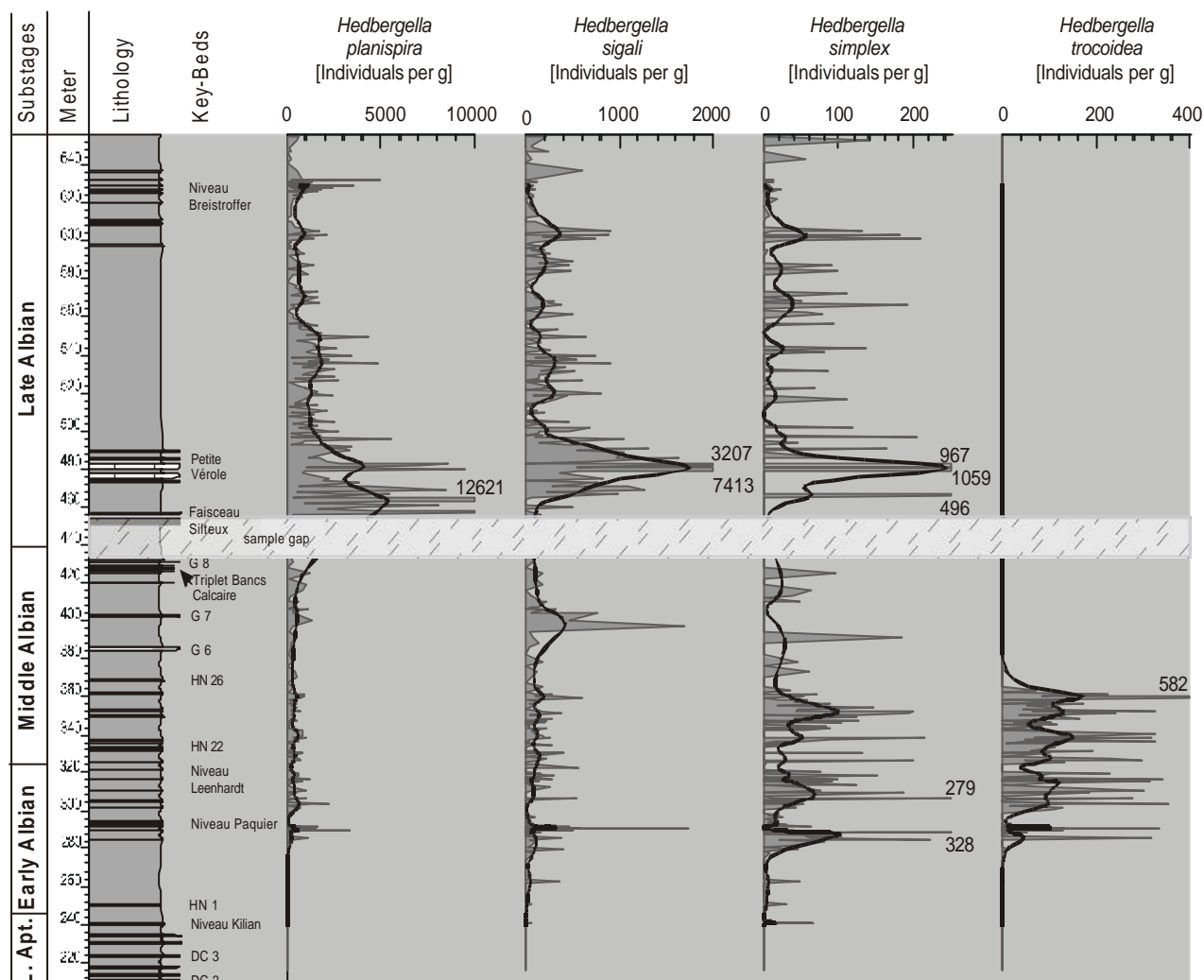


Fig. 20: Abundance of the planktic foraminifera *Hedbergella planispira*, *Hedbergella sigali*, *Hedbergella simplex* and *Hedbergella trocoidea* given in individuals per g sediment from the Late Aptian to Late Albian in SE-France (Vocontian Basin).

Hedbergella trocoidea can only be described from the Early and Middle Albian with values of about 400 Ind./g (Fig. 20).

Heterohelix spp. predominates the fauna and occurs discontinuously throughout the studied section (Fig. 21). Highest abundances of *Heterohelix moremani* (1993 and 1750 Ind./g) can be observed in the early Late Albian just above the Petite Vérole (Fig. 21). No distinct fluctuation in abundances can be observed (Fig. 21). *Heterohelix reussi* reaches highest abundances just above the Faisceau Silteux (2313 Ind./g) and shows no distinct fluctuation as well (Fig. 21).

Heterohelix striata occurs only in the Niveau Breistroffer with max. values of 529 Ind./g (Fig. 21).

Praeglobotruncana delrioensis appears only in the late Late Albian and reaches maximum values in the Niveau Breistroffer (15 Ind./g; Fig. 21).

The two species of *Planomalina* spp. occur only in the Late Albian. *Planomalina praebuxtorfi* shows max. values 50 m below the Niveau Breistroffer (0.25 Ind./g; Fig. 22) and *Planomalina buxtorfi* has two maxima with 4.5 Ind./g 23 m below and 17 Ind./g directly at the Niveau Breistroffer.

SE-France
(Vocontian Basin)

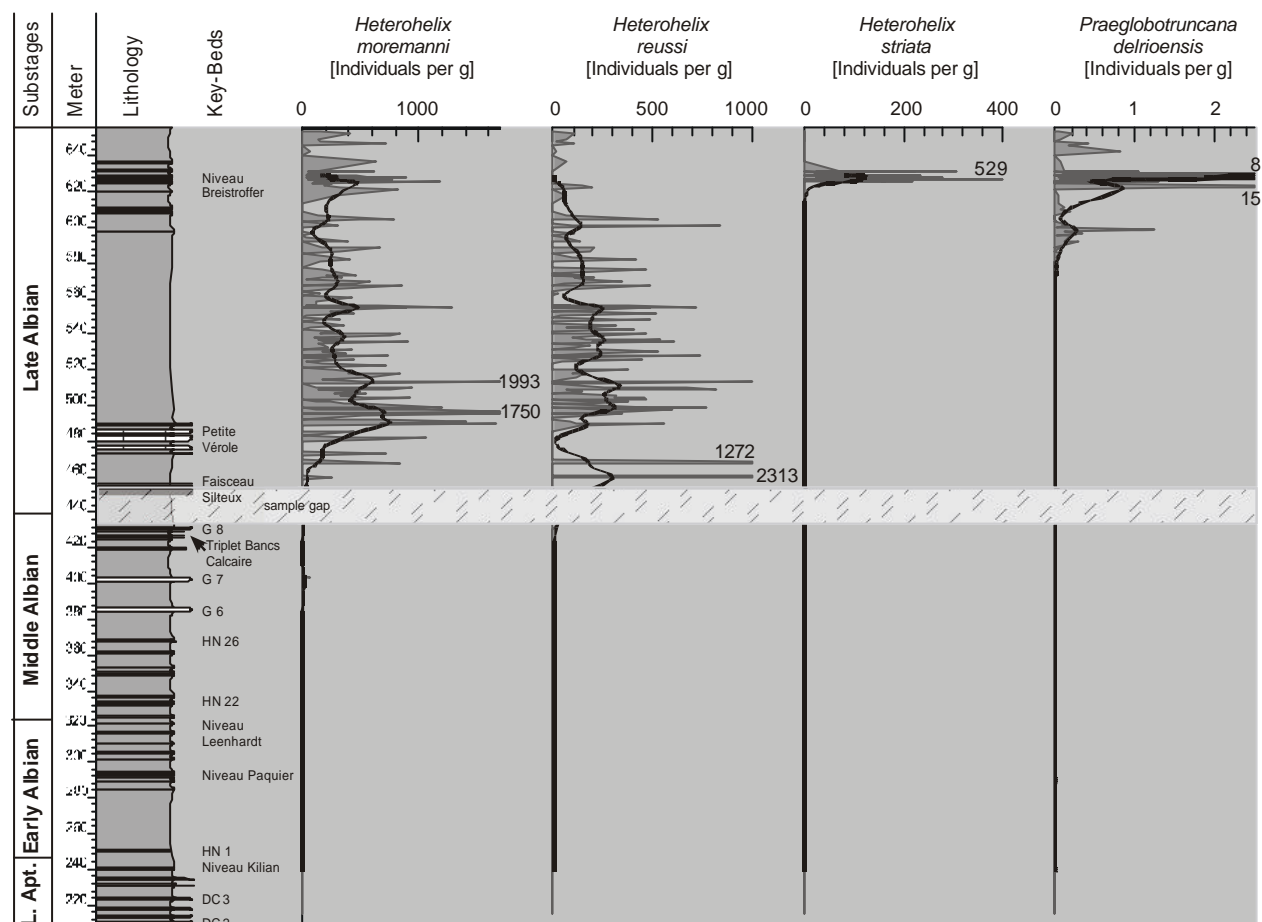


Fig. 21: Abundance of the planktic foraminifera *Heterohelix moremani*, *Heterohelix reussi* and *Heterohelix striata* as well as *Praeglobotruncana delrioensis* given in individuals per g sediment of the Late Aptian to Late Albian in SE-France (Vocontian Basin).

Rotalipora appenninica, *Rotalipora subticinensis* and *Rotalipora ticinensis* show maximum values in the Late Albian. In detail, high abundances of *R. appenninica* (83 Ind./g; Fig. 22) can be observed at the Niveau Breistroffer. *Rotalipora subticinensis* is marked at the Petite Vérole (0.35 Ind./g; Fig. 22) and *R. ticinensis* 60 m above the Petite Vérole by a distinct maximum (1.89 Ind./g; Fig. 22).

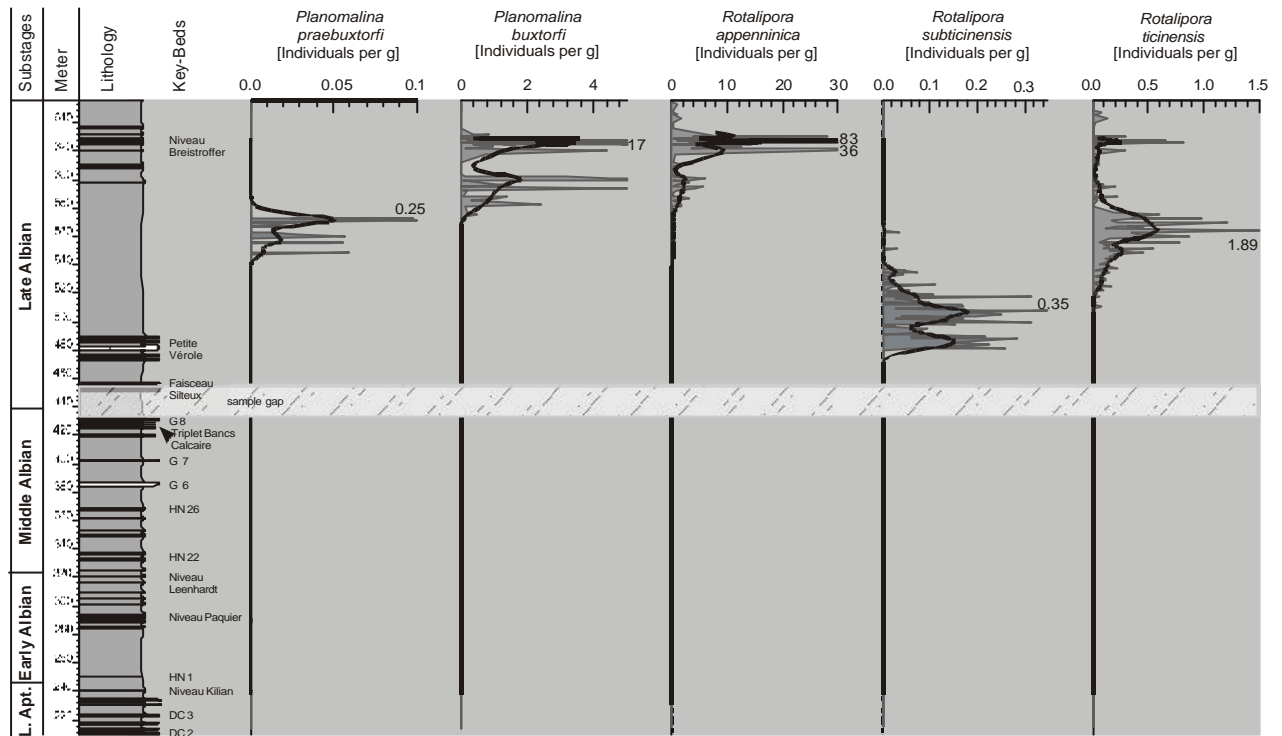
The four species of the genus *Ticinella* occur discontinuously throughout the whole section. *Ticinella bejaouaensis* occurs only in the Late Aptian with values of about 0.03 Ind./g (Fig. 23). *Ticinella praeticinensis* shows highest abundances (0.4 Ind./g) in the Petite Vérole (Fig. 23) and *Ticinella primula* can be observed from the Niveau Leenhardt to the Faisceau Silteux

with max. values between the sandlayers G 6 and G 7 (~4000 Ind./g; Fig. 23). *Ticinella roberti* appears only on the Late Albian and shows one maximum about 60 m below the Niveau Breistroffer (306 Ind./g; Fig. 23).

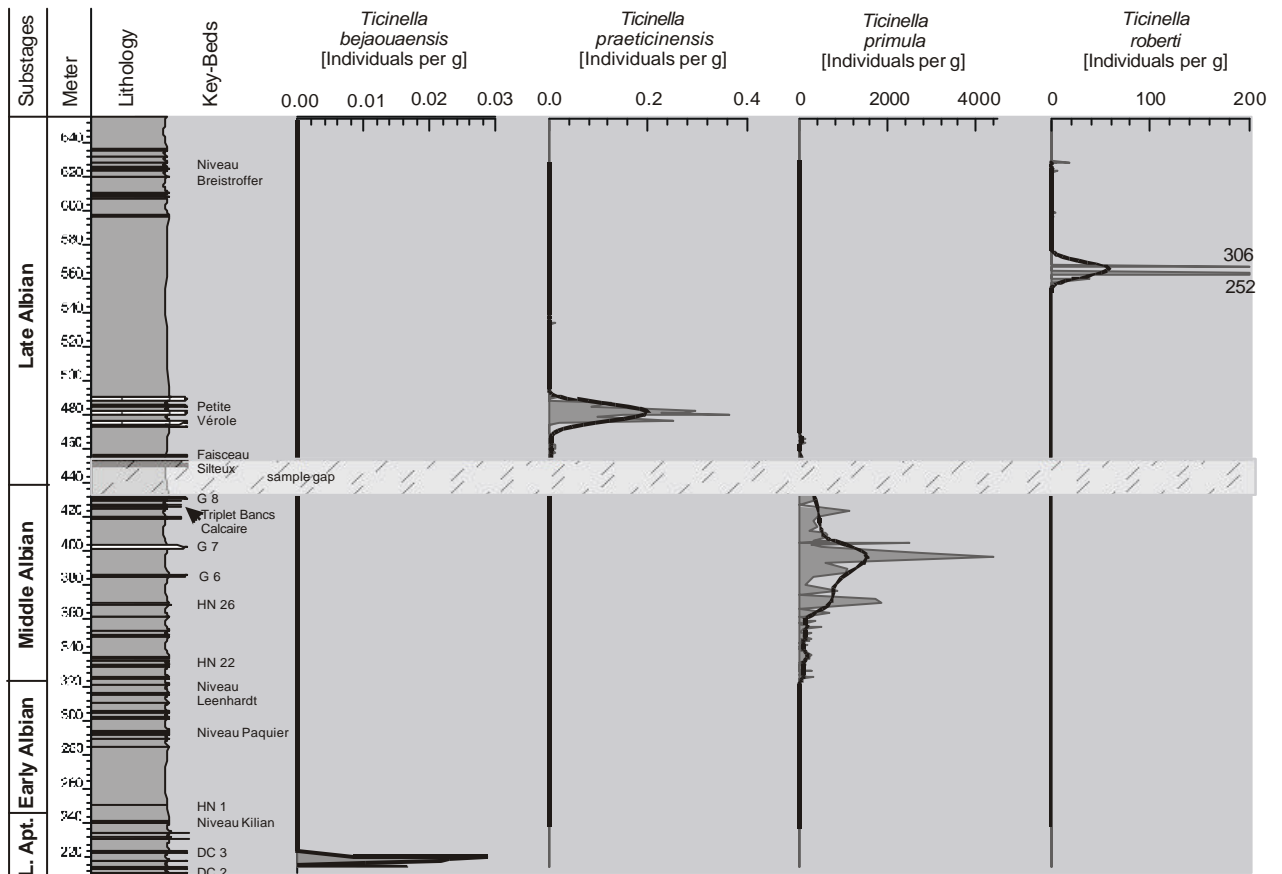
Fig. 23: Abundances of the planktic foraminifera *Ticinella bejaouaensis*, *Ticinella praeticinensis*, *Ticinella primula* and *Ticinella roberti* given in individuals per g sediment of the Late Aptian to Late Albian in SE-France (Vocontian Basin).

Fig. 22: Abundance of the planktic foraminifera *Planomalina praebuxtorfi*, *Planomalina buxtorfi*, *Rotalipora appenninica*, *Rotalipora subticinensis* and *Rotalipora ticinensis* given in individuals per g sediment of the Late Aptian to Late Albian in SE-France (Vocontian Basin).

SE-France
(Vocontian Basin)



SE-France
(Vocontian Basin)



3.3.3. First and Last Appearance Datums of Planktic Foraminifera

In the studied section in SE-France (Vocontian Basin) a total of 21 first appearance datums (FADs) and 16 last appearance datums (LADs) can be recognised in the interval between DC 2 and the end of the succession (0-441 m; Fig. 24). In the lower part of the combined sections from the DC 2 to 8 m below the Niveau Paquier no FADs can be observed.

After this point the number of FADs increases in two intervals: The first interval from 8 m below the Niveau Paquier to 4 m above the Niveau Leenhardt shows 5 FADs. In the second interval about 7 m below the sand layer G 7 to the end of the section the number of FADs (13) increases continuously (Fig. 24). In the following table all FADs and LADs from bottom to top are compiled, the stratigraphically important taxa are shown in bold type (Tab. 2).

Tab. 2: Compilation of first and last appearance datums (FADs, LADs) of planktic foraminifera of the Late Aptian to Late Albian in SE-France (Vocontian Basin). The position is given in metres in reference to the distinct lithological marker. The stratigraphically important FADs and LADs are indicated by bold type.

Depth (m)	Depth in relation to a marker horizon	First Appearance Datum (FAD)	Last Appearance Datum (LAD)
648	18 m above the Niveau Breistroffers		<i>Planomalina buxtorfi</i>
635	5 m above the Niveau Breistroffers		<i>Globigerinelloides ultramicra</i>
630	Within the Niveau Breistroffer		<i>Heterohelix striata</i>
630	Within the Niveau Breistroffer		<i>Hedbergella trocoidea</i>
630	Within the Niveau Breistroffer		<i>Globigerinelloides bentonensis</i>
629	Within the Niveau Breistroffer		<i>Ticinella roberti</i>
626	Within the Niveau Breistroffer		<i>Biticinella breggiensis</i>
626	Within the Niveau Breistroffer	<i>Hedbergella flandrini</i>	<i>Hedbergella flandrini</i>
625	Within the Niveau Breistroffer	<i>Heterohelix striata</i>	
596	27 m below the Niveau Breistroffers		<i>Hedbergella maslakovae</i>
586	37 m below the Niveau Breistroffers		<i>Ticinella primula</i>
580	43 m below the Niveau Breistroffers	<i>Praeglobotruncana delrioensis</i>	
575	48 m below the Niveau Breistroffers		<i>Guembelitra cretacea</i>
573	50 m below the Niveau Breistroffers	<i>Planomalina buxtorfi</i>	
572	51 m below the Niveau Breistroffers		<i>Planomalina praebuxtorfi</i>
548	75 m below the Niveau Breistroffers	<i>Planomalina praebuxtorfi</i>	
541	53 m above the Petite Vérole		<i>Hedbergella bizonae</i>
540	52 m above the Petite Vérole	<i>Rotalipora appenninica</i>	

537	49 m above the Petite Vérole		<i>Rotalipora subticinensis</i>
534	46 m above the Petite Vérole		<i>Ticinella praeticinensis</i>
520	32 m above the Petite Vérole	<i>Rotalipora ticinensis</i>	
482	At the Petite Vérole	<i>Rotalipora subticinensis</i>	
457	Just above the Faisceau Silteux	<i>Guembelitra cretacea</i>	
435-453	Within a sample gap (broken line in Fig. 34)	<i>Ticinella praeticinensis</i>	
435-453	Within a sample gap (broken line in Fig. 34)	<i>Biticinella breggiensis</i>	
435	4 m above the sandlayer Grés 8 (G 8)	<i>Heterohelix reussi</i>	
431	Just above the sandlayer Grés 8 (G 8)	<i>Ticinella roberti</i>	
411	9 m above the sandlayer Grés 7 (G 7)	<i>Ticinella raynaudi</i>	
405	3 m above the sandlayer Grés 7 (G 7)	<i>Heterohelix moremani</i>	
324	8 m above the Niveau Leenhardt	<i>Ticinella primula</i>	
318	2 m above the Niveau Leenhardt	<i>Globigerinelloides ultramicra</i>	
310	5 m below the Niveau Leenhardt	<i>Globigerinelloides bentonensis</i>	
288	1 m below the Niveau Paquier	<i>Hedbergella bizonae</i>	
286	3 m below the Niveau Paquier	<i>Hedbergella maslakovae</i>	
222	1 m below the Délits Calcaires 3 (DC 3)		<i>Ticinella bejaouaensis</i>
218	5 m below the Délits Calcaires 3 (DC 3)	<i>Hedbergella gorbachikae</i>	

3.3.4. Stable Isotopes

The carbon ($\delta^{13}\text{C}$) and oxygen ($\delta^{18}\text{O}$) isotope measurements of the 317 m thick succession in SE-France (Vocontian Basin) are based on 518 bulk rock samples. The average sample distance varies between 5 and 100 cm. The $\delta^{13}\text{C}$ record shows values from 0.3 to 2.55 ‰ and is characterised by a major fluctuation from 0.5 and 1.0 ‰ (smoothed white curve; Fig. 25). In detail, from the Haut Noire 21 (HN 21) to 6 m below Haute Noir 23 (HN 23), the $\delta^{13}\text{C}$ values increase from 1.85 to 2.2 ‰. From 6 m below HN 23 to 9 m below G7 the $\delta^{13}\text{C}$ values decrease again (1 ‰), followed by an increase (0.9 ‰) up to the Triplet Banc Calcaire. From the Triplet Banc Calcaire to 11 m below the

Petite Vérole the $\delta^{13}\text{C}$ values decrease again (0.5 ‰). The succession from 11 m below to 54 m above the Petite Vérole is marked by increasing $\delta^{13}\text{C}$ values of 0.7 ‰. From 54 m above the Petite Vérole to the base of the Niveau Breistroffer the $\delta^{13}\text{C}$ record show balanced values between 1.3 and 1.6 ‰. The Niveau Breistroffer is marked by two distinct negative excursions in the $\delta^{13}\text{C}$ values (about 0.4 ‰). Above the Niveau Breistroffer the carbon isotope values increase from 1.5 ‰ up to 2.0 ‰. The oxygen isotope ($\delta^{18}\text{O}$; Fig. 25) record in SE-France is characterised by frequent fluctuation. Generally, the values vary between 4.3 to -3.2 ‰ (smoothed white curve). In the

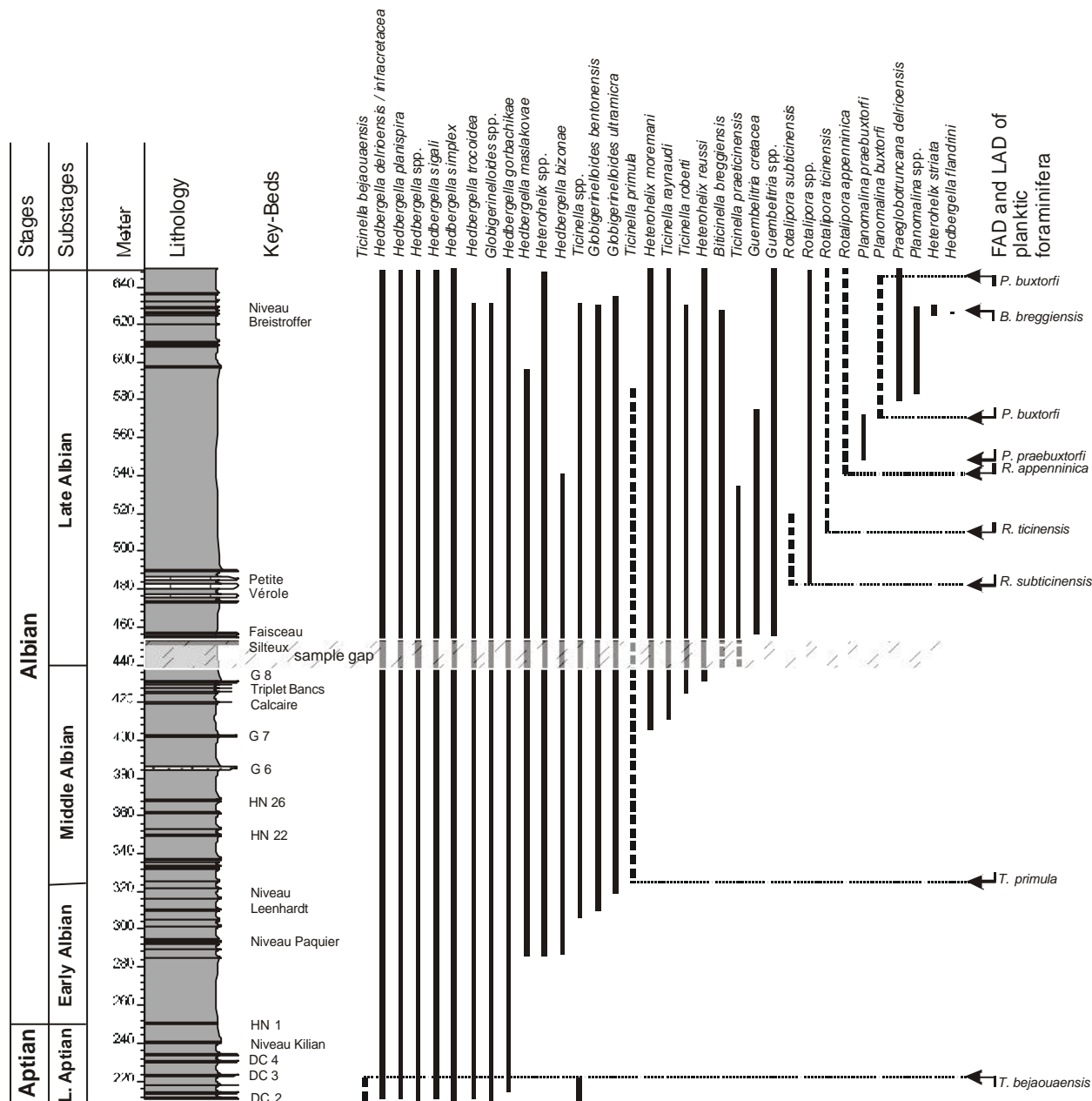


Fig. 24: Range chart of planktic foraminifera of SE-France (Vocontian Basin) with respect to the lithology. The distribution of the stratigraphically important taxa is given in broken lines.

lower part from the HN 22 to Haute Noirs 25 (HN 25), the $\delta^{18}\text{O}$ curve is marked by balanced values about -3.3‰ and decrease then to 0.7‰ lighter values. The interval from HN 25 to 52 m below the Niveau Breistroffer the oxygen isotope shows balanced values about -4.1‰ . 51 m below the Niveau Breistroffer the $\delta^{18}\text{O}$ values increase (0.4‰) again. From 51 m below the Niveau Breistroffer to the Niveau itself the values are about -3.8‰ . The Niveau Breistroffer is characterised by a negative

excursion in $\delta^{18}\text{O}$ values of about 0.5‰ , followed by a positive excursion of about 0.7‰ . From just above the Niveau Breistroffer to the end of the section the oxygen isotopes show balanced values about 3.6‰ . The distinct decrease at the HN 25 and the increase 51 m below the Niveau Breistroffer goes along with section boundaries between the sections Serre Amande / Col de Palluel II (lower part) and Col de Palluel IV / V (upper part).

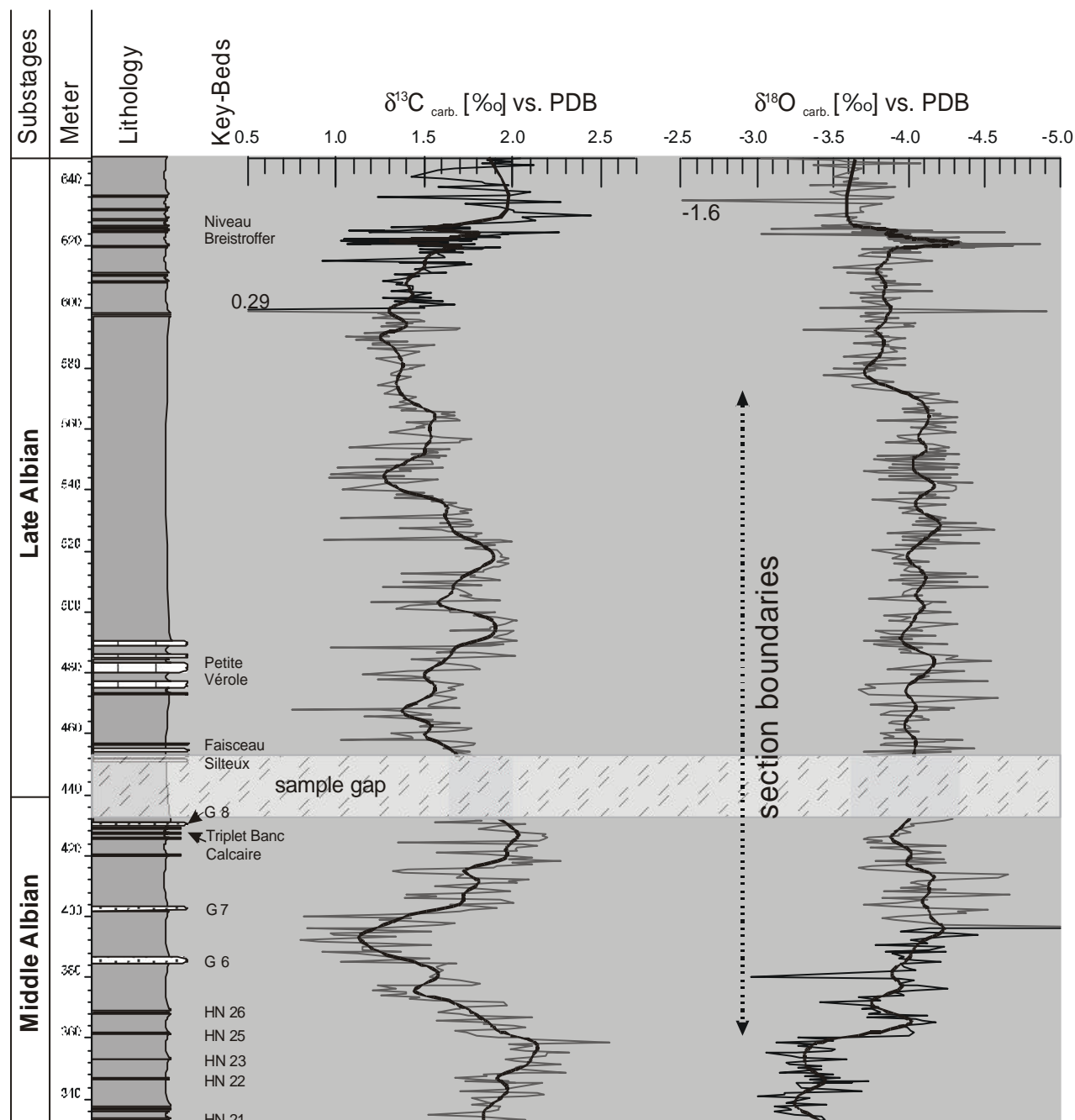


Fig. 25: $\delta^{13}\text{C}$ and $\delta^{18}\text{O}$ values of the Middle and Late Albian of SE-France. A smoothed curve is given in white colour. The pronounced negative $\delta^{18}\text{O}$ values from HN25 to 52 m below Niveau Breistroffer reflect section boundaries (see this Chapter below).

3.4. Discussion SE-France

3.4.1. Preservation of Planktic Foraminifera of SE-France

For an interpretation and discussion of preservational modes of the planktic foraminifera of SE-France no raticular data are available.

Subjectively, the planktic foraminifera are good to moderately preserved, so that the count of the species and the first and last appearance datums seem to be reliable.

3.4.2. Isotopic Signatures and Diagenesis

Calcareous sections are dominated by calcareous nannofossils, planktic foraminifera and benthic foraminifera in descending order (Herrle, 2002). Therefore, it is assumed that the isotope signal represents predominantly a surface water signal. However, the original isotopic signal may be influenced by various early and late diagenetic effects. The observed long- and short term fluctuation in the $\delta^{13}\text{C}$ record in SE-France can be correlated with comparable variations in the sections at the

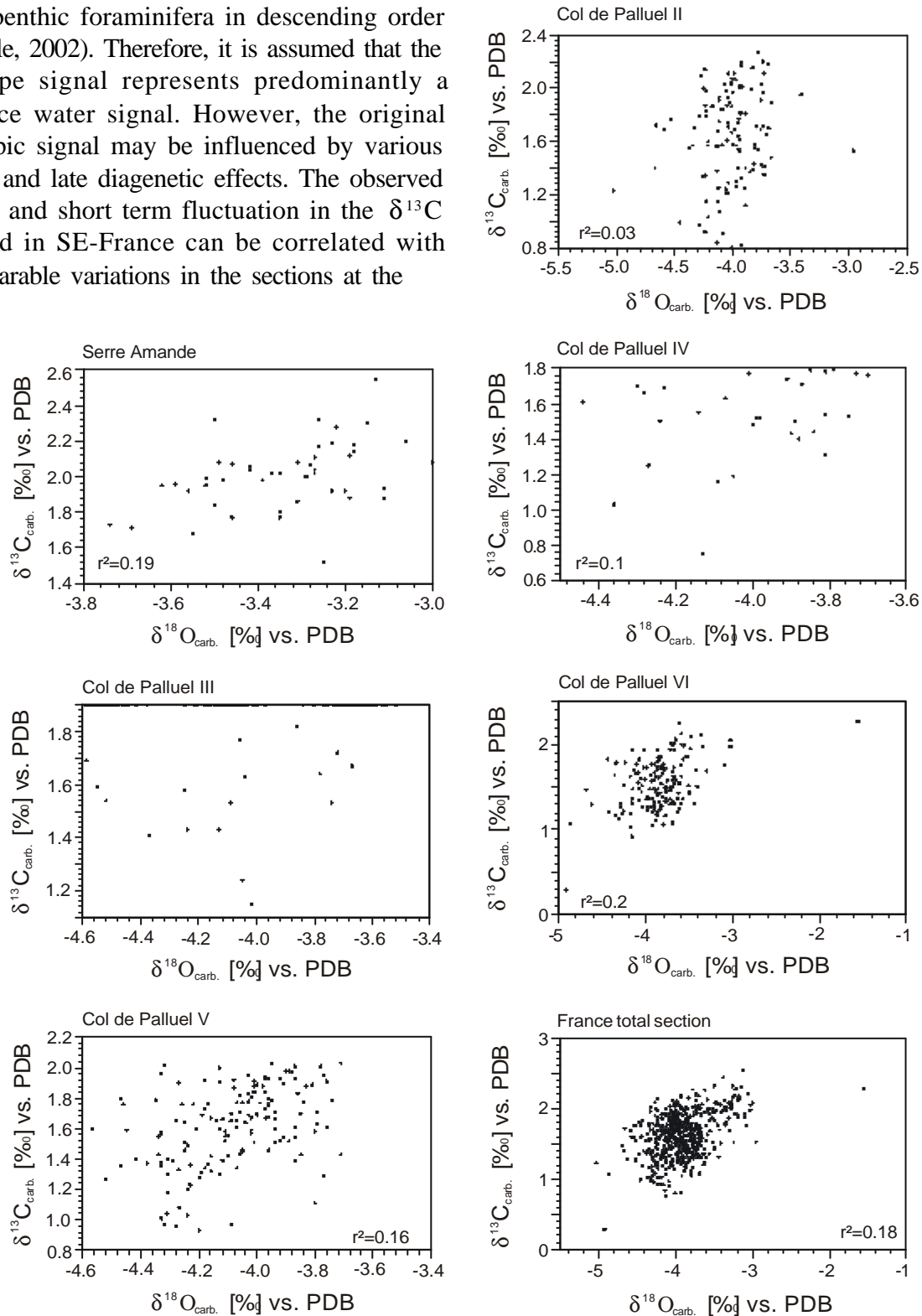


Fig. 26: $\delta^{13}\text{C}$ and $\delta^{18}\text{O}$ of bulk carbonate samples from the different SE-France sections showing a weak to insignificant positive correlations.

DSDP Site 545, 547, Mazagan Plateau (Nederbragt, et al., 2001; Herrle, 2002), ODP Site 1052 (Blake Nose Plateau; Wilson & Norris, 2001) and in NE-Texas (this thesis; see Chapter 3.4.5; Fig. 57). Therefore, it can be assumed that the carbon isotope signal is barely influenced by diagenesis. Even when the absolute carbon values are altered by isotopically light cement, this alteration did not mask the high-amplitude fluctuation in the carbon isotope stratigraphy (Weissert & Br  h  ret, 1991). If the sediments were affected by burial diagenesis and calcite precipitation from marine pore-fluids, the carbon and oxygen isotope values should show a positive correlation (Jenkyns & Clayton, 1986; Jenkyns, 1996). Herrle (2002) stated the correlation between carbon and oxygen isotope values for the sections Tarendol ($r^2=0.5$), Pr  -Guittard ($r^2=0.69$) and l'Arboudeysse ($r^2=0.71$) as weak positive and for the interval Les Oustaus ($r^2=0.37$) and Col de Palluel I ($r^2=0.39$) as insignificant. The in this study investigated sections Serre Amante ($r^2=0.19$), Col de Palluel II ($r^2=0.03$), Col de Palluel IV ($r^2=0.1$), Col de Palluel V ($r^2=0.16$) and Col de Palluel VI ($r^2=0.2$) are also insignificantly correlated (Fig. 26). The section Col de Palluel III did not reveal enough values to calculate a reliable correlation. The low covariance between the $\delta^{13}\text{C}$ and $\delta^{18}\text{O}$ values in France implies an insignificant alteration during diagenesis (Fig. 26). Even though the correlation would be strongly positive, Rao (1996) supposed that this would not necessarily indicate a diagenetic signal. Whereas the carbon isotope signal can be seen as insignificantly affected by diagenesis, the oxygen signal is more likely to have been altered. The oxygen isotopes of the sediments are more solvable in pore waters than carbon isotopes (Scholle & Arthur, 1980). Additionally, the oxygen isotope record is more susceptible to temperature fractionation than the carbon isotope (Freedman & O'Neil, 1977). It seems likely, that the abrupt decrease of the $\delta^{18}\text{O}$ values in SE-France (360 m) of about 1.1‰ and the later increase of 0.9‰ (572 m), coinciding with section boundaries, is caused by varying diagenesis of the different section intervals (Fig. 25).

3.4.3. Planktic Foraminiferal Record

During the Late Aptian to Late Albian, the evolution of planktic foraminiferal fauna was characterised by major evolutionary changes (diversification and stasis). These changes can be observed in abundance, size, diversity and composition of the planktic foraminiferal fauna. Using these faunal proxies, the Late Aptian to Late Albian can be divided into two evolutionary phases (I and II): The first evolutionary phase of "no evolution" (phase I) from Late Aptian and Early Albian in SE-France is characterised by low total abundances of planktic foraminifera, a lack of planktic foraminifera greater than 250 μm and a low diversity with highly fluctuating values (Fig. 17). The beginning of this phase was not subject of this study. It ends at the Haut Noir 22 (HN 22), where planktic foraminifera greater than 250 μm reappear and the strong fluctuation in diversity ends. The phase I of "no evolution" can be divided into an interval of "stasis" (I a) with low total abundances and an interval of "starting" (I b) with increasing total abundances (Fig. 27). The afore mentioned phase of "no evolution" seems to be globally distributed. Leckie et al. (2002) and Premoli-Silva & Sliter (1999) also describe small sized foraminifera (< 230 μm) and low diversity from the Aptian/Albian boundary of several sites around the world. The dichotomy of phase I, caused by the earlier increase of total abundance of planktic foraminifera (Fig. 27) is not figured out by Leckie et al. (2002) and Premoli-Silva & Sliter (1999), but the general trend of low total abundances is similar. The interval of "no evolution" is also characterised by a turnover in other planktic organisms (radiolarians; Erbacher, 1994), increased oceanic crust production (Bralower et al., 1997), low sea level, (Haq et al., 1987) and a strong influence of monsoonal activity, especially in the Vocontian Basin (SE-France; Herrle et al., 2003 a, b). The number of causes for a phase of "no evolution" could be numerous. For example food availability, water temperature, oxygen content and pH values of the water as well as watermass structure are presumed. As Herrle (2003 a, b) pointed out,

SE-France

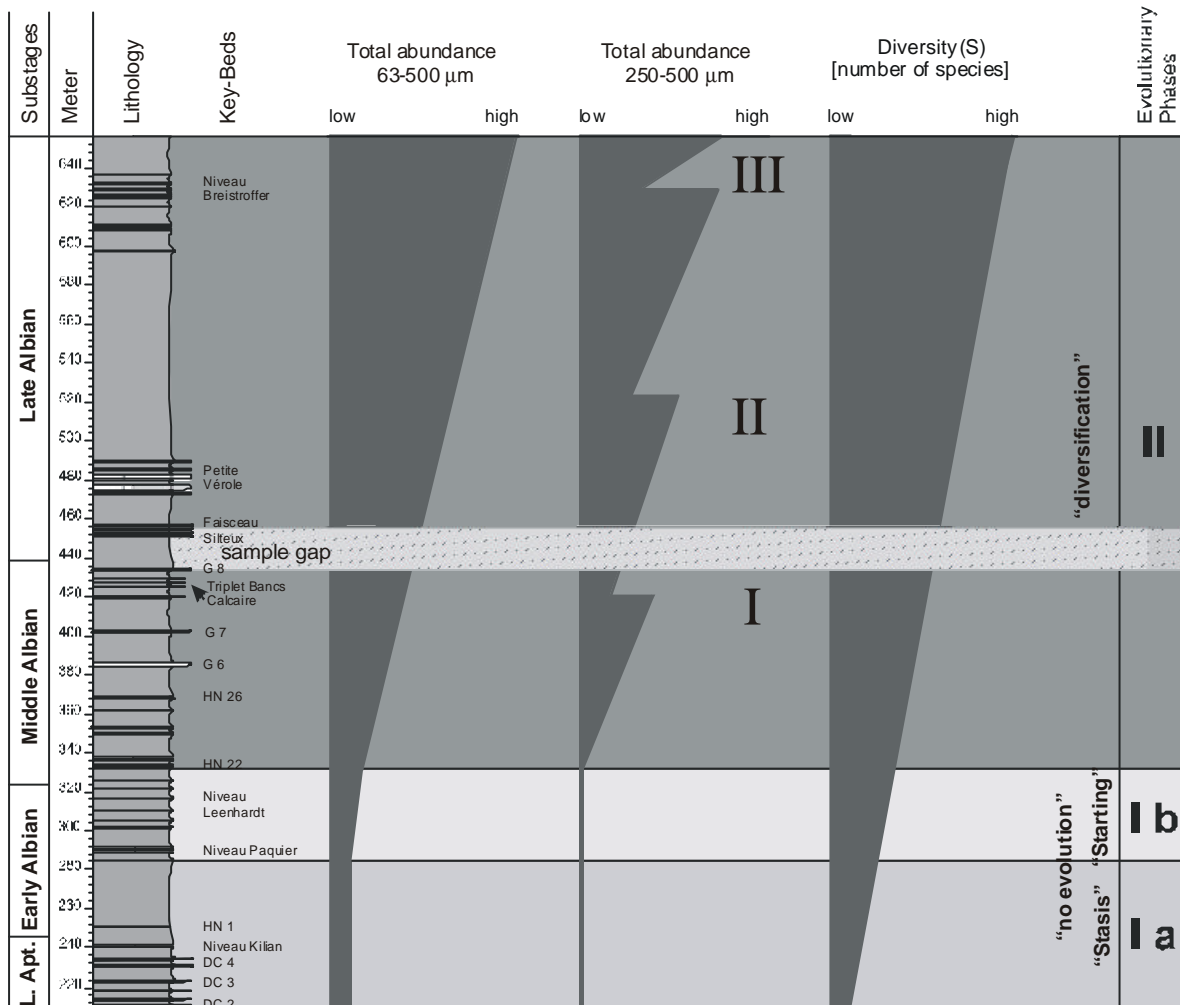


Fig. 27: Total abundance of planktic foraminifera of the fraction 63-500 µm, 250-500 µm, 63-250 µm (Ind./g) and diversity (number of species) in SE-France with a proposed “evolutionary” zonation.

surface water fertility in the Vocontian Basin during the Aptian/Albian boundary interval was controlled by a strong influence of the monsoonal circulation. Based on nannofossil and carbon isotope data, Herrle (2003 a, b) shows that low temperatures coincide with low surface water fertility and vice versa. Low fertility means less nannoplankton and therefore less food for planktic foraminifera. The interval between the Niveau Kilian and Niveau Paquier (Aptian/Albian boundary) in the Vocontian Basin is estimated as cooler (Herrle & Mutterlose, 2003). Combining the described low total abundances of planktic foraminifera and the estimated low temperatures, a negative feedback mechanism of lower fertility, lower food availability can be presumed for the Aptian/

Albian boundary interval. Changing nutrient availability and/or changing upper water column structure near the change Aptian/Albian is assumed by Leckie et al. (2002) as well. Premoli-Silva & Sliter (1999) presumes that a weakening/disrupting thermocline provokes low abundances, low diversity and a fauna composed only of opportunists. Also dissolution is mentioned by Premoli-Silva & Sliter (1999) as cause for the observed low abundances and diversity. The second evolutionary phase (phase II) from the HN 22 until the end of the section is characterised by increasing or and generally higher abundances than in phase I, increasing size (rising abundances of foraminifera >250 µm) and iversity (Fig. 17, 27). It can be described as “diversification”. This step in the evolution

of planktic foraminifera can also be reproduced with the abundances of selective foraminifera species. For example, the abundances of the phylogenetic succession of *Ticinella primula*, *Ticinella praeticinensis*, *Rotalipora subticinensis*, *Rotalipora ticinensis* and *Rotalipora appenninica* (Gandolfi, 1955; Wonders, 1980; Fig. 28) and *Planomalina praebuxtorfi* and *Planomalina buxtorfi* (Wonders, 1980; Fig. 28) show successional peaks. The diversification observed globally, could have been caused by numerous reasons. According to Stanley & Hardie (1998), the higher rate of hydrothermal activity combined with alteration of ocean carbonate concentration have encouraged the development of calcite-secreting plankton. This benefit to calcite-secreting plankton may be seen in the increasing size of planktic foraminifera, respectively in the increasing number of individuals of the fraction 250-500 μm (Fig. 27).

Also the appearance of heavier calcified species in the ocean (*Ticinella*, *Rotalipora*, *Planomalina*; Fig. 28) have gone along with the initiation of a more calcareous dominated sedimentation (above Haute Noire 26; Fig. 28). Caused by the altered circulation, sea level rise and global warming, the availability of food for planktic foraminifera have changed as well (Leckie et al., 2002). The nutrients were possibly fixed in the warmer epicontinental seas (Codispoti, 1997) and have encouraged the productivity of cyanobacteria and coccolithophorids (e.g. Falkowski et al., 1998). Maybe because of the fixed nutrients and the increasing amount of phytoplankton, the planktic foraminifera have changed food preference, have developed deeper habitats and have adapted their morphology to the changes, as can be seen in the abundances of the phylogenetic sequence in Fig. 28. The succession *T. primula*, *T. praeticinensis*, *R. subticinensis*, *R. ticinensis* and

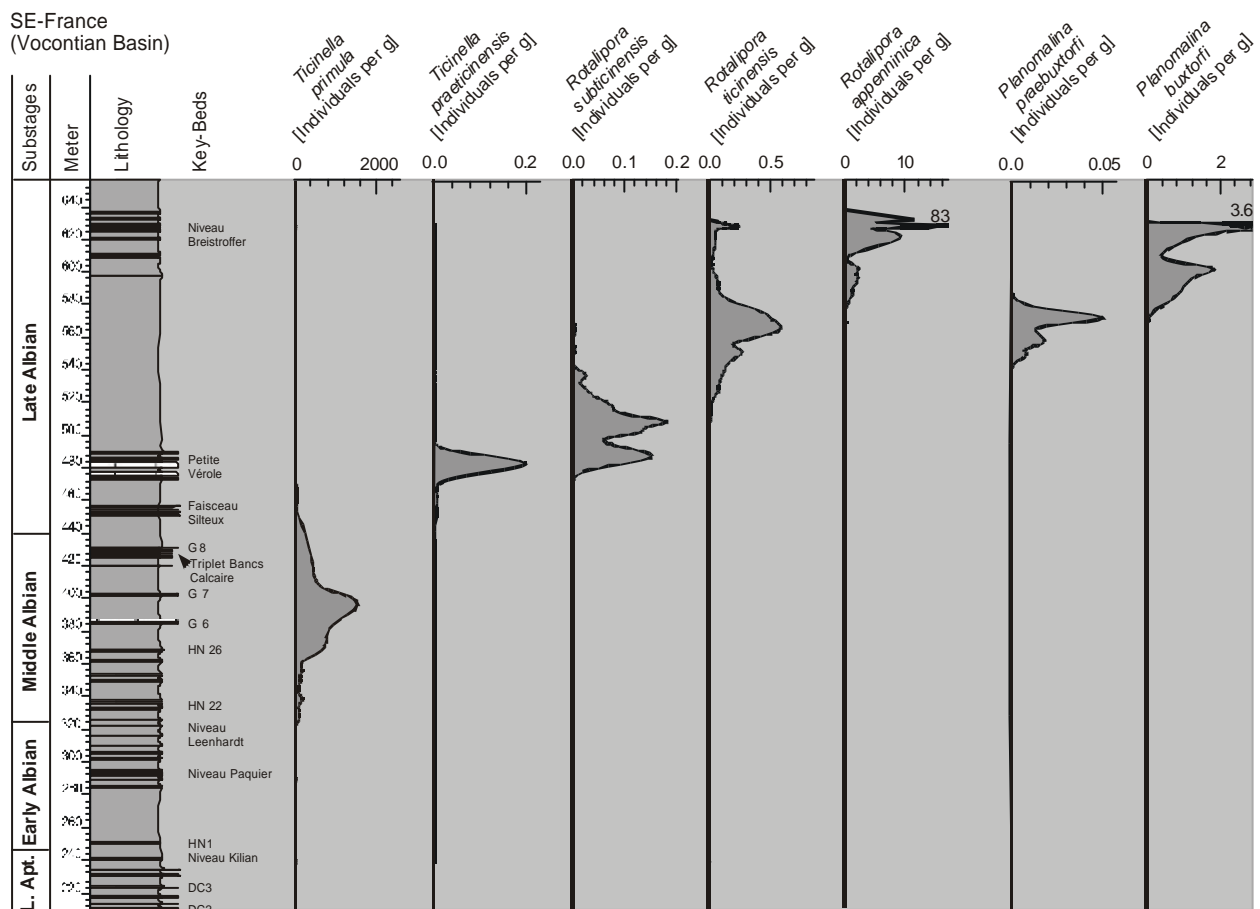


Fig. 28: Total abundances of the successive appearance of *Ticinella primula*, *Ticinella praeticinensis*, *Rotalipora subticinensis*, *Rotalipora ticinensis* and *Rotalipora appenninica* as well as *Planomalina praebuxtorfi* and *Planomalina buxtorfi* in mean values (Ind./g).

R. appenninica reflects an evolution from the middle calcified (Huber et al., 1995), planispiral (Caron, 1985), mid water depth (Hart & Bailey, 1979) species *Ticinella primula* to the heavily calcified (Huber et al., 1995), keeled, deep water depth (Hart & Bailey, 1979) species *Rotalipora appenninica*. Whereas the food preference of *T. primula* is unknown, for *R. appenninica* phytodetritus is presumed, conferring to the modern analogy of *Globorotalia truncatulinoides* (Hart & Bailey, 1979).

3.4.4. Biostratigraphy of the Late Aptian to Late Albian

A revised, detailed, high resolution stratigraphical zonation based on planktic foraminifera, with 10 zones and subzones for the Late Aptian to Late Albian (Délits Calcaires 2 to Niveau Breistroffer; Fig. 29) is compared with previous works (e.g. Moullade, 1966; Caron in Bréhéret et al., 1986; Bréhéret, 1997). Especially in the Late Albian, two additional

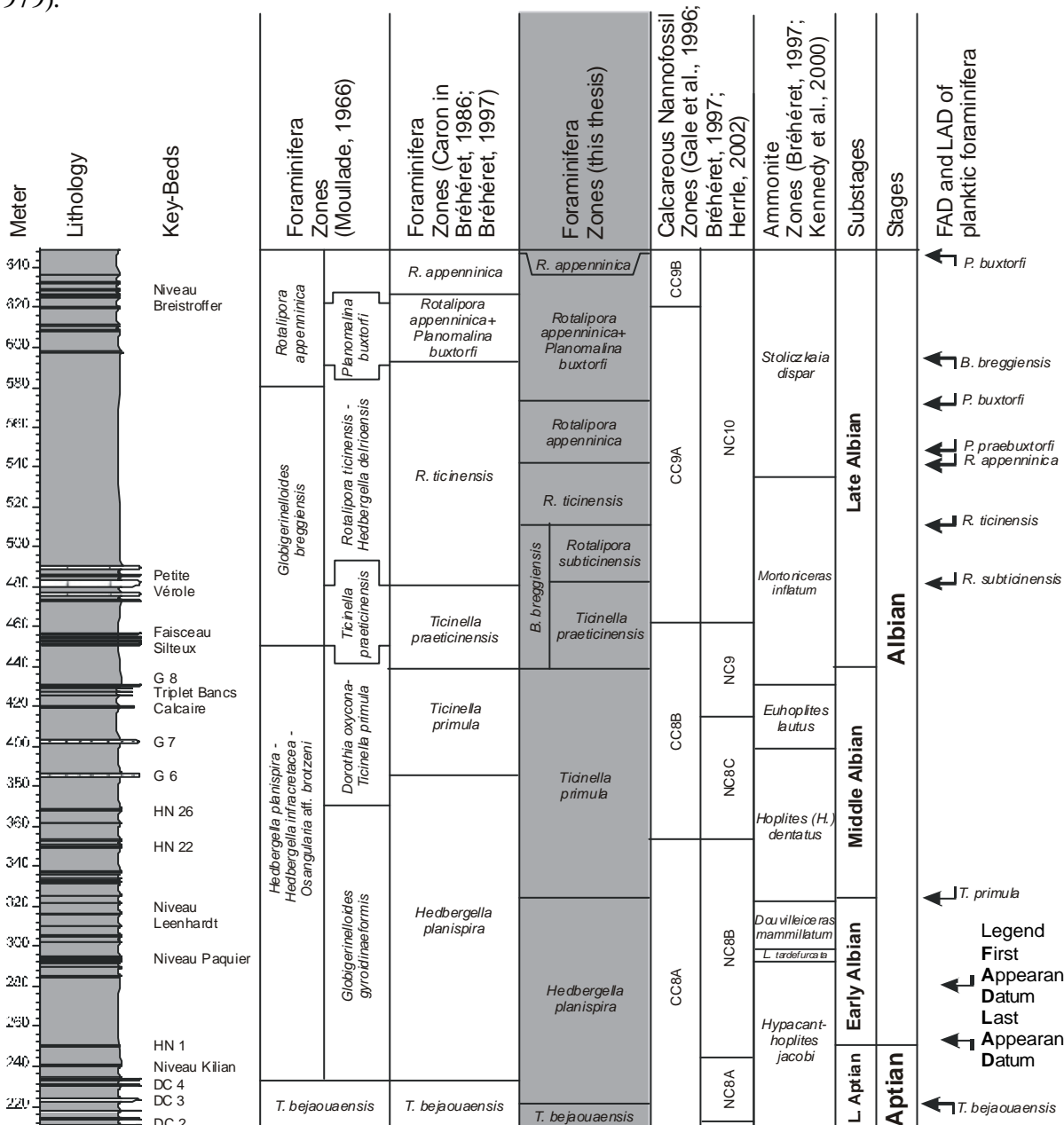


Fig. 29: Biostratigraphic zonation for the Later Aptian and Albian of SE-France (grey shaded) based on planktic foraminifera compared with the work of Moullade (1966), Caron in Bréhéret (1986) and Bréhéret (1997). In addition, the calcareous nannofossil and ammonite zonation (Gale, 1996; Bréhéret, 1997; Herrle & Mutterlose, 2003) is shown.

(subzones) are identified. The stratigraphy based on the observed first and last appearances (FADs and LADs; Fig. 24) and adopted the biostratigraphical view of Caron (1985), Sliter (1989,1992) and Robaszynski & Caron (1995) for the Tethyan realm. The stratigraphical zonation of planktic foraminifera (Fig. 29) is completed with zonation schemes of calcareous nannofossils and ammonites (Gale et al., 1996; Br  h  ret, 1997; Kennedy et al., 2000; Herrle; 2002). Following planktic foraminifera zones can be recognised (Fig. 29):

Ticinella bejaouaensis zone

Base: First appearance datum (FAD) of *Ticinella bejaouaensis*

Top: Last appearance datum (LAD) of *Ticinella bejaouaensis*

Range: The base of the *T. bejaouaensis* zone is not studied. The top of this zone is situated 1 m below the horizon D  lits Calcaires 3 (DC 3). Moullade (1966) and the relating work of Br  h  ret (1997) placed the top of the *T. bejaouaensis* zone near the D  lits Calcaire 4 (DC 4), a few metres below the Niveau Kilian (Fig. 29).

Remarks: In the upper part of this zone *Prediscosphaera columnata* emerges for the first time. The top of this zone is characterised by the carbonate layers D  lits Calcaires 3 and 4 (DC 3 and 4).

Hedbergella planispira zone

Base: LAD of *Ticinella bejaouaensis*

Top: FAD of *Ticinella primula*

Range: The *H. planispira* zone includes the interval from 1 m below DC 3 to the Haut Noirs 19 (HN 19). Moullade (1966) defined a *Hedbergella planispira*/*Hedbergella infracretacea*/*Ossangularia* aff. *brotzeni* zone for this section. This zone reaches until the Faisceau Silteux and can be divided into the *Globigerinelloides gyroidinaeformis* and *Dorothia oxycona*/*Ticinella primula* subzones. Caron (in Br  h  ret, 1986) and Br  h  ret (1997) placed the *H. planispira* zone between the top of DC 3 and the sand layer G 6 (Fig. 29).

Remarks: In the lower part of the *H. planispira* zone the first appearance of the calcareous

nannoplankton *Hayesites albiensis* can be observed. Also the FADs of the ammonites *Leymeriella tardefurcata*, *Hoplites dentatus* und *Douvilleiceras mammillatum* are described. Br  h  ret (1997) and Kennedy et al. (2000) observe a mass-appearance of *L. tardefurcata* at the base of the Niveau Paquier. In the *H. planispira* zone 12 m below the Niveau Paquier an increase in the abundance of planktic foraminifers (63-500 μ m) can be described (see Fig. 17). This superregionally observed increase either mark the end of a crisis in the evolution of planktic foraminifers (Br  h  ret & Delamette, 1989; Premoli-Silva & Sliter, 1999) or the end of reinforced carbonate dissolution (Erba, 1992; Premoli-Silva & Sliter, 1999). This interval is also characterised by the superregionally distributed black shale event Niveau Paquier (Oceanic Anoxic Event 1b, OAE 1b) and the regionally occurring Niveau Leenhardt black shale.

Ticinella primula zone

Base: FAD of *Ticinella primula*

Top: FAD of *Ticinella praeticinensis*

Range: This zone comprises the section from Haute Noirs 19 (HN 19) to 6 m above the sandy turbidite G 8 (Fig. 29). Moullade (1966) defines the *T. primula* zone together with *Dorothia oxycona* as a subzone within the *H. planispira* zone. After Br  h  ret (1997) the *T. primula* zone reaches from the turbidite G 6 to G 8. Caron in Br  h  ret et al. (1986) and Kennedy et al. (2000) describe the base of this zone between 35 m (Br  h  ret et al., 1986) and 55 m (Kennedy et al., 2000) above the Niveau Leenhardt.

Remarks: Within the *T. primula* zone the FAD of *Tranolithus orinatus* 29 m below G 6 and of *Axopodorhabdus albianus* 12 m above G 7 can be observed. Additionally, the ammonites *Euhoplites lautus* (2 m below G 7) and *Mortoniceras inflatum* (2 m below G 8) occur for the first time (Br  h  ret, 1997). At the base of the *T. primula* zone, 10 m above the Niveau Leenhardt, planktic foraminifers > 250 μ m re-emerge (Fig. 17). The lower part of this zone is characterised by the black shales of the Niveau Leenhardt to Haute Noirs 26 (HN 26), the upper part by the turbidites G6 to G 8.

Biticinella breggiensis zone

Base: FAD of *Biticinella breggiensis*

Top: FAD of *Rotalipora ticinensis*

Range: The *B. breggiensis* zone starts 4 m above the turbidite G 8 and reaches until 28 m above the Petite Vérole (Fig. 29). For this interval, Moullade (1966) described a *Globigerinelloides breggiensis* zone which is divided into the *Ticinella praeticinensis* and *Rotalipora ticinensis/Hedbergella delrioensis* subzone. Bréhéret (1997) specified no *B. breggiensis* zone but subdivided the section into the *Ticinella praeticinensis* and *Rotalipora ticinensis* zone. In the previous works of Moullade (1966) and Bréhéret (1997) these planktic foraminifera zones comprise more than half of the Late Albian. Based on the observed FAD of *Rotalipora subticinensis* and due to the international stratigraphy from Sliter (1989; 1992) and Robaszynski & Caron (1995), the *R. subticinensis* subzone is inserted between the *T. praeticinensis* subzone and the *R. ticinensis* zone. The result is a higher resolution of the Late Albian (Fig. 29).

Ticinella praeticinensis subzone

Base: FAD of *Ticinella praeticinensis*

Top: FAD of *Rotalipora subticinensis*

Range: This zone starts 6 m above the turbidite G 8 and ends in the Petite Vérole. *T. praeticinensis* and *B. breggiensis* emerge synchronously in SE-France (Fig. 29).

Remarks: The calcareous nannofossil *Eiffellithus turriseiffelii* first occurs 12 m below the Petite Vérole (Bréhéret, 1997). FAD of ammonites can not be observed. This interval is characterised by small glauconitic silt- and sandlayers (Faisceau Silteux).

Rotalipora subticinensis subzone

Base: FAD *Rotalipora subticinensis*

Top: FAD *Rotalipora ticinensis*

Range: The base of this subzone is located in the Petite Vérole and ends 32 m above it (Fig. 29).

Remarks: In this subzone no first occurrences of calcareous nannofossils or ammonites can be described. The interval is characterised by the limy beds of the Petite Vérole.

Rotalipora ticinensis zone

Base: FAD of *Rotalipora ticinensis*

Top: FAD of *Rotalipora appenninica*

Range: The base of the *R. ticinensis* zone is located 22 m above the Petite Vérole and ends 52 m above it (Fig. 29). Moullade (1966) and Bréhéret (1997) located the range of the *R. ticinensis* zone from the Petite Vérole to 30-40 m below the Niveau Breistroffer. According to the stratigraphical data of this thesis, the *R. ticinensis* zone comprises a smaller time interval compared with Moullade (1966) and Bréhéret (1997), which leads to a higher resolution of the Late Albian (Fig. 29).

Remarks: The ammonite *Stoliczkaia dispar* first occurs 46 m above the Petite Vérole. The *R. ticinensis* zone is characterised by a lime- / marlstone alternation.

Rotalipora appenninica zone

Base: FAD of *Rotalipora appenninica*

Top: FAD of *Rotalipora globotruncanoides* (younger synonym of *Rotalipora brotzeni*; after González Donoso & Linares in Robaszynski et al., 1994)

Range: The *Rotalipora appenninica* zone begins 83 m below the Niveau Breistroffer. The FAD of *R. globotruncanoides* can not be observed in the studied succession. Due to the FAD of *Planomalina buxtorfi* 50 m below and the LAD 18 m above the Niveau Breistroffer, a *R. appenninica/P. buxtorfi* partial range zone can be described (Fig. 29). Moullade (1996) and Bréhéret (1997) also show a *R. appenninica* and a *R. appenninica/P. buxtorfi* partial range zone in the Late Albian. The data shows that *P. buxtorfi* occurs after *R. appenninica*. Consequently the *R. appenninica* zone is here divided into three and not only two (Bréhéret, 1997) subzones (Fig. 29).

Remarks: In its upper part the *R. appenninica/P. buxtorfi* partial range zone is characterised by the black shales of the Niveau Breistroffer. The Niveau Breistroffer is marked by a high abundance of *R. appenninica* and *R. ticinensis* (see Fig. 22). This *Rotalipora* acme may as well be observed in the boreal realm (Weiss, 1997). This marker horizon may have a good correlation potential because of the referring LAD of

Hayesites albiensis 3 m below the Niveau Breistroffer (Gale et al., 1996).

3.4.5. High resolution Carbon Isotope Stratigraphy of the Late Aptian to Late Albian

Based on the work of Scholle & Arthur (1980), different authors (Weissert & Lini, 1991; Menegatti et al., 1998; Bralower et al., 1999; Herrle, 2002) have shown the applicability of carbon isotopes for regional to global correlation. The exact terms to describe the carbon isotope curves ($\delta^{13}\text{C}$) of the Aptian and Albian are still discussed (Menegatti et al., 1998; Bralower et al., 1999; Herrle, 2002). The studies of Scholle & Arthur (1980), Menegatti et al. (1998) and Nederbragt et al. (2001) deal only with short intervals of the Aptian or Albian. Previous studies which cover longer time intervals are low-resolution curves (5 to 10 m). However the $\delta^{13}\text{C}$ curve of this study is in high resolution (2 to 60 cm) and comprises the Early/Middle Albian and Late Albian (Fig. 30). The results of this study are supplemented with $\delta^{13}\text{C}$ data of Herrle (2002) for the Late Aptian and Early Albian, from Bornemann (2000) for the Late Albian interval of the Niveau Breistroffer and Gale et al. (1996) for the Early Cenomanian (Fig. 30). These data are used to establish a CIS for the Early Albian to Early Cenomanian in SE-France. The 26 zones of the CIS are based on a structuring of the $\delta^{13}\text{C}$ record in intervals with increasing, decreasing and stable values. These single intervals are of superregional significance and can be correlated with comparable intervals at the DSDP Site 545 (Herrle, 2002) and 547 (Nederbragt et al., 2001) at the Mazagan Plateau (Fig. 30), and the ODP Site 1052 (Wilson & Norris, 2001) at the Blake Nose Plateau (Fig. 31).

The nomenclature of the CIS for the Early Albian (Al 7 to Al 22) to Early Cenomanian (Ce 1 to Ce 3) is established in this study. It is based on Herrle (2002) and continues his work for the Aptian and Early Albian (Ap 1 to Al 6; only Ap 15 to Al 6 used herein). In the following, the segments Al 7 to Ce 3 of the CIS are described with respect to planktic foraminifera, calcareous nannofossils and ammonite biostratigraphy

(Fig. 30). For a detailed description of the units Ap 15 to Al 6 see Herrle (2002).

Al 7 Zone

Definition: This unit is marked by balanced $\delta^{13}\text{C}$ values about 2 ‰. The start and the end of this interval is characterised by a shift of the values about 0.2 ‰.

Range: Middle Albian. Lower part of the *Ticinella primula* zone, at the base of the NC8C calcareous nannofossil subzone and in the middle part of the *Hoplites H. dentatus* ammonite zone.

Remarks: This interval is marked by the black shale horizons of the Haute Noirs 23, 24 and 25.

Al 8 Zone

Definition: Slow decrease of the $\delta^{13}\text{C}$ values by up to 1.2 ‰.

Range: Middle Albian. In the middle part of the *T. primula* zone, NC8C nannofossil subzone and the top of the *H. H. dentatus* zone.

Remarks: In the lower part of this unit black shale horizons (HN 26) and in the upper part sandy turbidites (G 6) occur.

Al 9 Zone

Definition: This interval is marked by slow increasing $\delta^{13}\text{C}$ values up to 1.5 ‰.

Range: Upper Middle Albian. Top of the *T. primula* zone, top of the NC8C and base of the NC9 calcareous nannofossil zone and *Euhoplites lautus* ammonite zone.

Remarks: This unit is characterised in the lower part by the sandy turbidite G 7 and in the top by the Triplet Banc Calcaire.

Al 10 Zone

Definition: Slight decrease of about 0.6 ‰.

Range: Base of the Late Albian. *Biticinella breggiensis* zone (upper part of the *Ticinella praeticinensis* subzone), top of the NC9 and base of the NC10 calcareous nannofossil zone and middle of the *Mortoniceras inflatum* ammonite zone.

Remarks: The base of this interval is marked by the siliceous Faisceau Silteux and the top by the carbonaceous layers of the Petite Vérole.

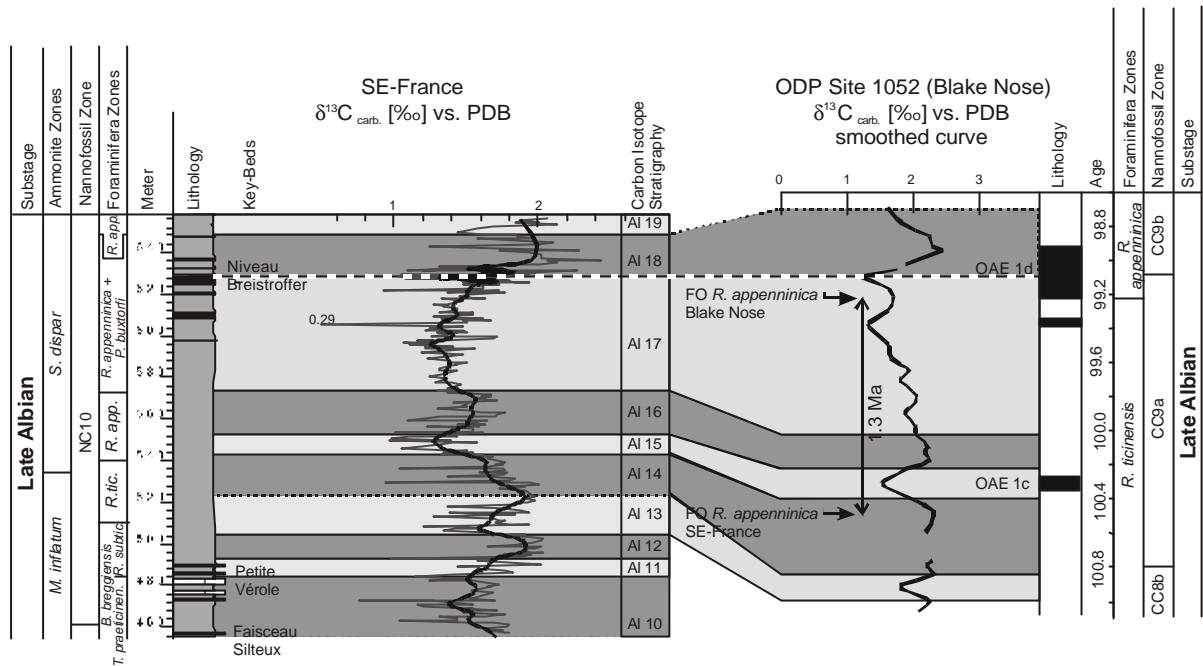


Fig. 31: Correlation of the Carbon isotope record of SE-France and the $\delta^{13}\text{C}$ record of the ODP Site 1052 (Wilson & Norris, 2001) at the Blake Nose Plateau. Additionally, a detailed correlation of the black shale horizon Niveau Breistroffer and the OAE 1d (black dotted line) is shown.

Al 11 Zone

Definition: Rapid positive $\delta^{13}\text{C}$ excursion about 0.8 ‰.

Range: Late Albian. Middle of the *B. breggiensis* zone and base of the *Rotalipora subticinensis* subzone, NC10 calcareous nannofossil zone and middle of the *M. inflatum* ammonite zone.

Remarks: This interval comprises the top of the carbonaceous event Petit Vérole.

Al 12 Zone

Definition: This interval is characterised by balanced $\delta^{13}\text{C}$ values about 2‰.

Range: Late Albian. Top of the *B. breggiensis* zone (also top of the *R. subticinensis* subzone), NC10 calcareous nannofossil zone and *M. inflatum* ammonite zone.

Remarks: This unit ends with a sharp decrease in $\delta^{13}\text{C}$ values about 0.4 to 0.6 ‰.

Al 13 Zone

Definition: Slight increase in carbon isotope values of about 0.6 ‰.

Range: Late Albian. Top of the *B. breggiensis* zone (also top of the *R. subticinensis* subzone) and base of the *Rotalipora ticinensis* zone, NC10

and *M. inflatum* zone.

Al 14 Zone

Definition: Slight decrease in carbon isotope values of about 0.6 ‰

Range: Late Albian. Top of the *Rotalipora ticinensis* zone, NC10, *M. inflatum* zone and base of the *Stoliczkaia dispar* zone.

Al 15 Zone

Definition: This interval is marked by a decrease in $\delta^{13}\text{C}$ values about 0.7 ‰.

Range: Late Albian. Base of the *Rotalipora appenninica* zone, NC10 calcareous nannofossil zone and lowermost part of the *S. dispar* ammonite zone.

Al 16 Zone

Definition: A rapid increase of about 0.2 ‰, followed by a slight decrease of also 0.2 ‰.

Range: Late Albian. Part of the *R. appenninica* zone, NC10 calcareous nannofossil zone and part of *S. dispar* ammonite zone.

Al 17 Zone

Definition: A slight decrease in $\delta^{13}\text{C}$ values by

up to 0.6 ‰. This unit ends with a sharp negative excursion of about 1 ‰.

Range: Late Albian. This unit comprises two thirds of the *Rotalipora appenninica/Planomalina buxtorfi* partial range zone, NC10 calcareous nannofossil zone and *S. dispar* ammonite zone.

Remarks: The negative excursion at the top of this interval is accompanied by the basinwide and probably globally distributed black shale horizons of the Niveau Breistroffer (OAE 1d).

Al 18 Zone

Definition: Rapid increase of the $\delta^{13}\text{C}$ values by up to 1.2 ‰ (positive excursion) with a slight decrease of about 0.6 ‰.

Range: Late Albian. Top of the *R. appenninica/P. buxtorfi* partial range zone, NC10 calcareous nannofossil zone and *S. dispar* ammonite zone.

Al 19 Zone

Definition: Rapid increase of the $\delta^{13}\text{C}$ values by up to 0.8 ‰.

Range: Late Albian. In the *Rotalipora appenninica* zone immediately above the top of the *R. appenninica/P. buxtorfi* partial range zone, NC10 calcareous nannofossil zone and *S. dispar* ammonite zone.

Al 20 Zone

Definition: This interval is marked by balanced $\delta^{13}\text{C}$ values about 2.3 ‰.

Range: Late Albian. *Rotalipora appenninica* zone, NC10 calcareous nannofossil zone and *S. dispar* ammonite zone

Al 21 Zone

Definition: Short negative excursion of 0.8 ‰.

Range: Upper part of the *Rotalipora appenninica* zone, NC10 calcareous nannofossil zone and *S. dispar* ammonite zone.

Al 22 Zone

Definition: This unit is characterised by balanced $\delta^{13}\text{C}$ values about 2.2 ‰.

Range: Late Albian and Early Cenomanian. This interval comprises the top of the *R. appenninica* zone and the base of the *Rotalipora globotruncanoides* zone, NC10 calcareous

nannofossil zone, the top of the *S. dispar* and the base of the *Mantelliceras mantelli* ammonite zone.

Ce 1 Zone

Definition: A short negative excursion of about 1.0 ‰.

Range: Early Cenomanian. Lowermost part of the *R. globotruncanoides* zone, NC10 calcareous nannofossil zone and lower part of the *M. mantelli* ammonite zone.

Ce 2 Zone

Definition: Short increase in the $\delta^{13}\text{C}$ values by up to 0.8 ‰.

Range: Early Cenomanian. Lower part of the *R. globotruncanoides* foraminifera zone, NC10 calcareous nannofossil zone and base of the *M. mantelli* zone.

Remarks: This interval is marked by a change to more limy intercalations in the sediment succession.

Ce 3 Zone

Definition: This unit is characterised by stable values about 1.6 ‰.

Range: Early Cenomanian. *Rotalipora globotruncanoides* foraminifera zone, NC10 calcareous nannofossil zone and *M. mantelli* ammonite zone.

3.4.6. Aptian/Albian Stage and Albian Substage Boundaries in SE-France

Aptian/Albian Stage Boundary

The Albian Stage was introduced by d'Orbigny (1842-43) for the interval between the Aptian and the Cenomanian. Breistroffer (1947) defines the beginning of the Albian by the *Leymeriella tardefurcata* zone with *Leymeriella schrammeni* at the base (Hart et al., 1996). At the 1st Symposium on Cretaceous Stage Boundaries in Copenhagen (1983), the *L. schrammeni* zone was deemed to be a "better" base of the Albian than *Hypacanthoplites jacobi*. However, this species is unfortunately limited to the Boreal Northern Europe (Birkelund et al., 1984; Hancock, 1991, 2001). In Brussels at the 2^d Symposium on Cretaceous Stage Boundaries

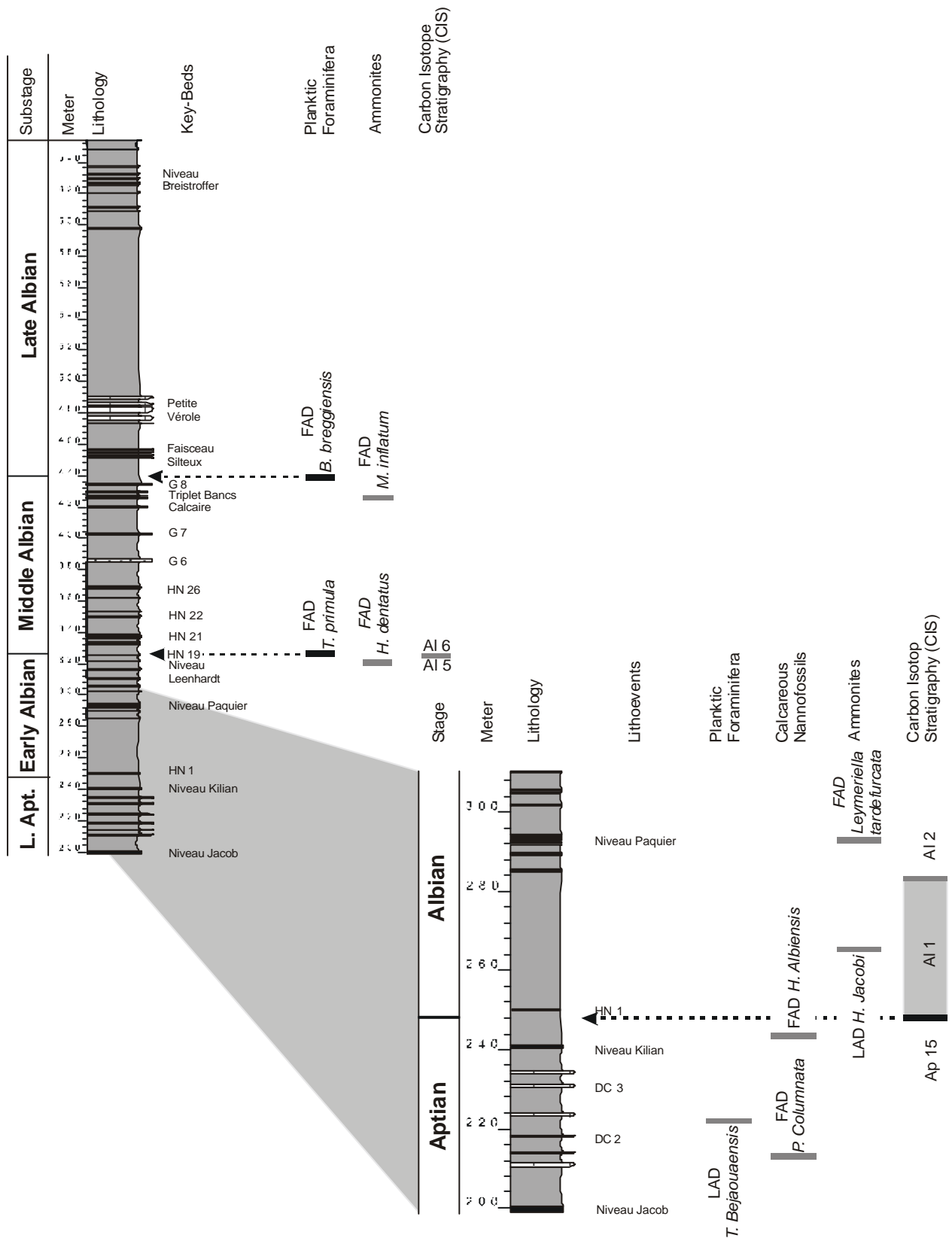


Fig. 32: Overview of the Late Aptian to Late Albian of SE-France with bio-, isotopic- and lithostratigraphic marker horizons. Additionally on a detailed view of the Aptian/Albian stage boundaries interval and useable stage boundary markers. First appearance datum (FAD) of planktic foraminifera and lithological events (this thesis), FAD of calcareous nannofossils and isotope stratigraphy for the Late Aptian and Early Albian (Gale et al., 1996; Herrle & Mutterlose, 2003), ammonites in accordance with Kennedy et al. (2000).

(1995), the sections in Vöhrum (NW-Germany) and at the Col de Pré Guittard (SE-France) were proposed to be “Global Boundary Stratotype Sections and Points” (GSSP). Whereas 1995 not enough data for a decision were available, Kennedy et al. (2000) and the present thesis provide new insights into the definition of the Aptian/Albian stage boundary based on the Col de Pré Guittard section. After the evaluation of the sections Tarendol, Col de Pré Guittard, Les Oustaus and Arboudeysse, the following bio-, isotopic- and lithostratigraphic markers for the definition of the Aptian/Albian boundary in the interval between the Niveau Jacob and the Niveau Paquier are available (Fig. 32): From bottom to top (Niveau Jacob to 16 m above the Niveau Paquier), this is the last appearance datum (LAD) of *Ticinella bejaouaensis* (this thesis), for the planktic foraminifera and the first appearance datum (FAD) of *Prediscosphaera columnata* and *Hayesites albiensis* (Herrle & Mutterlose, 2003) for calcareous nannofossils can be described. The LAD of *T. bejaouaensis* is not considered as boundary marker, because this LAD is regarded as diachronous (see chapter 5.1). Superregionally, isochronous FADs or LADs of planktic foraminifera can not be demonstrated for this time interval. In addition, the FAD of *Hypacanthoplites jacobii* (Hart et al., 1996; Kennedy et al., 2000) and of *Leymeriella tardefurcata* (Bréhéret et al., 1986; Kennedy et al., 2000) are found in the interval from the Niveau Jacob to Niveau Paquier. The exclusive distribution of *L. tardefurcata* in the Tethyan realm limited the applicability of this species as Aptian/Albian boundary marker. Because of the endemism of ammonite faunas and the widespread gaps in the successions comprising this stage boundary, Hancock (2001) assumed that a world-wide event at around 112 Ma -as usable international standard- or the Aptian/Albian boundary- will never be found. Therefore, Hancock (2001) suggested to move the boundary to the nearest horizon, the base of the *Lyelliceras lyelli* zone. Unfortunately, *L. lyelli* is commonly used as base of the Middle Albian and a precise definition of the base of the *L. lyelli* zone is not possible. Regarding these objections

it may not be wise to use *L. lyelli* as boundary criterion. It should be considered to abandon ammonite FADs as markers for the Aptian/Albian boundary. As Hancock (2001) concludes a completely different datum should be chosen. The Aptian/Albian boundary interval is marked by a long-term decrease in carbon isotope values (in the CIS: the transition from zone Ap15 to Al1; Herrle 2002). The correlation of the carbon isotope record of SE-France with the Mazagan Plateau (Fig. 30) shows that this decrease is a global signal, which can be found in pelagic/hemipelagic as well as in shallow marine environments (Grötsch et al., 1998). The Aptian/Albian boundary interval is also marked by the black shales of the Niveau Jacob, Niveau Kilian and Niveau Paquier. Lithological events as the aforementioned black shales cannot be traced in shallow marine environments and consequently are not qualified as boundary markers. After considering all bio-, isotopic- and lithostratigraphic markers described above, the Aptian/Albian boundary will now be defined (in this thesis) 5.5 m above the Niveau Kilian at the base of the long-term decrease in the $\delta^{13}\text{C}$ record (Ap15 to Al1), as Herrle (2002) suggested (Fig. 32).

Early/Middle Albian Substage Boundary

At the 1st Symposium of Cretaceous Stage Boundaries in Copenhagen (1983; Birkelund et al., 1984) the *Lyelliceras lyelli* zone was defined as base of the Middle Albian, it was acknowledged that further investigations were needed (Hart et al., 1996). It should be noted that *L. lyelli* cannot be observed in SE-France and consequently is not available as boundary marker in the Vocontian Basin. But, considering the suggestion of Hancock (2001) to move the Aptian/Albian boundary, then it will have significant effects on the Middle Albian. It will result in ignoring the Early Albian completely (Fig. 1 in Hancock, 2001). Alternatively, the base of the *Hoplites (H.) dentatus* zone could be used as Middle Albian boundary (Owen, 1984; Hancock, 1991). For a definition of the base of the Middle Albian, several bio- and lithological markers are available (Fig. 32): firstly, there is the FAD of *Ticinella primula* 7.5 m above the

Niveau Leenhardt. Secondly, according to Bréhéret (1997), the FAD of *H. (H.) dentatus* 4.5 m above the Niveau Leenhardt, as well as the change from a short termed decrease in the $\delta^{13}\text{C}$ record (Al5) to an interval of more stable carbon isotope values (Al 6) can be observed. Now the base of the Middle Albian is defined by the FAD of *T. primula* 7.5 m above the Niveau Leenhardt (Fig. 32).

Middle/Late Albian Substage Boundary

Breistroffer (1947) defined the Late Albian boundary by the base of the *Dipoloceras cristatum* ammonite subzone, which is equivalent to the base of the *Mortoniceras inflatum* zone. The discussion at the symposiums in Copenhagen (1983) and Brussels (1995), accepted these results (Hart et al., 1996). In this thesis, the base of the Late Albian is defined by the FAD of *Biticinella breggiensis* 6 m above the sandstone G8 (Bréhéret, 1997; Fig. 32), accompanied by the FAD of *Mortoniceras inflatum* 2 m below G8.

4. NE-Texas

4.1. Geology and Palaeogeography of Texas

The geology of Texas is characterised by the Palaeozoic Llanorian geosyncline. In the Ordovician to Permian Appalachian Orogeny the geosyncline was folded to the Quachita-Marathon-Mountains (Fig. 33), the most southern and independent part of the Appalachian Mountain chain (Schuchert, 1943; Eisbacher, 1988). Most of the Quachita-Marathon-Mountains and their borderland are now buried under 1000 m thick sediments of the Gulf of Mexico, which emerges since the Late Jurassic over the Palaeozoic basement (Schuchert, 1943; Finsley, 1996; Fig. 33). The ancient foreland of the mountain belt with its Permian and Triassic terrestrial sediments can be found only in the Panhandle (Fig. 33). The Mesozoic (mainly Cretaceous) and Cenozoic sediment successions result from the transgression of the Gulf of Mexico and follow the morphology of the Gulf Coast. (Finsley, 1996; Fig. 33).

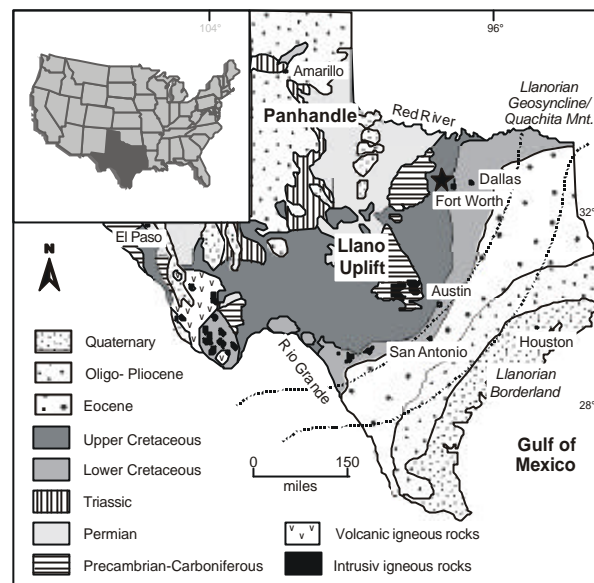


Fig. 33: Geological map of Texas (modified after Finsley, 1996) with the study area marked by an asterisk.

During the Cretaceous, the investigated area of NE-Texas was part of the widespread continental Comanchean Shelf and situated at a palaeolatitude of 40° N (Voigt, 1996). The shelf was divided from south to north into the McKnight Basin, Kirschberg Lagoon, the East Texas Embayment (ETB) and carbonate platforms (Murray, 1961; Hayward & Brown, 1967). The Stuart City and the Central Texas Reef trend separated the Comanchean Shelf and the East Texas Embayment (ETB) from the western Atlantic (Scott, 1990; Fig. 34). The region of investigation in NE-Texas is situated in the eastern part of the East Texas Embayment. The sedimentation in the East Texas Embayment during the upper mid-Cretaceous was controlled by third order long-term transgressive-regressive deposition cycles (Scott et al. 2000). The Middle to Late Albian in the ETB is characterised by the cyclic deposition of lime-, silt-, marl- and mudstones (Hendricks, 1967; Scott et al., 1994). The thickness of the whole succession and the single cycles varies vertically and laterally and shows a movement of the basin depotcenter during time. The palaeo-water depth of the ETB is estimated at about 50 to 100 m by faunal data (Scott et al., submitted).

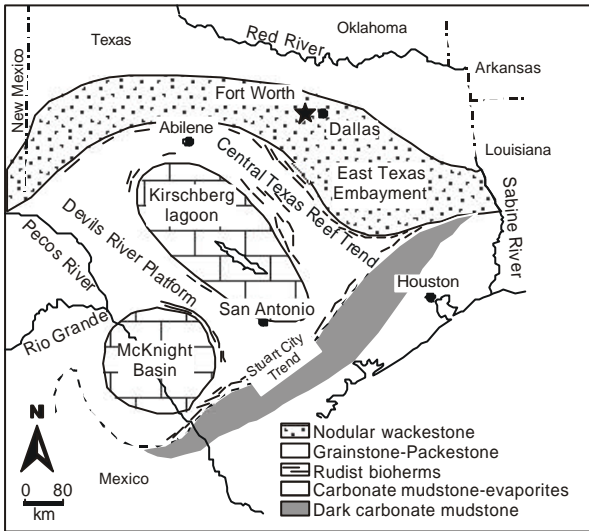


Fig. 34: Palaeogeographic map of NE-Texas during the Albian (after Fisher & Rodda, 1969). The area of study is marked by an asterisk.

The mid-Cretaceous of NE-Texas is represented in the sediments of the so-called Comanchean Series, which ranges from the late Early Aptian to the Early Cenomanian (114.5 to 94.4 Ma; Scott et al., 2000). This series is a time-stratigraphic unit defined by its unconformable bounding surfaces (e.g. Hill, 1901; Salvador, 1991; Wilson & Ward, 1993). The Comanchean Series is divided into the Trinity, Fredericksburg and Washita groups (Mosteller, 1970; Rose, 1972) comprising several formations (Fig. 35). These terms are lithostratigraphical and not chronostratigraphical units representing long-term transgressive-regressive depositional cycles (Scott et al., submit). In this thesis, the upper part of the Fredericksburg and the main part of the Washita group is studied. The Fredericksburg group (108.2 to 104.0 Ma; Scott et al., 2000) represents a second order depositional cycle (Scott et al. 2000) and is divided into the Paluxy, Walnut and Goodland formation in NE-Texas (Scott et al., submitted; Fig. 35). The Washita group (104.0 to 94.4 Ma; Scott et al., 2000) also represents a second order depositional cycle comprising 9 formations. These lithostratigraphic units are the Kiamichi, Duck Creek, Fort Worth, Denton, Weno, Pawpaw, Main Street, Grayson and Buda formation. The formations do not exactly coincide with the

6 shale-limestone couplets (Scott, 1976; Scott et al., 1978) representing third-order transgressive-regressive depositional cycles (Fig. 35). The contact between the Fredericksburg and the Washita group is represented by a transgressive flooding surface at the boundary between the Goodland and Kiamichi formations. The origin of this sedimentation cyclicity is assumed in subsidence rates, wave base depth and sediment input (Scott et al., 1978) and results in changing basin and shelf depositional conditions (Scott et al., submitted). Eustatic sea-level changes are also presumed as originator (Scott et al., 1994, Immenhauser et al., 1999;

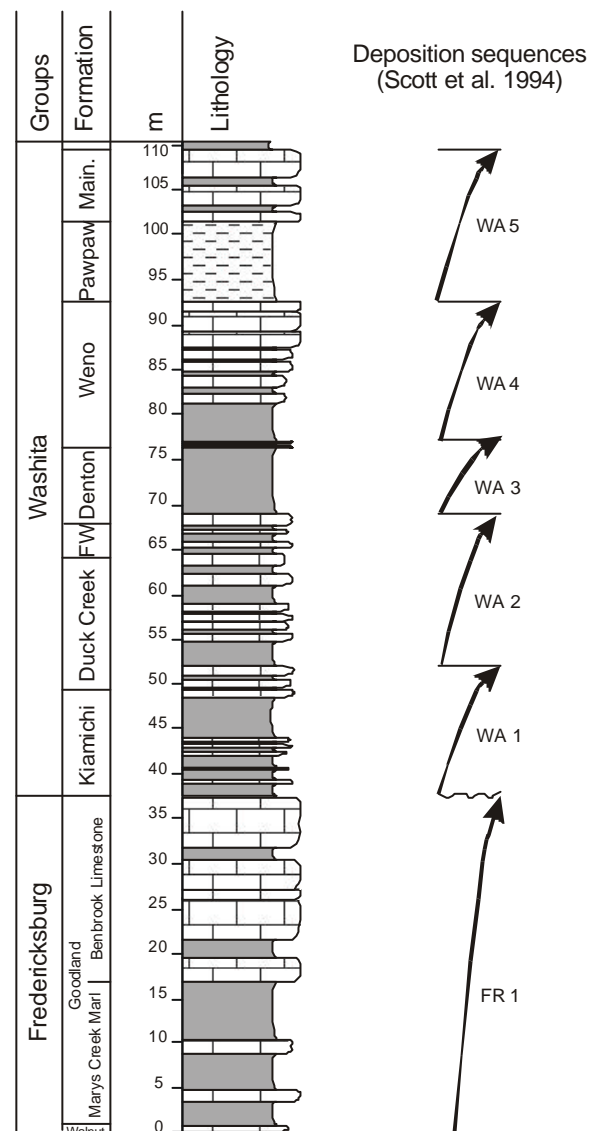


Fig. 35: Litho- and cyclostratigraphic structuring of the Middle to Late Albian sediment succession of NE-Texas (modified after Scott et al., 2000)

Scott et al., 2000) of these cycles. Correlations of these cycles with the Western Interior (Scott et al., 1994), Northern Mexico (Scott et al., submitted) and the Arabian platform (Scott et al., 2000) are possible.

4.2. Lithology and Description of Investigated Sections NE-Texas

The upper Middle Albian to lowermost Early Cenomanian of NE-Texas was studied in 9 sections (Marys Creek I-II, Vickery Boulevard., Meacham Field, Seminary Drive, Lancaster Avenue, Interstate 30 & Ben Street, Interstate 30 & Menzer Street and Sunset Oaks) in the area of Fort Worth (Fig. 36), comprising 185 samples. The successions are correlated with distinct lithological formation boundaries after Scott (pers. com.). The samples were taken in 0.10 to 0.60 m intervals. The co-ordinates for the measured sections are given in UTM due to the 1:24000 scale of the topographic maps (TM) of the USGS. A road map of NE-Texas with the location of these sections is given in Appendix 1.

Fig. 36: →

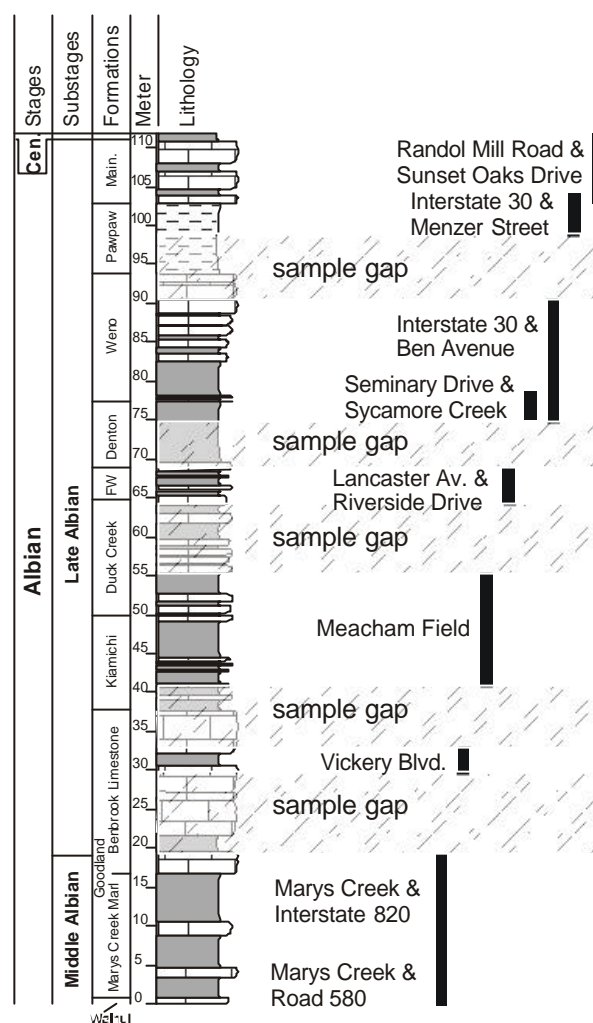
Overview of the investigated sections and their stratigraphical ranges in NE-Texas.

4.2.1. Marys Creek I

Location and grid reference: East cutbank of Marys Creek, at the north side of 580 (US 80-180), about 1.4 km west of Westland (Fig. 36, Appendix 15). TM Benbrook Quadrangle, co-ordinates X: 97°29'00'', Y: 32°42'37''.

Stratigraphic range: Middle Albian, Walnut and Goodland Formation (Marys Creek Marl).

Lithology: The 9 m thick section of Marys Creek I starts with a bioclastic lime-wackestone and ends with a limestone layer (1.60 m). This interval comprises a dark to blue marlstone light grey lime-wackestone alternation. Generally, the limestone in the lower part of the succession is nodular and characterised by bioclastic debris (Fig. 37). In the upper part, the limestone is stratified. A rich fauna of bivalves, texitryphaeid oysters, gastropods, ammonites and echinoids can be found in this succession (Perkins, 1960).



Main.=Main Street
FW=Fort Worth

Legend

- | | | | |
|--|-------------------|--|------------------|
| | Oystershellbed | | Gastropods |
| | Limestone | | Ammonites |
| | Marly Limestone | | Echinoids |
| | Limy marlstone | | Wood |
| | Marlstone | | Bioturbation |
| | Mudstone | | Studied sections |
| | Nodular limestone | | |
| | Limy nodules | | |
| | Lumachelle | | |
| | Bivalves | | |
| | Inocerams | | |
| | Oysters | | |

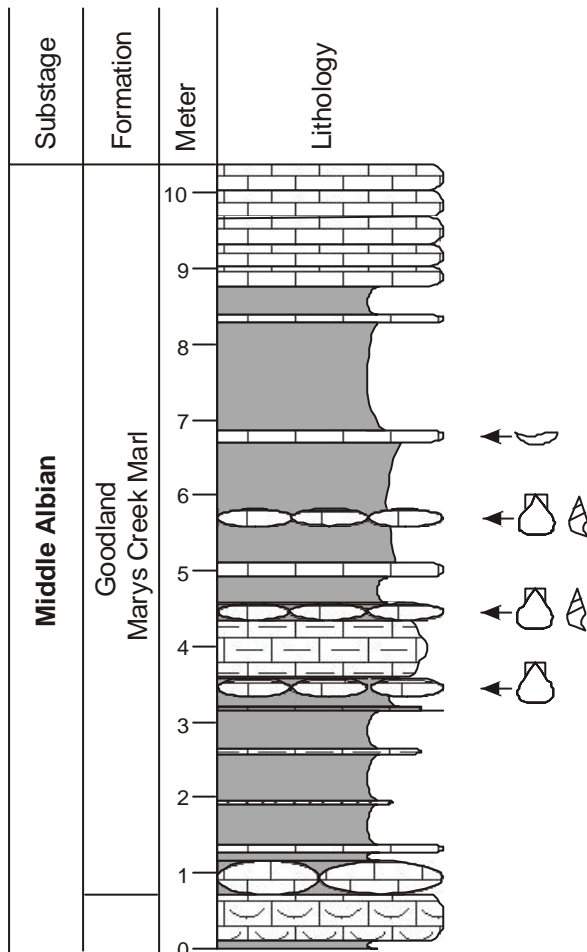


Fig. 37: Schematic lithological column of the Marys Creek I section. A detailed lithological column with sample distribution is given in Appendix 15. For lithological explanations and abbreviations see Fig. 36.

4.2.2. Marys Creek II

Location and grid reference: South cutbank of Marys Creek, about 1.4 km east of FM 2871 and west of the Interstate 820 (Fig. 36, Appendix 16). TM Aledo Quadrangle, co-ordinates X: 97°30'10'', Y: 32°43'25''.

Stratigraphic range: Middle to Late Albian, Goodland Formation (Marys Creek Marl and Benbrook Limestone).

Lithology: This section starts directly above the 1.6 m thick limestone (Marys Creek I) and ends 3 m above an abrupt change from marl/limestone alternation to limestone. In the lower part, the succession consists of interbedded marl- and limestone. The upper part is characterised by light grey, stratified, mollusc lime-wackestones. The limestone in the lower part is mainly

nodular and in the upper part stratified. Numerous limestone layers are characterised by bioclastic debris (bivalves, oysters, gastropods) or oysters (Fig. 38). The abrupt lithological change from marl- to limestone in the top of the section marks the boundary between Marys Creek Marl and Benbrook Limestone of the Goodland Formation (Perkins, 1960; Scott, pers. com., 2001). The fauna contains mainly oysters (*Gryphaea*) and gastropods, ammonites are common (Perkins, 1960; Lehmann, pers. com.,

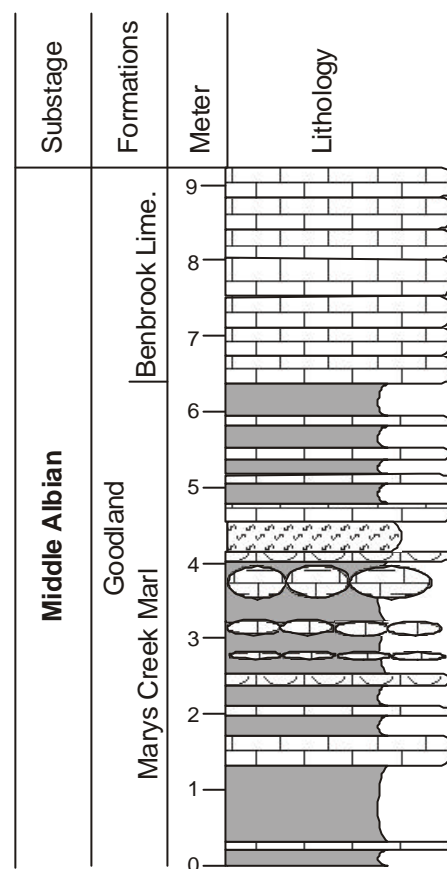


Fig. 38: Schematic lithological column of the Marys Creek II section. A detailed lithological column with sample distribution is given in Appendix 16. For lithological explanations and abbreviations see Fig. 36.

4.2.3. Vickery Blvd.

Location and grid reference: This section is situated south of Vickery Blvd., at the level of Almar York company next to the railroad tracks (Fig. 36; Appendix 17). TM Fort Worth Quadrangle, co-ordinates X: 97°20'30'', Y: 32°44'30''.

Stratigraphic range: Late Albian, Goodland Formation (Benbrook Limestone).

Lithology: This 3 m thick section starts with a marly limestone and ends with a limestone layer. The succession is dominated by light grey, stratified, lime-wackestone interbedded with dark grey marl intervals (Fig. 39). The first two layers are very rich in gastropods, ammonites (mass occurrence of *Oxytropidoceras*; pers. com. Lehmann, 2003) and echinoids (*Toxaster*).

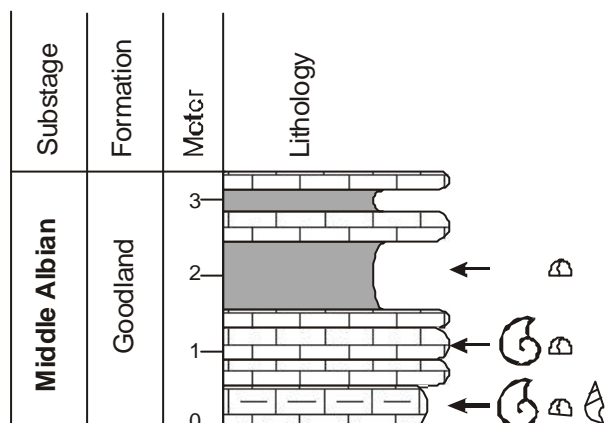


Fig. 39: Schematic lithological column of the Vickery Blvd. section. A detailed lithological column with sample distribution is given in Appendix 17. For lithological explanations and abbreviations see Fig. 36.

4.2.4. Meacham Field

Location and grid reference: This succession represents the north and south side of an old, disused quarry (Saginaw quarry) north of the Interstate 820 and east of the Old Decatur Road (Fig. 36; Appendix 18). TM Lake Worth Quadrangle, co-ordinates X: 97°22'30'', Y:32°52'50''.

Stratigraphic range: Late Albian, Kiamichi and basal Duck Creek Formation.

Lithology: The 17 m thick section starts with a limestone layer and ends about 0.5 m above a distinct oystershellbed. This succession consists of a dark arenaceous marlstone light grey and yellow limestone alternation. The lower part is characterised by nodular limestone, limy nodules and silty intercalations (Fig. 40). The stratified limestone of the upper part is dominated by bioclastic debris (bivalves,

oysters for example *Lopha*, *Aetostrea*) and bioturbation (*Planolites*, *Chondrites*). Ammonites are very abundant in the whole section. At about 8 m above the base of the section a lot of carbonised fossil wood can be found.

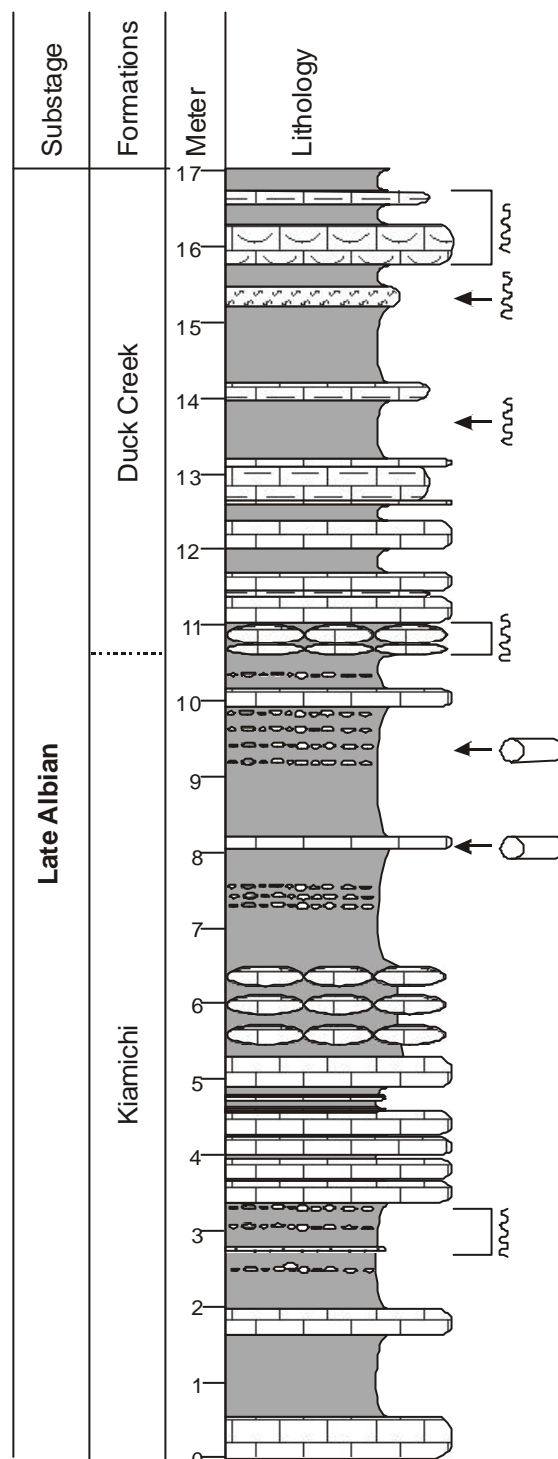


Fig. 40: Schematic lithological column of the Meacham Field section. A detailed lithological column with sample distribution is given in Appendix 18. For lithological explanations and abbreviations see Fig. 36.

4.2.5. Lancaster Avenue

Location and grid reference: This outcrop is located 100 m south of the southwest corner of Lancaster Avenue und Riverside Drive near a garage (Fig. 36; Appendix 19). TM Fort Worth Quadrangle, co-ordinates X: 97°18'10'', Y: 32°44'50''.

Stratigraphic range: Late Albian, Upper Duck Creek and Fort Worth Formation.

Lithology: The 4.5 m thick section starts with a limy marlstone interval and ends with a limestone layer. The lower 1 m consists of partial nodular grey limy marlstone and the remaining 3.5 m of the succession consist of a dark marlstone and light grey limestone alternation (Fig. 41). The boundary between Duck Creek and Fort Worth Formation is marked by the change from limy marlstone to marl- limestone alternation (Perkins, 1960; Scott, pers. com., 2001). From section meter 1 to 2.7, the limestones are characterised by a high abundance of the burrows of *Thalassinoides*.

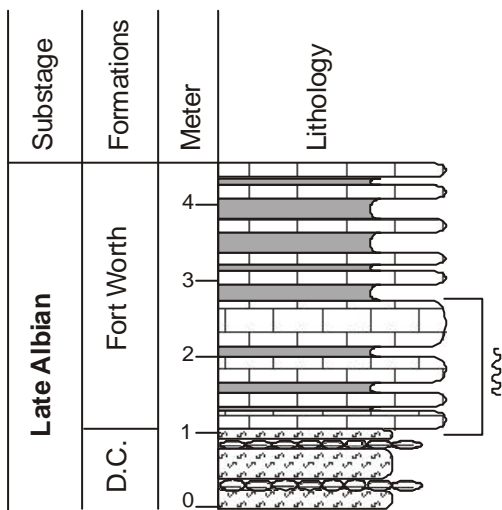


Fig. 41: Schematic lithological column of the Lancaster Avenue section. A detailed lithological column with sample distribution is given in Appendix 19. For lithological explanations and abbreviations see Fig. 36.

4.2.6. Seminary Drive

Location and grid reference: The succession is situated at the westbank of the Sycamore Creek, about 200 m north of the Seminary Drive (Fig. 36; Appendix 20). TM Fort Worth Quadrangle, co-ordinates X: 97°18'20'', Y: 32°41'10''.

Stratigraphic range: Late Albian, Denton and basal Weno Formation.

Lithology: This 4 m thick section starts with mudstone and ends with two distinct limestone layers. The succession consists of dark marl and mudstone with intercalated light grey limestone layers. The marlstone at the base is marked by an oystershellbed (Fig. 42). The boundary between Denton and Weno Formation is given by the base of the two distinct limestone layers in the upper part of the succession (Scott, pers. com, 2001). The marlstones and mudstones at the base are generally characterised by whole oysters and the limestone by *Thalassinoides*.

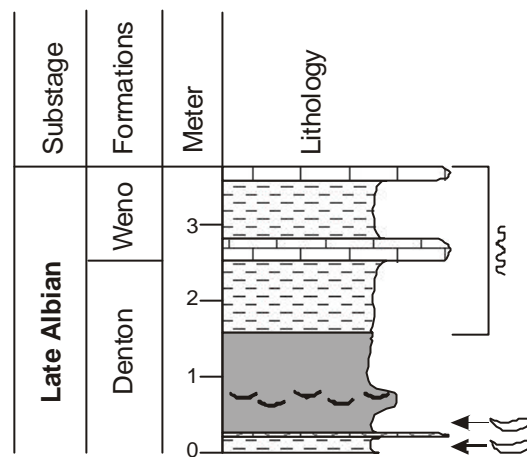


Fig. 42: Schematic lithological column of the Seminary Drive section. A detailed lithological column with sample distribution is given in Appendix 20. For lithological explanations and abbreviations see Fig. 36.

4.2.7. Interstate 30 & Ben Avenue

Location and grid reference: This section represents a roadcut south of Interstate 30 between Oakland and Beach Street, accessible from Ben Avenue (Fig. 36; Appendix 21). TM Haltom City Quadrangle, co-ordinates X: 97°16'30'', Y: 32°45'5''.

Stratigraphic range: Late Albian, Weno Formation.

Lithology: This 15.5 m thick section starts 1.2 m below the two limestone layers (Seminary Drive) and ends with a 1.5 m thick limestone layer. This succession can be separated into two parts. The lower part up to 11 m is dominated by dark marlstones with intercalated limy

marlstone beds and light grey limestone horizons. The part begins with a dark marlstone and nodular limestone alternation and then changes to light grey stratified limestone (Fig. 43). The connection between this succession and the section at Seminary Drive are the two limestone layers at the base. These double layers also mark the boundary Denton-Weno Formation (Scott, pers. com, 2001). In general, the limestone is more fossiliferous with bivalves, inoceramids and ammonites (Perkins, 1960). The middle part of the succession is characterised by slight bioturbation (*Chondrites*).

4.2.8. Interstate 30 & Menzer Street

Location and grid reference: Roadcut at the Interstate 30, about 250 m west of Oakland Street, accessible from West Menzer Street (Fig. 36; Appendix 22). TM Haltom City Quadrangle, co-ordinates X: 97°16'15'', Y: 32°45'15''.
Stratigraphic range: Late Albian, Pawpaw Formation.

Lithology: The section is about 6.5 m thick and starts with dark mudstones and ends with stratified limestones. The lower part up to 5 m consists of well laminated dark mudstone and the upper part of bioclastic packstone (Fig. 44). The boundary between the Pawpaw and the Main Street Formation is marked by the change from dark mudstone to bedded limestone (Scott, pers.com., 2001). The fauna in the mudstone is characterised by pyrite and nacre bivalves and ammonites as well as echinoids. In the upper part, the limestone is less fossiliferous, but bioturbation is abundant.

4.2.9. Sunset Oaks

Location and grid reference: This section is combined from roadcuts in Sunset Oaks Drive at Randol Mill Road, one block west of Bridgewood Drive and an excavation bank east of the Bridgewood Drive on the northern side of the fence (Fig. 36; Appendix 23). TM Hurst Quadrangle, co-ordinates X: 97°13'40'', Y: 32°46'30''.

Stratigraphic range: Late Albian to Lower Cenomanian, Mainstreet and basal Grayson Formation.

Lithology: This 9 m thick section starts with

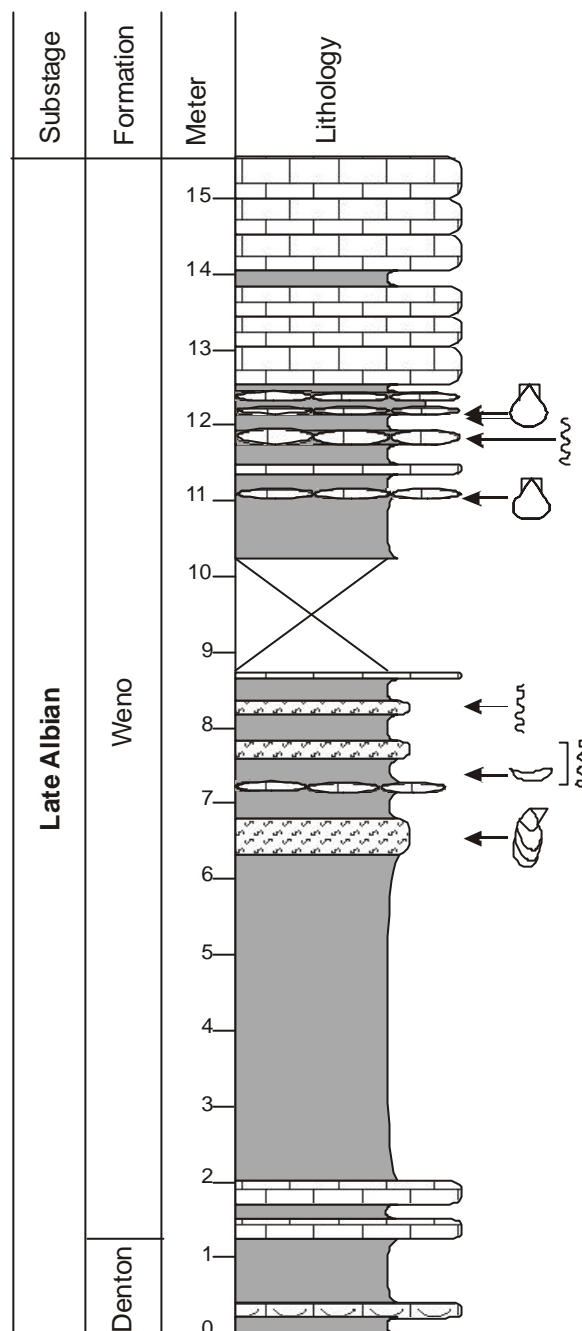
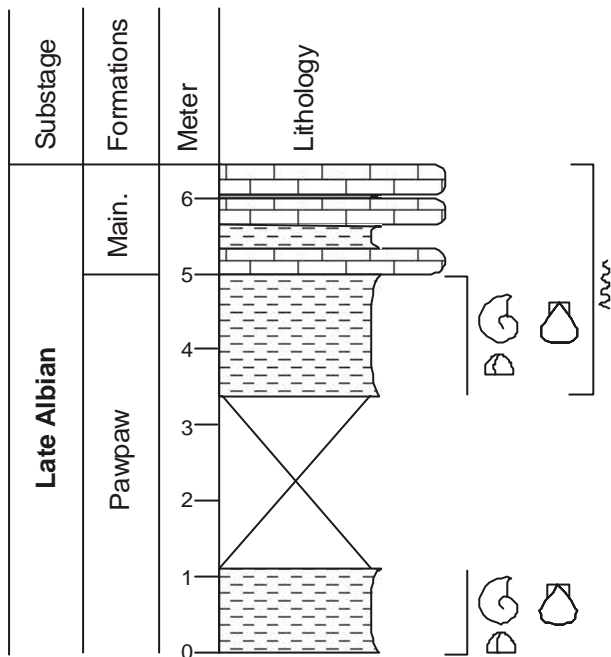


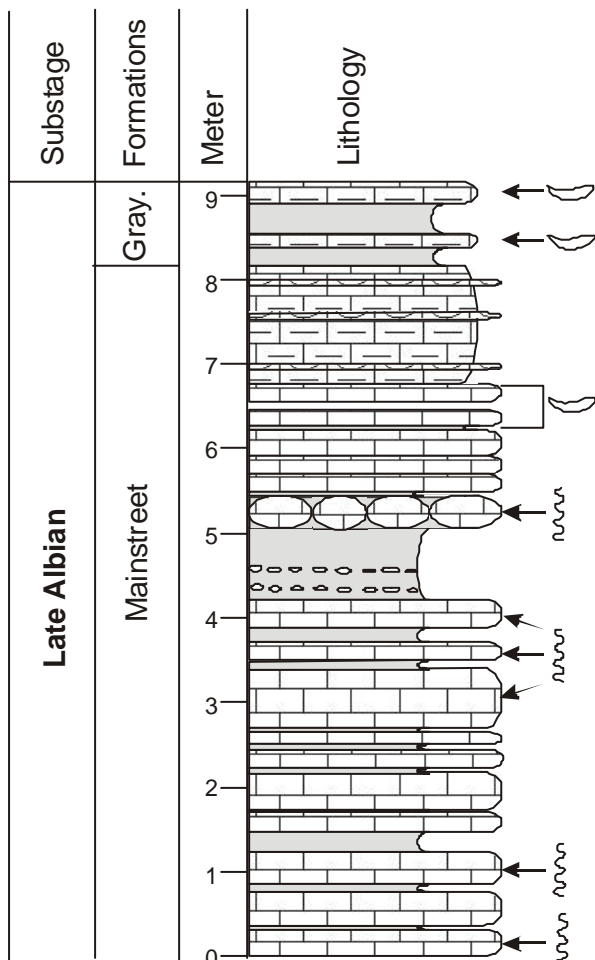
Fig. 43: Schematic lithological column of the Interstate 30 & Ben Avenue section. A detailed lithological column with sample distribution is given in Appendix 21. For lithological explanations and abbreviations see Fig. 36.

stratified bioclastic packstone and ends with a marly limestone. The whole succession consists of a grey marlstone light grey limestone alternation, the upper part is more marly (Fig. 45). The boundary between the Main Street and Grayson Formation is marked by a change to a more marly sedimentation at about 8 m above



the base of the section (Scott, pers. com., 2001). The limestone in the lower part is characterised by bioclastic debris (bivalves, gastropods). Ammonites and bioturbation (*Chondrites*, *Thalassinoides*) are very abundant. In the upper part texitrypaeid oysters are very common.

← Fig. 44: Schematic lithological column of the Interstate 30 & Menzer Street section. A detailed lithological column with sample distribution is given in Appendix 22. For lithological explanations and abbreviations see Fig. 36.



← Fig. 45: Schematic lithological column of the Sunset Oaks section. A detailed lithological column with sample distribution is given in Appendix 23. For lithological explanations and abbreviations see Fig. 36.

4.3. Results NE-Texas

4.3.1. Preservation of Planktic Foraminifera

The preservation of planktic foraminifera in NE-Texas varies between poor and very good. Some samples are characterised by foraminifera with fillings of the shells with calcite. In other samples the planktic foraminifera are not filled. In samples in which unfilled foraminifera dominate more shell debris and broken tests can be found than in samples in which filled planktic foraminifera dominate.

4.3.2. Planktic Foraminiferal Record

The total abundance of planktic foraminifera (63-500 µm) in this compiled succession

fluctuates between 0 and 3014 individuals per g sediment (Ind./g; Fig. 46). In the lower part of the section (Goodland formation) the values are very low (0-32 Ind./g; \bar{x} 3.5 Ind./g; Fig. 46). In the Kiamichi formation, the total abundance reaches a maximum of 11654 Ind./g (\bar{x} 3014 Ind./g). In the interval Duck Creek to Main Street, the abundance decreases again (1802 Ind./g; \bar{x} 402 Ind./g; Fig. 46). The total abundance shows small increases in the Weno and Main Street formation. Individuals of the fraction 250-500 μ m occur throughout the

succession. The lower part (Goodland formation) is also characterised by low abundances of max. 1.3 Ind./g (\bar{x} 0.21 Ind./g; Fig. 46). In the Kiamichi and Fort Worth formation, the abundance increases up to a maximum of 97 Ind./g (\bar{x} 15.7 Ind./g; Fig. 46). The interval from the top of the Denton to the base of the Main Street formation is marked by low values of max. 2.05 Ind./g (\bar{x} 0.5 Ind./g; Fig. 46). In the Main Street formation, the total abundance is increasing again up to a maximum of 27 Ind./g (\bar{x} 5.37 Ind./g; Fig. 46). The fluctuation of the abundance of

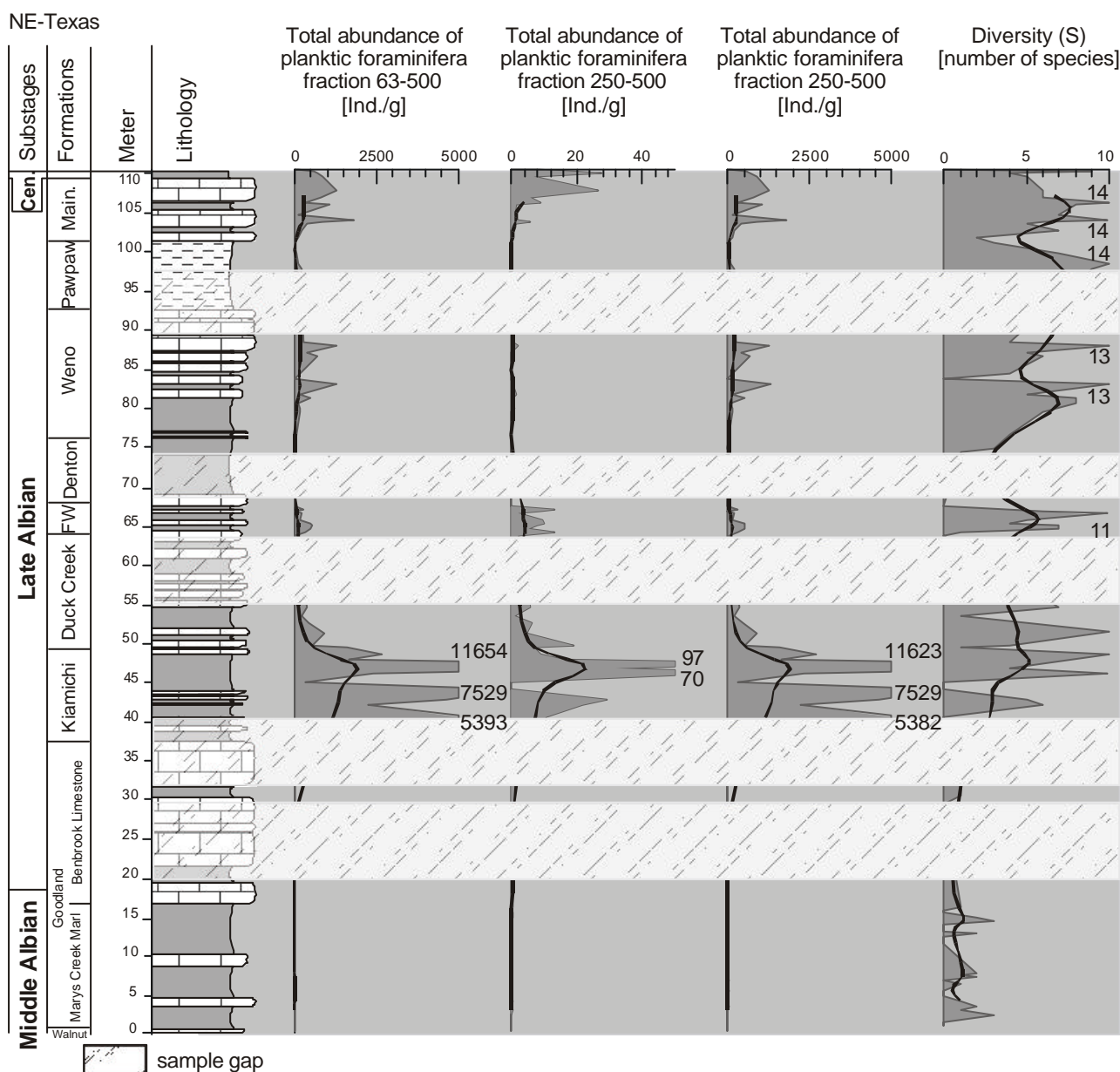


Fig. 46: Total abundance of planktic foraminifera of the fraction 63-500 μ m, 250-500 μ m and 63-250 μ m is given in individuals per g sediment and the diversity is given in number of species of the Middle and Late Albian succession in NE-Texas. The faint hatched parts represent sample gaps.

the fraction 63-250 μm shows comparable variation to the abundances of fraction 63-500 μm (Fig. 46). In the Kiamichi formation the total abundance of the fraction 63-250 μm reaches a maximum with 11623 Ind./g (ø 3014 Ind./g). The diversity (number of species) of planktic foraminifera in the Middle and Late Albian is fluctuating. In the lower part of the section (Goodland formation), the species richness is low with a maximum of 5 species. The remaining succession is characterised by increasing and varying numbers of species to a maximum of 7 to 10 species (Fig. 46). The planktic foraminiferal assemblage in NE-Texas is

composed of 18 species (Tab. 3), belonging to 10 genera.

Tab. 3: List of occurring planktic foraminiferal species of NE-Texas in alphabetical order.

- Ascoliella nitida* (Michael, 1972)
- Ascoliella quadrata* (Michael, 1972)
- Ascoliella scitula* (Michael, 1972)
- Favusella hiltermanni* (Loeblich & Tappan, 1961)
- Favusella washitensis* (Carsey, 1926)
- Globigerinelloides bentonensis* (Morrow, 1934)
- Globigerinelloides caseyi*

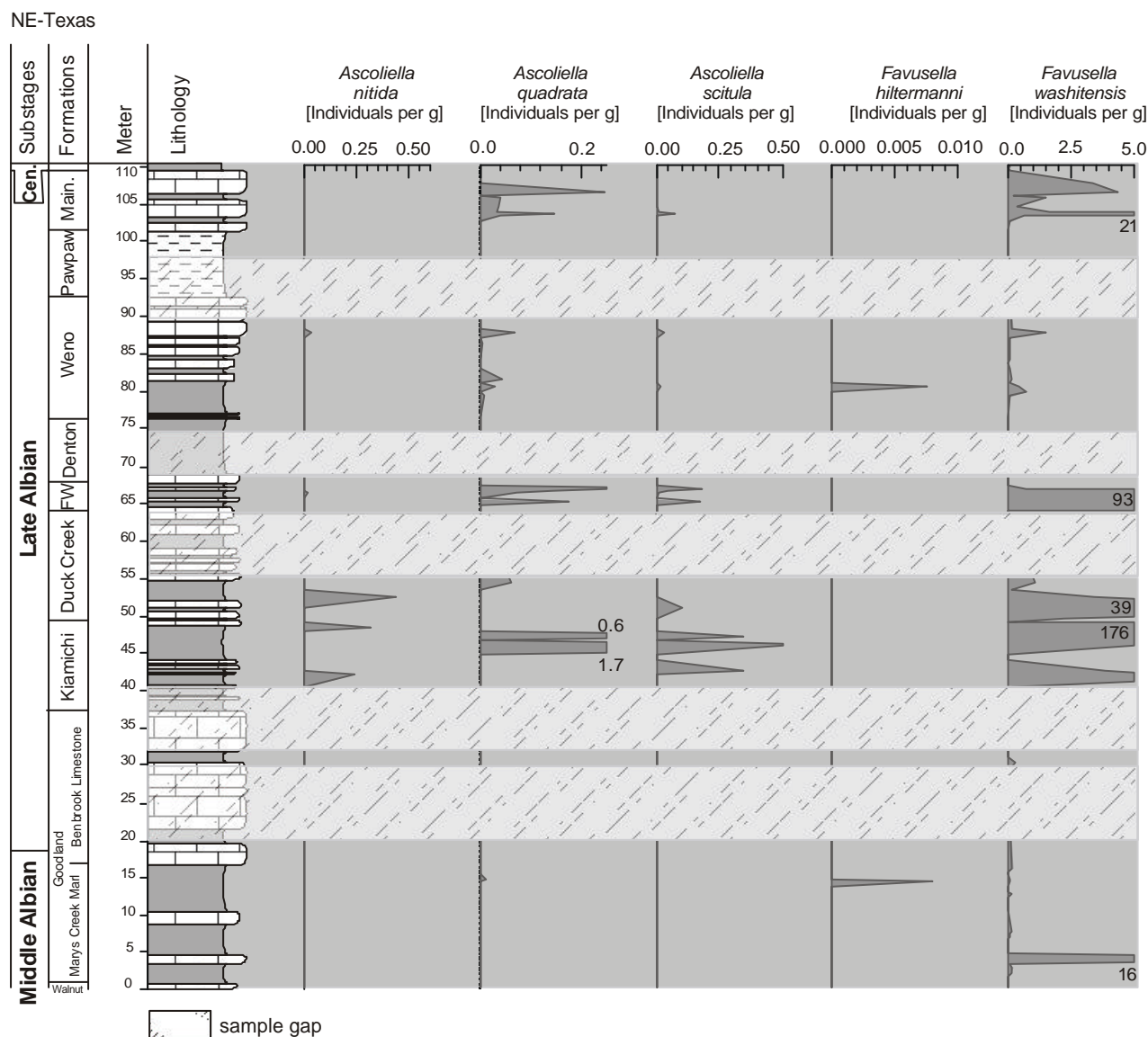


Fig. 47: Abundance of the planktic foraminifera *Ascoliella nitida*, *Ascoliella quadrata* and *Ascoliella scitula* as well as *Favusella hiltermanni* and *Favusella washitensis* given in individuals per g sediment of the Middle and Late Albian of NE-Texas. The faint hatched parts represent sample gaps.

(Bolli, Loeblich & Tappan, 1957)
Guembelitria spp. (Cushman, 1933)
Hedbergella delrioensis/ infracretacea
 (Carsey, 1926)
Hedbergella implicata (Michael, 1972)
Hedbergella intermedia (Michael, 1972)
Hedbergella planispira (Tappan, 1940)
Hedbergella punctata (Michael, 1972)
Heterohelix moremanni (Cushman, 1938)
Heterohelix reussi (Cushman, 1938)
Praeglobotruncana delrioensis
 (Plummer, 1931)
Rotalipora evoluta / appenninica (Sigal, 1948)
Ticinella primula (Luterbacher, 1963)

Because of the incompleteness of the whole section only general trends and maximum values can be described.

The genus *Ascoliella* spp. is represented by *Ascoliella nitida*, *Ascoliella quadrata* and *Ascoliella scitula*. *Ascoliella nitida* in the Late Albian shows very low abundances with maximum values of about 0.5 Ind./g in the Kiamichi and lower Duck Creek Formation (Fig. 47). *Ascoliella quadrata* is characterised by low values, with maxima in the Kiamichi (1.7 Ind./g), Fort Worth (0.2 Ind./g) and Main Street (0.22 Ind./g) Formation (Fig. 47).

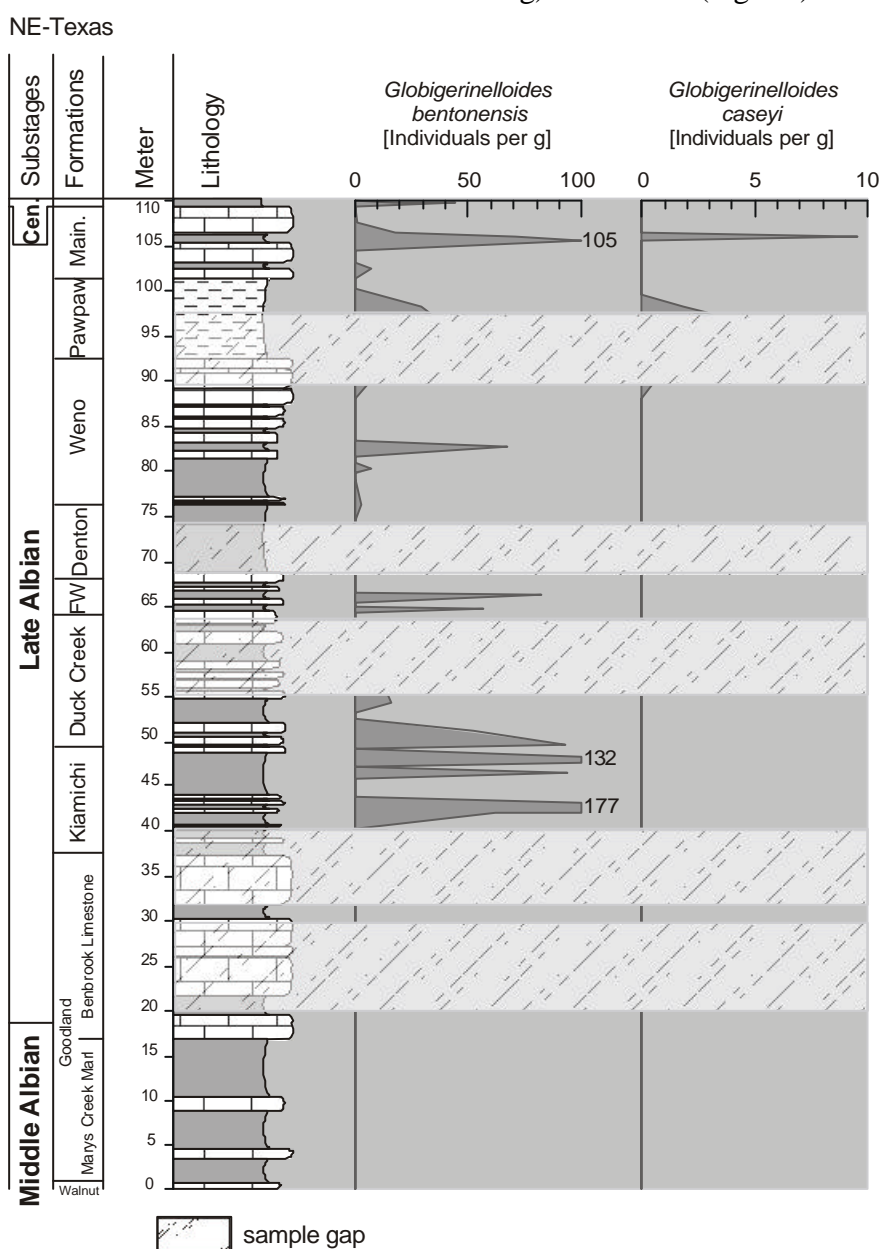


Fig. 48: Abundance of the planktic foraminifera *Globigerinelloides bentonensis* and *Globigerinelloides caseyi* given in individuals per g sediment of the Middle and Late Albian of NE-Texas.

Ascoliella scitula occurs in the Late Albian with maximum values in the Kiamichi Formation (0.5 Ind./g; Fig. 47).

Favusella spp. is represented by *Favusella hiltermanni* and *Favusella washitensis*. *F. hiltermanni* shows extreme low values in only two samples (~0.008 Ind./g) and occurs nowhere else (Fig. 47). *Favusella washitensis* is abundant in the Middle and Late Albian and maximum values can be described from the Marys Creek Marl (16 Ind./g), the Kiamichi (282 Ind./g), the Fort Worth (93 Ind./g) and the Main Street (21 Ind./g) Formation.

The abundance of *Globigerinelloides bentonensis* shows fluctuation between 0 Ind./g

and 177 Ind./g (Fig. 48), the highest values can be described from the Kiamichi Formation.

Globigerinelloides caseyi occurs only in the Pawpaw and Main Street Formation and reaches max. values of 9.5 Ind./g (Fig. 48)

Hedbergella spp. consists of *Hedbergella delrioensis/infracretacea*, *Hedbergella implicata*, *Hedbergella intermedia*, *Hedbergella planispira* and *Hedbergella punctata*.

Hedbergella delrioensis/infracretacea can be found from the Marys Creek Marl up to the Grayson Formation and reaches the highest values in the Kiamichi (4013 Ind./g) and Main Street/Grayson Formation (307 Ind./g; Fig. 49). The values between the Kiamichi and Pawpaw

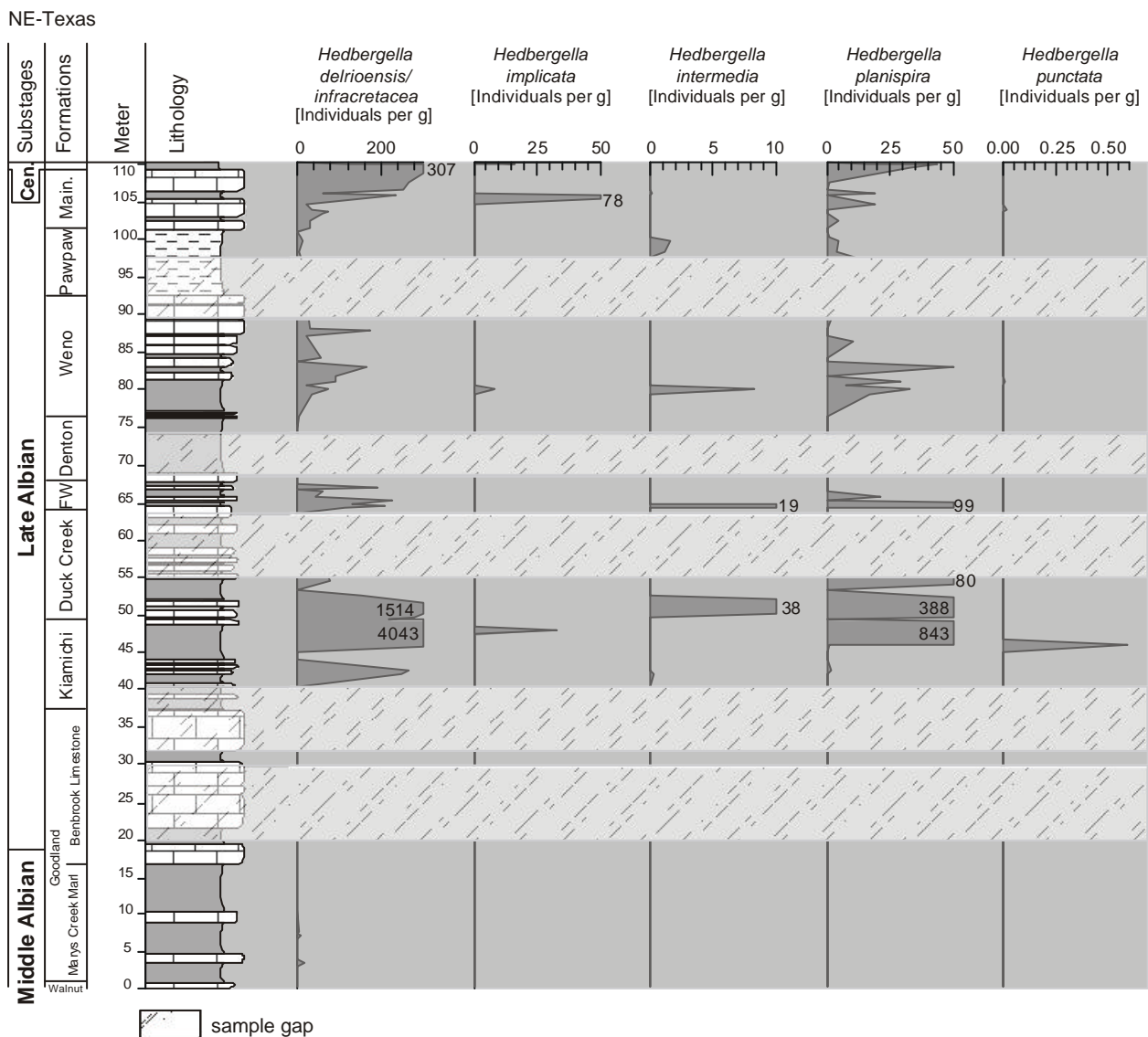


Fig. 49: Abundance of the planktic foraminifera *Hedbergella delrioensis/infracretacea*, *Hedbergella implicata*, *Hedbergella intermedia*, *Hedbergella planispira* and *Hedbergella punctata* given in individuals per g sediment of the Middle and Late Albian of NE-Texas. The faint hatched parts represent sample gaps.

Formation are lower and increase slowly in the Pawpaw and Main Street Formation (Fig. 49). *Hedbergella planispira* shows comparable fluctuation, as well this species shows highest values in the Kiamichi- (843 Ind./g) and Main Street Formation (43 Ind./g; Fig. 49). *Hedbergella implicata*, *H. intermedia* and *H. punctata* shows only selective occurrences with max. values of 78 Ind./g (*H. implicata*), 38 Ind./g (*H. intermedia*) and 0.5 Ind./g (*H. punctata*) in the Late Albian (Fig. 49).

Heterohelix spp. is composed of *Heterohelix moremani* and *Heterohelix reussi* and occurs in the Late Albian. The abundance of *H. moremani* increases rapidly in the Weno Formation and remains on this higher level (426-847 Ind./g; Fig. 50). The number of individuals per g of *H. reussi* increases in two steps. First step in the Denton

and Weno Formation with max. values of 278 Ind./g and the second step in the Pawpaw and Main Street Formation up to values of 318 Ind./g (Fig. 50).

Praeglobotruncana delrioensis shows only one peak in the Main Street Formation with 0.15 Ind./g (Fig. 50).

Rotalipora evoluta/appenninica can only be found in the Main Street and Grayson Formation (Late Albian to Early Cenomanian) with a maximum of 16 Ind./g (Fig. 50).

Ticinella primula occurs only in some beds in the Late Albian (Kiamichi Formation) with maxima values of 55 and 41 Ind./g in the Kiamichi and Fort Worth Formation (Fig. 50). The values seem to decrease after the Fort Worth Formation.

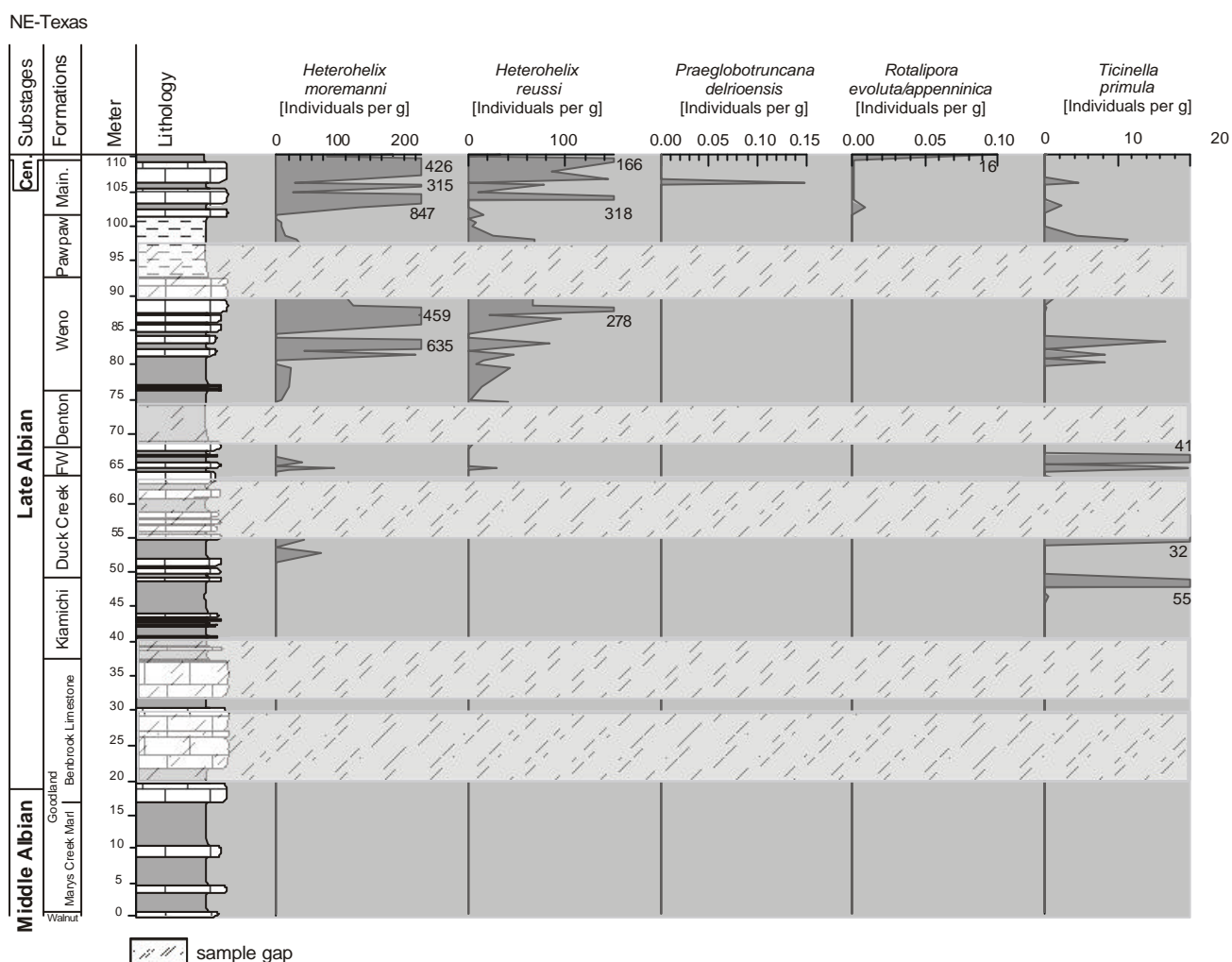


Fig. 50: Abundance of the planktic foraminifera *Heterohelix moremani* and *Heterohelix reussi* as well as *Praeglobotruncana delrioensis*, *Rotalipora evoluta/appenninica* and *Ticinella primula* given in individuals per g sediment of the Middle and Late Albian of NE-Texas. The faint hatched parts represent sample gaps.

4.3.3. First and Last Appearance Datums of Planktic Foraminifera

The studied section from the base of the Goodland formation to the base of the Grayson formation in NE-Texas is characterised by a total of 14 first appearance datums (FADs) and 5 last appearance datums (LADs, Fig. 51). The first appearance datums emerge in four major units. The first unit contains 3 FADs and is settled 2.5 m below the boundary Marys Creek

Marl and Benbrook Limestone in the middle of the Goodland formation. The next unit with 7 FADs occurs in the Kiamichi Formation. In the Fort Worth formation only one FADs can be recognised (unit III). The fourth unit with 3 gradually emerging species is settled in the Pawpaw and Main Street formation in the upper part of the studied succession (Fig. 51). In the following table FADs and LADs are compiled (Tab.4). Stratigraphical important taxa are in bold.

Tab. 4: Compilation of first and last appearance datums (FADs, LADs) of planktic foraminifera of the Middle to Late Albian of the NE-Texas, the position is given in m in reference to distinct lithological formation boundaries, the stratigraphical important FADs are marked by bolt type.

Depth (m)	Depth in relation to the lithostratigraphic formation	First Appearance (FAD)	Last Appearance Datum (LAD)
106.7	About 5.4 m above the base of the Main Street formation		<i>Ascoliella quadrata</i>
106.1	About 4.8 m above the base of the Main Street formation	<i>Praeglobotruncana delrioensis</i>	
103.9	About 2.6 m above the base of the Main Street formation		<i>Hedbergella punctata</i>
103.9	About 1.6 m above the base of the Main Street formation		<i>Ascoliella scitula</i>
102.5	About 1.2 m above the base of the Main Street formation	<i>Rotalipora evoluta</i>	
97.7	3.6 m below the base of the Main Street formation	<i>Globigerinelloides caseyi</i>	
87.8	3.6 m below the base of the Main Street formation		<i>Ascoliella nitida</i>
80.4	20.9 m below the base of the Main Street formation		<i>Favusella hiltermanni</i>
64.7	About 0.2 m above the base of the Fort Worth formation	<i>Heterohelix reussi</i>	
45.9	About 6 m above the base of the Kiamichi formation	<i>Ticinella primula</i>	
45.9	About 4.8 m above the base of the Kiamichi formation	<i>Hedbergella punctata</i>	
45.9	About 4.8 m above the base of the Kiamichi formation	<i>Hedbergella implicata</i>	
41.9	About 4.8 m above the base of the Kiamichi formation	<i>Hedbergella planispira</i>	
41.9	About 4.8 m above the base of the Kiamichi formation	<i>Hedbergella intermedia</i>	
41.9	About 4.8 m above the base of the Kiamichi formation	<i>Globigerinelloides bentonensis</i>	
41.9	About 4.8 m above the base of the Kiamichi formation	<i>Ascoliella nitida</i>	
14,4	2.5 m below the boundary Marys Creek Marl to Benbrook Limestone	<i>Ascoliella quadrata</i>	

14,4	2.5 m below the boundary Marys Creek Marl to Benbrook Limestone	<i>Heterohelix moremani</i>	
14,4	2.5 m below the boundary Marys Creek Marl to Benbrook Limestone	<i>Favusella hiltermanni</i>	

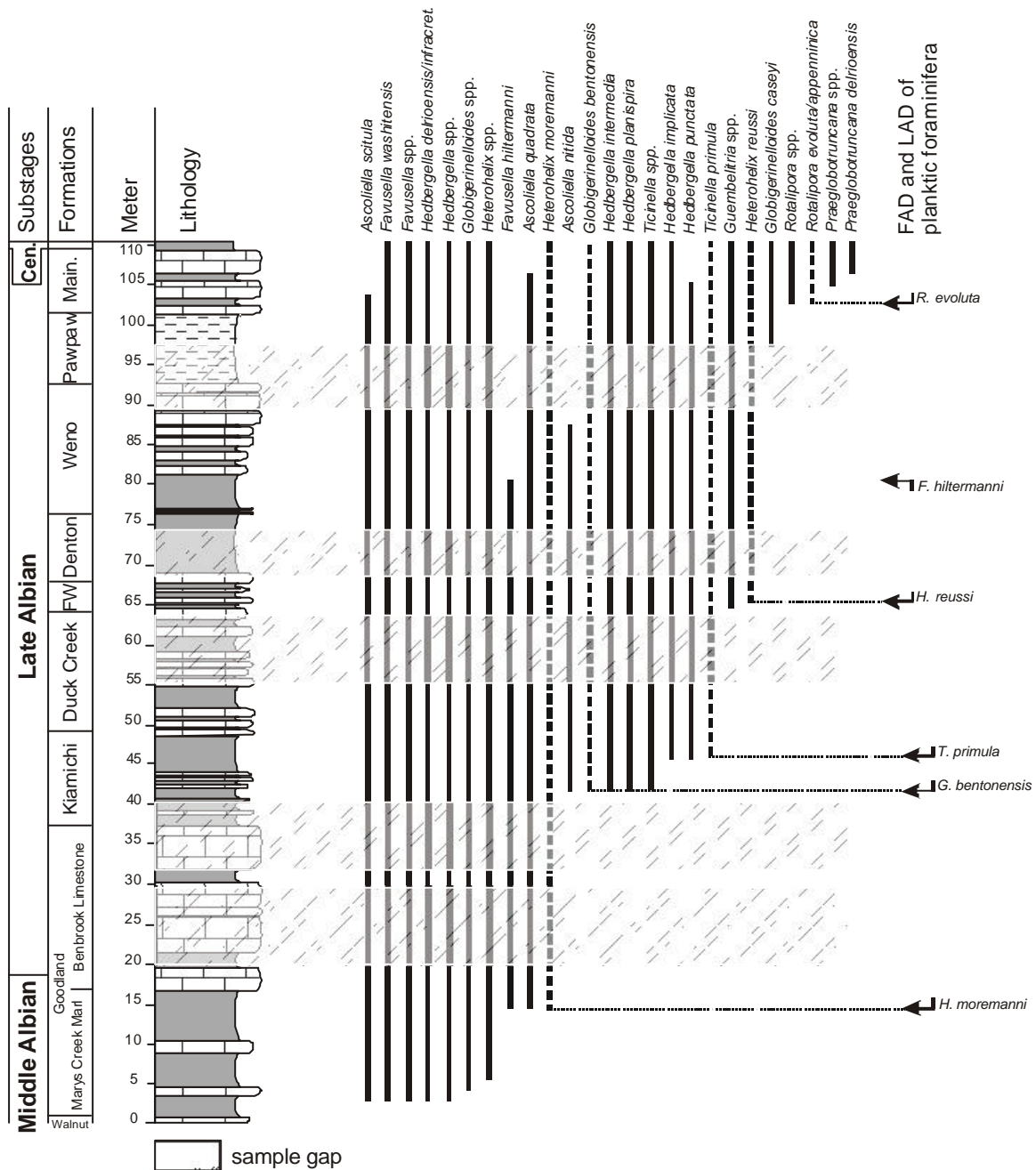


Fig. 51: Range chart of planktic foraminifera of the Middle and Late Albian of NE-Texas with respect to the lithostratigraphic subdivisions. The distribution of the stratigraphical important taxa are given in broken lines

4.3.4. Stable Isotopes

The oxygen and carbon isotope curve of the 110 m thick succession in NE-Texas is based on 165

bulk rock samples. The average sample distance varies between 5 and 60 cm. The carbon isotope curve fluctuates from 0.6 to 3.1 ‰ (Fig. 52). The carbon isotope values ($\delta^{13}C$)

NE-Texas

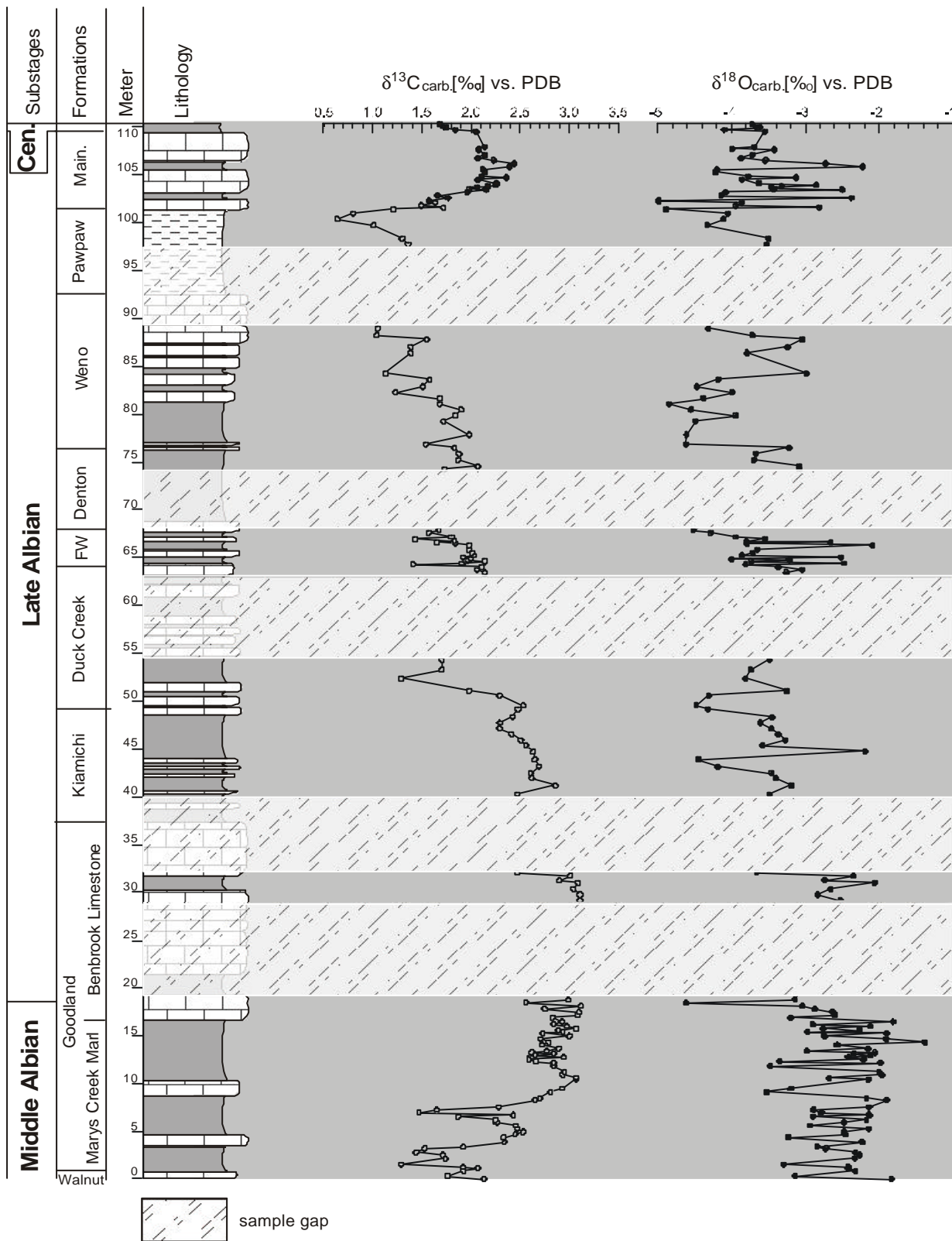


Fig. 52: $\delta^{13}\text{C}$ and $\delta^{18}\text{O}$ values of the Middle and Late Albian of NE-Texas. The gaps in the isotope record are due to the bad accessibility of sections or section parts.

at the base of the section in NE-Texas (Goodland formation) are characterised by two distinct negative excursions of about 1 ‰. In the successive interval from the top of Marys Creek Marl (Goodland formation) to the base of the Kiamichi formation the $\delta^{13}\text{C}$ values are balanced (2.8 ‰). This stable interval follows a long persistent decrease about 1.5 ‰ from the lower Kiamichi to the upper Pawpaw formation. The upper Pawpaw formation is marked by a short term negative excursion in the $\delta^{13}\text{C}$ values (0.8 ‰). At the crossover from the Pawpaw to the Main Street formation a short term positive excursion about 1.9 ‰ can be recognised (Fig. 52). The oxygen isotope curve ($\delta^{18}\text{O}$) varies between -1.8 and -5 ‰ (Fig. 52). Generally the oxygen isotopes show a trend from heavier (-2.3 ‰) to lighter (-3.7 ‰) values. Compared with the $\delta^{18}\text{O}$ curve in SE-France, this curve shows no distinct long or short term variations (Fig. 52).

4.4. Discussion NE-Texas

4.4.1. Preservation of Planktic Foraminifera

The preservation of the planktic foraminifera in NE-Texas is better, compared with SE-France (subjective observation). A less number of shells are filled with secondary calcite, but a higher number is not filled, at all. Compared with the filled ones, the non-filled shells are more often broken and have more damages. In NE-Texas, there are no species that were more favourably affected by diagenesis than others.

4.4.2. Planktic Foraminiferal Record

Unfortunately, parts of the succession are not accessible. Consequently, it was not possible to make a detailed analysis of the abundance record of planktic foraminifera in NE-Texas. However, general trends can be interpreted. The abundance of planktic foraminifera of the fractions 63-500 μm , 250-500 μm , 63-250 μm and the diversity (number of species) are the main proxies to analyse the fauna. The total abundance of planktic foraminifera (63-500 μm) shows a similar trend as the abundance of planktic foraminifera of the size 250-500 μm and 63-250 μm in NE-Texas.

All three curves are marked by a major peak (highest abundances) in the Kiamichi formation (Fig. 53). This peak corresponds to a major transgression on the Comanchean shelf proposed by Scott et al. (2000) for this time interval (Fig. 53). Therefore, this maximum in planktic foraminifera can be a result of the transgression onto the shelf. Due to the transgression more nutrients were washed out of the newly flooded shores (Erbacher, 1994) and have favoured a higher phytoplankton production, which, lead to more food for planktic foraminifera. In the succeeding formations (Duck Creek, Fort Worth, Denton, Weno), the abundances of all fractions of planktic foraminifera are lower again. This can be interpreted such that the number of planktic foraminifera got normalised, because of lesser food, after the first phytoplankton bloom. The next increase in abundances is in the Pawpaw, Main Street and Grayson formations corresponding with a major transgression as well (Scott, et al. 2000). The diversity shows no small scaled trend like the abundances (Fig. 53), but it can be observed that the number of species is increasing until the Kiamichi Formation. Possibly, the diversity does not correspond to the transgression cycles (WA 1 to 5), but follows the general Middle and Late Albian radiation/diversification trend (Fig. 2).

Following species of planktic foraminifera in NE-Texas can be used for palaeoceanographic implications; *Hedbergella delrioensis/infracretacea*, *Hedbergella planispira*, *Heterohelix moremani*, *Heterohelix reussi*. The trend in the data set of *Hedbergella delrioensis/infracretacea* and *Hedbergella planispira* is similar. Both have maximum values in the Kiamichi Formation, show lower values later and increasing abundances again in the Pawpaw, Main Street and Grayson Formation (Fig. 54). This observed fluctuation of *H delrioensis/infracretacea* and *Hedbergella planispira* coincide with the variation of the total abundances of all fractions. It can be assumed the same nutrient input because of transgression and respectively higher food availability is the cause for this fluctuation, as above. These two opportunistic *Hedbergella* species,

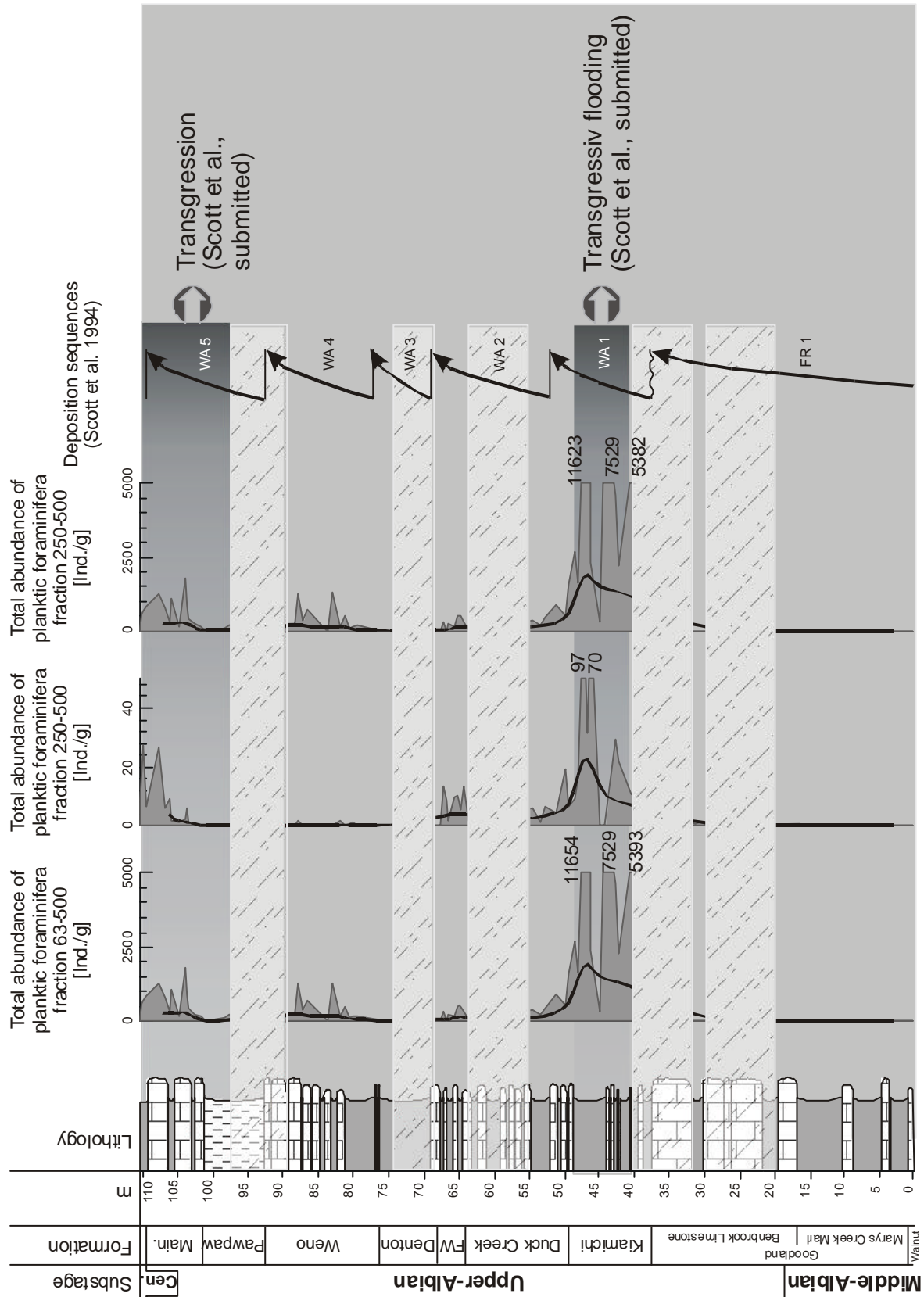


Fig. 53: Total abundances of planktic foraminifera in NE-Texas of the fraction 63-500 μm, 250-500 μm, 63-250 μm (Ind./g) and the diversity (number of species) compared with the transgression cycles in NE-Texas proposed by Scott et al. (1994).

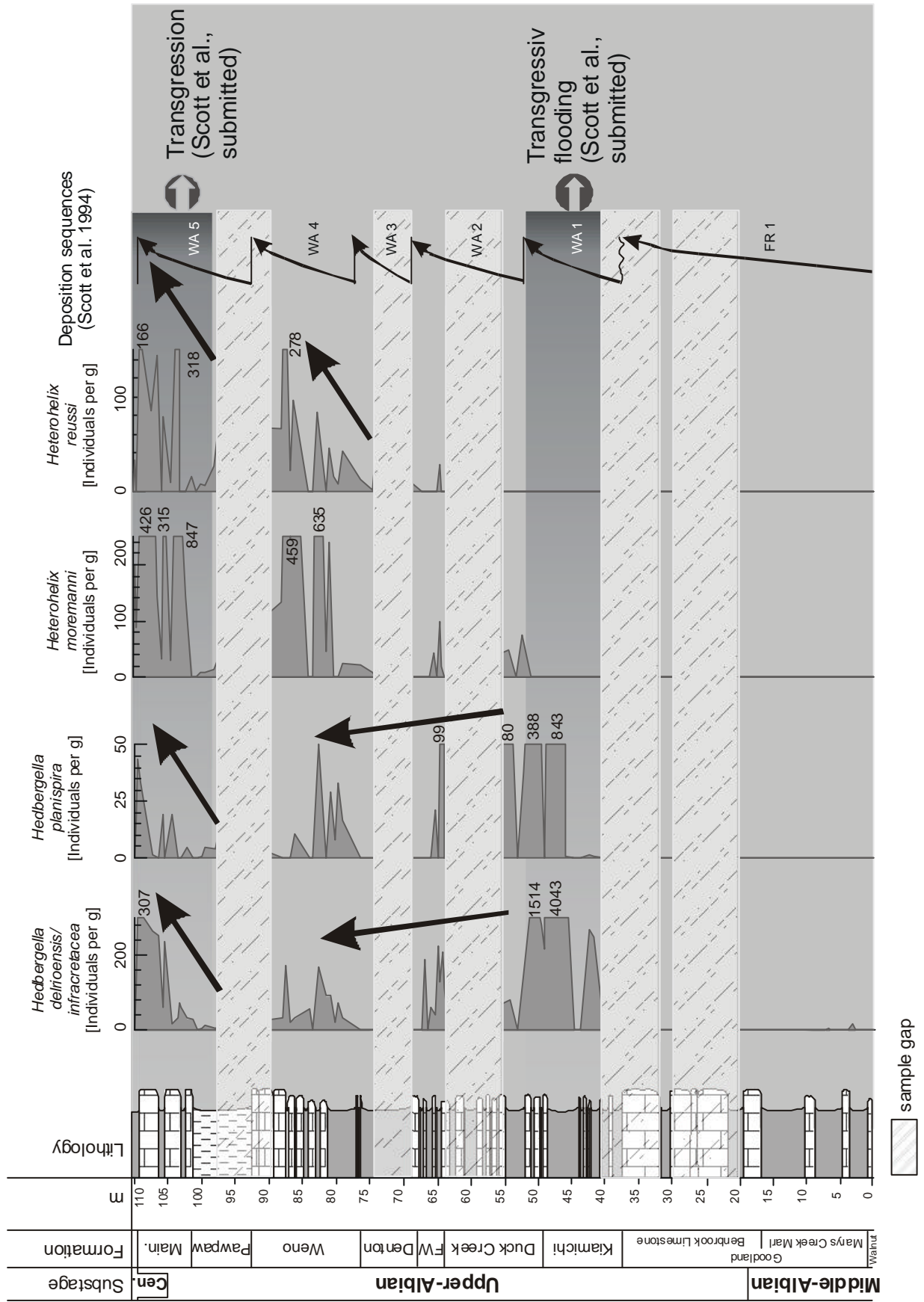


Fig. 54: Total abundance of *Hedbergella delrioensis/infracretacea*, *Hedbergella planispira*, *Heterohelix moremani* and *Heterohelix reussi* given in individuals per g sediment compared with the transgressions cycles proposed for NE-Texas (Scott et al., 1994).

(Premoli-Silva & Sliter, 1999), seem to prefer high nutrient conditions/ high food availability and live in the highest part of the upper water column (Premoli-Silva & Sliter, 1999). *Heterohelix moremani* and *Heterohelix reussi* show a clear increase and maximum values from the Denton Formation to the end of the section (in the case of *H. reussi* two increases; Fig. 54). The trend in the abundance of *Heterohelix* does not coincide with *Hedbergella*. This could lead to the assumption that the Heterohelids follows other controlling factors than *Hedbergella*. It may be possible that the appearance of *H. moremani* and *H. reussi* on the shallow shelf is steered by the second order sealevel rise (UZA1.3-1.5; Haq et al., 1988) and not by the nutrient availability.

4.4.3. Biostratigraphy of the Middle/Late Albian

Based on the material from NE-Texas, a detailed stratigraphical zonation with planktic foraminifera and ammonites could be worked out (Fig. 55). Compared to a previous work with a lower sampling resolution (Michael, 1972), a revised, high resolution stratigraphy with 6 planktic foraminiferal zones for the Middle to Late Albian (Goodland to Main Street formation) could be elaborated (Fig. 55). A lack of open marine taxa like *Biticinella* or *Rotalipora*, or the late first occurrence of *Ticinella* limited a direct comparison between the stratigraphic zonation suggested for the Gulf of Mexico (Longoria, 1984; Premoli-Silva & McNulty, 1989) as well as the European realm (Robaszynski & Caron, 1995). The stratigraphy is based on observed first and last appearance datums (FADs and LADs; Fig. 51) and not as in Michael (1972) on assemblage zones. Following planktic foraminiferal zones could be described.

Favusella washitensis zone

Base: FAD of *Favusella washitensis*

Top: FAD of *Heterohelix moremani*

Range: The base of this zone is not recorded. The top is recognised two metres below the lithological change from the Marys Creek Marl to the Benbrook Limestone. Michael (1972)

described a *Favusella washitensis* assemblage zone for the Goodland formation (Fig. 55).

Remarks: The ammonite fauna of NE-Texas is characterised by endemic forms. However, faunal associations and a few superregional distributed ammonites enable correlations with the European realm (Lehmann, pers. com.). Therefore, this zone is marked by the Middle Albian *Euhoplites lautus* ammonite zone.

Heterohelix moremani zone

Base: FAD of *Heterohelix moremani*

Top: FAD of *Globigerinelloides bentonensis*

Range: This zone comprises the interval from two metres below the lithological change from Marys Creek Marl to Benbrook Limestone to 5 metres above the lithological changes from Benbrook Limestone (Goodland formation) to the silty marlstones of the Kiamichi formation (Fig. 55). Michael (1972) described the base of the *Hedbergella implicata* assemblage subzone at the boundary Goodland to Kiamichi formation.

Remarks: This zone comprises the top of the *E. lautus* and the lower to middle part of the Late Albian *Mortoniceras inflatum* ammonite zone.

Globigerinelloides bentonensis zone

Base: FAD of *Globigerinelloides bentonensis*

Top: FAD of *Ticinella primula*

Range: This zone starts 5 m above the base of the Kiamichi formation and ends 3 m below the base of the Duck Creek formation (lithological change from silty marlstone to limestone layers; Fig. 55). The *G. bentonensis* zone is equivalent with the lower part of the *H. implicata* assemblage subzone (Michael, 1972).

Remarks: This zone is situated in the upper third of the *M. inflatum* ammonite zone, in the *Hysterocheras varicosum* subzone.

Ticinella primula zone

Base: FAD of *Ticinella primula*

Top: FAD of *Heterohelix reussi*

Range: This zone begins 3 m below the base of the Duck Creek formation and ends at the base of the Fort Worth formation (Fig. 55). This zone

comprises the middle and upper part of the *H. implicata* assemblage subzone and the base of the *Hedbergella punctata* assemblage subzone (Michael, 1972).

Remarks: This zone comprises the top of the *M. inflatum* and the lower part of the Late Albian *Stoliczkaia dispar* ammonite zone.

Heterohelix reussi zone

Base: FAD of *Heterohelix reussi*

Top: FAD *Rotalipora evoluta*

Range: This zone comprises the base of the Fort Worth formation and ends 1.5 m above the base

of the Mainstreet formation (Fig. 55). Michael (1972) described the *Hedbergella punctata* and the lower and middle part of the *Hedbergella delrioensis* assemblage subzone for this interval.

Remarks: This zone is equivalent with the middle and upper part of the Late Albian *S. dispar* ammonite zone.

Rotalipora evoluta zone

Base: FAD of *Rotalipora evoluta*

Top: FAD of *Rotalipora cushmani* or *greenhornensis*

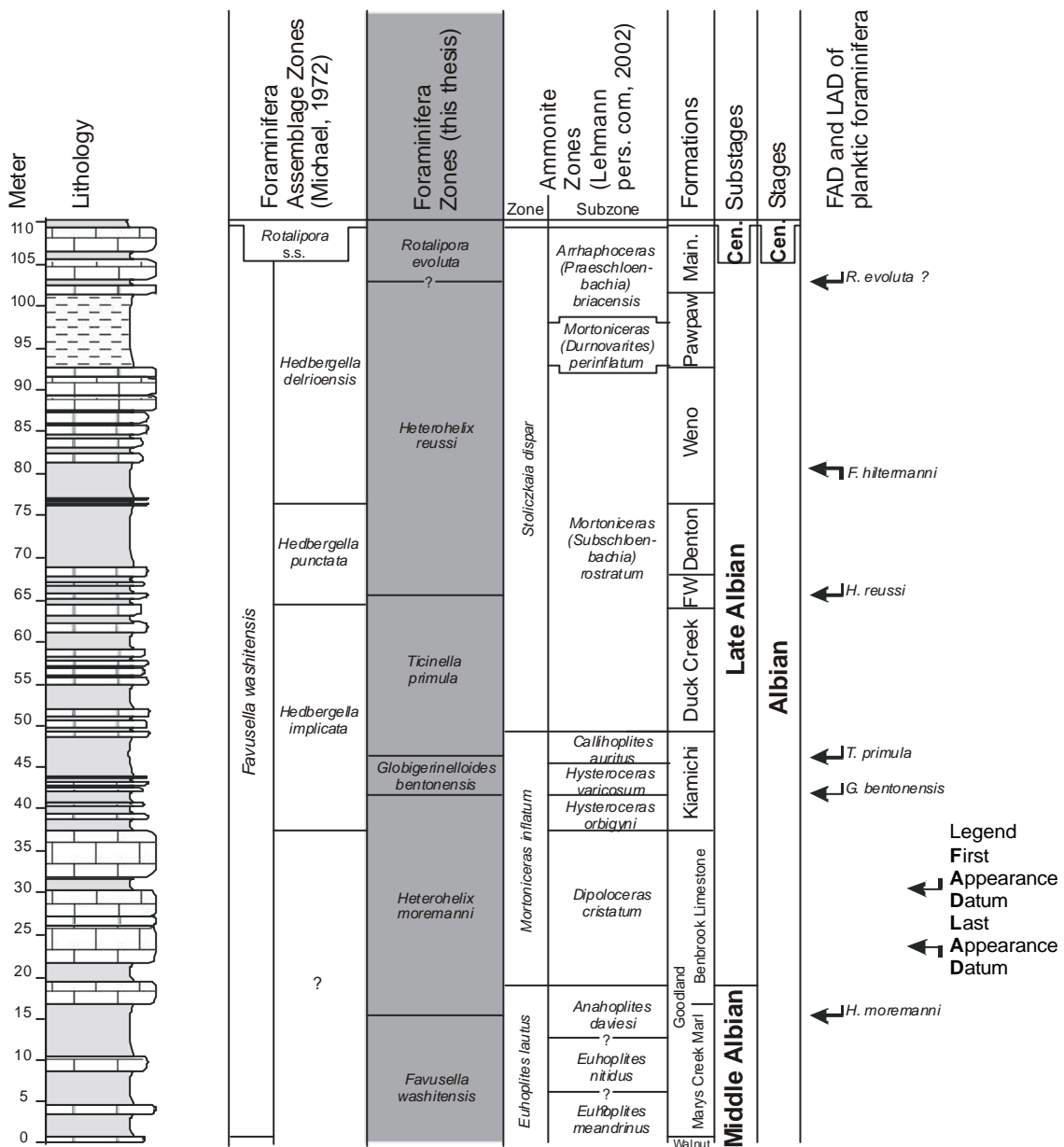


Fig. 55: Biostratigraphic zonation for the Middle and Late Albian of NE-Texas (grey shaded) based on planktic foraminifera compared with the work of Michael (1972).

Range: This zone comprises the interval from 1.5 m above the base of the Mainstreet formation and ends outside the recorded section (Fig. 55). Michael (1972) described the upper part of the *H. delrioensis* assemblage subzone and the *Rotalipora* s.s. assemblage zone. The base of his *R. evoluta* zone is situated higher in the lithological succession (Grayson formation). The *Rotalipora* s.s. zone according to Pessagno (1969) can be divided into the *Rotalipora evoluta* assemblage subzone and the *Rotalipora cushmani-greenhornensis* assemblage subzone. Many foraminiferal specialists synonymise *R. evoluta* with *R. appenninica* (Scott et al., submitted). In North Texas it may be a proxy for *R. globotruncanoides*, the marker for the Cenomanian base (Scott et al., submitted).

Remarks: This zone is characterised by the top of the *S. dispar* ammonite zone.

4.4.4. Isotopic Signature and Diagenesis

The carbon and oxygen isotope record of the 9 sections in NE-Texas were measured with bulk calcium carbonate samples. The carbonate is dominated by calcareous nannofossils, planktic foraminifera and benthic foraminifera, in descending order. Therefore it is assumed that the signal predominantly represents a surface water signal. However, the original isotopic signal can be influenced by different early and late diagenetic effects. If the sediments were affected by burial diagenesis and calcite precipitation from marine pore-fluids, the carbon and oxygen isotope values would show

a positive correlation (Jenkyns & Clayton, 1986; Jenkyns, 1996). None of the 9 single sections in Texas do contain enough values to allow a separate calculation. The complete section in Texas shows an insignificant correlation ($r^2=0.25$; Fig. 56). The low covariance between the $\delta^{13}\text{C}$ and $\delta^{18}\text{O}$ values in Texas implies an insignificant alteration during diagenesis (Fig. 56). Even though the correlation would be strong positive, Rao (1996) supposed that this would not necessarily indicate a diagenetic signal.

4.4.5. Correlation of the Carbon Isotope Record of NE-Texas with SE-France

As it is shown in chapter 3.4.5., the carbon isotope curve can be correlated superregionally. It was the aim of the correlation of the $\delta^{13}\text{C}$ record of NE-Texas and SE-France, to prove the applicability of the CIS on shallow marine environments like NE-Texas, where early diagenesis and alteration of the original marine isotopic signature could be expected (Grötsch et al., 1998). The $\delta^{13}\text{C}$ fluctuation in NE-Texas is extremely difficult to correlate with the variations in SE-France (Fig. 57), because of the sampling gaps. Only three major fluctuations in NE-Texas can be transferred to SE-France (Fig. 57). The top of Al 9 in the Middle Albian, the zone Al 14 in the late Albian and the major increase of $\delta^{13}\text{C}$ values in the late Late Albian between zone Al 17 and Al 18 can be found in NE-Texas.

4.4.6. Albian/Cenomanian Stage and Albian Substage Boundaries in NE-Texas

Middle/Late Albian Substage Boundary

As discussed in chapter 3.4.6., classically the Middle/Late Albian boundary can be defined by the FAD of *Dipoloceras cristatum*. For the definition of the Middle/Late Albian boundary in NE-Texas, different bio- and lithostratigraphical horizons are available. There are the FAD of *H. moremani* 1.4 m below the distinct lithological change from Marys Creek Marl to the Benbrook Limestone and the FAD of *Dipoloceras cristatum* 2 m above the litho -

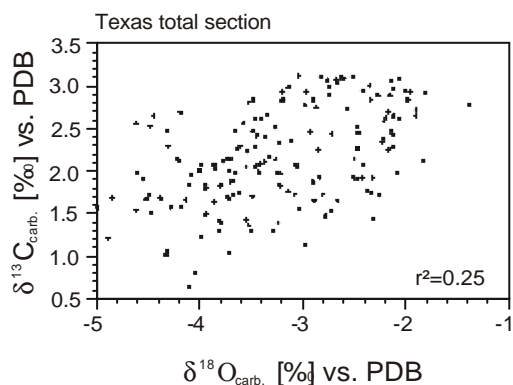


Fig. 56: $\delta^{13}\text{C}$ and $\delta^{18}\text{O}$ of bulk carbonate samples from NE-Texas showing a weak to insignificant positive correlation.

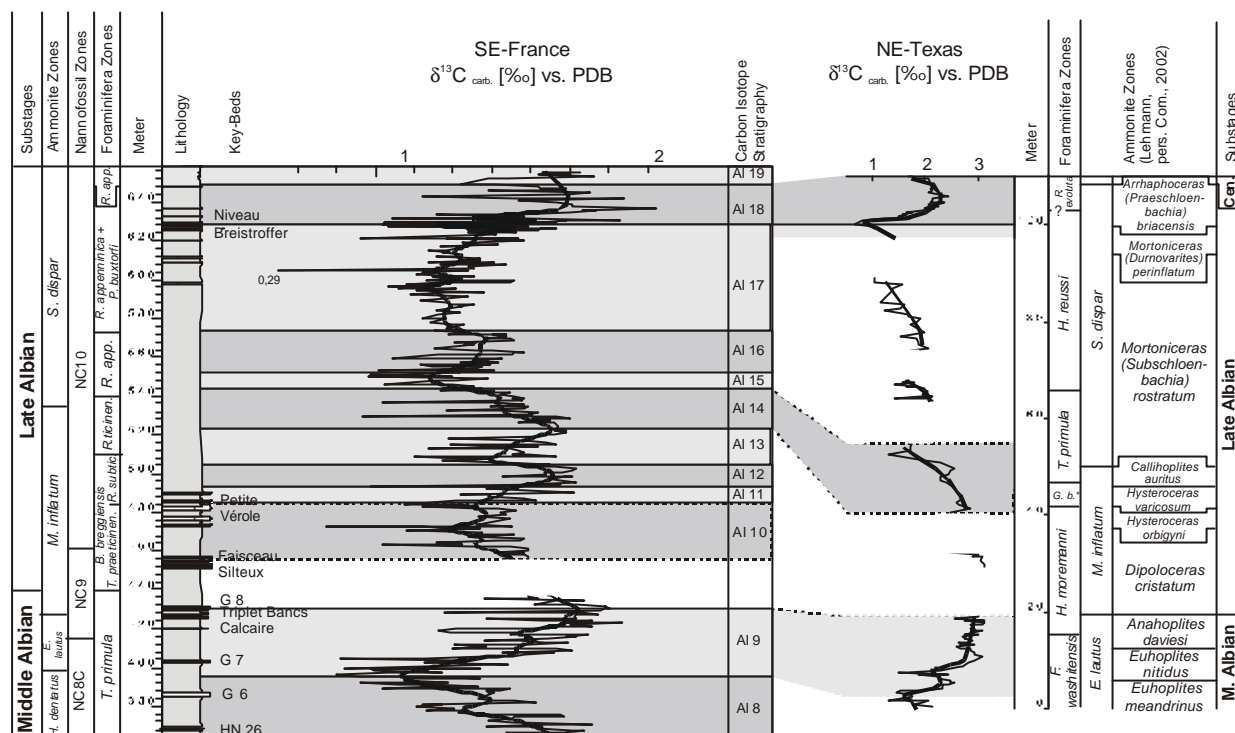


Fig. 57: Correlation of the Carbon isotope record of SE-France and the $\delta^{13}\text{C}$ record of the NE-Texas.

logical change. The distinct lithological change from marlstones (Marys Creek) to limestones (Benbrook), 16 m above the base of the succession, can be used as boundary marker as well. The Middle/Late Albian substage boundary is defined in NE-Texas by the FAD *D. cristatum* (Young, 1967; Hancock et al., 1993) known from the upper part of the Goodland formation (Kennedy et al., 1999; Scott et al., submitted; Fig. 58).

Albian/Cenomanian Stage Boundary

After Scott et al. (submitted) the Albian/Cenomanian stage boundary can be defined by a cycle boundary in the upper meter of the Main Street formation (Fig. 58). This cycle boundary can be correlated by graphic correlation with the proposed boundary in France (Scott et al., submitted). Clark (1965) and Young (1967) stated that the Albian/Cenomanian boundary lies at the top of the Pawpaw formation. The upper part (Pawpaw, Main Street and Grayson formation) contains a typical Cenomanian ammonite fauna (Mancini, 1979). Based on planktic foraminifera (FAD of *Rotalipora evoluta/appenninica*) this boundary could be

placed into the Grayson formation (Pessagno, 1967; Michael, 1972). But the FAD of *R. evoluta/appenninica* is not reliable because there are evidences (discussed in chapter 5.1.) that the first appearance is not time equivalent to the FAD of *Rotalipora appenninica* in SE-France, for example.

For the placement of the Albian/Cenomanian stage boundary in NE-Texas, the following bio-, litho-, isotope- and cyclostratigraphic datums are available: the FAD of *R. evoluta* in the lower Main Street formation (1 above the base), the lithological change from the limestones of the Main Street to the marlstones of the Grayson formation (1 m below the top of the total succession). Also the change from the isotope zone Al 17 to Al 18 (1 m below the base of the Main Street formation) and the cycle boundary WA 5 to WA 6 (1 m below the top of the succession).

In this thesis the Albian/Cenomanian stage boundary is defined by the cycle boundary between cycle WA 5 and WA 6 suggested by Scott et al. (submitted; Fig. 58). This coincides with the lithological boundary between the Main Street and Grayson formation.

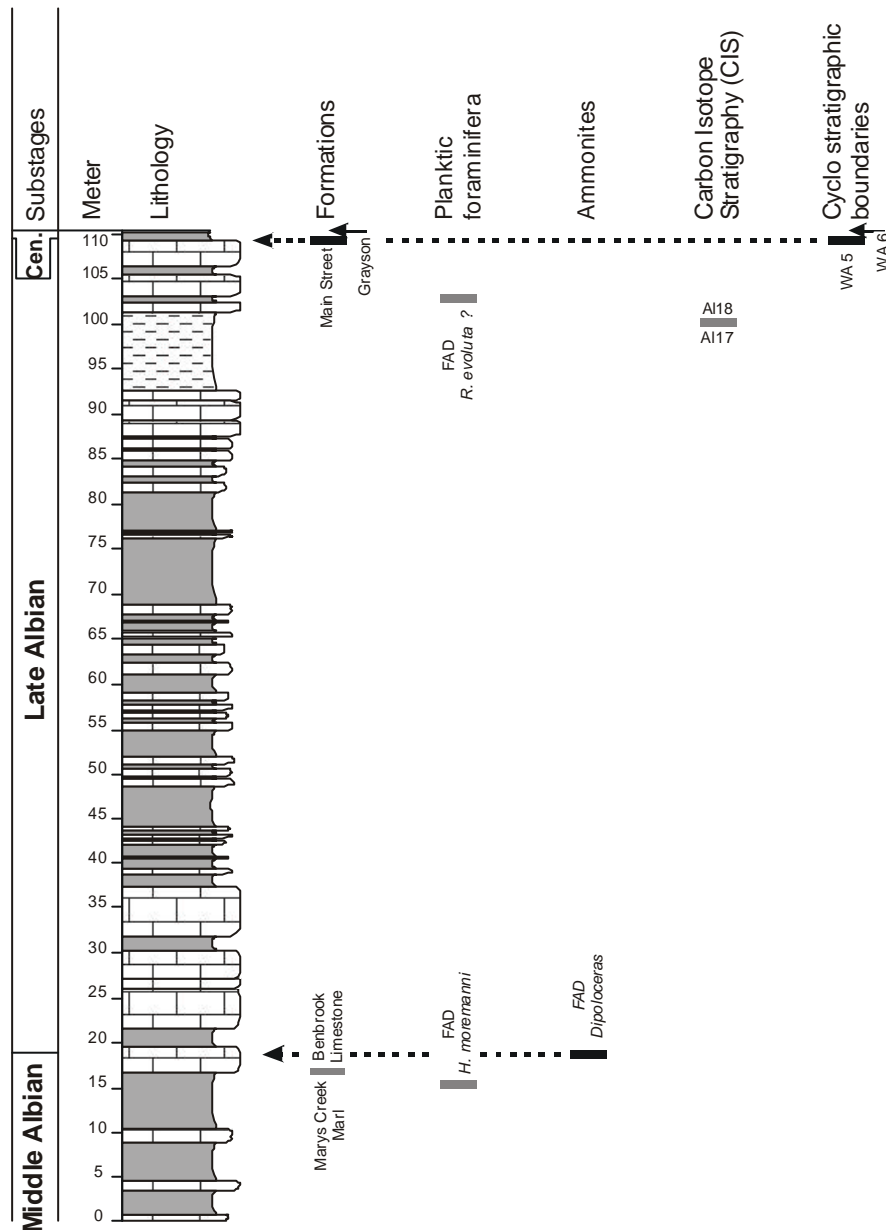


Fig. 58: Overview of the Middle and Late Albian of NE-Texas with bio-, isotope- and lithostratigraphic marker horizons for the Middle/Late Albian substage and Albian/Cenomanian stage boundary. First appearance datums of planktic foraminifera, isotope stratigraphy and lithological events (this thesis), ammonites (Lehmann pers. com.).

5. Integrated Stratigraphy of the Late Aptian to Late Albian: Implications for Planktic Foraminiferal Evolution

5.1. Comparison of First and Last Appearance Datums of Planktic Foraminifera with an isochronous $d^{13}C$ signal

Based on the assumption that the carbon isotope signal is a global isochronous signal (Hilbrecht & Hoefs, 1986; Voigt & Hilbrecht,

1997; Bralower et al., 1999) and due to the correlation of Fig. 30, 31 and 57, syn- and diachronous first and last appearance datums of planktic foraminifera can be described (Fig. 59).

Ticinella bejaouaensis

The last appearance of *T. bejaouaensis* in SE-France is recorded in the middle part of isotope zone Ap 15. At the Mazagan Plateau it occurs at the base of zone Al 2 (Fig. 59). This leads to the assumption that the LAD of *T. bejaouaensis*

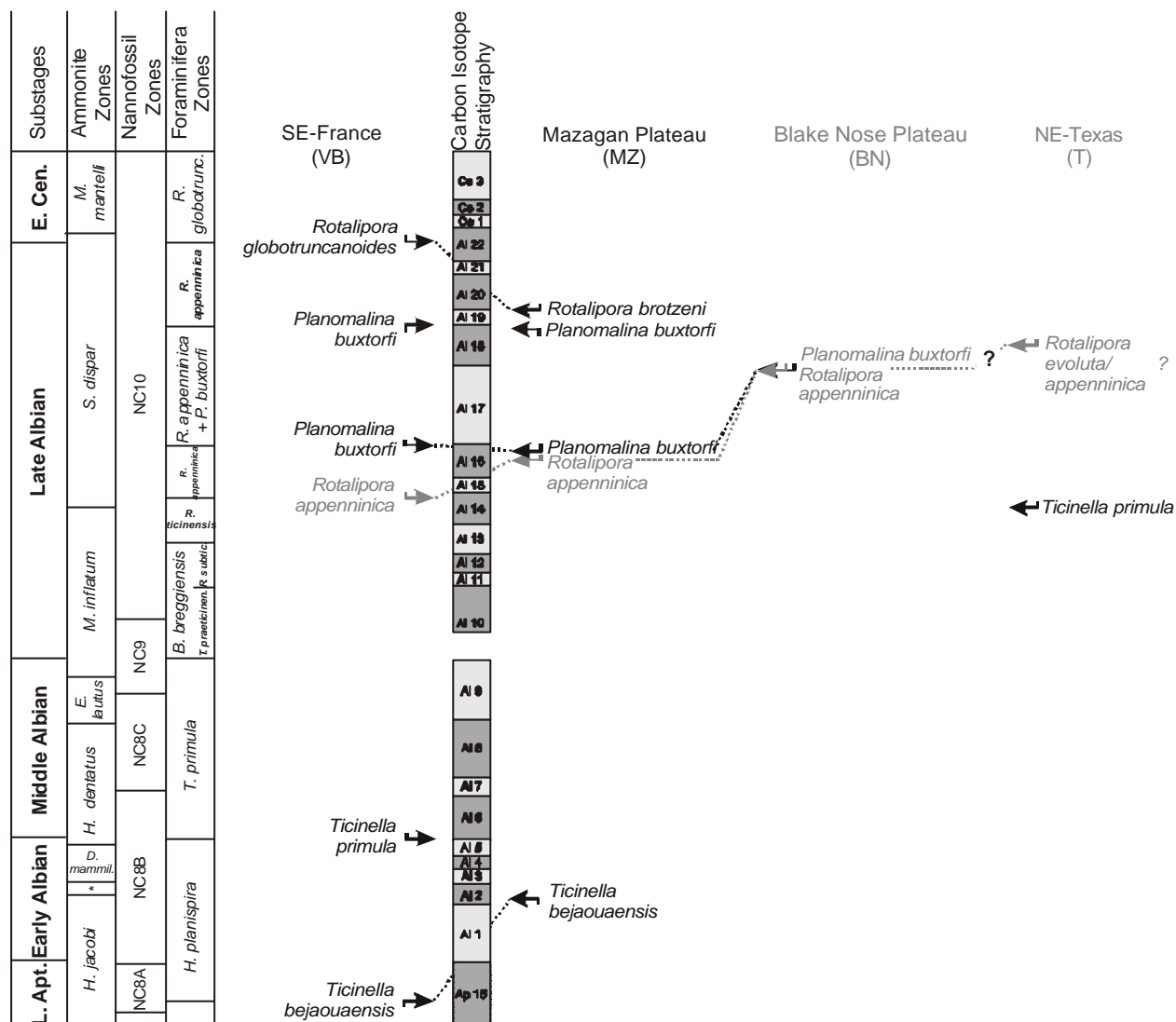


Fig. 59: Comparison of first appearance datum (FAD) of planktic foraminifera of the Aptian and Early Cenomanian of SE-France, DSDP Site 545 and 547 (Mazagan Plateau, NW-Africa), ODP Site 1052 (Blake Nose Plateau; western Atlantic) and NE-Texas. The FADs of planktic foraminifera in SE-France and NE-Texas based on this thesis, FADs of the Mazagan Plateau based on Leckie (1984) and the FADs of the Blake Nose Plateau on Bellier & Moullade (2002) and Wilson & Norris (2001).

is diachronous as Kennedy et al. (2000) presumed. This species died out first in the western Tethys and about 2.1 Ma later in the eastern Atlantic (the sedimentation rate for the Late Aptian/Early Albian is estimated as ~3 cm / 1000 years; Köbller et al., 2001). Due to missing data no statements about the western Atlantic can be made.

Ticinella primula

T. primula first appears in SE-France at the base of Al 6. There does not exist any data from the eastern and western Atlantic. In NE-Texas

T. primula first occurs in the middle of Al 14 (Fig. 59). This long gap (2.9 to 6.8 Ma; depending on sedimentation rates of 7 cm per 1000 years for the Late Albian and 3 cm per 1000 years for the Late Aptian) between these two FADs and there is evidence that a paleoceanographic mechanism controlled the FAD of *T. primula* in NE-Texas (see chapter 6.6.2.). The FAD of *T. primula* is presumed to be diachronous (Kennedy et al., 2000). Based on biostratigraphical comparison, the reappearance of *Ticinella* with *T. primula* is diachronous between various European

(Robaszynski & Caron, 1995) and Tethyan (Tornaghi et al., 1989) sections.

Rotalipora appenninica

Correlations of the FADs of *R. appenninica* show an earlier record in SE-France (isotope zone Al 14) than at the Mazagan Plateau (Al 16). At the Blake Nose Plateau (western Atlantic) *R. appenninica* occurs somewhat later than at the Mazagan Plateau (top of Al 17; Fig. 59). According to this new observation the FADs of *R. appenninica* could be placed chronologically. *Rotalipora appenninica* first evolves in the western Tethys then emerges into the eastern Atlantic and from there into the western Atlantic (Fig. 60). The estimated time periods, calculated by sedimentation rates and absolute ages can be assumed as follows: The duration of the late Albian is assumed as 3.1 Ma (Gradstein et al., 1995), with 203 m of sediments in the late Albian in SE-France a sedimentation rate of about 5 to 7 cm / 1000 a is calculated. The sedimentation rate for the Mazagan Plateau is estimated about 3 cm / 1000 a (Leckie, 1984), and for the Blake Nose Plateau about 9 to 10 cm / 1000 a (Wilson & Norris, 2001). Based on these sedimentation rates and supported by absolute ages (Gradstein et al., 1995, Wilson & Norris, 2001), the migration of *R. appenninica*

from the western Tethys to the eastern Atlantic took 0.3-0.4 Ma and from the eastern to the western Atlantic 0.7-0.9 Ma (Fig. 60). The total time period of the migration from the western Tethys to the western Atlantic is estimated as 1.0-1.3 Ma. The distribution of *R. appenninica* from east to west may be compared with the migration of *Globorotalia truncatulinoides* / *Globorotalia tosaensis* in the Pliocene. *Globorotalia truncatulinoides*, respectively its ancestor *Globorotalia tosaensis*, migrates during 2.3 and 1.9 Ma from the southwest Pacific into the Indian and Atlantic oceans via the Indonesian passage (Spencer-Cervato & Thierstein, 1997).

Planomalina buxtorfi

P. buxtorfi first occurs in SE-France and at the Mazagan Plateau at the top of isotope zone Al 16. At the Blake Nose Plateau *P. buxtorfi* first emerges at the top of Al 17. It seems that the FAD of *P. buxtorfi* in SE-France and at the Mazagan Plateau is more or less synchronous (Fig. 61). The time period between the FAD in SE-France and the FAD at the Mazagan Plateau is ~0.06 Ma, which is shorter than the sample distance at the Mazagan Plateau (0.14-0.24 Ma). The time between the FAD in SE-France / Mazagan Plateau and the Blake Nose Plateau is

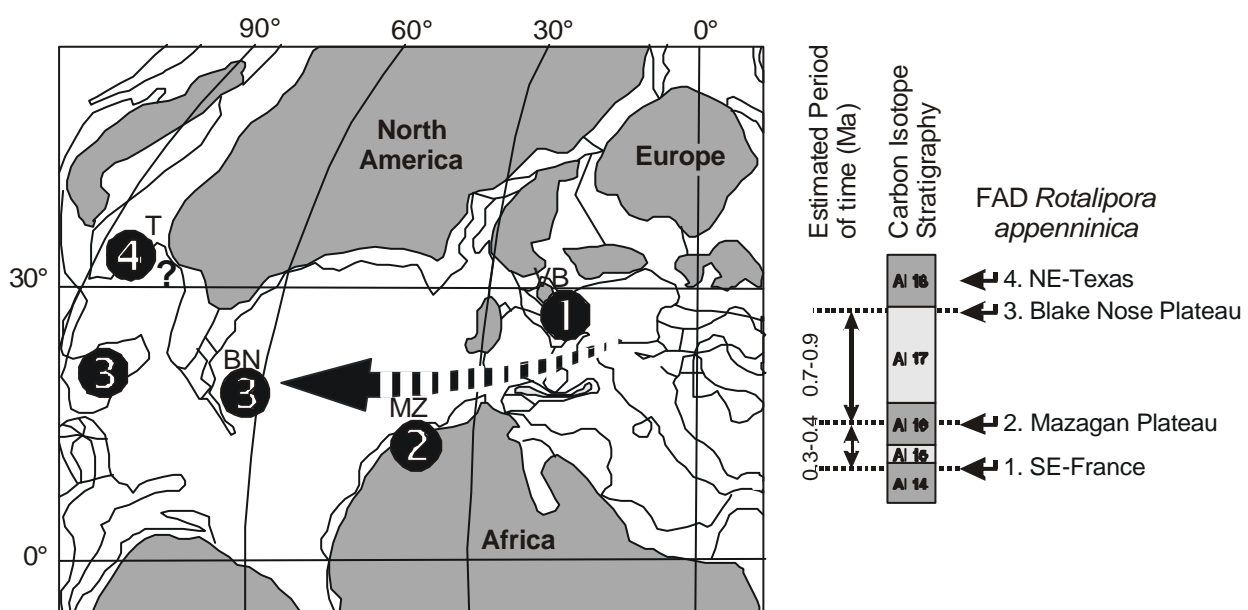


Fig. 60: Palaeogeographic map of the northern hemisphere in the Late Albian (modified after Voigt, 1996). The FADs of *R. appenninica* are shown chronologically in black numbers.

about 0.7 to 0.9 Ma (Fig. 61).

Rotalipora globotruncanoides

In SE-France *R. globotruncanoides* emerges for the first time in the isotope zone Al 22, and *R. brotzeni* (older synonym of *R. globotruncanoides*; after González Donoso & Linares in Robaszynski et al., 1994) at the Mazagan Plateau at the top of Al 19 (Fig. 59). This indicates that this rotaliporid species evolved 0.7 Ma (sedimentation rate ~6 cm per 1000 years) earlier in the eastern Atlantic than in the western Tethys.

significant effect on the transport of planktic foraminifera as Schmuker & Schiebel (2002) pointed out. Transportation of recent shallow and deep dwelling foraminifera *Globorotalia truncatulinoides* by currents (Subtropical Underwater; Schmuker & Schiebel, 2002; Azores Current; Schiebel et al., 2002) is proposed. It has to be asked what kind of mechanism might have forced the delay of the FAD of *R. appenninica* between SE-France and NW-Africa and not that of the later occurring *P. buxtorfi*. For example, Spencer-Cervato & Thierstein (1997) proposed oceanographic

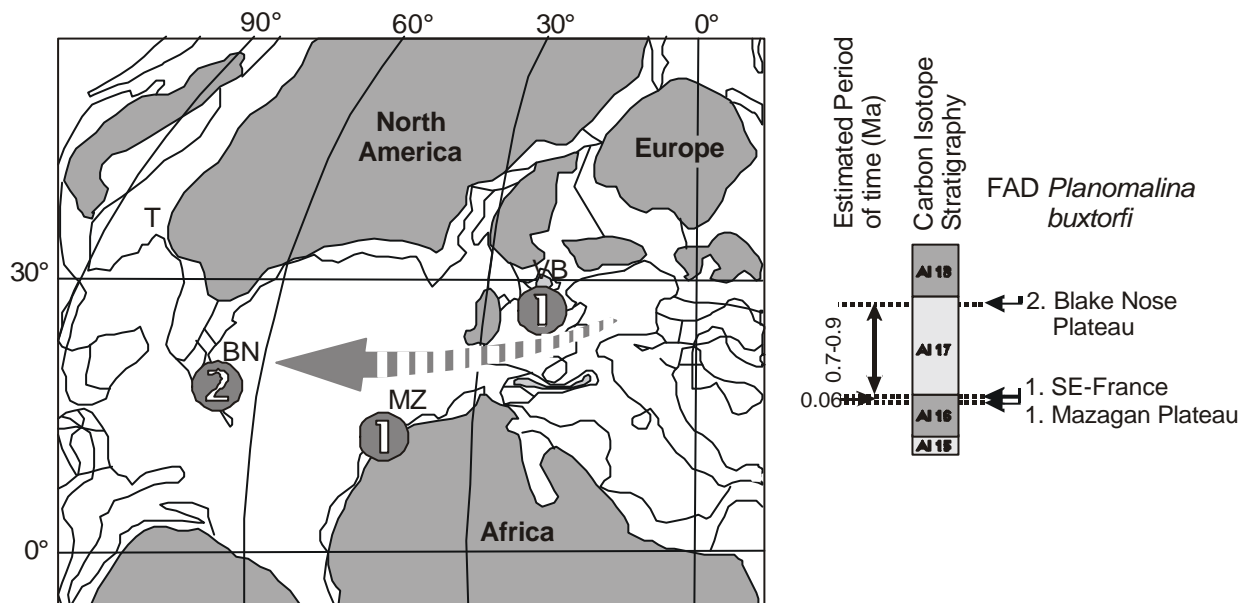


Fig. 61: Palaeogeographic map of the northern hemisphere in the Late Albian (modified after Voigt, 1996). The FADs of *P. buxtorfi* are shown chronologically in light grey numbers.

5.2. Palaeoceanographic Implications of diachronous FADs of *R. appenninica* and *P. buxtorfi* at the Mazagan Plateau (eastern Atlantic).

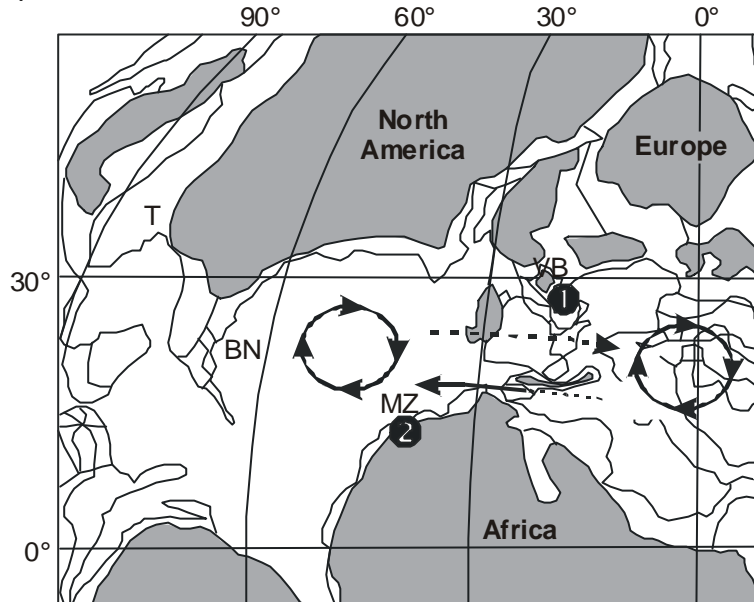
Rotalipora appenninica appears diachronously in the western Tethys and the eastern Atlantic, with a time lack of 0.3-0.4 Ma, whereas *P. buxtorfi* occurs synchronously 0.45 Ma later (Fig. 60, 61). The transport mechanism of *R. appenninica* and *P. buxtorfi* may be the clockwise surface water currents in the western Tethys and Central Atlantic gyres (Barron & Peterson, 1990; Poulsen et al., 2001). It seems to be evident that water currents had a

barriers for a delayed and a following transgression for spurred migration of *G. truncatulinoides* respectively *G. tosaensis*. But oceanographic barriers in the mid Cretaceous between the western Tethys and the eastern Atlantic can be ruled out: The Betic Seaway with a depth of ~ 2500 m represented no hindrance to planktic foraminifera. For the Albian Betic Seaway an open deep water connection to the North Atlantic is suggested (Reicherter et al., 1994). For the mid-Cretaceous (Late Albian) ocean circulation, clockwise gyres in the Tethys and the central Atlantic are proposed (Barron & Peterson, 1990; Poulsen et al., 2001). The Betic Seaway is dominated by a

westward outflow from the Tethys into the central Atlantic and a small backflow in the northern part into the Tethys (Poulsen et al., 2001; Fig. 62). Possibly the intensity of the surface water currents can be supposed as

cause for the diachronous appearance of *R. appenninica* (0.3-0.4 Ma) or the synchronous appearance of *P. buxtorfi* between SE-France and the Mazagan Plateau. Nowadays, currents in east to west direction (for example

a) FAD *R. appenninica*



b) FAD *P. buxtorfi*

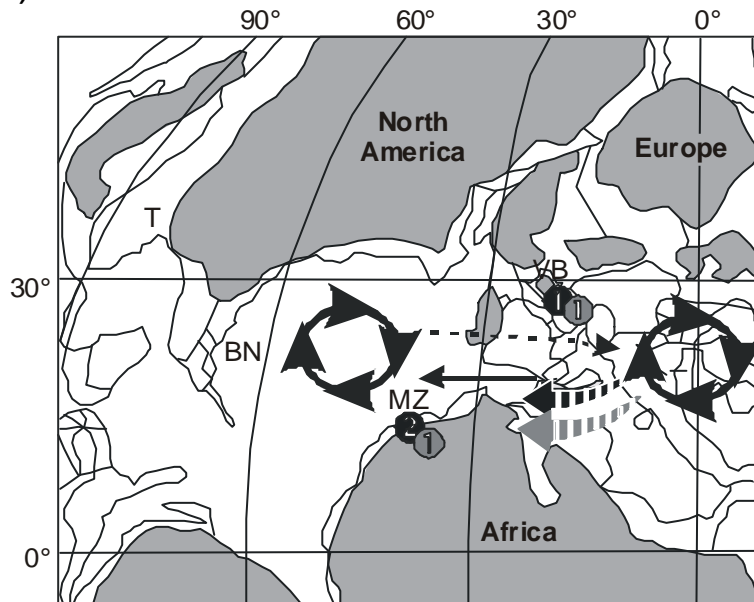


Fig. 62: Palaeogeographic map of the northern hemisphere in the Late Albian (modified after Voigt, 1996) with the FADs of *R. appenninica* (black numbers) and *P. buxtorfi* (grey numbers) in a preliminary chronology. Black arrows indicate the simplified water currents for the western Tethys and the Atlantic, modified after Barron & Peterson (1990) and Poulsen (2001). The thickness of the arrows shows the presumed intensity of the surface water currents. Broken arrows indicate the possible distribution of *R. appenninica* (black) and *P. buxtorfi* (grey).

the Canary Current) flow with slow 0.1 to 2.0 km/h compared to the Gulf Stream that flows in north south direction (2.0 to 5.0 km/h; Ingle, 1999). If we assume that the 0.3-0.4 Ma long migration of *R. appenninica* is for the Cretaceous a “normal” time period it remains questionable why *P. buxtorfi* migrates /appears in SE-France and at the Mazagan Plateau synchronous without or minor delay. Enhanced water current velocity and therefore a higher transport speed can be achieved by enforced surface water circulation. An amplified monsoonal activity in the course of global warming would lead to a greater wind speed and consequently to enforced surface water velocity. For the northern hemisphere in the mid Cretaceous, due to the land-ocean distribution, a monsoon system, comparable to the modern Asian monsoon system, is proposed by Oglesby & Park (1989). The Late Albian is characterised by a global warming (102 Ma to CTBE; Abreu et al. 1998) as well, which is supported by oxygen isotope data from the Exmouth Plateau (104-98 Ma; Clark & Jenkyns, 1999). Therefore, it may be speculated that in the Late Albian between the FAD of *R. appenninica* at the Mazagan Plateau (Fig. 62a) and the FAD of *P. buxtorfi* in SE-France/ Mazagan Plateau (Fig. 62b) the global warming enforced

the monsoonal system and subsequently the surface water circulation. Consequently, the migration of *P. buxtorfi* (Fig. 62b) would have been accelerated compared with the distribution of *R. appenninica* (Fig. 62a). Furthermore, an amplified monsoonal system would not only have speed up the transportation velocity in the clockwise gyres in the Atlantic and Tethys, but in addition also transport warm water from the subtropics into high latitudes. In NW-Germany, the planktic foraminifera data of the Kirchrode borehole shows influences of warm water in the Late Albian (Weiss, 1997).

5.3. Palaeoecological Implications for diachronous FADs of *R. appenninica* and *P. buxtorfi* at the Blake Nose Plateau (western Atlantic).

Due to the ongoing global warming in the Late Albian (Abreu et al., 1998; Clark & Jenkyns, 1999), it may be presumed that an enhanced monsoonal activity and surface water circulation exist and so a faster migration of planktic foraminifera species possibly could be expected. Comparing the FADs of *R. appenninica* and *P. buxtorfi* between the Mazagan and Blake Nose section, both species occur at the Blake Nose

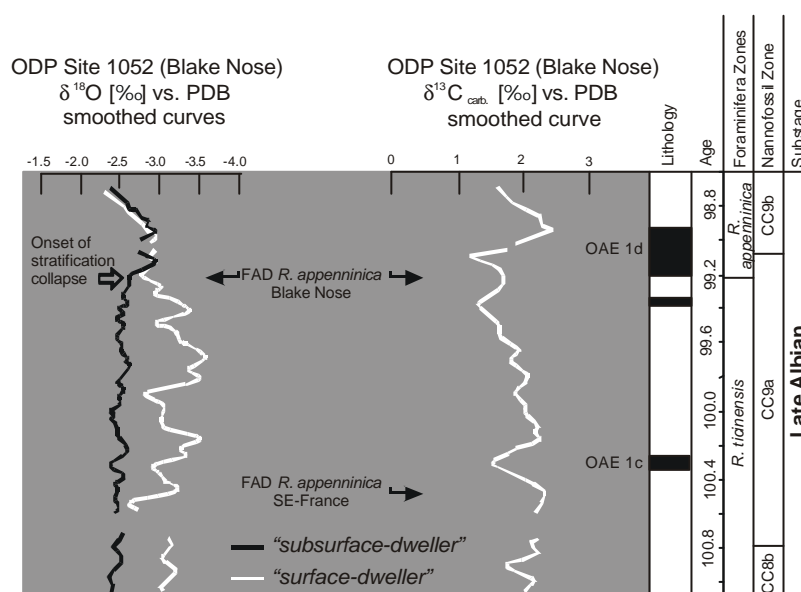


Fig. 63: Carbon and oxygen isotope record of ODP Site 1052 at the Blake Nose Plateau (Wilson & Norris, 2001) marked with the first appearance of *Rotalipora appenninica* in SE-France and at the Blake Nose Plateau.

Plateau simultaneously 0.7-0.9 Ma later than at the Mazagan Plateau (and 1.0-1.3 Ma later than in SE-France; Fig. 60, 61). The migration/distribution of these two species between NW-Africa (eastern Atlantic) and off Florida (western Atlantic) seems to be as well delayed. In addition to the above mentioned paleo-oceanographic changes (current velocity), palaeoecological factors like food availability can be considered as cause for the retarded migration of these species. Both species (*R. appenninica*, *P. buxtorfi*) are assumed to have lived in the deeper part of the photic zone (Hart, 1980; Wonders, 1980) and to have preferred waters with low nutrient concentration and less phytoplankton (e.g. Premoli-Silva & Sliter, 1999). Like their modern counterparts, these k-type species (Premoli-Silva & Sliter, 1999) seemed to be most specialised in the living habitat and food preference. Recent keeled foraminifera like *Globorotalia menardii* live in the deeper part of the surface waters near the thermocline about 50-100 m (Kemle von Mücke & Oberhänsli, 1999) and prefer mainly phytoplankton (diatoms, coccoliths) and detrial remains as food source (Hemleben et al., 1977; Spindler et al., 1984). Based on morphological comparisons this food preference might be as

signed to the Cretaceous keeled forms like *Rotalipora* and *Planomalina*.

In the Late Albian the Atlantic is described as an ocean basin which has ceased to be an extension of a silled Tethys Seaway, with an estuarine circulation and a deep connection to other deep oceans (Norris et al., 2001). The sediments at the Blake Nose Plateau are accumulated in an open marine environment. The estimated Sea Surface Temperature (SST) is proposed to have been at least 30-31°C during the Late Albian and Early Cenomanian (Norris & Wilson, 1998). At the Blake Nose Plateau, the $\delta^{18}\text{O}$ signal of surface and subsurface dwelling planktic foraminifera shows converging values near the onset of the OAE1d (Wilson & Norris, 2001). This converging is interpreted as a collapse of the upper ocean thermal gradient (stratification), an increase in the depth of the mixed layer and/or a shift in the thermocline is under debate (Wilson & Norris, 2001; Fig. 63). The converging $\delta^{18}\text{O}$ values of surface and subsurface planktic foraminifera could also be interpreted as a habitat change of the foraminifera. Wilson & Norris (2001) argue against a habitat change, because of the coherency of the $\delta^{18}\text{O}$ signal. The delayed FADs of *R. appenninica* and *P. buxtorfi* at the Blake

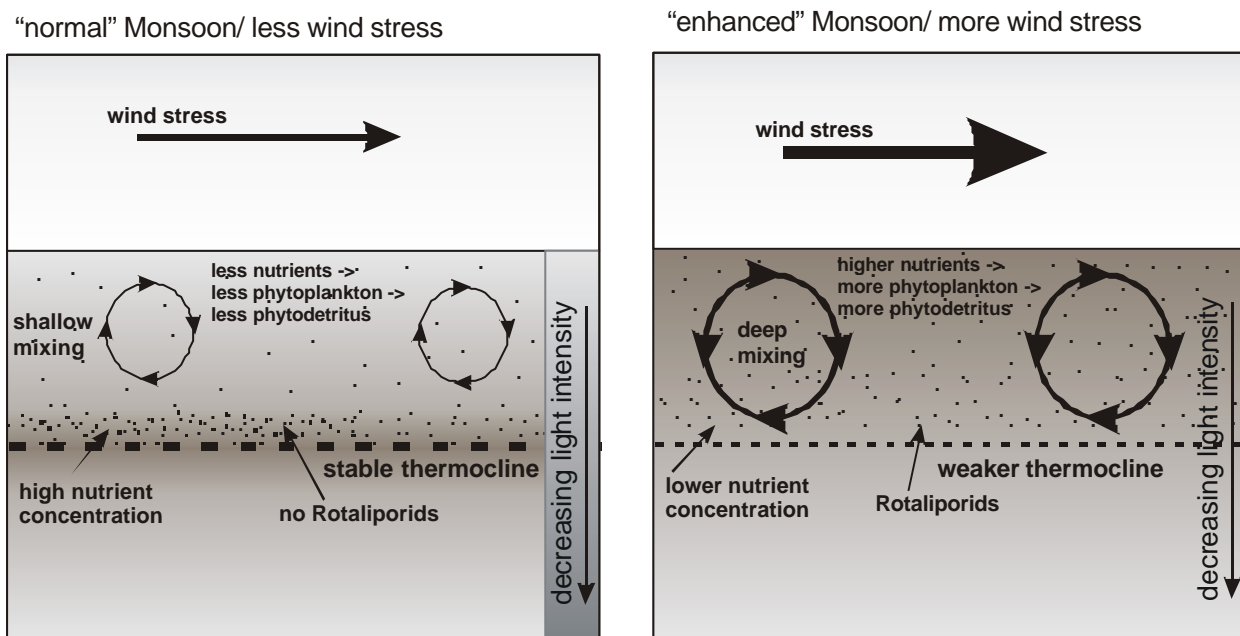


Fig. 64: Model of nutrient distribution in the upper water column at the Blake Nose Plateau before and during the collapse of the stratification.

Nose Plateau correspond with the collapse of the stratification (Fig. 63). Therefore, it is assumed that the ecological circumstances at the Blake Nose before the stratification collapse prevented the settlement of these species and/or the ecological changes following the collapse may have advanced the settlement. The collapse of the stratification, which lead to a better mixing of the surface water and the water of the deeper photic zone, could be the cause itself. The break-down of the stratification might have lead to more oxygen in the deeper photic zone and redistribution of the nutrients. The better mixing could have provided that the nutrients, which are accumulated in the deeper photic zone during a time with a more stable thermocline (Fig. 64a), to be evenly distributed in all of the photic zone and that the deeper photic zone will become relatively depleted (entrainment; Fig. 64b; Schiebel et al., 2001). Whereas the nutrient condition in the deeper photic zone before the mixing can be characterised as fairly high, the mixing depleted most of the nutrients. A rather nutrient depleted condition is more appropriate for deep dwelling, k-type species like *R. appenninica* and *P. buxtorfi*, according to Premoli Silva & Sliter (1999). When nutrients accumulated in the deeper photic zone with reduced light intensity (Fig. 64a) not enough phytodetritus food for *R. appenninica* and *P. buxtorfi* may have been available. In the upper part of the surface water with higher light intensity, not many nutrients may have been present and consequently the amount of phytodetritus was small. If nutrients have been more evenly distributed due to the mixing and the nutrient concentration in the upper part of the photic zone have been increased (Fig. 64b), more phytoplankton may have been produced and more food for keeled foraminifera would have been present in the deeper photic zone. Wilson & Norris (2001) assumed that the variability in stratification is related to local changes in proto-western boundary current waters and subtropical gyres. Furthermore, it is suggested that a stratification collapse is accompanied by a general increase in deep winter mixing and generally reduced summer stratification, analogous to modern seasonal

cycles in the subtropics (Wilson & Norris, 2001) added over longer time periods. Meyers & Doose (1999) and Herrle et al. (2003 a, b) assumed that enhanced monsoonal activity is characterised by stronger winds allowing a better mixing of the surface waters and the entrainment of nutrients into the upper photic zone (Fig. 64). Therefore enhanced monsoonal activity forced by global warming can be considered as cause for the collapse in the stratification.

5.4. Transgression related First Appearance Datums in NE-Texas and Implications for Biostratigraphy

First appearances of planktic foraminifera in NE-Texas seem to occur in two major intervals in the Kiamichi and in the Pawpaw to Main Street formation (Fig. 65). The first interval in the lower Late Albian Kiamichi formation shows five FADs in a very short succession. This interval is characterised by the first occurrence of *Ticinella primula*. Michael (1972) also described this FAD in the Kiamichi formation. *Ticinella primula* is regarded as Middle Albian (e.g. Longoria, 1984) or used as basal marker of the Middle Albian (Br  h  ret, 1997; Fiet et al. 2001). For example, Longoria (1984) and Premoli-Silva & McNulty (1989) described the FAD of *T. primula* from the Gulf of Mexico as Middle Albian. Compared with SE-France (CIS) the FAD of *T. primula* in NE-Texas lies in the Late Albian (Fig. 65). This observation of a late appearance of *T. primula* is supported by the ammonite stratigraphy of NE-Texas (Lehmann pers. com.), which placed the Kiamichi formation into the Late Albian. The Kiamichi formation is more or less equivalent to the Washita depositional cycle 1 (WA 1), which represents a transgressive flooding period (after Scott et al. submitted; Fig. 65). Regarding the late FAD of *T. primula* in NE-Texas compared to SE-France, and the simultaneous transgression, it is possible that this first occurrence is induced by the transgression. The higher total abundance of planktic foraminifera (Fig. 46, 53) supports that hypothesis. It is supposed that *T. primula*, present in

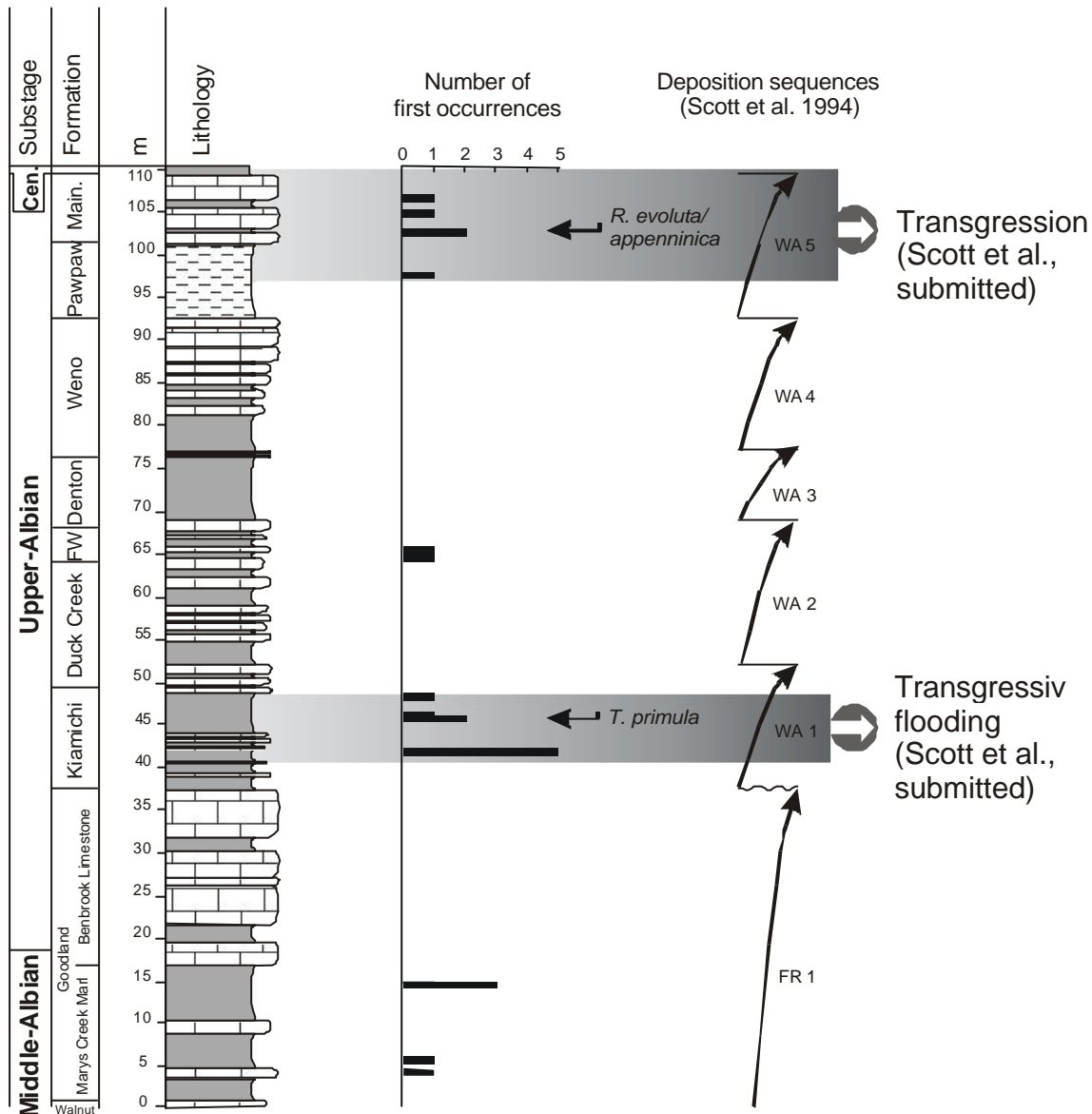


Fig. 65: The FADs and LADs of planktic foraminifera in NE-Texas of the Middle and Late Albian compared with the cyclostratigraphy based on Scott et al. (submitted).

the western Atlantic (Gulf of Mexico) in the Middle Albian, migrated to NE-Texas not until the Late Albian because of the shallow marine environment on the Comanchean shelf. Therefore, this FAD can only be used for a regional stratigraphic zonation in NE-Texas, but can not be compared superregional with, for example, SE-France. The second interval from the upper Pawpaw to the upper Main Street formation is marked by 1 to 2 FADs in a short succession as well. This interval is characterised by the FAD of *R. evoluta* (Fig. 65). After Scott et al. (submitted), *R. evoluta* is synonymous to *R. appenninica*. The appearance of *R. evoluta/*

appenninica in the uppermost Albian to lowermost Cenomanian (Main Street to Grayson formation) in NE-Texas is supported by Pessagno (1967), Michael, (1972) and Mancini (1979). Also the FAD of *R. evoluta/appenninica* is described for example in the middle Late Albian (early *S. dispar* ammonite zone) from SE-France (this thesis) and the Late Albian (upper part of the *S. dispar* ammonite zone) from the Gulf of Mexico (Longoria, 1984). In the east (Western Tethys; SE-France), *R. appenninica* occurs earlier than in the west (Western Atlantic, Blake Nose Plateau) and in the Gulf of Mexico (Longoria, 1984; Fig. 66). The

delayed appearance of *R. evoluta/appenninica* in NE-Texas compared with the Gulf of Mexico (Fig. 66) can be explained by the shallow neritic environment in NE-Texas during most of the Late Albian. *R. evoluta/appenninica* had the first opportunity to migrate into NE-Texas along with a major transgression (Fig. 66; dark grey arrow), which Scott et al. (submitted) postulated for the Late Albian Pawpaw and Main Street formation (WA 5 cycle). Also in the Kiamichi Formation, the influence of transgression on the planktic foraminifera occurrences is supported by the increasing total abundances (chapter 4.4.2.).

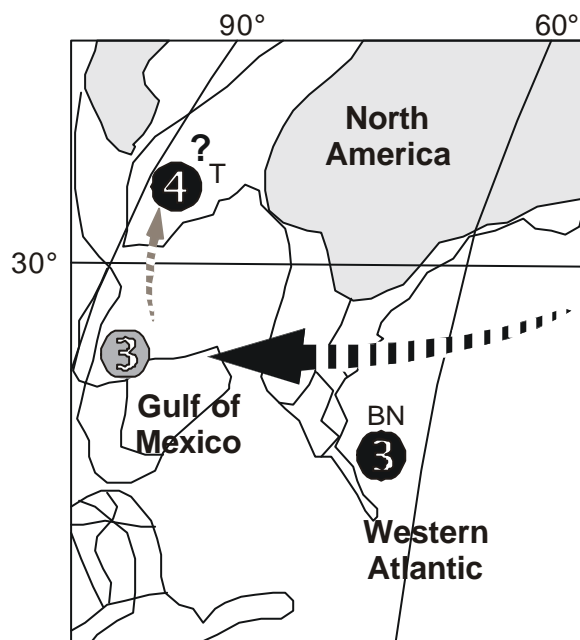


Fig. 66: Palaeogeographic map of the Western Atlantic in the Late Albian (modified after Voigt, 1996). The FADs of *R. appenninica* in this area are shown chronologically in black numbers. The dark grey number 3 is based on data from Longoria (1984). The dark grey arrow induced the transgression derived first occurrence of *R. appenninica* in NE-Texas.

6. Conclusions

- Based on first and last occurrences of planktic foraminifera, a detailed planktic foraminifer's biostratigraphic zonation for the Late Aptian to Albian of the Vocontian Basin (western Tethys) and the Middle to Late Albian of NE-Texas (western Atlantic) is established.

For NE-Texas a biostratigraphic zonation based on first and last appearance datums of planktic foraminifera, and not on foraminifera assemblages, is presented. The planktic foraminifera biostratigraphy of the Vocontian Basin and NE-Texas is calibrated to the carbon isotope stratigraphy and the existing ammonite and calcareous nannofossil biostratigraphy for the western Tethys and the western Atlantic.

- A high resolution carbon isotope stratigraphy for the Early, Middle and Late Albian of the Vocontian Basin (SE-France) has been established and verified by comparison with the carbon isotope record ($\delta^{13}\text{C}$) of the Mazagan Plateau, the Blake Nose Plateau and NE-Texas.

- After integrating all biostratigraphic (planktic foraminifera, calcareous nannofossils and ammonites) and isotope stratigraphic data, the following markers for stage and substage boundaries are presented: The Aptian/Albian Stage boundary in SE-France is determined 5.5 m above the Niveau Kilian black shale, characterised by the onset of the negative $\delta^{13}\text{C}$ excursion. The Early/Middle Albian substage boundary in SE-France is marked by the first appearance datum (FAD) of the planktic foraminifer *Ticinella primula*. The Middle/Late Albian substage boundary is defined by the FAD of the planktic foraminifer *Biticinella breggiensis* accompanied by the FAD of the ammonite *Mortoniceras inflatum*. The Middle/Late Albian substage boundary in NE-Texas is determined by the FAD of the ammonite *Dipoloceras cristatum*. The Albian/Cenomanian Stage boundary is defined by the cycle boundary between the sedimentation cycle WA 5 and WA 6 in NE-Texas.

- Based on the correlation of the $\delta^{13}\text{C}$ record of the sections in SE-France (western Tethys), the Mazagan Plateau (eastern Atlantic), the Blake Nose Plateau (western Atlantic) and NE-Texas (western Atlantic) syn- and diachronous first and last appearances of planktic foraminifera can be described. *Ticinella bejaouaensis* disappears (LAD) in SE-France about 2.1 Ma earlier than at the Mazagan Plateau. *Rotalipora appenninica* emerges at the Mazagan Plateau 0.3-0.4 Ma later than in SE-

France and 0.7-0.9 Ma later at the Blake Nose Plateau than at the Mazagan Plateau. The first appearance of *Planomalina buxtorfi* in SE-France and at the Mazagan Plateau seems to be synchronous, but at the Blake Nose Plateau this species occurs 0.7-0.9 Ma later. *Rotalipora globotruncanoides* first occurs at the Mazagan Plateau and can be recognised about 0.7 Ma later in SE-France. In NE-Texas, *Ticinella primula* and *Rotalipora evoluta/appenninica* first occur with time lags of 2.9 to 6.8 Ma (*Ticinella primula*, compared to SE-France) and *Rotalipora evoluta/appenninica* appears about 0.6 Ma later than at the Blake Nose Plateau (1.5 Ma compared with SE-France).

- These syn- and diachronous first and last appearances of planktic foraminifera have the following palaeoceanographic and palaeoecologic implications: The delayed transport of *R. appenninica* between SE-France and the Mazagan Plateau as well as the faster transport of *P. buxtorfi* may be caused by the influence of the enhanced monsoonal system on the surface water circulation. The synchronous FAD of *R. appenninica* and *P. buxtorfi* at the Blake Nose Plateau coincides with the collapse of stratification of the upper water column. A direct palaeoecologic link between the FADs and the collapse is assumed and can be explained by a redistribution of nutrients within the photic zone due to the enhanced monsoonal activity. The delayed appearances of planktic foraminifera in NE-Texas may be caused by the shallow marine environment of the Comanchean shelf. The FADs of planktic foraminifera in NE-Texas are mainly influenced by sea level induced transgressions, which prevented a settling of *T. primula* and *R. evoluta/appenninica*.

7. Literature

- Abreu, V.; Hardenbol, J.; Haddad, G.A.; Baum, G.R.; Droxler, A., W. & Vail, P.R.** (1998): Oxygen isotope synthesis: a Cretaceous ice-house.- *In* de Graciansky, P.-C.; Hardenbol, J.; Jacquin, T. & Vail, P., R. (eds.) Mesozoic and Cenozoic sequence stratigraphy of European Basins, *SEPM Special Publication*, **60**, 75-80.
- Arkin, Y. & Hamaoui, M.** (1967): The Judea Group (Upper Cretaceous) in Central and Southern Israel.- *Geological Survey of Israel Bulletin*, **42**, 1-17.
- Arnaud, H. & Lemoine, M.** (1993): Structure and Mesozoic-Cenozoic evolution of the South-East France Basin (SFB).- *Géologie Alpine*, **3**, 3-58.
- Arnaud-Vanneau, A. & Arnaud, H.** (1990): Hauterivian to Lower Aptian carbonate shelf sedimentation and sequence stratigraphy in the Jura and northern subalpine Chains (south-eastern France and Swiss Jura).- *In* Tucker, M.E.; Wilson, J.L.; Crevello, P.D.; Sarg, J.R. & Read, J.F. (eds.) Carbonate Platforms, *International Association of Sedimentologists, Special Publication*, **9**, 203-233.
- Arnaud-Vanneau, A. & Arnaud, H.** (1991): Sédimentation et variations relatives du niveau de la mer sur les plate-formes carbonatées du Berriasien-Valanginien inférieur et du Barrémien dans les massifs subalpins septentrionaux et le Jura (Sud-Est de la France).- *Bulletin Société Géologique de France*, **8**, 535-545.
- Arthur, M.A.; Dean, W.E. & Schlanger, S.O.** (1985): Variations in the global carbon cycle during the Cretaceous related to climate, volcanism, and changes in atmospheric CO₂.- *In* Sundquist, E.T.S. & Broecker, W.S. (eds.) The Carbon Cycle and Atmospheric CO₂: Natural variations Archean to Present, *Geophysical Monograph*, 504-529.
- Arthur, M.A.; Brumsack, H.J.; Jenkyns, H.C. & Schlanger, S.O.** (1990): Stratigraphy, geochemistry, and Palaeoceanography of organic carbon-rich Cretaceous sequences.- *In* Ginsburg, R.N. & Beaudoin, B. (eds.) Cretaceous Resources, Events and Rhythms, 75-119.
- Ayala, C.A.** (1962): Morfología y estructura de algunas foraminíferos planetónicos del Cenomaniano de Cuba.- *Societa Geologia Mexicanas Bulletin*, **25**, 1-63.
- Barr, F.T.** (1972): Cretaceous biostratigraphy and planktonic foraminifera of Lybia.- *Micropalaeontology*, **18**, 1-46.
- Barron, E.J.** (1987): Global Cretaceous Palaeogeography.- *Palaeogeography, Palaeoclimatology, Palaeoecology*, **59**, 207-214.
- Barron, E.J. & Washington, W.M.** (1985): Warm Cretaceous climates: High atmospheric CO₂ as plausible mechanism.- *In* Sundquist, E.T. & Broecker, W.S. (eds.), The Carbon Cycle and Atmospheric CO₂: Natural variations Archean to Present, *Geophysical Monograph*, 546-553.
- Barron, E.J. & Peterson, W.H.** (1990): Mid-Cretaceous ocean circulation: results from model sensitivity studies.- *Palaeoceanography*, **5** (3), 319-337.
- Barron, E.J.; Fawcett, P.J.; Peterson, W.H.; Pollard, D. & Thompson, S.L.** (1995): A simulation of mid-Cretaceous climate.- *Palaeoceanography*, **10** (5), 953-962.
- Bellier, J.P. & Moullade, M.** (2002): Lower Cretaceous planktonic foraminiferal biostratigraphy of the western North Atlantic (ODP Leg 171B), and taxonomic clarification of key index species.- *Revue de Micropaléontologie*, **45**, 9-26.
- Birkelund, T.; Hancock, J.M.; Hart, M.B.; Rawson, P.F.; Remane, J.; Robaszynski, F.; Schmid, F. & Surlyk, F.** (1984): Cretaceous stage boundaries - Proposals.- *Bulletin of the Geological Society of Denmark*, **33**, 3-20.
- Blow, W.H.** (1970): Validity of biostratigraphic correlations based on the *Globigerinacea*.- *Micropalaeontology*, **16**, 257-268.
- Bolli, H.M.** (1945): Zur Stratigraphie der oberen Kreide in den höheren helvetischen Decken.- *Ecolgae Geologicae Helvetiae*, **37**, 217-329.

- Bolli, H.M.** (1959): Planktonic foraminifera from the Cretaceous of Trinidad, B.W.I.- *Bulletins of American Palaeontology*, **39**, 257-277.
- Bornemann, A.** (2000): Paläozeanographische Untersuchungen an Schwarzschiefern des Ober-Alb (Unter-Kreide) von SE-Frankreich.- Diploma thesis, Bochum.
- BouDagher-Fadel, M.K.; Banner, F.T. & Whittaker, J.E.** (1997): The *Favusellidae*- the Cretaceous acme of the *Favusellacea*.- In BouDagher-Fadel, M.K.; Banner, F.T. & Whittaker, J.E. (eds.) *The Early Evolutionary History of Planktonic Foraminifera*, 57-77.
- Bralower, T. J.; Sliter, W. V.; Arthur, M. A.; Leckie, M. R.; Allard, D. & Schlanger, S.** (1993): Dysoxia/Anoxia Episodes in the Aptian-Albian (Early Cretaceous).- *The Mesozoic Pacific, Geophysical Monograph*, **77**, 5-37.
- Bralower, T. J.; Arthur, M. A.; Leckie, M. R.; Sliter, W. V.; Allard, D. & Schlanger, S.** (1994): Timing and palaeoceanography of oceanic dysoxia/anoxia in the Late Barremian to Early Aptian (Early Cretaceous).- *Palaios*, **9**, 335-369.
- Bralower, T.J.; Fullagar, P.D.; Paull, C.K.; Dwyer, G.S. & Leckie, M.R.** (1997): Mid-Cretaceous strontium-isotope stratigraphy of deep-sea sections.- *Geological Society of America Bulletin*, **109**, 1421-1442.
- Bralower, T.J.; CoBabe, E.; Clement, B.; Sliter, W.V.; Osburn, C.L. & Longoria, J.** (1999): The record of global changes in mid-Cretaceous (Barremian-Albian) sections from the Sierra Madre, northeastern Mexico.- *Journal of Foraminiferal Research*, **29**, 418-437.
- Bréhéret, J.-G.** (1983): Sur des niveaux de black-shales dans l'Albien inférieur et moyen du domaine vocontien (Sud-Est de la France): Étude de nannofaciès et signification des paléoenvironnements.- *Bulletin du Muséum National d'Histoire Naturelle*, **5C**, 113-159.
- Bréhéret, J.-G.** (1986): Indices d'un événement anoxique étendu à la Téthys alpine, à l'Albien inférieur événement Paquier.- *Comptes Rendu de l'Académie des Sciences*, **300**, 355-358.
- Bréhéret, J.-G.** (1988): Episodes de sédimentation riche en matière organique dans les marnes bleues d'âge aptien et albien de la partie pelagique du bassin vocontien.- *Bulletin Société Géologique de France*, **8**, 349-356.
- Bréhéret, J.-G.** (1997): L'Aptien et l'Albien de la Fosse vocontienne; Evolution de la sédimentation et enseignements sur les événements anoxiques.- *Société Géologique du Nord*, **25**, pp. 602.
- Bréhéret, J.-G.; Caron, M. & Delamette, M.** (1986): Niveaux riches en matière organique dans l'Albien Vocontien; quelques caractères du palaeoenvironnement; essai d'interprétation génétique.- *Documentaire de Bureau géologique et minéralogique*, **110**, 141-191.
- Bréhéret, J.-G. & Delamette, M.** (1987): Séquences de dépôt et couches riches en matière organique (CRMO) dans les marnes bleues aptiennes et albiennes du bassin vocontien.- In Ferry, S. & Rubino, J.L. (eds.) *Eustatisme et séquences de dépôt dans le Crétacé du Sud-Est de la France.- Géotrope*, **1**, 83-93.
- Bréhéret, J.-G. & Delamette, M.** (1989): Faunal fluctuation relates to oceanographical changes in the Vocontian Basin (S-France) during Aptian-Albian time.- *Geobios, Mémoire spéciale*, **11**, 267-277.
- Breistroffer, M.** (1947): Sur les Zones d'Ammonites dans l'Albien de France et d'Angleterre.- *Travaux du Laboratoire de Géologie de l'Université de Grenoble*, **26**, 17-104.
- Caron, M.** (1985): Cretaceous planktic foraminifera.- In Bolli, H.M.; Saunders, J.B. & Perch-Nielsen K. (eds.) *Plankton Stratigraphy*, 17-86.
- Caron, M. & Homewood, P.** (1983): Evolution of early planktic foraminifers.- *Marine Micropalaeontology*, **7**, 453-462.
- Carsey, D.J.** (1926): Foraminifera of the Cretaceous of central Texas.- *Bulletin of the University of Texas Bureau of Economic Geology and Technology*, **2612**, 1-56.
- Clark, D.L.** (1965): Heteromorph ammonoids from the Albian and Cenomanian of Texas and adjacent regions.- *Geological Society of America, Mémoire*, **95**.

- Clarke, L.J. & Jenkyns, H.C.** (1999): New oxygen isotope evidence for long-term Cretaceous climatic change in the Southern Hemisphere.- *Geology*, **27**, 699-702.
- Coccioni, R.; Erba, E. & Premoli-Silva, I.** (1992): Barremian-Aptian calcareous plankton biostratigraphy from the Gorgo Cerbara section (Marche, central Italy) and implications for plankton evolution.- *Cretaceous Research*, **13**, 517-537.
- Coccioni, R. & Premoli Silva, I.** (1994): Planktonic foraminifera from the Lower Cretaceous of Rio Argos sections (southern Spain) and biostratigraphic implications.- *Cretaceous Research*, **15**, 645-687.
- Codispoti, L.A.** (1997): The limits to growth.- *Nature*, **387**, 237-238.
- Courtillot, V.; Jaeger, J.J.; Yang, Z.; Feraud, G. & Hofmann, C.** (1996): The influence of continental flood basalts on mass extinctions; where do we stand?- In Ryder, G.; Fastovsky, D. & Gartner, S. (eds.) The Cretaceous-Tertiary event and other catastrophes in Earth history, *Geological Society of America, Special Paper*, **307**, 513-525.
- Cotillon, P. & Rio, M.** (1984): Cyclicité comparée du Crétacé inférieur pélagique dans les chaînes subalpines méridionales (France SE), l'Atlantique central (Site 534 DSDP) et le Golfe du Mexique (Sites 535 et 540 DSDP). Implications paléoclimatiques et application aux corrélations stratigraphiques transthysiennes.- *Bulletin de la Société Géologique de France*, **26**, 47-61.
- Curnelle, R. & Dubois, P.** (1986): Evolution mésozoïque des grands bassins sédimentaires français (bassins de Paris, d'Aquitaine et du Sud-Est).- *Bulletin de Société Géologique de France*, **8**, 529-546.
- Eisbacher**, (1988): Nordamerika.- *Enke Verlag*, pp. 176.
- Erba, E.** (1992): Calcareous Nannofossil distribution in pelagic rhythmic sediments (Aptian-Albian Piobbico core, Central Italy).- *Rivista Italia Palaeontologia Stratigraphia*, **97**, 455-484.
- Erba, E.** (1996): The Aptian Stage.- *Bulletin Institut Royal Nature Belgique*, **66**, 31-43.
- Erbacher, J.** (1994): Entwicklung und Paläozeanographie mittelkretazischer Radiolarien der westlichen Tethys (Italien) und des Nordatlantiks.- *Tübinger Mikropaläontologischen Mitteilungen*, **12**, 120.
- Erbacher, J.; Thurow, J. & Littke, R.** (1996): Evolution patterns of radiolaria and organic matter variations: A new approach to identify sea-level changes in mid-Cretaceous pelagic environments.- *Geology*, **24**, 499-502.
- Erbacher, J. & Thurow, J.** (1997): Influence of oceanic anoxic events on the evolution of mid-Cretaceous radiolaria in the North Atlantic and western Tethys.- *Marine Micropalaeontology*, **30**, 139-158.
- Erbacher, J.; Hemleben, C.; Huber, B.T. & Markey, M.** (1999): Correlating environmental changes during early Albian oceanic anoxic event 1b using benthic foraminiferal palaeoecology.- *Marine Micropalaeontology*, 7-28.
- Erbacher, J.; Huber, B.T.; Norris, R.D. & Markey, M.** (2001): Increased thermohalin stratification as a possible cause for an ocean anoxic event in the Cretaceous period.- *Nature*, **409**, 325-327.
- Falkowski, P.G.; Barber, R.T. & Smetacek, V.** (1998): Biochemical controls and feedbacks on ocean primary productivity.- *Science*, **281**, 200-206.
- Fiet, N.; Beaudoin, B. & Parize, O.** (2001): Lithostratigraphic analysis of Milankovitch cyclicity in pelagic Albian deposits of central Italy: Implications for duration of the stage and substages.- *Cretaceous Research*, **22**, 265-275.
- Finsley, C.** (1996): A field guide to fossils of Texas.- *Gulf Publishing Company*, pp. 211.
- Fisher, W.L. & Rodda, P.U.** (1969): Edwards Formation (Lower Cretaceous), Texas: Dolomitization in a carbonate platform system - *American Association of Petroleum Geologist Bulletin*, **53**, 55-72.
- Flandrin, J.** (1963): Remarques stratigraphiques, paléontologiques et structurales sur la région de Séderon.- *Bulletin du Service de la Carte Géologique de la France*, **272**, 815-845.
- Friedmann, I. & O'Neil, J.R.** (1977): Compilation of stable isotope fractionation factors of

geochemical interest.- In Fleischer, M. (ed.) *Data of Geochemistry, U.S. Geological Survey Professional Paper*, **440**, 12.

Gale, A.S.; Kennedy, W.J.; Burnett, J.A.; Caron, M. & Kidd, B.E. (1996): The Late Albian to Early Cenomanian succession at Mont Risou near Rosans (Drome, SE-France): an integrated study (ammonites, inoceramids, planktonic foraminifera, nannofossils, oxygen and carbon isotopes).- *Cretaceous Research*, **17**, 515-606.

Galeotti, S. (1998): Planktic and benthic foraminiferal distribution patterns as a response to changes in surface fertility and ocean circulation: a case study from the Late Albian "Amadeus Segment" (Central Italy).- *Journal of Micropalaeontology*, **17**, 87-96.

Gandolfi, R. (1942): Ricerche micropalaeontologiche e stratigrafiche sulla Scaglia e sul flysch cretacicci die Dintorni di Balema (Canton Ticino).- *Rivista Italiana Palaeontologia Stratigrafia*, **48**, 1-160.

Gandolfi, R. (1955): The genus *Globotruncana* in Northeastern Colombia.- *Bulletin American Palaeontology*, **36**, 7-118.

Gradstein, F.M.; Agterberg, F.P.; Ogg, J.G.; Hardenbol, J.; Veen, P.V.; Thierry, J. & Huang, Z. (1995): A Triassic, Jurassic and Cretaceous time scale.- *Society of Economic Palaeontologists and Mineralogists, Special Publication*, **54**, 95-126.

Grötsch, J.; Billing, I. & Vahrenkamp, V. (1998): Carbon-isotope stratigraphy in shallow-water carbonates: Implications for Cretaceous black-shale deposition.- *Sedimentology*, **45**, 623-634.

Gwinner, M.P. (1971): Geologie der Alpen. Stratigraphie, Paläogeographie, Tektonik.- *Schweizerbart Verlag*, pp. 477.

Haig, D.W. (1979): Global distribution patterns for mid-Cretaceous foraminiferids.- *Journal of Foraminiferal Research*, **9**, 29-40.

Hancock, J.M. (1991): Ammonites scales for the Cretaceous System.- *Cretaceous Research*, **12**, 259-291.

Hancock, J.M.; Kennedy, W.J. & Cobban, W.A. (1993): A correlation of the Upper Albian to basal Coniacian sequence of Northwest Europe, Texas and the United States Western Interior.- In Caldwell, W.G.E. & Kaufman, E.G. (eds.) Evolution of the Western Interior Basin, *Geological Association of Canada, Special Paper*, **39**, 453-476.

Hancock, J.M. (2001): A proposal for a new position for the Aptian/Albian boundary.- *Cretaceous Research*, **22**, 677-683.

Haq, B.U.; Hardenbol, J. & Vail, P.R. (1988): Mesozoic and Cenozoic chronostratigraphy and cycles of sea-level changes.- *SEPM Special Publication*, **42**, 71-108.

Hart, M.B. (1980): A water depth model for the evolution of planktonic Foraminiferida.- *Nature*, 252-254.

Hart, M.B. (1999): The evolution and biodiversity of Cretaceous planktonic foraminiferida.- *Geobios*, **32**, 247-255.

Hart, M.B. & Bailey, H.W. (1979): The distribution of planktic foraminiferida in the mid-Cretaceous of NW-Europe.- In Wiedmann, J. (ed.) Aspekte der Kreide Europas., IUGS Series A, **6**, 527-542.

Hart, M.B.; Amedro, F. & Owen, H. (1996): The Albian stage and substage boundaries.- *Bulletin Institut Royal Nature Belgique*, **66**, 45-56.

Hay, W.W.; DeConto, R. M.; Wold, Ch. N.; Wilson, K. M.; Voigt, S.; Schulz, M.; Wold-Rosby, A.; Dullo, W.-Ch.; Ronov, A. B.; Balukhovskiy, A. N. & Soeding, E. (1999): An alternative global Cretaceous palaeogeography.- In Barrera, E.J. & Claudia C. (eds.) The evolution of the Cretaceous Ocean-Climate System, *Special Papers of the Geological Society of America*, **332**, 1-47.

Haynes, J.R. (1981): The Globigerinida.- Foraminifera, MacMillan Publisher, pp. 433.

Hayward, O.T. & Brown, L.F. (1967): Comanchean (Cretaceous) rocks of central Texas.- *Society of Economic Palaeontologists and Mineralogists, Permian Basin Section*, **67-8**, 30-48.

- Hemleben, C.; Bé, A.W.H.; Anderson, R.O. & Tuntivate, S.** (1977): Test morphology, organic layers and chamber formation of the Planktonic foraminifer *Globorotalia menardii* (d'Orbigny).- *Journal of Foraminiferal Research*, **7**, 1-25.
- Hendricks, L.** (1967): Comanchean stratigraphy of the Cretaceous of North Texas.- *Society of Economic Palaeontologists and Mineralogists, Permian Basin Section*, **67-8**, 51-64.
- Herrle, J.O.** (2002): Palaeoceanographic and palaeoclimatic implications on Mid-Cretaceous black shale formation in the Vocontian Basin and Atlantik: Evidence from calcareous nannofossils and stable isotopes.- *Tübinger Mikropaläontologische Mitteilungen*, **27**, 114.
- Herrle, J.O. & Mutterlose, J.** (2003): Calcareous nannofossils from the Aptian -Lower Albian of southeast France: palaeocological and biostratigraphic implications.- *Cretaceous Research*, **24**, 1-22.
- Herrle, J.O.; Pross, J.; Friedrich, O. & Hemleben, Ch.** (2003 a): Short-term changes in the Cretaceous Tethyan Ocean: micropalaeontological evidence from Early Albian Oceanic Anoxic Event 1b.- *Terra Nova*, **15**, 14-19.
- Herrle, J.O.; Pross, J.; Friedrich, O. Köbler, P. & Hemleben, Ch.** (2003 b): Forcing mechanisms for mid-Cretaceous black shale formation: evidence from the Upper Aptian and Lower Albian of the Vocontian Basin (SE France).- *Palaeogeography, Palaeoclimatology, Palaeoecology*, **190**, 399-426.
- Hilbrecht, H. & Hoefs, J.** (1986): Geochemical and palaeontological studies of the $\delta^{13}C$ anomaly in Boreal and north Tethyan Cenomanian-Turonian sediments in Germany and adjacent areas.- *Palaeogeography, Palaeoclimatology, Palaeoecology*, **53**, 169-189.
- Hill, R.T.** (1887): The present condition of knowledge of the geology of Texas.- *U.S. Geological Survey Bulletin*, **45**, 95 p.
- Hill, R.T.** (1901): Geography and Geology of the Black and Grand Prairies, Texas.- *U.S. Geological Survey*, **21**, 292.
- Huber, B.T.; Hodell, D.A. & Hamilton, C.P.** (1995): Middle-Late Cretaceous climate of the southern high latitudes: Stable isotopic evidence for minimal equator-to-pole thermal gradients.- *Geological Society of America Bulletin*, **107**, 1164-1191.
- Immenhauser, A. & Scott, R.W.** (1999): Global correlation of middle Cretaceous sea-level events.- *Geology*, **27**, 551-554
- Ingle, J.C.** (1999): Atmosphere-Ocean coupling and surface circulation of the ocean.- In Ernst, W.G. (ed.) *Earth System*, Cambridge University Press, 152-169.
- Jahren, A.H. & Arens, N.C.** (1998): Methane hydrate dissociation implicated in Aptian OAE events.- *Geological Society of America Abstracts with Programs*, **30**, 53.
- Jansa, L.F.; Steiger, T.H. & Bradshaw, M.** (1984): Mesozoic carbonate deposition on the outer continental margin off Morocco. - In Hinz, K. & Winterer, E.L. (eds.) *Initial Reports of the Deep Sea Drilling Project*, **79**, 857-891.
- Jenkins, D.G.** (1971a): New Zealand Cenozoic Planktonic Foraminifera.- *Bulletin of the Geological Survey of New Zealand*, **42**, 1-278.
- Jenkins, D.G.** (1971b): The reliability of some Cenozoic planktonic foraminiferal "datum planes" used in biostratigraphic correlation.- *Journal of Foraminiferal Research*, **1**, 82-86.
- Jenkyns, H.C.** (1996): Relative sea-level change and carbon isotopes: Data from Upper Jurassic (Oxfordian) of central and southern Europe.- *Terra Nova*, **8**, 75-85.
- Jenkyns, H.C. & Clayton, C.J.** (1986): Black shales and carbon isotopes in pelagic sediments from the Tethyan Lower Jurassic.- *Sedimentology*, **33**, 87-106.
- Kemle-von Mücke, S. & Oberhänsli, H.** (1999): The distribution of living planktic foraminifera in relation to Southeast Atlantic Oceanography.- In Fischer, G. & Wefer, G. (eds.) *Use of proxies in Palaeoceanography: Examples from the South Atlantic*. Springer-Verlag, 91-115.
- Kennedy, W.J. & Cooper, M.** (1975): Cretaceous ammonite distributions and the opening of the

- South Atlantic.- *Journal of the Geological Society London*, **131**, 283-288.
- Kennedy, W.J.; Gale, A.S.; Hancock, J.M.; Crampton, J.S. & Cobban, W.A.** (1999): Ammonites and Inoceramid Bivalves from close to the middle-upper Albian Boundary around Fort Worth, Texas.- *Journal of Palaeontology*, **73**, 1101-1125.
- Kennedy, W.J.; Gale, A.S.; Bown, P.R.; Caron, M.; Davey, R.J.; Gröcke, D. & Wray, D.S.** (2000): Integrated stratigraphy across the Aptian-Albian boundary in the Marne Bleues, at the Col de Pre-Guittard, Arnayon (Drome), and at Tartonne (Alpes-de Haute-Provence), France: A candidate Global Boundary Stratotype Section and Boundary Point for the base of the Albian Stage.- *Cretaceous Research*, **21**, 591-720.
- Köbller, P.; Herrle, J.O.; Appel, E.; Erbacher, J. & Hemleben, Ch.** (2001): Magnetic records of climatic cycles from mid-Cretaceous hemipelagic sediments of the Vocontian Basin, SE-France.- *Cretaceous Research*, **22**, 331-341.
- Koutsoukos, E.A.M.; Leery, P.N. & Hart, M.B.** (1989): *Favusella* Michael (1972): Evidence of ecophenotypic adaptation of a planktonic foraminifer to shallow-water carbonate environments during the mid-Cretaceous.- *Journal of Foraminiferal Research*, **19**, 324-336.
- Larson, R.L.** (1991): Geological consequences of superplumes.- *Geology*, **19**, 963-966.
- Leckie, M.R.** (1984): Mid-Cretaceous planktonic foraminiferal biostratigraphy off Central Morocco, Deep Sea Drilling Project Leg 79, Sites 545 and 547.- *Initial Reports of the Deep Sea Drilling Projects*, **79**, 579-620.
- Leckie, M.R.** (1987): Palaeoecology of mid-Cretaceous planktonic foraminifera: A comparison of open ocean and epicontinental sea assemblages.- *Micropalaeontology*, **33**, 164-176.
- Leckie, M.R.** (1989): A Palaeoceanographic Model for the early evolutionary history of planktonic foraminifera.- *Palaeogeography, Palaeoclimatology, Palaeoecology*, **73**, 107-138.
- Leckie, M.; Bralower, T.J. & Cashman, R.** (2002): Oceanic anoxic events and plankton evolution: Biotic response to tectonic forcing during the mid-Cretaceous.- *Palaeoceanography*, **17**, 1-29.
- Loeblich, A.R. & Tappan, H.** (1961): Cretaceous planktonic foraminifera: Part 1 -Cenomanian.- *Micropalaeontology*, **7**, 257-304.
- Longoria, J.F.** (1984): Cretaceous biochronology from the Gulf of Mexico region based on planktonic microfossils.- *Micropalaeontology*, **30**, 225-242.
- Lorenz, C.** (1980): Géologie des pays européens, France, Belgique, Luxembourg.- Paris.
- Lozo, F.E.** (1944): Biostratigraphic relations of some north Texas Trinity and Fredericksburg (Comanchean) foraminifers.- *American Midland naturalist*, **31**, 512-582.
- Luciani, V.; Cobianchi, M. & Jenkyns, H.C.** (2001): Biotic and geochemical response to anoxic events: The Aptian pelagic succession of Gargano Promotory (southern Italy).- *Geological Magazine*, **138**, 277-298.
- Mancini, E.A.** (1979): Late Albian and Early Cenomanian Grayson Ammonite biostratigraphy in North-Central Texas.- *Journal of Palaeontology*, **53**, 1013-1022.
- Maslakova, N.I.** (1963): On the classification of the genus Hedbergella. Translated from Russian.- *Oklahoma Geology Notes*, **24**, 130-135.
- Menegatti, A.P.; Weissert, H.; Brown, R.S.; Tyson, R.V.; Farrimond, P.; Strasser, A. & Caron, M.** (1998): High-resolution $\delta^{13}C$ stratigraphy through the early Aptian "Livello Selli" of the Alpine Tethys.- *Palaeoceanography*, **13**, 530-545.
- Meyers, P.A. & Dooze, H.** (1999): Sources, preservation, and thermal maturity of organic matter in Pliocene-Pleistocene organic-carbon-rich sediments of the Western Mediterranean Sea.- In Zahn, R.; Comas, M.C. & Klaus, A. (eds.) *Proceedings of the Ocean Drilling Program, Scientific Results*, **161**, 383-390.
- Michael, F.Y.** (1972): Planktonic Foraminifera from the Comanchean Series (Cretaceous) of Texas.- *Journal of Foraminiferal Research*, **2**, 200-220.
- Mosteller, M.A.** (1970): Subsurface stratigraphy of the Comanchean Series in east central Texas.-

Baylor Geological Studies, Bulletin, **19**, 34.

Moullade, M. (1966): Etude stratigraphique et micropaléontologique du Crétacé inférieur de la "Fosse vocontienne".- *Document Laboratoire Géologique Faculté Science Lyon*, **15**, 369.

Murray, G. (1961): Geology of the Atlantic and Gulf coastal province of North America, pp. 692.

Nederbragt, A.J.; Fiorentino, A. & Klosowska, B. (2001): Quantitative analysis of calcareous microfossils across the Albian-Cenomanian boundary oceanic anoxic event at DSDP Site 547 (North Atlantic).- *Palaeogeography, Palaeoclimatology, Palaeoecology*, **166**, 401-421.

Norris, R.D. & Wilson, P.A. (1998): Low-latitude sea-surface temperatures for the mid-Cretaceous and the evolution of planktic foraminifera.- *Geology*, **26**, 823-826.

Norris, R.D.; Kroon, D.; Huber, B.T. & Erbacher, J. (2001): Cretaceous-Palaeogene ocean and climate change in subtropical North Atlantic.- In Kroon, D.; Norris, R.D. & Klaus, A. (eds.) Western North Atlantic Palaeogene and Cretaceous Palaeoceanography, *The Geological Society Special Publication*, **183**, 1-22.

Oglesby, R. & Park, J. (1989): The effect of precessional insolation changes on Cretaceous climate and cyclic sedimentation.- *Journal of Geophysical Research*, **94**, 793-816.

Owen, H. (1984): The Albian Stage: European Province Chronology and Ammonite Zonation.- *Cretaceous Research*, **5**, 329-344.

Paquier, V. (1900): Recherches géologiques dans le Diois et les Baronnies orientales.- *Thèse Grenoble*, 402 p.

Perkins, B.F. (1960): Biostratigraphic studies in the Comanchean (Cretaceous) series of northern Mexico and Texas.- *Geological Society of America, Memoire*, **83**, 1-48.

Perkins, B.F. & Albritton (1955): The Washita group in the valley of the Trinity River, Texas; a field guide.- *Southern Methodist University Fordren Science Service*, **5**, 27 p.

Pessagno JR, E.A. (1967): Upper Cretaceous planktonic foraminifera from western Gulf Coastal Plain.- *Palaeontographica Americana*, **5**, 245-445.

Poulsen, C.J.; Seidov, D.; Barron, E.J. & Peterson, W.H. (1998): The impact of palaeogeographic evolution of the surface oceanic circulation and the marine environment within the mid-Cretaceous Tethys.- *Palaeoceanography*, **13**, 546-559.

Poulsen, C.J.; Barron, E.J.; Arthur, M.A. & Peterson, W.H. (2001): Response of mid-Cretaceous global oceanic circulation to tectonic and CO₂ forcings.- *Palaeoceanography*, **16**, 576-592.

Premoli-Silva, I. & McNulty, C.L. (1989): Planktonic foraminifera and calpionellids from Gulf of Mexico sites, Deep Sea Drilling Project Leg 77.- *Initial Reports of the Deep Sea Drilling Project*, **77**, 547-584.

Premoli-Silva, I. & Sliter, W.V. (1999): Cretaceous palaeoceanography: Evidence from planktonic foraminiferal evolution.- In Barrera, E.J. & Johnson, C.C. (eds.) Evolution of the Cretaceous Ocean-Climate System, *Geological Society of America, Special Publications*, **332**, 301-328.

Price, G.D. & Hart, M.B. (2002): Isotopic evidence for Early to mid-Cretaceous ocean temperature variability.- *Marine Micropalaeontology*, **46**, 45-58.

Price, G.D.; Sellwood, B.W.; Cornfield, R.M.; Clarke, L. & Cartlidge, J.E. (1998): Isotopic evidence for palaeotemperatures and depth stratification of middle Cretaceous planktonic foraminifera from the Pacific Ocean.- *Geological Magazine*, **135**, 183-191.

Prokoph, A. (1997): Palaeoenvironment and stratigraphy of Late Albian-Early Cenomanian planktonic foraminifera from NE-Germany.- *Freiberger Forschungsheft*, **C468**, 259-271.

Rao, C.P. (1996): Modern Carbonates: tropical, temperate, polar. Introduction to sedimentology and geochemistry.- *Printing Authority of Tasmania, Hobart*, 206.

Reicherter, K.; Pletsch, T.; Kuhnt, W.; Manthey, J.; Homeier, G.; Wiedmann, J. & Thurow, J. (1994): Mid-Cretaceous palaeogeography and palaeoceanography of the Betic Seaway (Betic Cordillera, Spain).- *Palaeogeography, Palaeoclimatology, Palaeoecology*, **107**, 11-33.

Renz, O. (1936): Stratigraphische und mikropalaeontologische Untersuchungen der Scaglia (obere

- Kreide-Tertiär) im zentralen Apennin.- *Eclogae Geologicae Helvetiae*, **29**, 1-149.
- Robaszynski, F.; Caron, M.; Amédéo, F.; Dupuis, C.; Hardenbol, J.; González Donoso, J.-M.; Linares, D. & Gartner, S.** (1994): Le Cénomanién de la région de Kalaat Senan (Tunisie central): litho-biostratigraphie et interprétation séquentielle.- *Revue Paléobiologie*, **12**, 351-505.
- Robaszynski, F. & Caron, M.** (1995): Foraminifères planctoniques du Crétacé: commentaire de la zonation Europe-Méditerranée.- *Bulletin Societe Geologique de France*, **166**, 681-692.
- Roemer, F.** (1849): Texas ... - *Adolf Marcus, Bonn*, 464 p.
- Rose, P.R.** (1972): Edwards Group, surface and subsurface, central Texas.- *University of Texas, Austin, Bureau of Economic Geology, Report of Investigations*, **74**, 198.
- Roth, P.H.** (1986): Mesozoic palaeoceanography of the North Atlantic and Tethys Oceans.- *In* Summerhays, C.P. & Shackleton, N.J. (eds.) North Atlantic Palaeoceanography, *Geological Society London*, **21**, 299-320.
- Salvador, A.** (1991): The origin and development of the Gulf of Mexico Basin.- *In* Salvador, A. (ed.) The Geology of North America, **3**, 389-444.
- Savostin, L.A.; Sibuet, J.; Zonenshain, L.P.; LePichon, X. & Poulet, M.J.** (1986): Kinematic evolution of the Tethys belt from Atlantic Ocean to Pamirs since Triassic.- *Tectonophysics*, **123**, 1-35.
- Schiebel, R.; Waniek, J.; Bork, M. & Hemleben, C.** (2001): Planktic foraminiferal production stimulated by chlorophyll redistribution and entrainment of nutrients.- *Deep Sea Research*, **48**, 721-740.
- Schiebel, R.; Schmuker, B.; Hemleben, C. & Alves, M.** (2002): Tracking the recent and Late Pleistocene Azores Front by the distribution of planktic foraminifers.
- Schlanger, S.O. & Jenkyns, H.C.** (1976): Cretaceous anoxic events: causes and consequences.- *Geologie en Mijnbouw*, **55**, 179-184.
- Schmuker, B. & Schiebel, R.** (2002): Planktic foraminifers and hydrography of the eastern and northern Caribbean Sea.- *Marine Micropalaeontology*, **46**, 387-403.
- Scholle, P.A. & Arthur, M.A.** (1980): Carbon isotope fluctuation in Cretaceous pelagic limestones: potential stratigraphic and petroleum exploration tool.- *American Association of Petroleum Geologist Bulletin*, **64**, 67-87.
- Schuchert, C.** (1943): Stratigraphy of the Eastern and Central United States.- *Wiley & Sons*, pp. 1013.
- Scott, R.W. & West, R.R.** (1976): Structure and classification of palaeocommunities, pp. 66.
- Scott, R.W.** (1990): Models and stratigraphy of Mid-Cretaceous reef communities, Gulf of Mexico.- *Society for Sedimentary Geology, Concepts in Sedimentology and Palaeontology*, **2**, pp.102.
- Scott, R.W.; Fee, D.; Magee, R. & Laali, H.** (1978): Epeiric depositional models for the Lower Cretaceous Washita-Group, North-Central Texas.- *Reports of Investigations, Bureau of Economic Geology*, **94**, p. 23.
- Scott, R.W.; Franks, P.C.; Stein, J.A.; Bergen, J.A. & Evetts, M.J.** (1994): Graphic correlation tests the synchronous Mid-Cretaceous depositional cycles: Western Interior and Gulf Coast, 89-98.
- Scott, R.W.; Benson, D.G.; Morin, R.W. & Shaffer, B.L.** (submitted): Integrated Albian-Lower Cenomanian Chronostratigraphy Standard, Trinity River section, Texas.
- Scott, R.W.; Schlager, W.; Fouke, B. & Nederbragt, S. A.** (2000): Are mid-Cretaceous eustatic events recorded in Middle East carbonate platforms? - *Society of Economic Palaeontologists and Mineralogists, Special Publication*, **69**, 77-88.
- Sellwood, B.W.; Price, G.D. & Valdes, P.J.** (1994): Cooler estimates of Cretaceous temperatures.- *Nature*, **370**, 453-455.
- Sigal, J.** (1952): Observation sur l'âge cenomanien d'une microfaune récemment décrite de la région de Taza (Maroc).- *Compte Rendu Sommaire des Seances de la Societe Geologique de France*, **13-14**, 309-311.

- Sigal, J.** (1955): Notes micropalaeontologiques nord-africaines; 1, Du cenomanien au santonian; zones et limites en facies pelagique.- *Compte Rendu Sommaire des Seances de la Société Géologique de France*, **7-8**, 157-160.
- Sigal, J.** (1965): Presence d'un foraminifère pelagique Hedbergella wshitensis (Carsey) du domaine Méditerranéen dans l'Albien du Bassin de Paris.- *Bureau Resh. Geol. Minier. Memoire*, **34**, 1-840.
- Sigal, J.** (1967): Essai sur l'état actuel d'une zonation stratigraphique a l'aide des principales espèces des Rosalines (Foraminifères).- *Compte Rendu Sommaire des Seances de la Société Géologique de France*, **1**, 48-50.
- Sliter, W.V.** (1989): Biostratigraphic zonation for Cretaceous planktonic foraminifers examined in thin section.- *Journal of Foraminiferal Research*, **19**, 1-19.
- Sliter, W.V.** (1992): Cretaceous planktonic foraminiferal biostratigraphy and palaeoceanographic events in the Pacific Ocean with emphasis on indurated sediment.- In Ishizaki, K.S. & Saito, T. (eds.) Centenary of Japanese Micropalaeontology, 281-299.
- Sliter, W.V. & Premoli-Silva, I.** (1990): Age and origin of Cretaceous planktonic foraminifers from Limestone of the Franciscan complex near Laytonville, California.- *Palaeoceanography*, **5**, 639-667.
- Spencer-Cervato, C. & Thierstein, H.R.** (1997): First appearance of *Globorotalia truncatulinoides*: cladogenesis and immigration.- *Marine Micropalaeontology*, **30**, 267-291.
- Spindler, M.; Hemleben, Ch.; Salomons, J.B. & Smit, L.P.** (1984): Feeding behavior of some planktonic foraminifers in laboratory cultures.- *Journal of Foraminiferal Research*, **14**, 237-249.
- Stanley, S.M. & Hardie, L.A.** (1998): Secular oscillations in the carbonate mineralogy of reef-building and sediment-producing organisms driven by tectonically forced siffs in seawater chemistry.- *Palaeogeography, Palaeoclimatology, Palaeoecology*, **144**, 3-19.
- Strasser, A.; Caron, M. & Gjermeni, M.** (2001): The Aptian, Albian and Cenomanian of Roter Sattel, Romandes Prealps, Switzerland: a high-resolution record of oceanographic changes.- *Cretaceous Research*, **22**, 173-199.
- Stoll, H.M. & Schrag, D.P.** (2000): High-resolution stable isotope records from the Upper Cretaceous rocks of Italy and Spain: Glacial episodes in a greenhouse planet.- *Geological Society of America Bulletin*, **112**, 308-319.
- Tornaghi, M.E.; Premoli-Silva, I & Ripepe, M.** (1989): Lithostratigraphy and planktonic foraminiferal biostratigraphy of the Aptia-Albian "scisti a Fucoidi" in the Piobbico Core, Marche, Italy: Background for cyclostratigraphy.- *Rivista Italiana Paleontologia Stratigrafia*, **95**, 223-264.
- Van Hinte, J.E.** (1965): An approach to *Orbitoides*.- *Proceedings K. ned. Akad. Wet. Series B*, **68**, 57-71.
- Voigt, S.** (1996): Paläobiogeographie oberkretazischer Inoceramen und Rudisten.- *Münchner Geowissenschaftliche Abhandlungen*, **31**, 1-101.
- Voigt, S. & Hilbrecht, H.** (1997): Late Cretaceous carbon isotope stratigraphy in Europe: Correlation and relation with sea level and sediment stability.- *Palaeogeography, Palaeoclimatology, Palaeoecology*, **134**, 39-59.
- Weiss, W.** (1997): Late Albian immigrations of planktonic foraminifera into the boreal sea: Results from Kirchrode I borehole (Hannover, NW-Germany).- *Newsletter Stratigraphy*, **35**, 1-27.
- Weissert, H.; McKenzie, J. & Hochuli, P.** (1979): Cyclic anoxic events in the Early Cretaceous Tethys Ocean.- *Geology*, **7**, 147-151.
- Weissert, H. & Breheret, J.G.** (1991): A carbonate carbon-isotope record from Aptian-Albian sediments of the Vocontian trough (SE France).- *Bulletin Société Géologique de France*, **162**, 1133-1140.
- Weissert, H. & Lini, A.** (1991): Ice age interludes during the time of Cretaceous Greenhouse climate?- In Müller, D.W.; McKenzie, J.A. & Weissert, H. (eds.) Controversies in modern geology: Evolution of geological theories in sedimentology, earth history and tectonics, 173-191.

- Weissert, H.; Lini, A.; Föllmi, K.B. & Kuhn, O.** (1998): Correlation of Early Cretaceous carbon isotope stratigraphy and platform drowning events: a possible link.- *Palaeogeography, Palaeoclimatology, Palaeoecology*, **137**, 189-203.
- Wick, W.** (1947): Aufbereitungsmethoden in der Mikropaläontologie.- *Jahresbericht der naturhistorischen Gesellschaft Hannover*, **98**, 35-41.
- Wiegand, G.E.** (1984): Cretaceous nannofossils from the Northwest African margin, Deep Sea Drilling Project Leg 79.- In Hinz, K. & Winterer, E.L. (eds.) *Initial Reports of the Deep Sea Drilling Project*, **79**, 563-578.
- Wilpshaar, M. & Leereveld, H.** (1994): Palaeoenvironmental change in the Early Cretaceous Vocontian Basin (SE France) reflected by dinoflagellate cysts.- *Review of Palaeobotany and Palynology*, **84**, 121-128.
- Wilpshaar, M. Leereveld, H. & Visscher, H.** (1997): Early Cretaceous sedimentary and tectonic development of the Dauphinois Basin (SE-France).- *Cretaceous Research*, **18**, 457-468.
- Wilson, J.L. & Ward, W.C.** (1993): Early Cretaceous carbonate platforms of northeastern and east-central Mexico.- In Simo, J.A.; Scott, R.W. & Masse, J.-P. (eds.) *Cretaceous Carbonate Platforms, American Association of Petroleum Geologists, Memoir*, **56**, 35-49.
- Wilson, P.A. & Norris, R.D.** (2001): Warm tropical ocean surface and global anoxia during the mid-Cretaceous period.- *Nature*, **412**.
- Winterer, E.L. & Hinz, K.** (1984): The evolution of the Mazagan continental margin: A synthesis of geophysical and geological data with results of drilling during Deep Sea Drilling Project Leg 79 U.S. Government Printing Office, Washington D.C., 893-919.
- Wissig, F.-N. & Herrig, E.** (1999): Arbeitstechniken der Mikropaläontologie.- pp. 191.
- Wonders, A.A.H.** (1980): Middle and late Cretaceous planktonic foraminifera of the western mediterranean area.- *Utrecht Micropalaeontological Bulletins*, 1-157.

8. Taxonomy

Ascoliella Banner & Desai, 1988

Ascoliella nitida (Michael, 1972)

1972 *Favusella nitida* Michael, p. 214, pl. 3, figs 10-12.

1973 *Favusella pessagnoii* Michael, pp. 214, 215, pl. 4, figs 4-6.

1976 *Favusella* aff. *washitensis* (Carsey), Ascoli, p. 661, 674, pl. 1, figs 4a-c.

1977 *Favusella hedbergellaeformis* Longoria & Gamper, p. 207, pl. 4, figs 1-3, 7-9.

1988 *Ascoliella scotiensis* Banner & Desai, p. 150, pl. 2, figs 3-4

1997 *Ascoliella nitida* (Michael) BouDagher-Fadel, p. 73, 77, pl. 4.5, figs 1-9; pl. 4.7, figs 1-3.

Range: This species appears in NE-Texas in the Late Albian, in the Kiamichi to the Weno formation (Fig. 51). Boudagher-Fadel et al. (1997) described *A. nitida* as the oldest known species of *Ascoliella*, ranging from the Late Aptian to Late Albian. In NE-Texas first recorded from the Duck Creek, Fort Worth and Denton formation (Michael, 1972).

Ascoliella quadrata (Michael, 1972)

1972 *Favusella quadrata* Michael, p. 215, pl. 4, figs 7-9.

1997 *Ascoliella quadrata* (Michael) BouDagher-Fadel, p. 73, pl. 4.5, figs 10-12.

Range: This species first occurs in the Middle to Late Albian (Goodland to lower Weno formation; Fig. 51). Michael (1972) observed this species in the Late Albian Duck Creek, Fort Worth and Denton formation.

Ascoliella scitula (Michael, 1972)

1973 *Favusella scitula* Michael, p. 215, pl. 4, figs 10-12.

1978 *Favusella papagayosensis* Longoria & Gamper, p. 207, pl. 4, figs 16-18 (holotypes), 19-21; pl. 5, figs 16-21 (paratypes).

1997 *Ascoliella scitula* (Michael) BouDagher-Fadel, p. 75, pl. 4.6, figs 1-3, 8-10.

Range: This species is known in NE-Texas in the Middle to Late Albian (Goodland to Main Street formation; Fig. 51). Michael (1971) described this species in NE-Texas from the Late Albian Duck Creek, Fort Worth and Denton formation.

Biticinella Sigal, 1956

Biticinella breggiensis (Gandolfi, 1942)

1942 *Anomalina breggiensis* Gandolfi, p. 102, pl. 3, figs 6a-c.

1956 *Biticinella breggiensis* Sigal, p.35, no. 3.

1962 *Biticinella breggiensis* Luterbacher & Premoli-Silva, p. 272, pl. 23, figs 2-4.

1966 *Ticinella* (*Biticinella*) *spectrum breggiensis* (Gandolfi) et Sigal, p. 193, pl. 1, figs 1-7; pl. 2, fig 2.

1969 *Biticinella breggiensis* (Gandolfi) Caron & Luterbacher, p. 25, pl. 7, fig 4a-c.

2001 *Biticinella breggiensis* (Gandolfi) Lipson-Benitah & Almogi-Labin, p. 240-243, pl. 1, figs 1-4; pl. 2, figs 1-3.

Range: This species (plate 1, fig. 2 a/b) appears in the Late Albian (*B. breggiensis* to *R. appenninica* zone) of SE-France (Caron, 1985; Fig. 24).

Favusella Michael, 1972

Favusella hiltermanni (Loeblich & Tappan, 1961)

1961 *Hedbergella hiltermanni* Loeblich & Tappan, p. 275, pl. 4, figs 12-13.

Range: This species occurs in NE-Texas in the Middle to Late Albian (Goodland to Weno formation; Fig. 51). Michael (1972) mentioned *F. hiltermanni* from the Duck Creek, Fort Worth and Denton formation (Late Albian) and Loeblich & Tappan (1961) and Boudagher-Fadel et al. (1997) in the Early Cenomanian of NW-Germany.

Favusella washitensis (Carsey, 1926)

1926 *Globigerina washitensis* Carsey, p. 44, pl. 7, fig 10; pl. 8, fig. 2.

1961 *Hedbergella washitensis* (Carsey) Loeblich & Tappan, p. 278, pl. 4, figs 9-11.

Remarks: The species *Favusella washitensis* was first described by Carsey (1926) as *Globigerina washitensis* and later assigned to the new genus *Favusella* by Michael (1972). The existence of this genus is still under debate. Koutsoukos et al. (1989) assumed that all *Favusella* taxa were ecophenotypic, controlled by peculiar ecological environmental terms (Hart et al., 1980) like shallow, warm, hypersalin, carbonate-saturated waters (Koutsoukos et al., 1989). The stratigraphical and faunal data in this thesis shows, that various species of *Favusella* have different stratigraphical ranges (Fig. 51). This leads to the assumption that the origin of this genus might be a change of environmental terms, but later becomes an independent genus. Boudagher-Fadel et al. (1997) assumption of different stratigraphical ranges and regional distributions of *Favusella* spp. supports the use of this genus as biostratigraphic marker.

Range: This species (plate 3, fig. 1) is known in NE-Texas in the Middle and Late Albian (Michael, 1972; Fig. 51). The same species was recorded from the Cenomanian of the Blake Plateau (Loeblich & Tappan, 1961), Cuba (Ayala, 1962) and Negev Desert (Arkin & Hamaoui, 1967). Sigal (1965) described *H. washitensis* from the Albian of Paris.

Globigerinelloides Cushman & Ten Dam, 1948

Globigerinelloides bentonensis (Morrow, 1934)

1934 *Anomalina bentonensis* Morrow, p. 201, pl. 30 figs 4a-b.

1957 *Planomalina caseyi* Loeblich & Tappan, pl. 1, figs 4-5.

1961 *Globigerinelloides eaglefordensis* (Moreman), Loeblich & Tappan, p. 268, pl. 2, figs 3-7.

1970 *Globigerinelloides bentonensis* (Morrow), Eicher & Worstell, p. 297, pl. 8, figs 17, 19; pl. 9, figs 3.

1977 *Globigerinelloides cushmani* (Tappan), Masters, p. 408, pl. 10, fig 4; pl. 11, figs 1-2.

1987 "*Blowiella*" *bentonensis* (Morrow) BouDagher-Fadel, p. 145, pl. 3, figs 1-9; pl. 4, fig. 6.

1997 *Alanlordella bentonensis* (Morrow) BouDagher-Fadel, p. 221-223, pl. 12.3, figs 1-9; pl. 12.4, figs 1-9, text-fig 12.1.

Range: This species (plate 3, fig. 5) occurs in SE-France from the Early to Late Albian (*H. planispira* to *R. appenninica* zone, Fig. 24) and in NE-Texas in the Late Albian (Kiamichi to end of section; Fig. 51). Caron (1985) described *G. bentonensis* from the Albian.

Globigerinelloides caseyi (Bolli, Loeblich & Tappan, 1957)

1957 *Planomalina caseyi* Bolli, Loeblich & Tappan, p. 24, pl. 1, figs 4a-5b.

1962 *Globigerinelloides caseyi* (Bolli, Loeblich & Tappan) Low, pp. 122-123;

1966 *Globigerinelloides caseyi* (Bolli, Loeblich & Tappan) Pessagno, p. 276, pl. 49, figs 2-5.

Range: This species appears in the uppermost Late Albian and Early Cenomanian (Pawpaw to end of section) of NE-Texas (Fig. 51). Michael (1972) mentioned *G. caseyi* as common in the Kiamichi and Duck Creek and rare in the Main Street and Grayson formation of NE-Texas. This species is also recorded as *G. eaglefordensis* (Loeblich & Tappan, 1961) from England (Gault Clay), Blake Plateau and Texas (Grayson and Del Rio formation).

Globigerinelloides ultramicra (Subbotina, 1949)

1949 *Globigerinella ultramicra* Subbotina, p. 33, pl. 2, figs 17-18.

1970 *Globigerinelloides caseyi* (Bolli, Loeblich & Tappan) Eicher & Worstell, p. 297, pl. 8, figs 11, 15-16.

1976 *Globigerinelloides ultramicra* (Subbotina) Masters, p. 413, pl. 12, figs 3-5.

1984 *Globigerinelloides ultramicrus* (Subbotina) Leckie, p. 614, pl. 11, figs 10-11.

Range: This species is known in SE-France in the Early to Late Albian (*H. planispira* to *R. appenninica* zone; Fig. 24). Leckie (1984) for example described *G. ultramicra* in the Late Albian and Cenomanian offshore Morocco (DSDP Site 545, 547).

Guembelitra Cushman, 1933

Guembelitra cretacea (Cushman, 1933)

1933 *Guembelitra cretacea* Cushman, p. 37, pl. 4, fig 12.

Range: This species occurs in SE-France in the Late Albian (*T. praeticinensis* to *R. appenninica* zone; Fig. 24). *Guembelitra cretacea* is also known in the Late Albian of NW-Germany (Prokoph, 1997).

Hedbergella Brönnimann & Brown, 1958*Hedbergella bizonae* (Chevalier, 1961)

1961 *Hastigerina bizonae* Chevalier, p. 34, pl. 1, figs 24a-c.

1972 *Hedbergella bollii* Longoria, p. 53, pl. 13, figs 12-14.

1973 *Hedbergella kuhryi* Longoria, p. 60, pl. 14, figs 4-6.

Range: *Hedbergella bizonae* is recorded in SE-France from the Early to Late Albian (*H. planispira* to *R. ticinensis* zone; Fig. 24).

Hedbergella delrioensis (Carsey, 1926)

1926 *Globigerina cretacea* d'Orbigny var. *delrioensis* Carsey, p. 43.

1937 *Globigerina infracretacea* Glaessner, p. 28, text-fig 1.

1961 *Hedbergella delrioensis* (Carsey) Loeblich & Tappan, p. 275, pl. 2, figs 11-13.

Remarks: *Hedbergella delrioensis* and *Hedbergella infracretacea* are considered as different species (Coccioni & Premoli-Silva, 1994). Maslakova (1963) and Caron (1985) regarded *H. infracretacea* as a younger synonym of *H. delrioensis*. Both species show a large variability in size, surface and number of chambers. These two taxa exhibit no clear distinguishing features and remain problematic (Coccioni & Premoli-Silva, 1994). Therefore these two species are in this thesis added together as *H. delrioensis/infracretacea*.

Range: This species (plate 2, fig. 2; plate 3, fig. 2) occurs in SE-France in the Late Aptian to the Late Albian (total section; Fig. 24) and in NE-Texas in the Middle to the Late Albian (as well total section; Fig. 51). *Hedbergella delrioensis/infracretacea* is global distributed and is recorded from various location like Roter Sattel (Switzerland; Strasser et al., 2001), California (Sliter & Premoli-Silva, 1990), Mexico (Longoria, 1984; Premoli-Silva & McNulty, 1989) and NW-Germany (Prokoph, 1997).

Hedbergella flandrini (Porthault, 1970)

1970 *Hedbergella flandrini* Porthault, pp. 64-65, pl. 10, figs 1-3.

Range: *Hedbergella flandrini* is described in SE-France only in a few samples in the Late Albian (*R. appenninica* zone; Fig. 24).

Hedbergella gorbachikae (Longoria, 1974)

1972 *Hedbergella gorbachikae* Longoria, p. 56, pl. 15, figs 1-16.

Range: This species appears in SE-France throughout the whole section in the Late Aptian to the Late Albian (Fig. 24).

Hedbergella implicata (Michael, 1972)

1972 *Hedbergella implicata* Michael, p. 208, pl. 2, figs 4-6.

Range: *Hedbergella implicata* is known in NE-Texas in the Late Albian to Early Cenomanian (Kiamichi to end of section; Fig. 51). Michael (1972) reports that this species is restricted to the

Late Albian Kiamichi and Duck Creek formation.

Hedbergella intermedia (Michael, 1972)

1971 *Hedbergella intermedia* Michael, p. 208, pl. 2, figs 7-9.

Range: This species is recorded in NE-Texas from the Late Albian to Early Cenomanian (Kiamichi to end of section; Fig. 51). *Hedbergella intermedia* is described by Michael (1972) for North Central Texas for the Late Albian Kiamichi, Duck Creek and Fort Worth formation.

Hedbergella maslakovae (Longoria, 1974)

1974 *Hedbergella maslakovae* Longoria, p. 61, 63, pl. 24, figs 11-12.

Range: *Hedbergella maslakovae* can be found in the Early to Late Albian (*Hedbergella planispira* to *Rotalipora appenninica* zone; Fig. 24) of SE-France. Caron (1985) mentioned *H. maslakovae* as common in the Aptian.

Hedbergella planispira (Tappan, 1940)

1940 *Globigerina planispira* Tappan, p. 122, pl. 19, fig 12.

1961 *Hedbergella planispira* (Tappan) Loeblich & Tappan, p. 276, pl. 5, figs 4-11.

1961 *Hedbergella trocoidea* (Gandolfi) Loeblich & Tappan, pp. 277-278, pl. 5, figs 1-2.

1967 *Hedbergella planispira* (Tappan) Pessagno, pp. 283-284, pl. 51, fig 1; pl. 53, figs 1-4.

Range: *Hedbergella planispira* (plate 2, fig. 4; plate 3, fig. 3) occurs in SE-France in the Late Aptian to Late Albian (Fig. 24). In NE-Texas this species is known from the Late Albian to Early Cenomanian (Kiamichi to end of section; Fig. 51). This species is as well as *H. delrioensis/infracretacea* a global distributed taxa. *Hedbergella planispira* is known in the Early Albian to Late Albian of the Blake Nose Plateau (Bellier & Moullade, 2002), Mexico (Longoria, 1984; Premoli-Silva & McNulty, 1989 and Roter Sattel (Switzerland; Strasser, 2001). From the Late Albian of California (Sliter & Premoli-Silva, 1990) and NW-Germany (Prokoph, 1997; Weiss, 1997)

Hedbergella punctata (Michael, 1972)

1970 *Hedbergella* (?) *punctata* Michael, p. 211, 214, pl. 3, figs 1-3; pl. 7, figs 1-2.

Range: This species appears in NE-Texas in the Late Albian (Kiamichi to Main Street formation, Fig. 51). *Hedbergella punctata* is recorded in North Central Texas in the Late Albian Kiamichi, Duck Creek and Denton formation (Michael, 1972).

Hedbergella sigali (Moullade, 1966)

1966 *Hedbergella* (*Hedbergella*) *sigali* Moullade, p. 87, pl. 7, figs 24-25.

1974 *Hedbergella sigali* (Moullade) Longoria, p. 68, pl. 21, figs 6-8; pl. 22, figs 1-13.

1979 *Hedbergella sigali* (Moullade) Sigal, pl. 1, figs 1-2.

1986 *Clavihedbergella sigali* (Moullade) Gorbachick, pl. 24, figs 1-2.

1989 *Hedbergella sigali* (Moullade) Puglisi & Coccioni, pl. 1, figs 18-23.

1993 *Praehedbergella sigali* (Moullade) Banner et al., pl. 7, pl. 2, figs 2-3.

Range: *Hedbergella sigali* occurs in SE-France throughout the total section (Late Aptian to Late Albian; Fig. 24). This species is also described in the Albian of Roter Sattel (Switzerland; Strasser et al., 2001).

Hedbergella simplex (Morrow, 1934)

1934 *Hastigerinella simplex* Morrow, p. 198-199, figs 6a-c (holotype)

1954 *Hastigerinella simplicissima* Magné & Sigal, pl. 14, figs 11a-c.

1961 *Clavihedbergella simplex* (Morrow) Loeblich & Tappan, p. 279-280, pl. 3, figs 11a-c.

1961 *Hedbergella amabilis* Loeblich & Tappan, p. 274, pl. 3, figs 1a-c (holotype), 2-4, 5a-c (paratypes), 6-10.

1976 *Hedbergella amabilis* (Loeblich & Tappan) Carter & Hart, p. 29-31, pl. 3, figs 22-23.

1977 *Hedbergella simplex* (Morrow) Weiss, p. 114, pl. 2, figs 1-2.

Range: This species (plate 2, fig. 3) can be found in SE-France in the Late Aptian to the Late Albian (Fig. 24). *Hedbergella simplex* is known in the Late Albian of California (Sliter & Premoli-Silva, 1990), Mexico (Premoli-Silva & McNulty, 1989) and NW-Germany (Prokoph, 1997).

Hedbergella trocoidea (Gandolfi, 1942)

1942 *Anomalina lorneiana* var. *trocoidea* Gandolfi, p. 99, pl. 2, figs 1-a-c.

1962 *Hedbergella trocoidea* (Gandolfi) Brönnimann & Brown, p. 16, fig 1.

1961 *Hedbergella trocoidea* (Gandolfi) Loeblich & Tappan, p. 277-278, pl. 5, figs 1a-c, 2a-c.

1969 *Hedbergella trocoidea* (Gandolfi) Caron & Luterbacher, p. 23, pl. 7, figs 1a-c, 2a-c (lectotypes).

1971 *Hedbergella trocoidea* (Gandolfi) Longoria, p. 69, pl. 17, figs 1-16; pl. 18, figs 3-5.

Range: *Hedbergella trocoidea* appears in the Late Aptian to Late Albian (begin of the section to *R. appenninica* zone; Fig. 24). This species is described in the Late Aptian to Early Albian of the Blake Nose Plateau (Bellier & Moullade, 2002) and in the Middle Albian of Mexico (Premoli-Silva & McNulty, 1989).

Heterohelix Ehrenberg, 1843

Heterohelix moremani (Cushman, 1938)

1937 *Guembelina moremani* Cushman, p. 10, pl. 2, figs 1a-3.

1967 *Heterohelix moremani* (Cushman) Pessagno, p. 260-261, pl. 48, figs 10-11; pl. 89, figs 1-2.

Range: This species (plate 2, fig. 5) occurs in SE-France in the Middle Albian to Late Albian (*T. primula* zone to the end of the section; Fig. 24). In NE-Texas *H. moremani* ranges from the Middle Albian to the Early Cenomanian (Goodland formation to the end of the section; Fig.). This species is known in the Late Albian of California (Sliter & Premoli-Silva, 1990), Mexico (Premoli-Silva & McNulty, 1989) and NW-Germany (Prokoph, 1997).

Heterohelix reussi (Cushman, 1938)

1937 *Gümbelina reussi* Cushman, p. 11, pl. 2, figs 6a-c.1985

1985 *Heterohelix reussi* (Cushman) Caron, p. 55, figs 24.10-11.

Range: *Heterohelix reussi* can be described in SE-France in the Middle Albian to Late Albian (*T. primula* zone to the end of the section; Fig. 24). In NE-Texas this species is mentioned in the Late Albian (Fort Worth formation to the end of section; Fig.). *Heterohelix reussi* is also known in the Early Cenomanian of California (Sliter & Premoli-Silva, 1990).

Heterohelix striata (Ehrenberg, 1840)

1840 *Textularia striata* Ehrenberg, p. 135, pl. 4, figs 1a, 2a, 3a.

1967 *Heterohelix striata* (Ehrenberg) Pessagno, p. 264, as fig 2a of Ehrenberg, 1840.

1985 *Heterohelix striata* (Ehrenberg) Caron, p. 55, figs 24.12-13

Range: *Heterohelix striata* appears in SE-France in the Late Albian (*R. appenninica* zone; Fig. 24) only in a few samples.

Planomalina Loeblich & Tappan, 1946***Planomalina buxtorfi*** (Gandolfi, 1942)

1942 *Planulina buxtorfi* Gandolfi, p. 103, pl. 3, figs 7a-c.

1946 *Planomalina apsodostroba* Loeblich & Tappan, p. 258, pl. 37, figs 22, 23.

1975 *Planomalina buxtorfi* (Gandolfi) emend. Wonders, pl. 1, fig. 4, text-fig 4, figs 3a-b, 4a-b.

1984 *Planomalina buxtorfi* (Gandolfi) Caron, p. 65, figs 29.1-2.

1997 *Planomalina buxtorfi* (Gandolfi) BouDagher-Fadel, p. 227, pl. 12.6, figs 7-9.

Range: *Planomalina buxtorfi* (plate 1, fig. 1 a/b) occurs in SE-France in the Late Albian within the *R. appenninica* zone (Fig. 24). This global distributed species is described from the Late Albian of Mazagan Plateau (Nederbragt et al., 2001), Blake Nose Plateau (Bellier & Moullade, 2002), Roter Sattel (Strasser et al., 2001), California (Sliter & Premoli-Silva, 1990) and Mexico (Longoria, 1984; Premoli-Silva & McNulty, 1989).

Planomalina praebuxtorfi (Wonders, 1975)

1975 *Planomalina praebuxtorfi* Wonders, pp. 90-91, pl. 1, figs 1-2, text-fig 4, fig 2.

1997 *Alanlordella praebuxtorfi* BouDagher-Fadel, Banner & Whittaker, pp. 224-227, pl. 12.5, figs 1-9, pl. 12.6, figs 1-6, fig 12.1.

Range: This species is known in SE-France in the Late Albian, in the lower *R. appenninica* zone (Fig. 24). *Planomalina praebuxtorfi* can be found in the Late Albian of Roter Sattel (Switzerland; Strasser et al., 2001), California (Sliter & Premoli-Silva, 1990) and Mexico (Longoria, 1984).

Praeglobotruncana Bermudez, 1952*Praeglobotruncana delrioensis* (Plummer, 1931)

1931 *Globorotalia delrioensis* Plummer, p. 199, pl. 13, figs 2a-c (holotypes).

1961 *Praeglobotruncana delrioensis* (Plummer) Loeblich & Tappan, p. 280-284, pl. 6, figs 9a-c, 10a-c (topotypes), 11, 12a-c.

Range: This species occurs in NE-Texas in the uppermost Late Albian and Early Cenomanian (Main Street formation to the end of the section; Fig. 51). *Praeglobotruncana delrioensis* is described in the Late Albian of California (Sliter & Premoli-Silva, 1990), Mexico (Premoli-Silva & McNulty, 1989) and NW-Germany (Prokoph, 1997).

Rotalipora Brotzen, 1942*Rotalipora appenninica* (Renz, 1936)

1936 *Globotruncana appenninica* Renz, p. 14, fig. 2; var. alpha Gandolfi, 1942, p. 117, text-figs 40a-c.

1961 *Rotalipora appenninica appenninica* (Renz) Luterbacher & Premoli-Silva, pp. 266-268, pl. 19, figs 1-2; pl. 20, figs 1-4; pl. 21, figs 1-4.

1969 *Rotalipora appenninica* (Renz) Caron & Luterbacher, p. 26, pl. 8, fig. 8. Robaszynski & Caron, 1979, p. 59, 64; pl. 4, figs 1a-3c; pl. 5, figs 1a-3c.

1980 *Thalmanninella appenninica* (Renz) Wonders, p. 141, pl. 2, figs 2a-c.

Range: *Rotalipora appenninica* (plate 1, fig. 3 a/b) first appears in SE-France in the upper part of the Late Albian (Fig. 24). This globally distributed species is known from the Late Albian of Switzerland (Strasser et al., 2001), Italy (Piobbico; Erbacher, 1994; Galeotti, 1998), Mazagan Plateau (Nederbragt et al., 2001), Blake Nose Plateau (Wilson & Norris, 2001; Bellier & Moullade, 2002), Mexico (Longoria, 1984), California (Sliter & Premoli-Silva, 1990) and even the Boreal Kirchrode (Weiss, 1997).

Rotalipora evoluta (Sigal, 1948)

1948 *Rotalipora cushmani* var. *evoluta* Sigal, p. 100, pl. 1, figs 3; pl. 2, figs 2.

1946 *Globorotalia delrioensis* Plummer, Loeblich & Tappan, p. 257, text-fig 4b.

1957 *Rotalipora* cf. *appenninica* (Renz) Bolli et al., p. 41, pl. 9, figs 5a-c.

1966 *Rotalipora* (*Thalmanninella*) *appenninica evoluta* (Sigal) Caron, p. 72, pl. 1, figs 3a-c.

1967 *Rotalipora evoluta* (Sigal) Pessagno, p. 294, pl. 49, figs 12-14; pl. 53, figs 6-8; pl. 98, fig 12.

Remarks: Many foraminiferal specialists synonymise *R. evoluta* with *R. appenninica* (Scott, submitted). In North Texas it maybe a proxy for *R. globotruncanoides*, the marker for the Cenomanian base (Scott, submitted).

Range: This species first can be found in NE-Texas in the Main Street formation (Fig. 51). Michael (1972) described *R. evoluta* from the upper Grayson formation of North Central Texas and Pessagno (1967) from the Cenomanian of Trinidad and Switzerland. Barr (1972) recorded *R. evoluta* from the Cenomanian of Libya.

Rotalipora subticinensis (Gandolfi, 1942)

- 1842 *Globotruncana ticinensis* var. *a* Gandolfi, p. 114, pl. 2, fig 4a-c (holotype).
 1957 *Globotruncana (Thalmaninella) ticinensis subticinensis* Gandolfi, p. 59, fig 1a-c.
 1978 *Pseudothalmanninella subticinensis* (Gandolfi) Wonders, p. 125. Pl. 1, figs 2a-c.
 1979 *Rotalipora subticinensis* (Gandolfi) Robaszynski & Caron, p. 107, pl. 19, figs 1a-c, 2a-d (topotypes).
 1980 *Pseudothalmanninella subticinensis* (Gandolfi) Wonders, p. 139, pl. 1, figs 2a-c.

Range: *Rotalipora subticinensis* first occurs in SE-France in the Late Albian (Fig. 24). This species is also known from the Late Albian of Switzerland (Strasser et al., 2001), Central Italy (Galeotti, 1998), the Blake Nose Plateau (Bellier & Moullade, 2002) and California (Sliter & Premoli-Silva, 1990).

Rotalipora ticinensis (Gandolfi, 1942)

- 1942 *Globotruncana ticinensis* Gandolfi, p. 113, pl. 2, figs 3a-c.
 1969 *Rotalipora ticinensis* (Gandolfi) Caron & Luterbacher, p. 25, pl. 8, figs 6a-c.
 1977 *Pseudothalmanninella ticinensis* (Gandolfi) Wonders, p. 128, pl. 1, figs 3a-c, 4a-c.
 1978 *Rotalipora ticinensis* (Gandolfi) Robaszynski & Caron, p. 111, pl. 20, fig 1a-d.
 1979 *Pseudothalmanninella ticinensis* (Gandolfi) Wonders, p. 139, pl. 1, figs 2a-c.

Range: *Rotalipora ticinensis* (plate 2, fig. 1 a/b) first appears in SE-France in the Late Albian (Fig. 24). This globally distributed species is known from the Late Albian of Switzerland (Strasser et al., 2001), Italy (Piobbico; Erbacher, 1994; Galeotti, 1998), the Mazagan Plateau (Nederbragt et al., 2001), Blake Nose Plateau (Wilson & Norris, 2001; Bellier & Moullade, 2002), California (Sliter & Premoli-Silva, 1990) and Mexico (Longoria, 1984)

Ticinella Reichel, 1950***Ticinella bejaouaensis*** (Sigal, 1966)

- 1966 *Ticinella roberti* var. *bejaouaensis* Sigal, pl. 5, figs 5-7.
 1966 *Ticinella bejaouaensis* (Sigal) emend. Moullade, p. 103.
 1985 *Ticinella bejaouaensis* (Sigal) Caron, p. 77, figs 36.1-3.

Range: *Ticinella bejaouaensis* is described in SE-France in the Late Aptian (from the start of the section to the LO of the nominal species; Fig. 24). This species is known also from the Aptian and Early Albian of the Blake Nose Plateau (Leckie, 1984) and the Aptian of Roter Sattel (Switzerland; Strasser et al., 2001)

Ticinella praeticinensis (Sigal, 1966)

- 1966 *Ticinella praeticinensis* Sigal, pp. 195-196, pl. 2, figs 3-5.
 1984 *Ticinella praeticinensis* (Sigal) Caron, p. 77, figs 36.8-9.

Range: This species occurs in SE-France in the Late Albian (*T. praeticinensis* to *R. appenninica* zone; Fig. 24). *Ticinella praeticinensis* is mentioned as well from the Late Albian of Mexico

of Mexico (Longoria, 1984; Premoli-Silva & McNulty, 1989).

Ticinella primula (Luterbacher, 1963)

1963 *Ticinella primula* Renz, Luterbacher & Schneider, p. 1085, text-fig 4.

Range: *Ticinella primula* appears in SE-France in the Middle to the Late Albian (*T. primula* to *R. appenninica* zone; Fig. 24). In NE-Texas this species is known in the Late Albian (Kiamichi formation to the end of the section; Fig. 51). This species is described in Roter Sattel (Switzerland; Strasser et al., 2001), California (Sliter & Premoli-Silva, 1990), Mexico (Premoli-Silva & McNulty, 1989) and NW-Germany (Prokoph, 1997).

Ticinella raynaudi (Sigal, 1966)

1966 *Ticinella raynaudi* Sigal, pp. 200-202, pl. VI, figs 1(a-c) - 3(a-c).

Range: *Ticinella raynaudi* is known in SE-France in the Middle to the Late Albian (*T. primula* zone to the end of the section, Fig. 24). This species is described in the Late Albian of California (Sliter & Premoli-Silva, 1990), Mexico (Premoli-Silva & McNulty, 1989) and NW-Germany (Prokoph, 1997; Weiss, 1997).

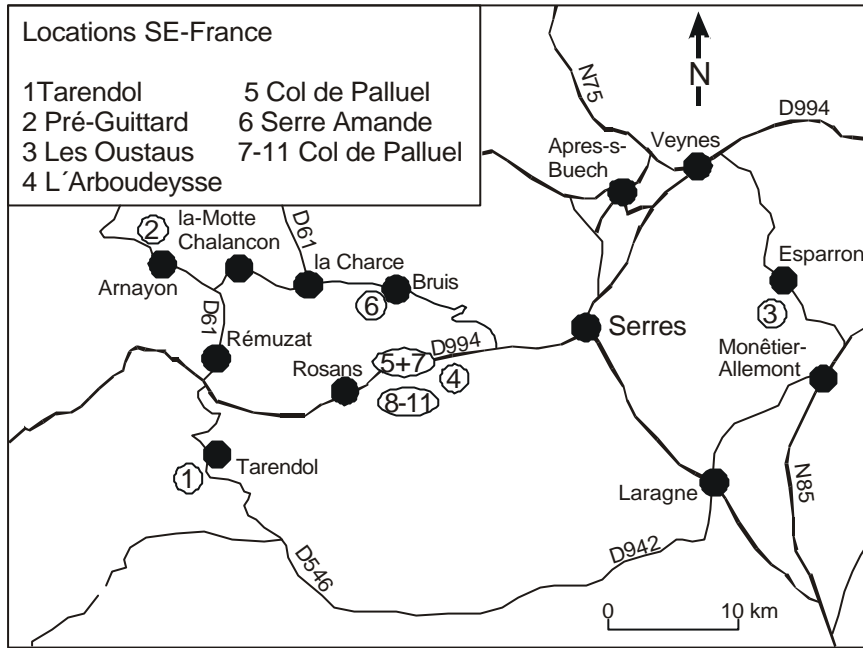
Ticinella roberti (Gandolfi, 1942)

1942 *Anomalina roberti* Gandolfi, p. 100, pl. 2, fig 2; pl. 4, figs 4-7, 20; pl. 5, fig 1; pl. 13, figs. 3,6.

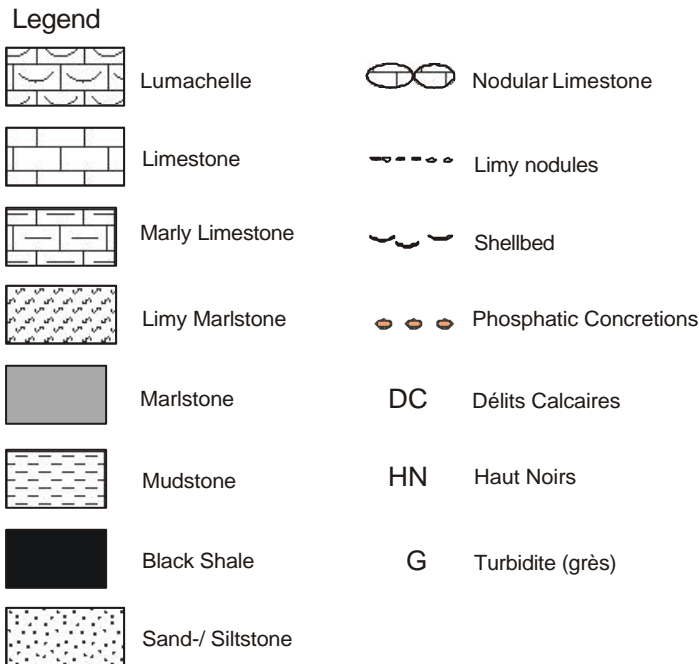
1949 *Globotruncana (Ticinella) roberti* (Gandolfi) Reichel, pp. 600-603, pl. 16, fig 1; pl. 17, fig 1.

1966 *Ticinella roberti* (Gandolfi) Sigal, pp. 203-207, pl. 4, figs 10-12; pl. 5, figs 1-4.

Range: This species occurs in SE-France from the uppermost Middle Albian to the uppermost Late Albian (*T. primula* to *R. appenninica* zone; Fig. 24). *Ticinella roberti* is known in the Albian of Libya and Switzerland (Barr, 1972).

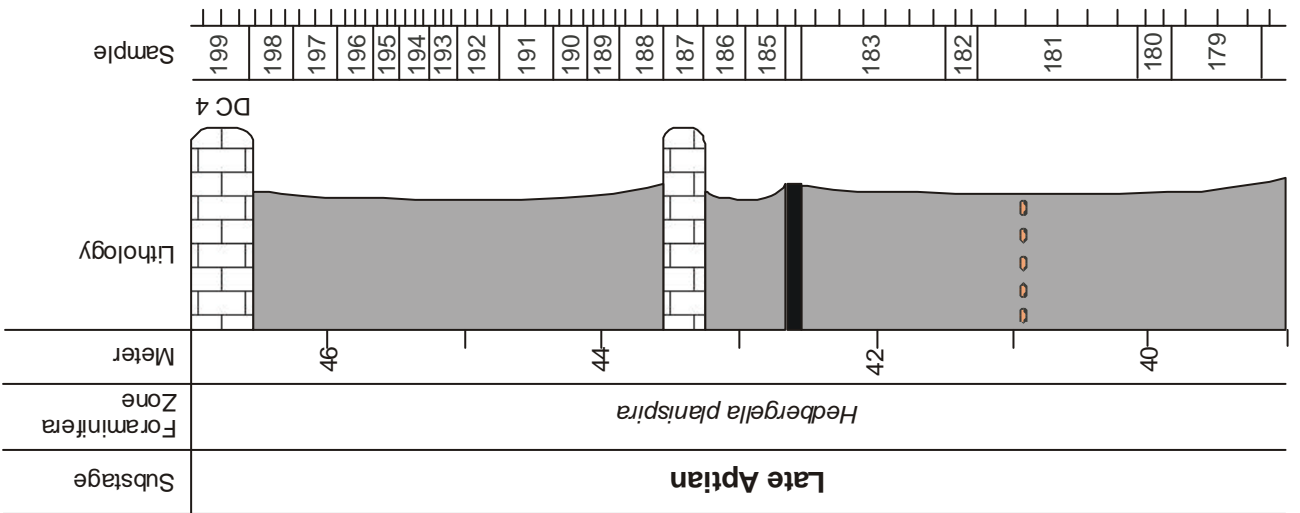
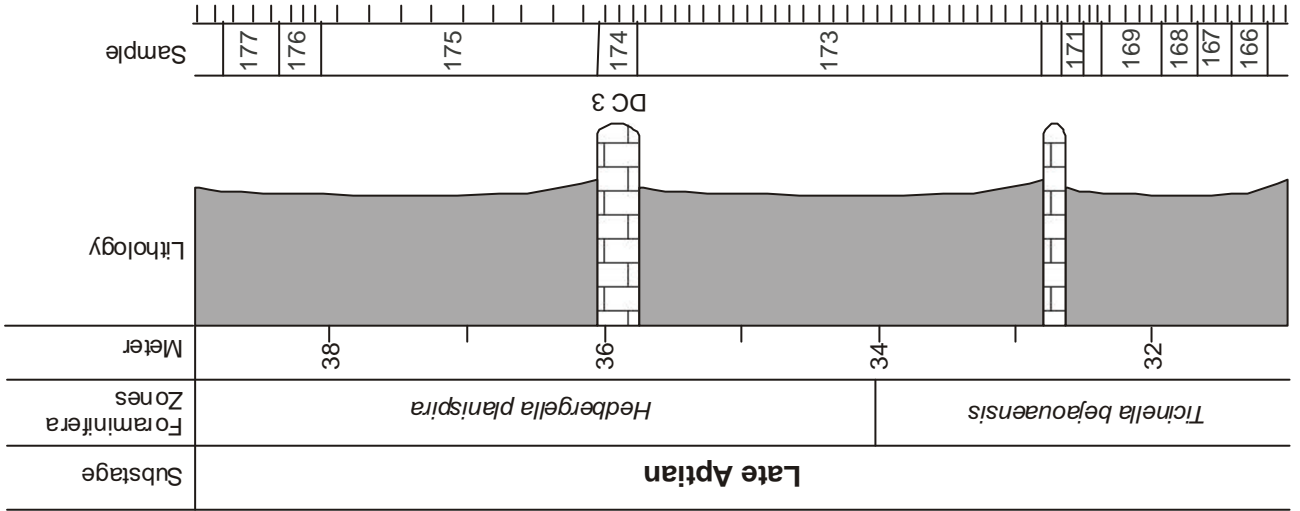
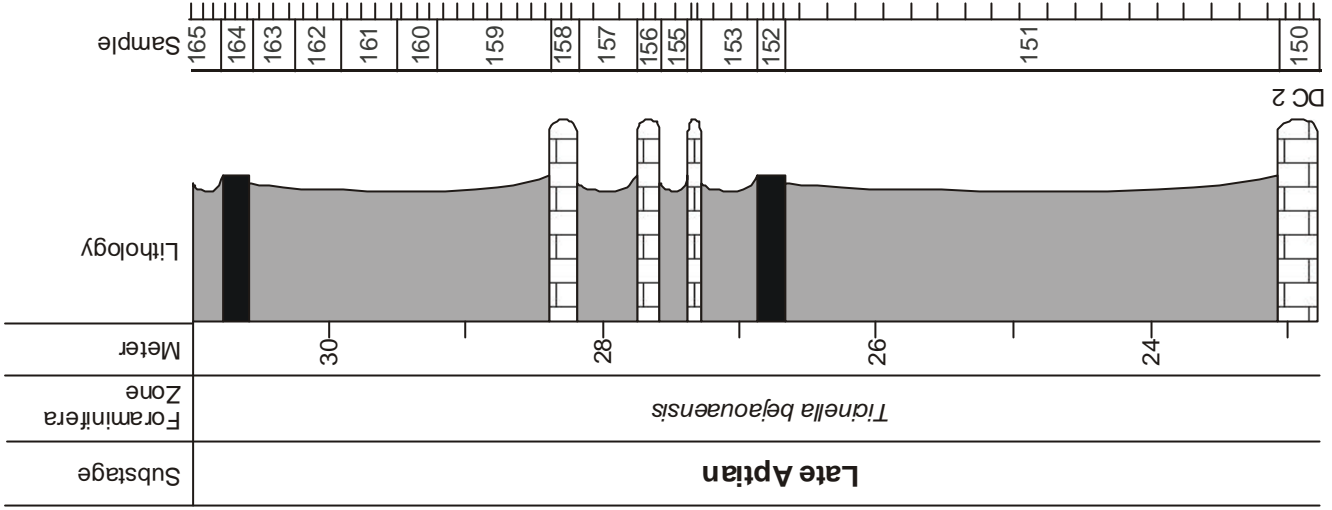


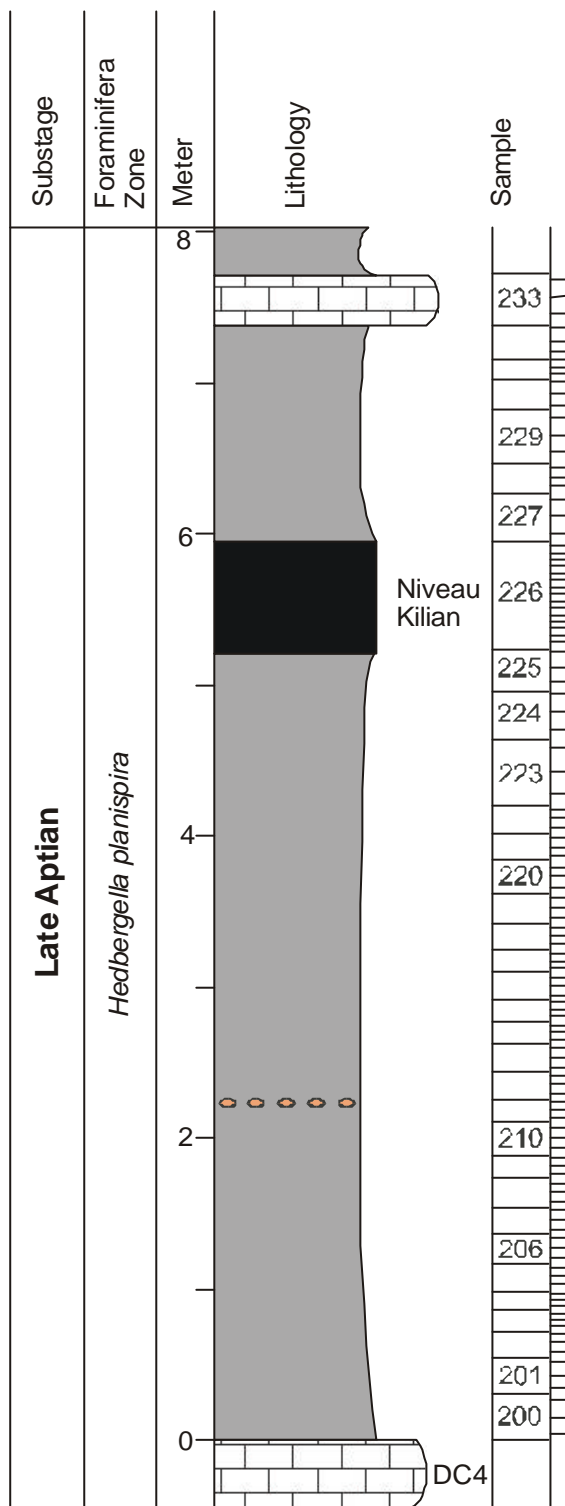
Appendix 1: Road map of SE-France with the location of the sections.



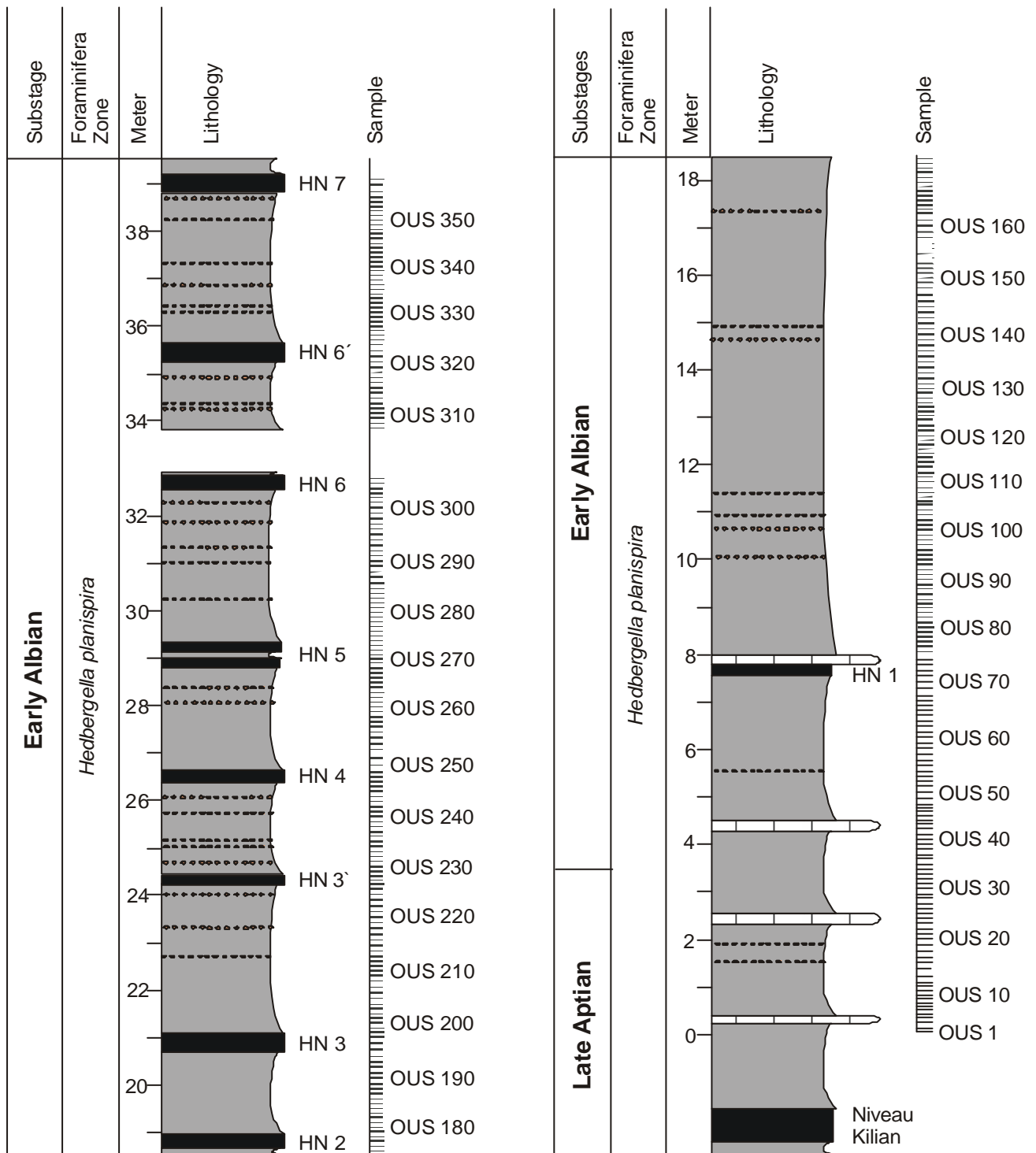
Appendix 2: Legend.

Appendix 3: Lithology and sample distribution of the Upper Aptian section 1 Tarendol, with respect to foraminifera stratigraphy (sample abbreviation = LF), see next page. For lithological explanation see Appendix 2.

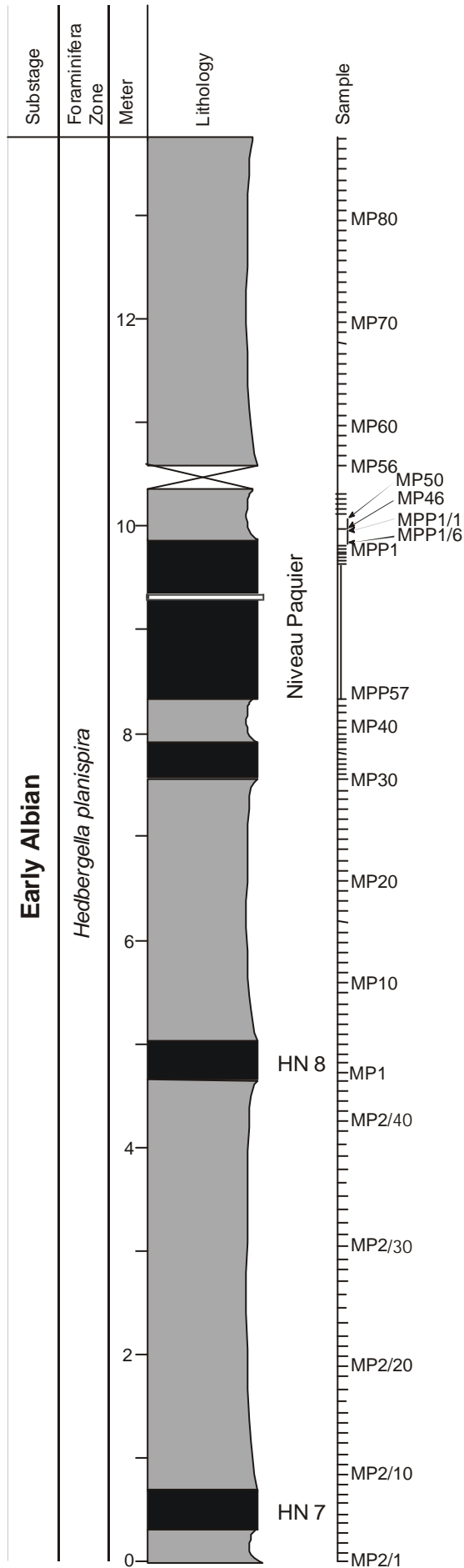




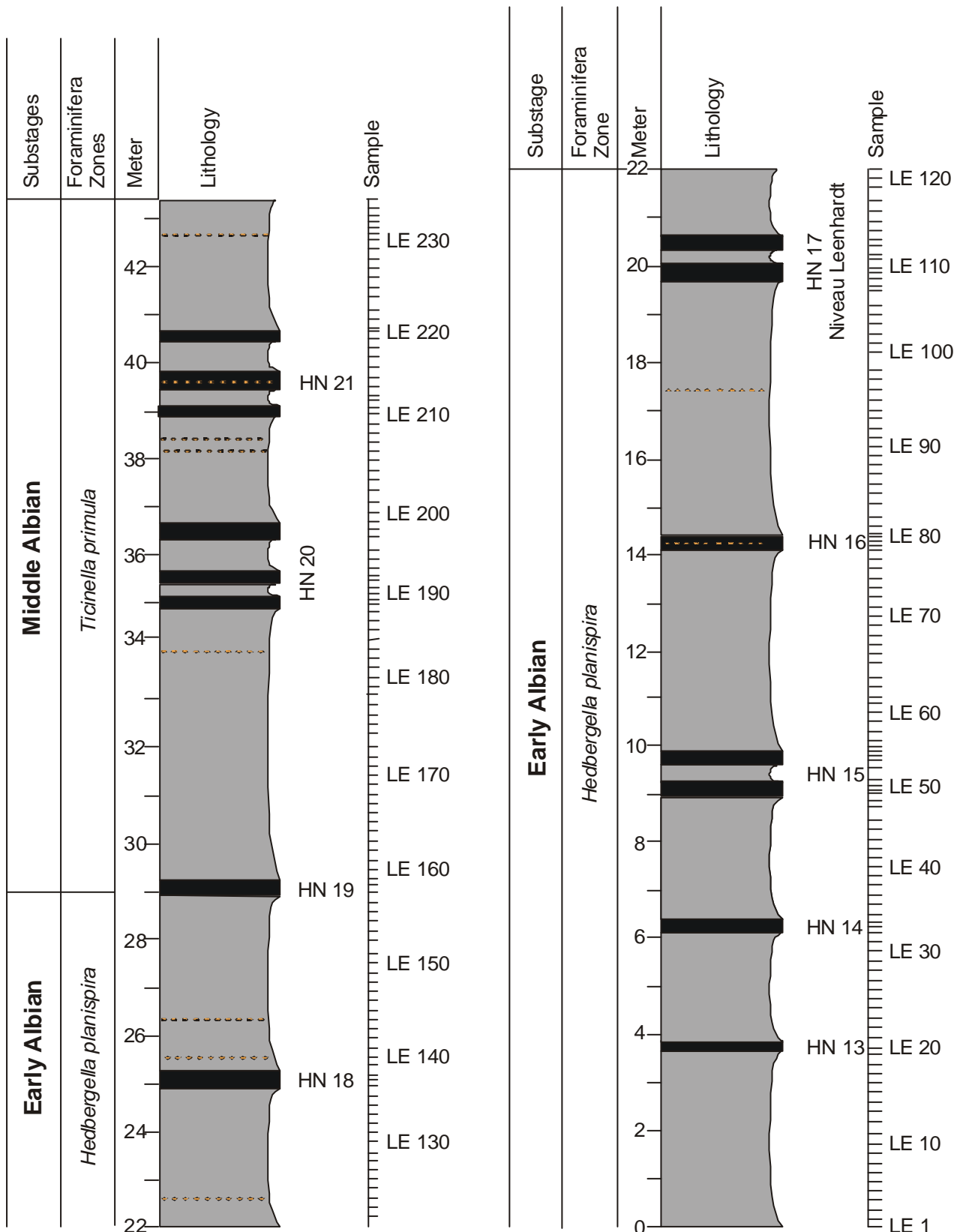
Appendix 4: Lithology and sample distribution of the Late Aptian section 2 Col de Pré Guittard near Arnanon, with respect to foraminifera stratigraphy (sample abbreviation = PG). For lithological explanation see Appendix 2.



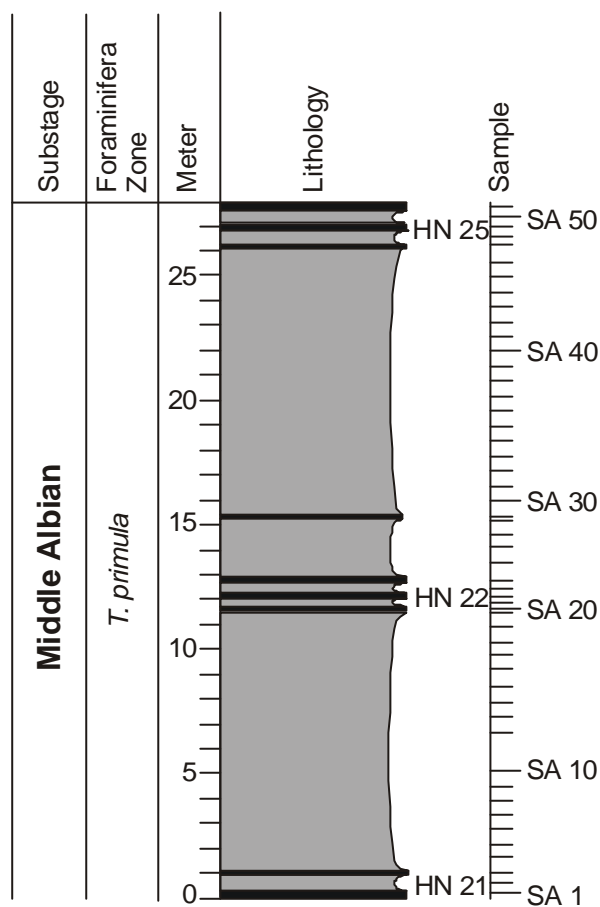
Appendix 5: Lithology and sample distribution of the Late Aptian to Early Albian section 3 Les Oustaus near Esparron, with respect to foraminifera stratigraphy (sample abbreviation = OUS). Lithological explanation see Appendix 2.



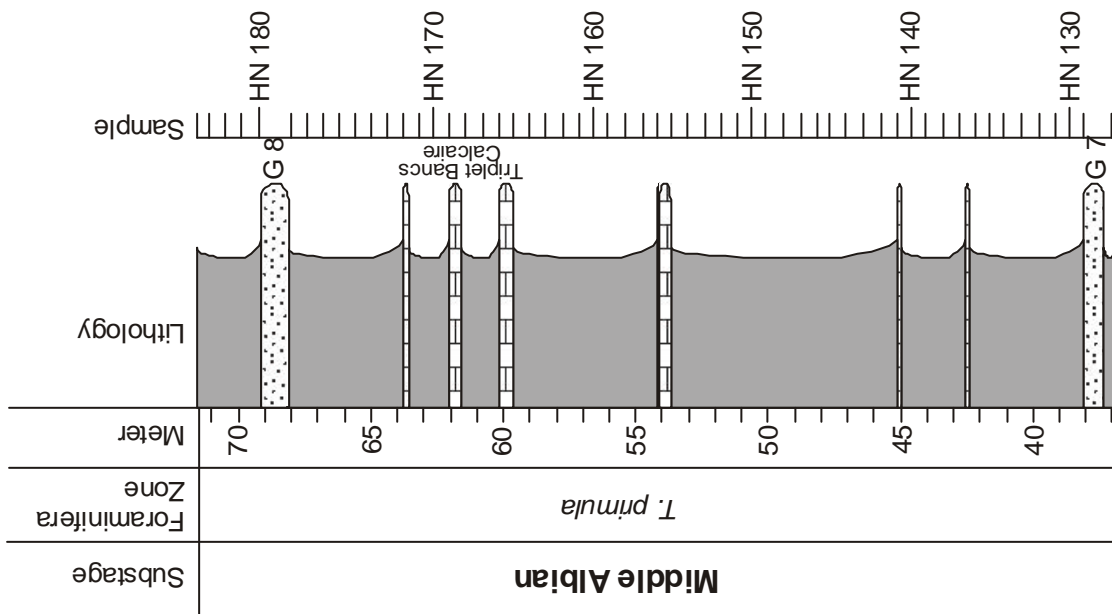
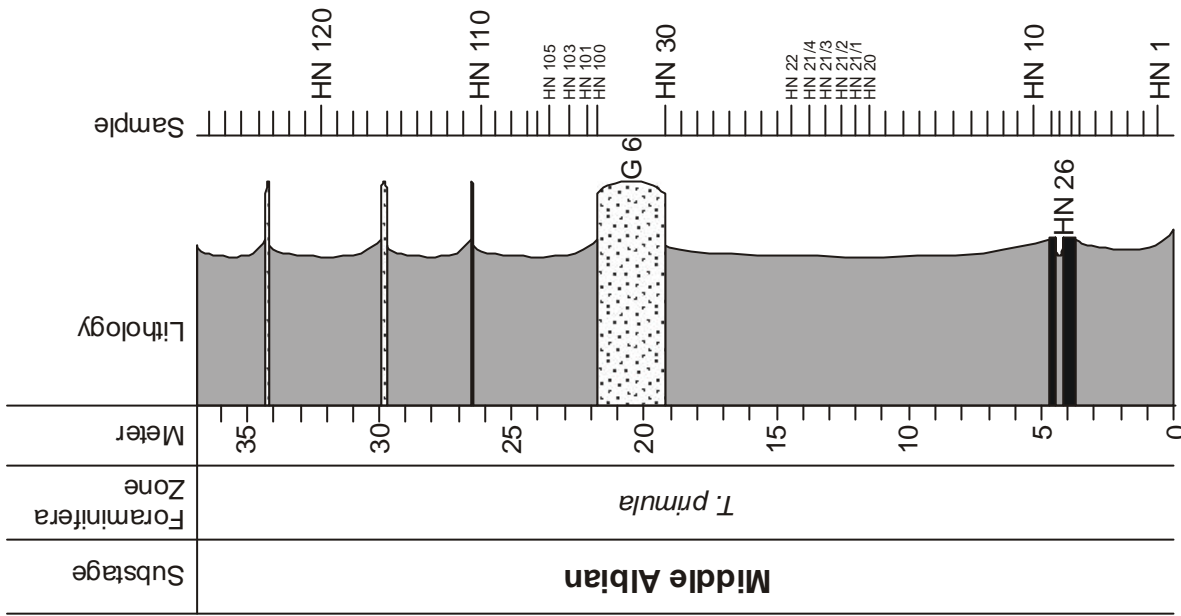
Appendix 6: Lithology and sample distribution of the Early Albian section 4 l'Arboudeysse near Moydans, with respect to foraminifera stratigraphy (sample abbreviation = MP, MP1, MP2 und MPP). For lithological explanation see Appendix 2.



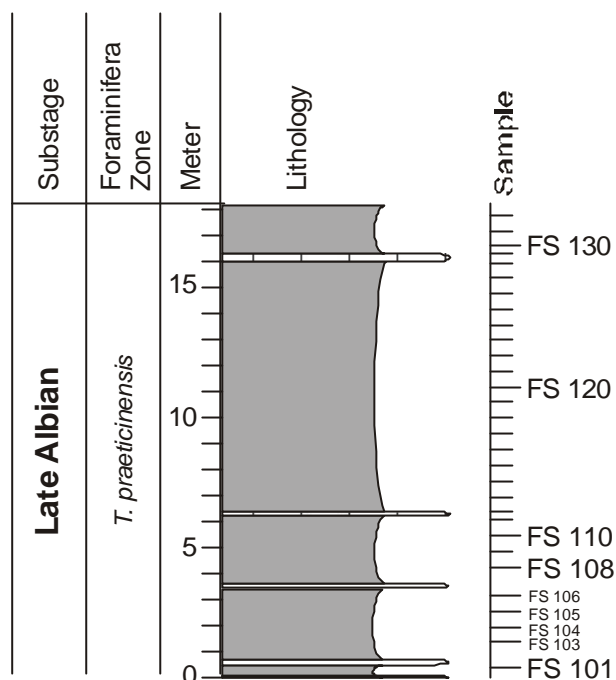
Appendix 7: Lithology and sample distribution of the Early to Middle Albian section 5 at the Col de Palluel (Les Jassines), with respect to foraminifera stratigraphy (sample abbreviation = LE). For lithological explanation see Appendix 2.



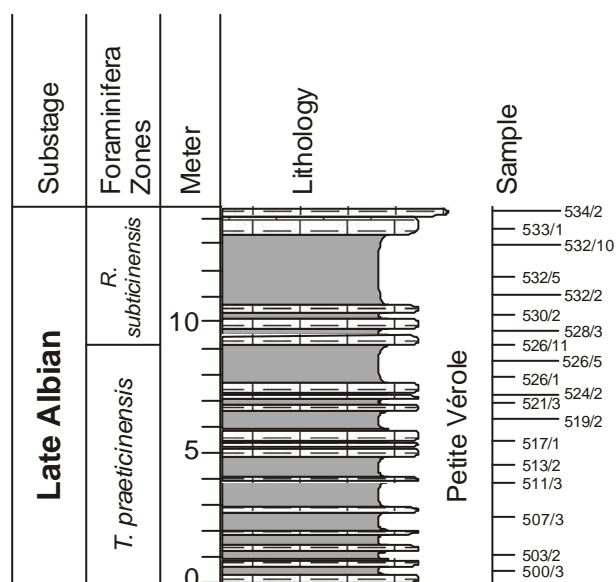
Appendix 8: Lithology and sample distribution of the Middle Albian section **6** at the Serre Amande near Bruis, with respect to foraminifera stratigraphy (sample abbreviation = SA). For lithological explanation see Appendix 2.



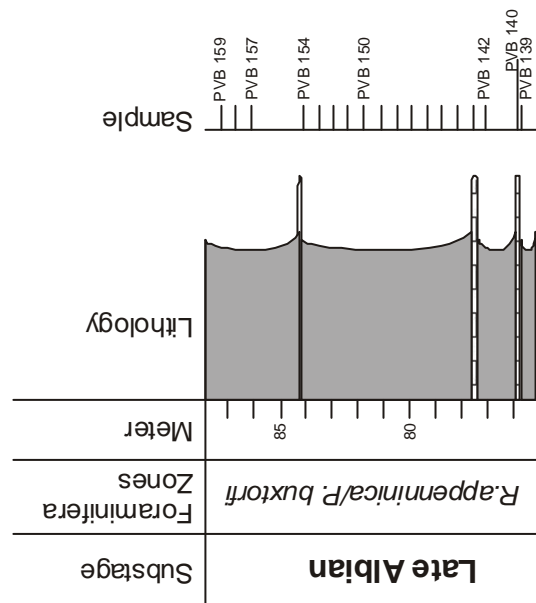
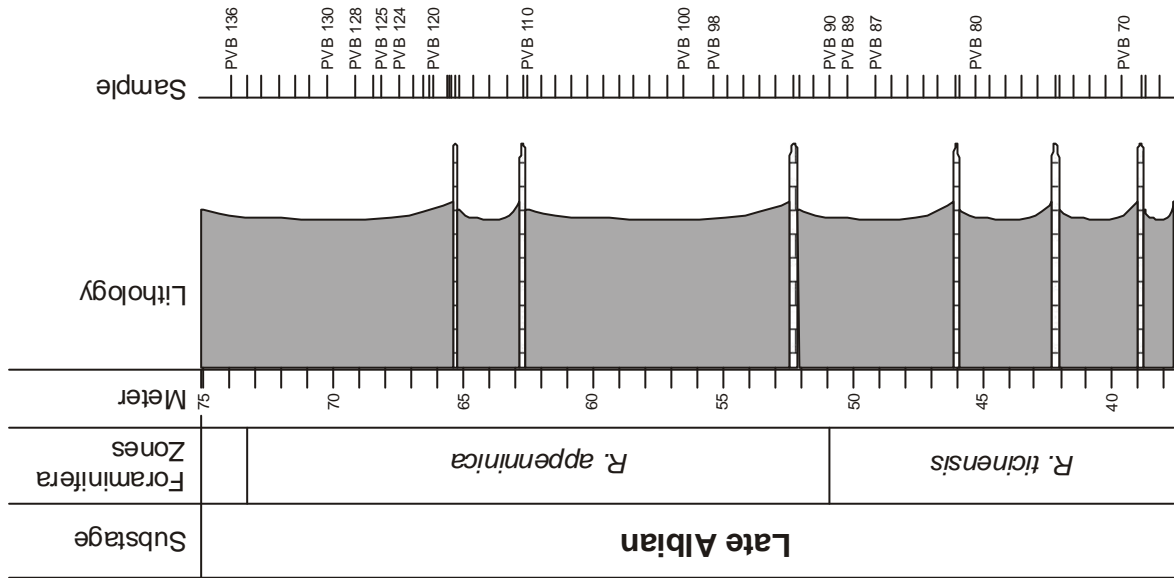
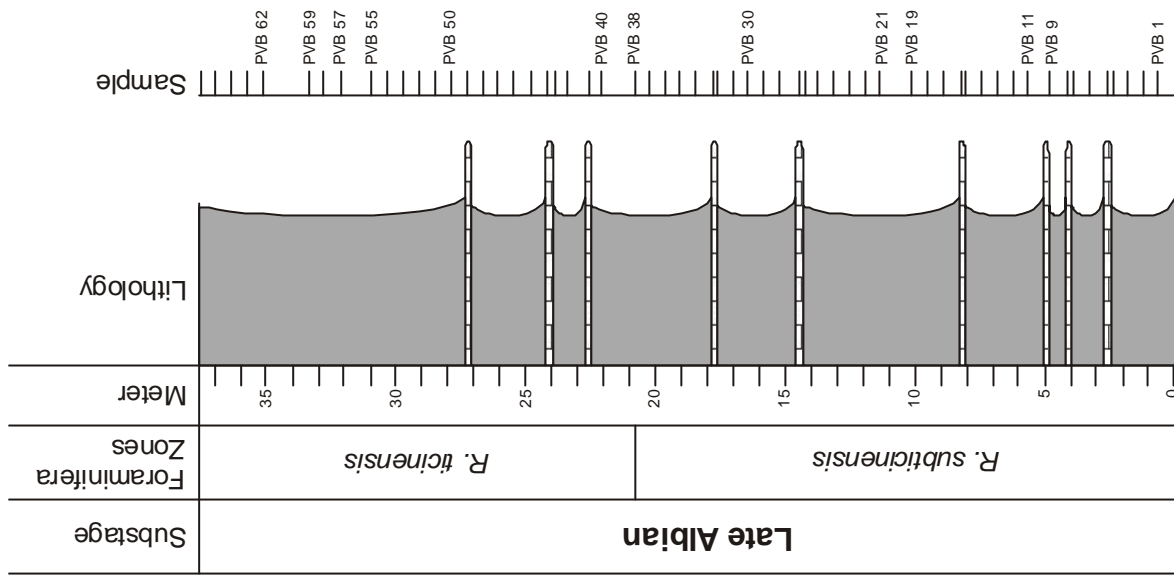
Appendix 9: Lithology and sample distribution of the Middle Albian section 7 at the Col de Palluel. Roadcut north of the D 994, between Moydans and Rosans. With respect to foraminifera stratigraphy (sample abbreviation = HN). For lithological explanation see Appendix 2.



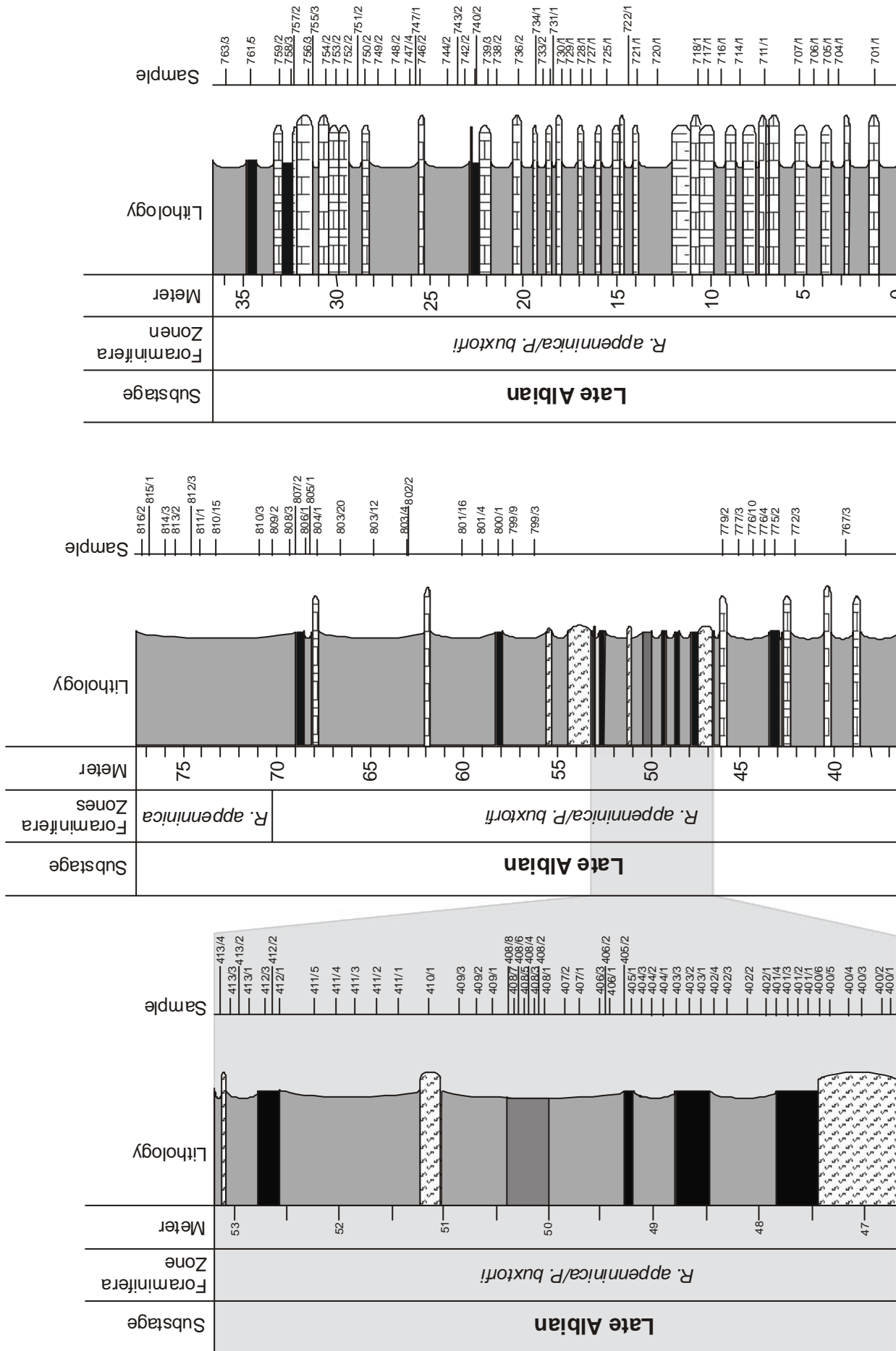
Appendix 10: Lithology and sample distribution of the Late Albian section **8** at the Col de Palluel, northern mountainside of the Mont Risou, with respect to foraminifera stratigraphy (sample abbreviation = FS). For lithological explanation see Appendix 2.



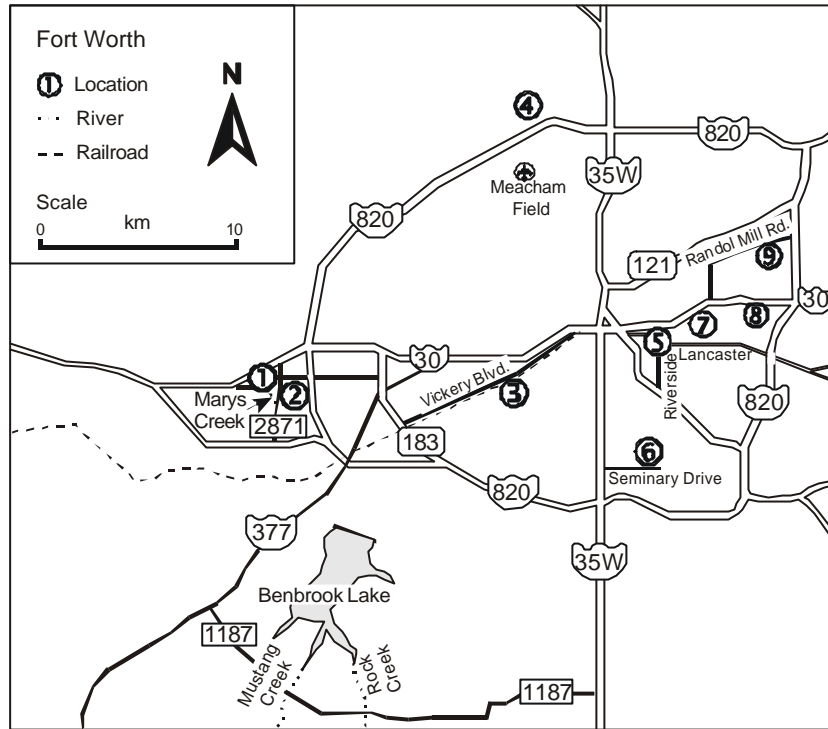
Appendix 11: Lithology and sample distribution of the Late Albian section **9** at the Col de Palluel, northern mountainside of the Mont Risou, with respect to foraminifera stratigraphy (sample abbreviation = PV). For lithological explanation see Appendix 2.



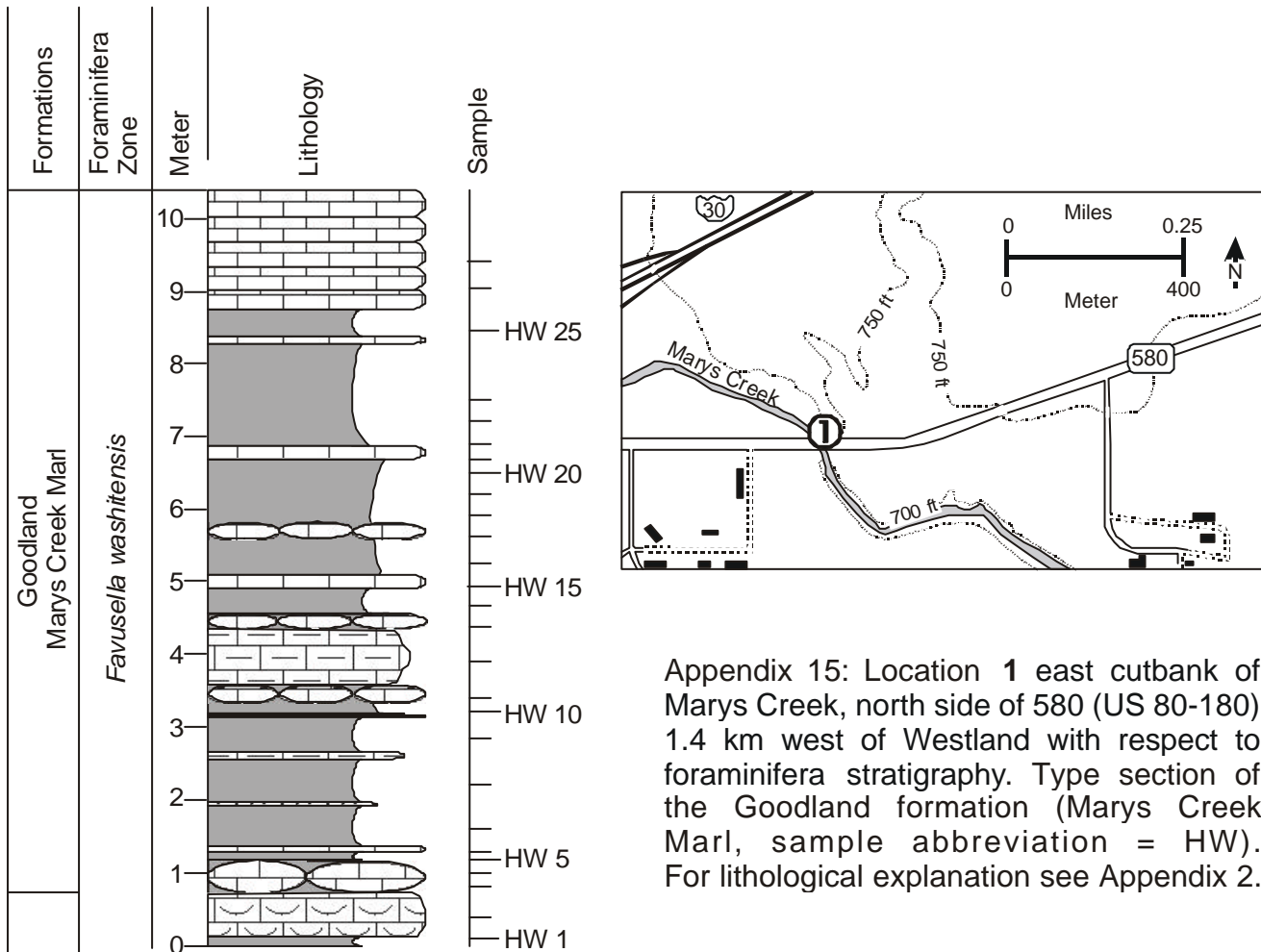
Appendix 12: Lithology and sample distribution of the Late Albian section **10** at the Col de Palluel, at the northern mountainside of the Mont Risou, with respect to foraminifera stratigraphy (sample abbreviation = PVB). For lithological explanation see Appendix 2.



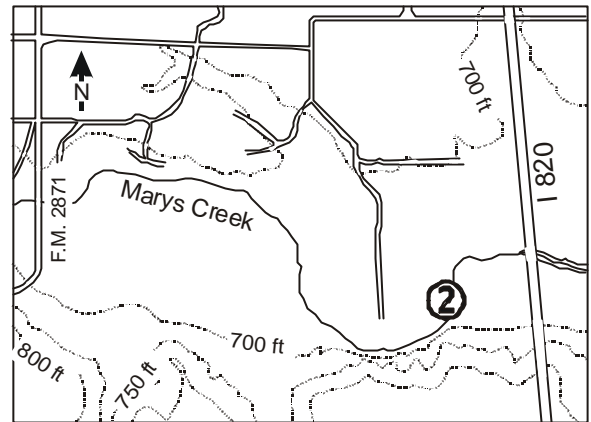
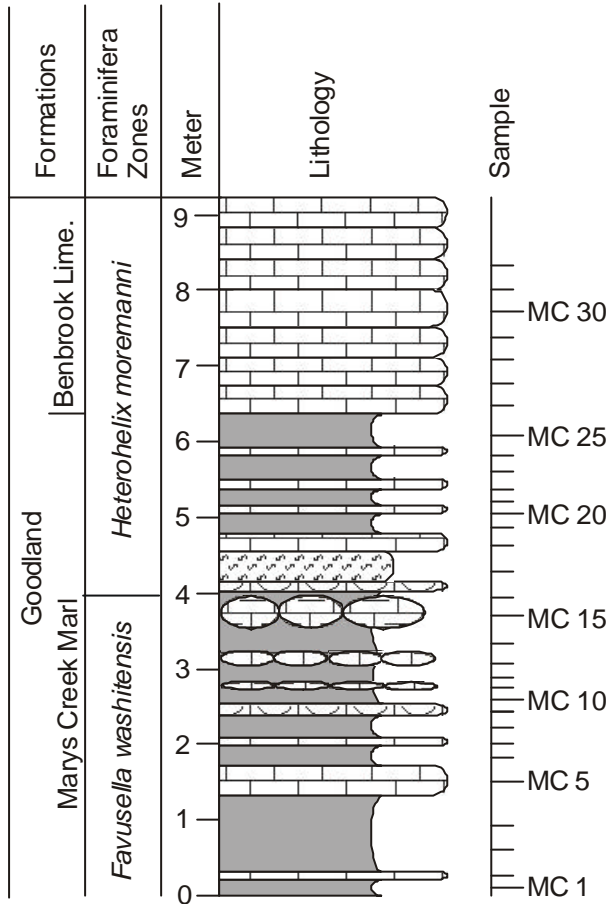
Appendix 13: Lithology and sample distribution of the Late Albian section 11 at the Col de Palluel, northern mountainside of the Mont Risou, with respect to foraminifera stratigraphy (sample abbreviation = BR). Additionally a detailed sketch of the Niveau Breistroffer. For lithological explanation see Appendix 2.



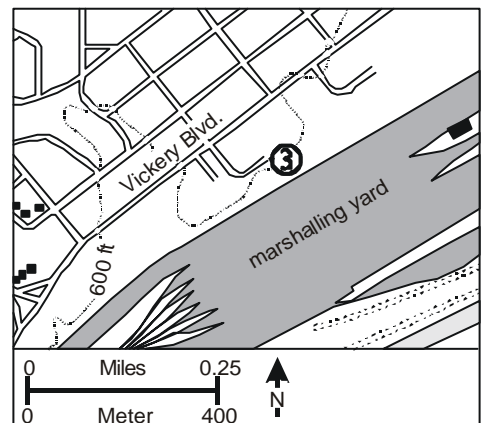
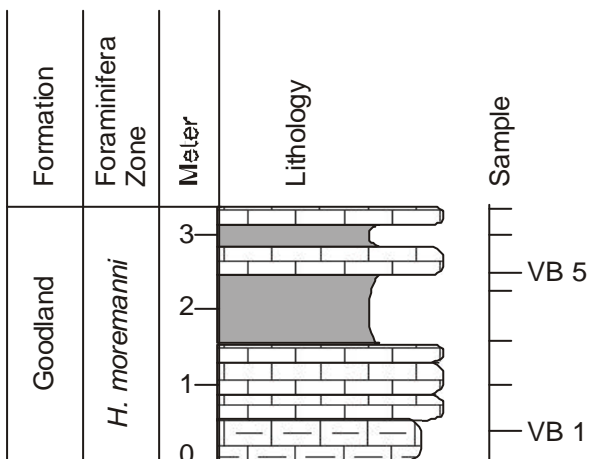
Appendix 14: Road map of Greater Fort Worth with the location of the section.



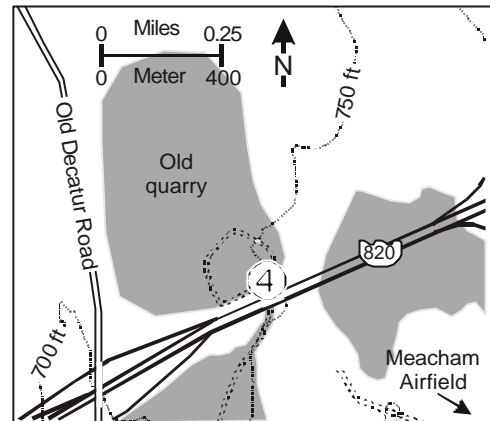
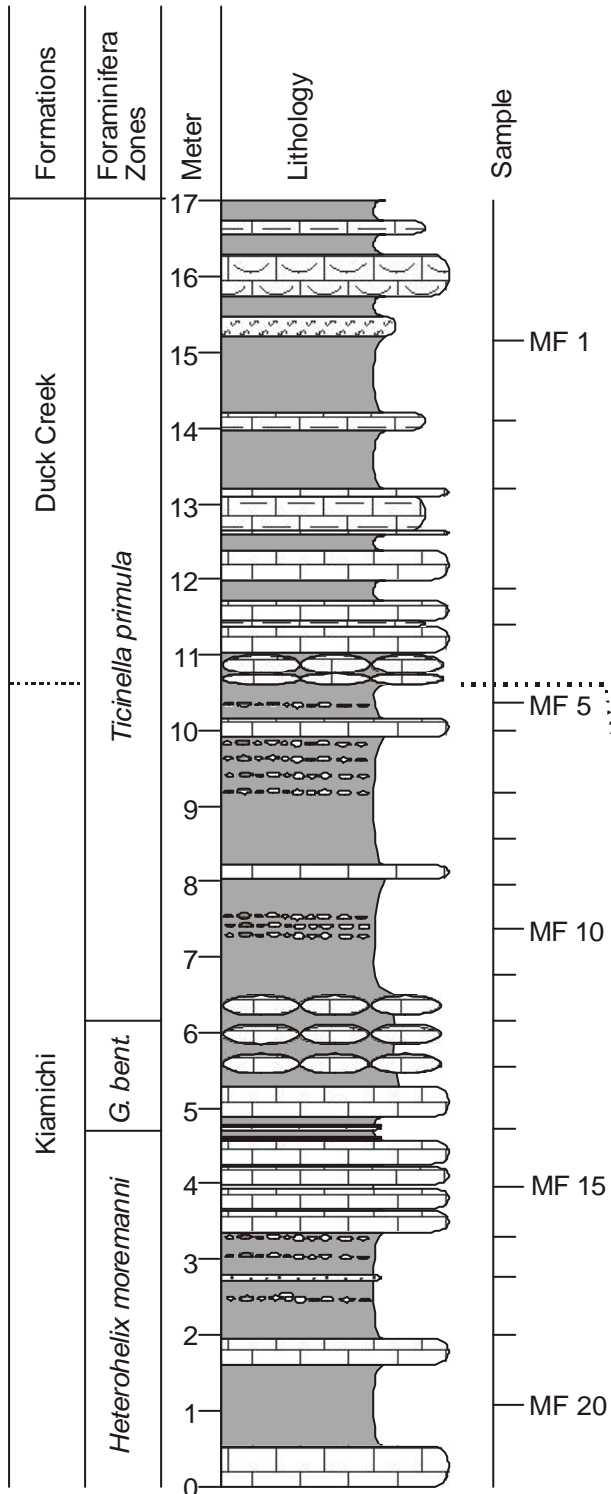
Appendix 15: Location 1 east cutbank of Marys Creek, north side of 580 (US 80-180) 1.4 km west of Westland with respect to foraminifera stratigraphy. Type section of the Goodland formation (Marys Creek Marl, sample abbreviation = HW). For lithological explanation see Appendix 2.



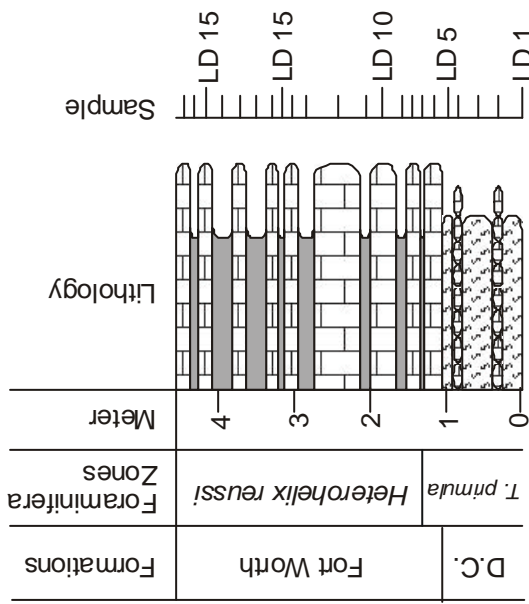
Appendix 16: Location **2** south cutbank of Marys Creek east of FM 2871 1.4 km and west of I-820 with respect to the foraminifera stratigraphy. Type section Goodland Formation (Benbrook Limestone, sample abbreviation = MC). For lithological explanation see Appendix 2.



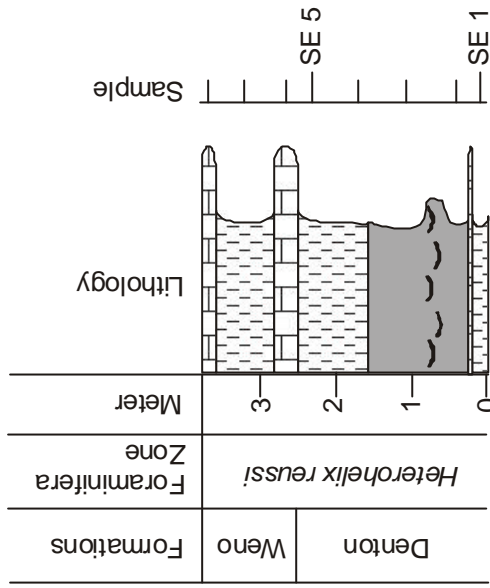
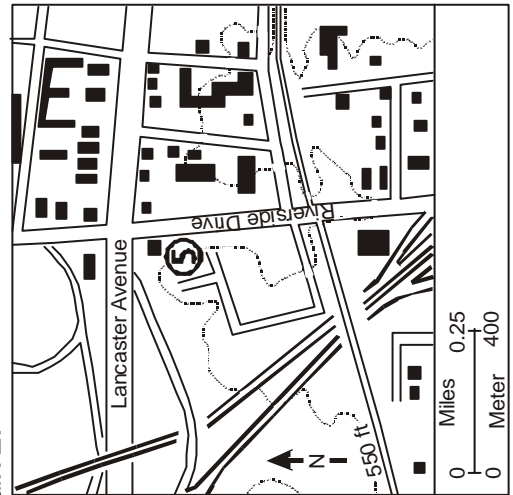
Appendix 17: Lithology and sample distribution of the section **3** south of Vickery Blvd, next to the railroad tracks with respect to foraminifera stratigraphy. (Sample abbreviation = VB). For lithological explanation see Appendix 2.



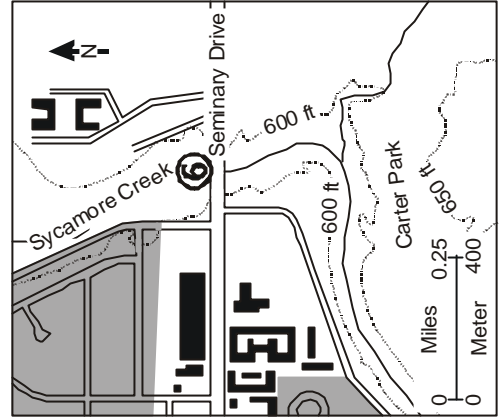
Appendix 18: Location 4 north and south side of an old, disused quarry (Saginaw quarry) north of the Interstate 820 and east of the Old Decatur Road with respect to foraminifera stratigraphy (sample abbreviation = MF). For lithological explanation see Appendix 2.

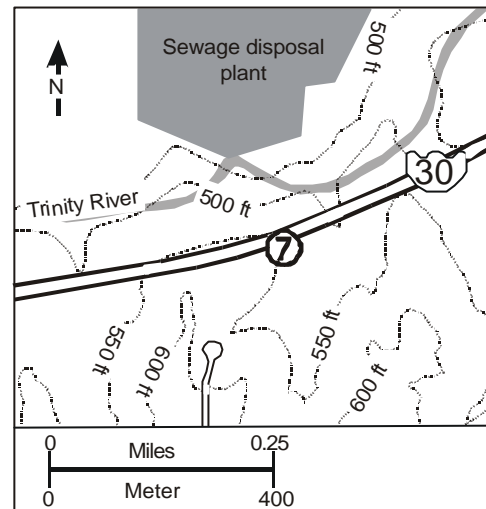
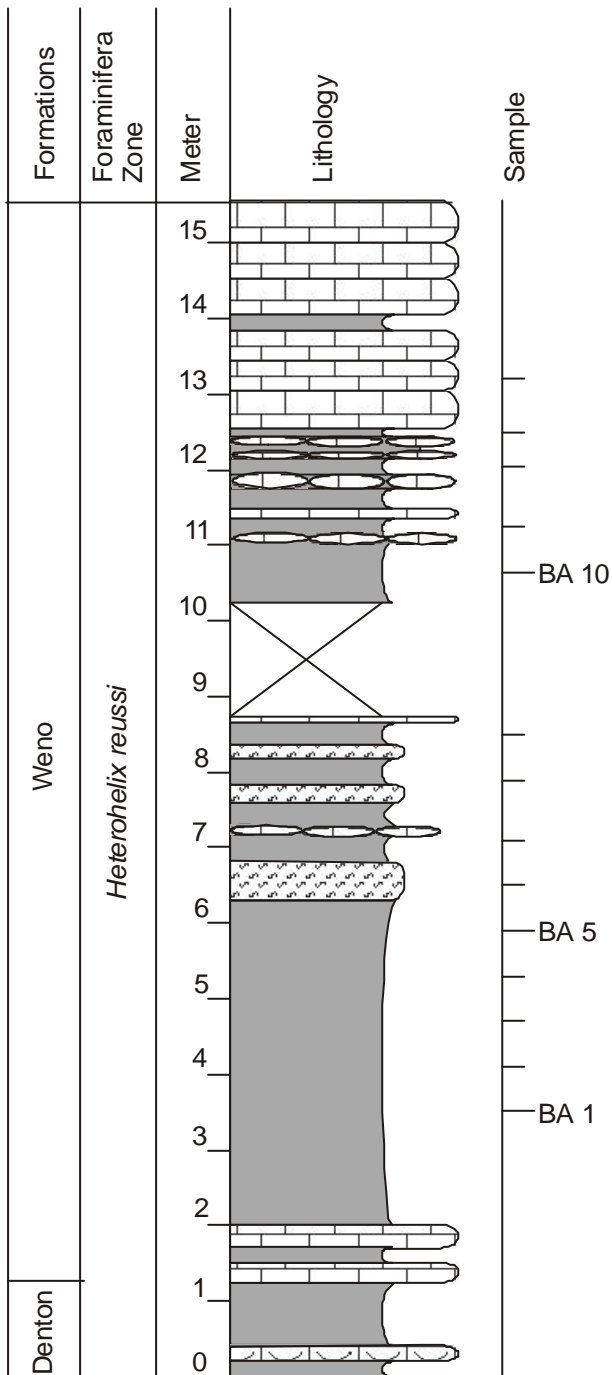


Appendix 19: Lithology and sample distribution of the section 5 southwest corner of Lancaster Avenue and Riverside Drive with respect to foraminifera stratigraphy. Duck Creek (D.C.) and Fort Worth Formation (sample abbreviation= LD). For lithological explanation see Appendix 2.

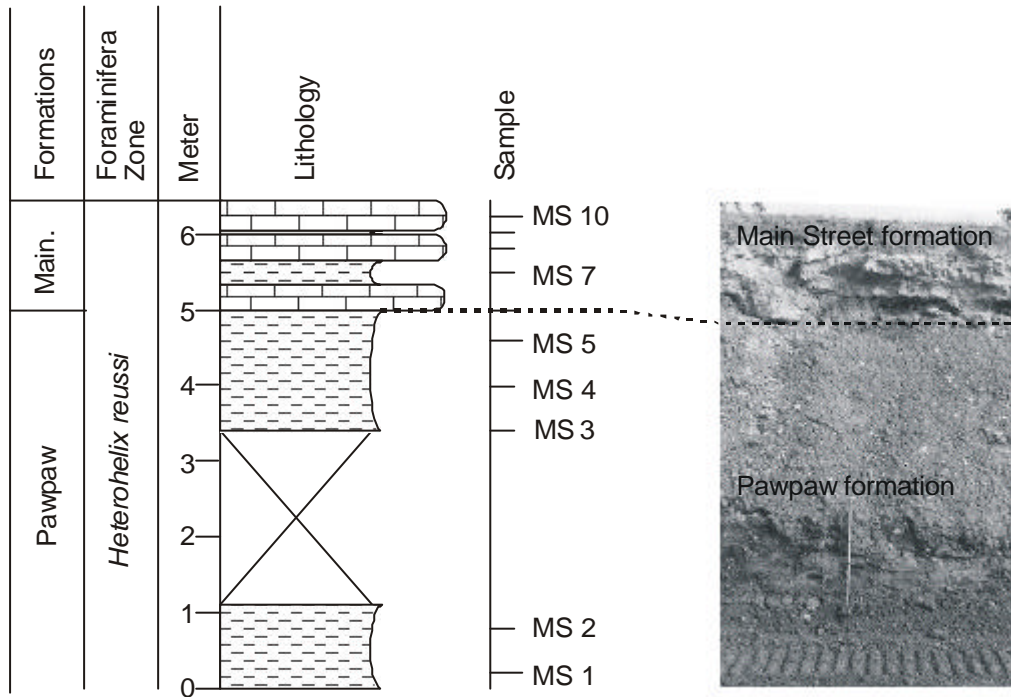


Appendix 20: Lithology and sample distribution of the section 6 westbank of the Sycamore Creek north of the Seminary Drive with respect to foraminifera stratigraphy (sample abbreviation = SE). For lithological explanation see Appendix 2.

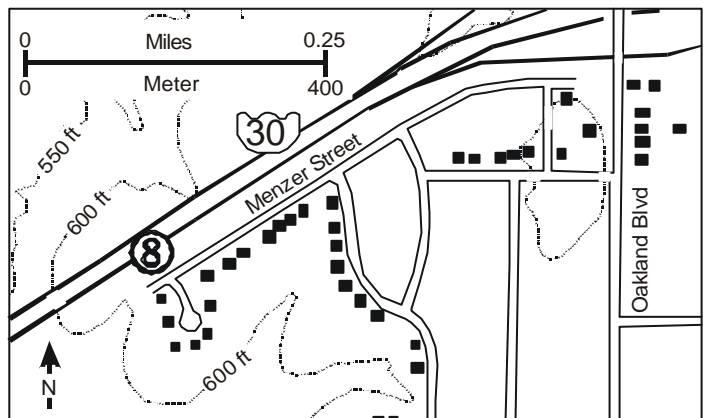


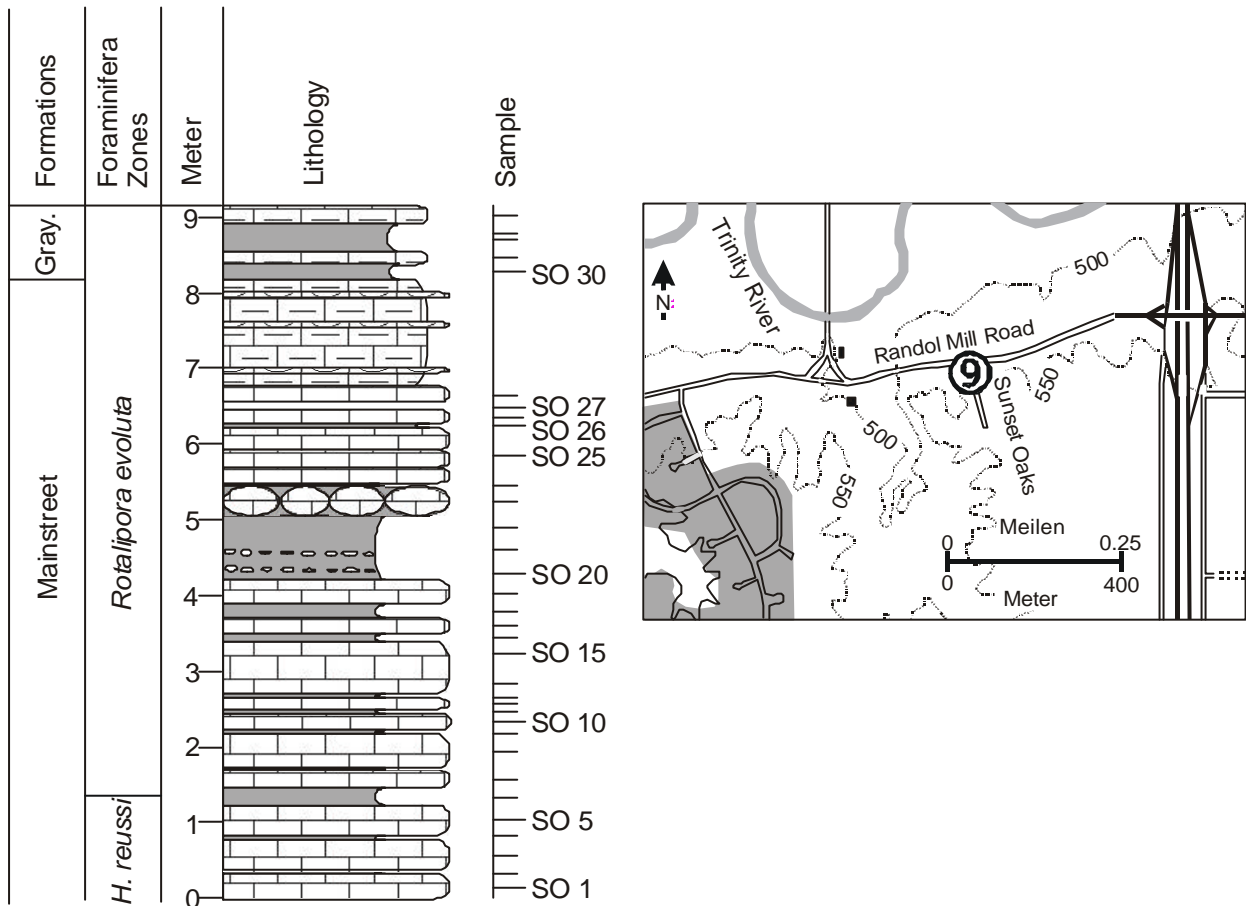


Appendix 21: Lithology sample distribution of the section 7. Roadcut south of Interstate 30 between Oakland and Beach Streets with respect to foraminifera stratigraphy (sample abbreviation = BA). For lithological explanation see Appendix 2.



Appendix 22: Lithology and sample distribution of section 8. Roadcut at the Interstate 30 west of Oakland Street with respect to foraminifera stratigraphy (accessible from West Menzer Street, sample abbreviation = MS). For lithological explanation see Appendix 2.





Appendix 23: Lithology and sample distribution of section 9. Roadcuts in Sunset Oaks Drive at Randol Mill Road one block west of Bridgewood Drive & excavation bank east of road on north side of fence with respect to foraminifera stratigraphy sample abbreviation = SO). For lithological explanation see Appendix 2.

Plate 1

- Fig. 1** *Planomalina buxtorfi* (Gandolfi, 1942)
SE-France, Section Col de Palluel VI, Late Albian,
a) umbilical view (330X), Sample BR 782/2
b) dorsal view (300X); Sample BR 782/1
- Fig. 2** *Biticinella breggiensis* (Gandolfi, 1942)
SE-France, Section Col de Palluel IV, Late Albian,
a) umbilical view (360X), Sample FS103
b) umbilical view (360X), Sample FS103
- Fig. 3** *Rotalipora appenninica* (Renz, 1936)
SE-France, Section Col de Palluel VI, Late Albian,
a) umbilical view (300X), Sample BR 789/6
b) dorsal view (350X); Sample BR 789/6



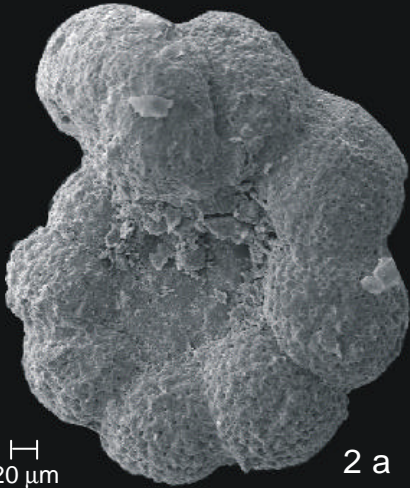
1a

20 μ m



1b

20 μ m



2 a

20 μ m



2 b

30 μ m



3a

20 μ m



3b

30 μ m

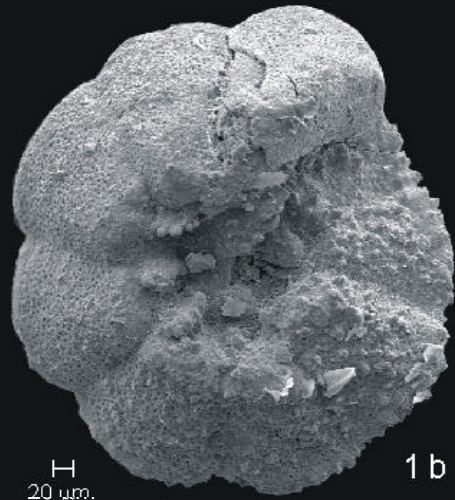
Plate 2

- Fig. 1** *Rotalipora ticinensis* (Gandolfi, 1942)
SE-France, Section Col de Palluel V, Late Albian,
a) dorsal view (250X), Sample PVB 107
b) umbilical view (300), Sample PVB 107
- Fig. 2** *Hedbergella delrioensis* (Carsey, 1926)
SE-France, Section Col de Palluel VI, Sample BR
781/ 2, Late Albian, dorsal view (380X)
- Fig. 3** *Hedbergella simplex* (Morrow, 1934)
SE-France, Section Col de Palluel VI, Late Albian,
dorsal view (420X), Sample BR 782/1,
- Fig. 4** *Hedbergella planispira* (Tappan, 1940)
SE-France, Section Col de Palluel VI; Sample BR
789/4, Late Albian, umbilical view (750X)
- Fig. 5** *Heterohelix moremani* (Cushman, 1938)
SE-France, Section Col de Palluel VI, Sample BR
794/2, Late Albian, (1000X)



30 μm

1 a



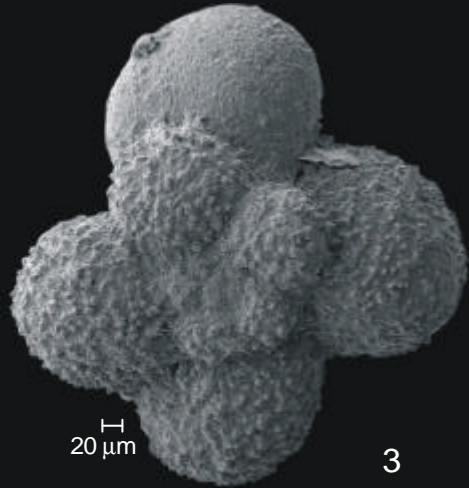
20 μm

1 b



20 μm

2



20 μm

3



20 μm

4

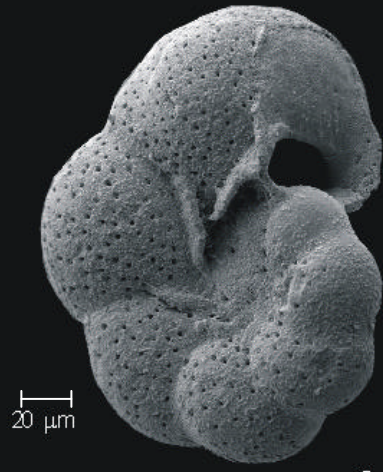
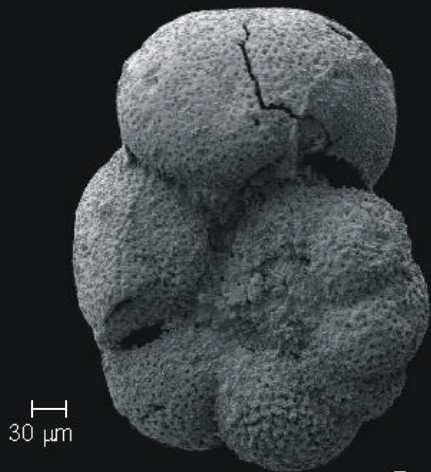
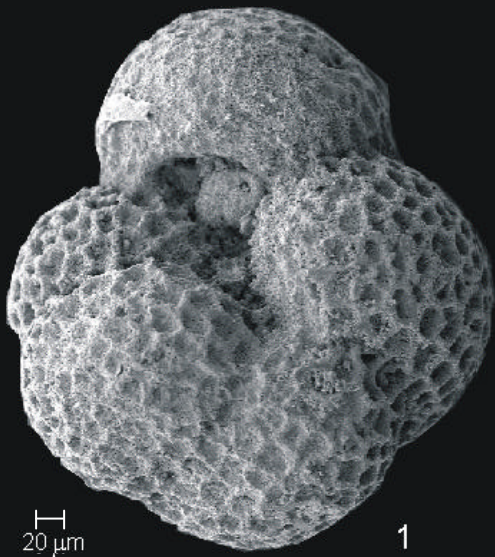


10 μm

5

Plate 3

- Fig. 1:** *Favusella washitensis* (Carsey, 1926)
NE-Texas, Section Lancaster Avenue, Sample
LD 13, Late Albian, umbilical view (400X)
- Fig. 2:** *Hedbergella delrioensis* (Carsey, 1926)
NE-Texas, Section Meacham Field, Sample MF 9
Late Albian, umbilical view (420X)
- Fig. 3:** *Hedbergella planispira* (Morrow, 1934)
NE-Texas, Section Interstate 30 & Menzer Street,
Sample MS 2, Late Albian, umbilical view (560X)
- Fig. 4:** *Hedbergella* sp. (Brönnimann & Brown, 1958)
NE-Texas, Section Meacham Field, Sample
MF 4, Late Albian, umbilical view (350X)
- Fig. 5:** *Globigerinelloides bentonensis* (Morrow, 1934)
NE-Texas, Section Meacham Field, Sample
MF 1, Late Albian, umbilical view, (360)
- Fig. 6:** *Globigerinelloides* sp. (Cushman & Ten Dam,
1948) NE-Texas, Section Interstate 30 & Menzer
Street, Sample MS 2, Late Albian, umbilical view
(820X)



Lebenslauf

Kerstin Reichelt

Geburtsdatum	15.04.1974
Geburtsort	Helmstedt
Wohnort	Derendingerstraße 105 72072 Tübingen

Universitätsausbildung

10.1999-09.2003	Promotion am Institut für Geowissenschaften der Universität Tübingen bei Prof. Dr. Ch. Hemleben
10.1993-09.1999	Studium der Geologie und Paläontologie (Diplom) and der Technischen Universität Braunschweig
1995-1999	Teilnahme an mehreren Grabungspraktika in Messel, Eckfelder Maar und Enspel

Schulische Bildung

08.1990-06.1993	Besuch des Theodor-Heuss-Gymnasiums in Wolfsburg, Abschluß mit Abitur, Note 2,2
08.1984-06.1990	Besuch der Orientierungsstufe und Realschule in Velpke, Abschluß mit dem Erweiterten Realschul- abschluß
08.1980-06.1984	Besuch der Dörfergemeinschaftsschule in Groß Twülpstedt (Grundschule)

Eidesstattliche Versicherung

Hiermit erkläre ich, Kerstin Reichelt, das ich diese Dissertation ohne unerlaubte und nur mit den in der Arbeit angegebenen Hilfsmitteln angefertigt habe.

Desweiteren versichere ich, das ich noch keinen Promotionsversuch unternommen habe.

Tübingen den